Basin and Range Province Seismic Hazards Summit III

Utah Geological Survey and Western States Seismic Policy Council

Day 4

Keynote

Technical Session 7 – Using Geodesy to Characterize Seismic Hazard in the Basin and Range Province:
Moderator: Bill Hammond, University of Nevada, Reno

Keynote

KINEMATICS OF THE WASATCH FAULT ZONE FROM GPS MEASUREMENTS, BLOCK MODELING, AND FAULT MODELING

Christine M. Puskas[1], Robert B. Smith[2], Wu-Lung Chang[3], Geoffrey Blewitt[4], and Christopher DuRoss[5]
[1] UNAVCO, 6350 Nautilus Dr., Boulder, Colorado 80301-5394
[2] Department of Geology & Geophysics, Frederick Albert Sutton Building, University of Utah, 115 S 1460 E, Salt Lake City, Utah 84112-0102
[3] Department of Earth Sciences, National Central University, 300, Jhongda Rd. Jhongli 32001, Taiwan
[4] Nevada Geodetic Laboratory, Nevada Bureau of Mines & Geology, University of Nevada, Mail Stop 178, Reno, Nevada 89557-0178
[5] Geologic Hazards Science Center, U.S. Geological Survey, 1711 Illinois St., Golden, Colorado 80401
Senior author email address: puskas@unavco.org

The Wasatch fault zone, which includes six primary, Holocene-active segments, marks the eastern boundary of the Basin and Range Province and accommodates ~3 mm/yr extension between the stable North American Plate and the extending Basin and Range Province (figure 1, 2). The Wasatch fault zone is seismically active, comprising the central part of the Intermountain seismic belt, and is considered capable of generating large, **M** 7+ earthquakes (figure 1). Approximately 80% of the population of Utah is concentrated in the valleys to the west of the Wasatch fault zone, living in an area of high earthquake risk.

For this study, we analyzed time-series from multiple regional Global Positioning System (GPS) networks to determine block interactions that best fit the observed regional extension, and we explored fault-loading geometries. Wasatch Front GPS stations used in this study are operated by the EarthScope Plate Boundary Observatory (PBO), University of Utah (UU), National Geodetic Survey Continuously Operating Reference Stations (CORS), and Utah Automated Geographic Reference Center's Utah Reference Network (TURN). All these stations are processed by the Nevada Geodetic Laboratory at the University of Nevada, Reno (UNR) using the GIPSY OASIS II software, and orbit/clock products from the Jet Propulsion Laboratory (JPL). Time series were spatially filtered and transformed into the NA12 North America-fixed reference frame, produced by UNR (figure 1). Station velocities were estimated from the slopes of the time series components using the analysis code of Langbein (2004) and Langbein and Johnson (1997).

The GPS time series were evaluated for quality by visual inspection, examining quality parameters from UNR, and checking the station state of health parameters from GPS data preprocessing from UNAVCO (Estey and others, 1999). Time periods with poor quality parameters (e.g., high RMS values, low signal-to-noise ratios, etc.) were removed from time series if they exceeded a period of a few months at the beginning or end of the observation period. Station time series were not used if they had less than two years of data, or if data quality was poor over the entire observation period.

To eliminate potential sources of nonlinear deformation, particularly in the vertical component, the GPS time series were compared with surface water loading models produced by UNAVCO. These models use as input the surface water mass stored in the soil and snowpack from the Global Land Data Assimilation System Land Surface Models (GLDAS LSM) (Rodell and others, 2004), and calculate the resulting elastic displacements at GPS site coordinates (van Dam and others, 2001; Meertens and others, 2011; Wahr and others, 2013). This surface loading is primarily a seasonal cycle with subsidence during late fall to early spring, when conditions are colder and wetter, and uplift in the summer to early fall, when conditions are warmer and drier. However, prolonged periods of drought can result in multiyear uplift. We also examined effects of surface lake loading of Great Salt Lake (Elósegui and others, 2003). For 2000–2014, the period studied, lake levels varied over a range of 10 feet (3 m) (Loving and others, 2000), resulting in differential loading that can be modeled with the same techniques as the surface loading models. GPS stations within a few kilometers of the lake may experience subsidence or uplift as lake levels fluctuate. These modeled hydrologic effects are not large: vertical, peak-to-peak seasonal amplitudes are typically ~2 mm, while additional uplift from drought is <1 mm, while maximum displacement range from lake loading is ~4 mm. The variations are not expected to affect velocities of most stations, but some stations operating less than 3–4 years may be affected.

Using the GPS velocities filtered for poor data and corrected for hydrologic loading, we then solved for block motions of the Wasatch fault zone. Tectonic blocks were identified using the distribution of normal faults in northern Utah. GPS stations were sorted depending on their position within a block, and those stations farthest from bounding faults were used to invert for the Euler poles of rotation of each block. Several block configurations were tested and evaluated based on the chi-square misfit between observed horizontal GPS velocities and modeled velocities from block motion.

Preliminary block models suggest that the fixed North America block is separated from the Basin and Range block by a narrow, intermediate block bounded to the west by the East Great Salt Lake and Oquirrh faults and to the east by the Wasatch fault zone, from the Provo segment to the Brigham City segment. South of this intermediate block, the Nephi and Levan segments of the Wasatch fault zone form the boundary between the fixed North America and Basin and Range block.

Once the block motions have been subtracted from the GPS velocities, the residuals are assumed to correspond to deformation from fault loading. Block motions should account for motion outside a fault zone, so subtracting the block rotations will leave non-zero velocities only across active fault traces. Vertical velocities are not affected by block rotation, but have a larger error and are more likely to have large scatter when compared to each other in profile (figure 2). The preliminary block modeling produces horizontal residuals <1 mm/yr. This is similar to the uncertainties in the GPS velocities, so using the residuals to constrain fault loading models is difficult. We explore possible fault loading geometries through forward modeling, looking at listric versus planar faulting at depth. We assume a crustal structure in which a fault in the upper, seismogenic crust is locked, but the same fault creeps in the mid to lower crust, exerting a load on the up-dip, locked segment. Prior studies using campaign GPS data by Chang (2004) and Chang and others (2006) demonstrate that fault loading rates depend on down-dip, creeping fault geometry and favor a shallow-dipping creeping fault (dip ~27º).

The proliferation of permanent GPS stations across the western US over the past 15 years has produced good geographic coverage of the Wasatch fault zone. Using the best available GPS data, we modeled the regional deformation with rotating tectonic blocks bounded by the Wasatch and other large normal faults. The block boundaries correspond to potentially active faults, and we use the residuals obtained by subtracting block motions from observed GPS motions to explore possible fault loading models. Fault geometries and loading rates are required for further studies of seismic hazard, and to constrain stress interactions between fault segments.

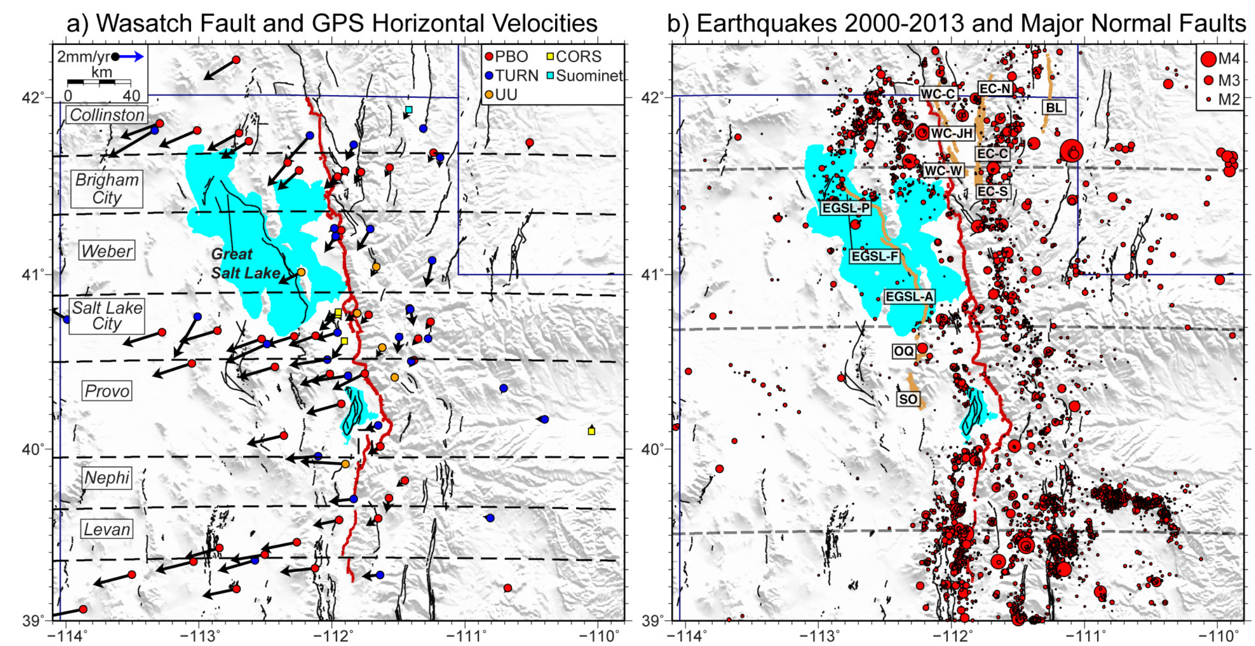

Figure 1. *(a) Horizontal GPS velocities across the Wasatch fault zone, and (b) earthquakes with M>2 for 2000-2014 and major normal faults in northern Utah. The Wasatch fault zone (thick, red) segments are labeled in (a) and separated by dashed lines. All Wasatch fault zone segments shown have been active in Holocene time except the Collinston segment, which is late Quaternary. GPS station symbols are coded by operating agency. All GPS horizontal velocities are shown and have not been sorted for quality. Other major normal faults (thick, brown) are shown in (b): EGSL=East Great Salt Lake fault with P=Promontory segment, F=Fremont segment, A=Antelope segment; OQ=Oquirrh fault; SO=South Oquirrh fault; WC=West Cache fault with C=Clarkston segment, JH=Junction Hills segment, W=Wellsville segment; EC=East Cache fault with N=Northern segment, C=Central segment, S=Southern segment; and BL=East Bear Lake fault. Earthquakes are from the ANSS catalog. Dashed lines show profile locations for figure 2. Topography is from the Marine Geoscience Data System (Ryan and others, 2009).*

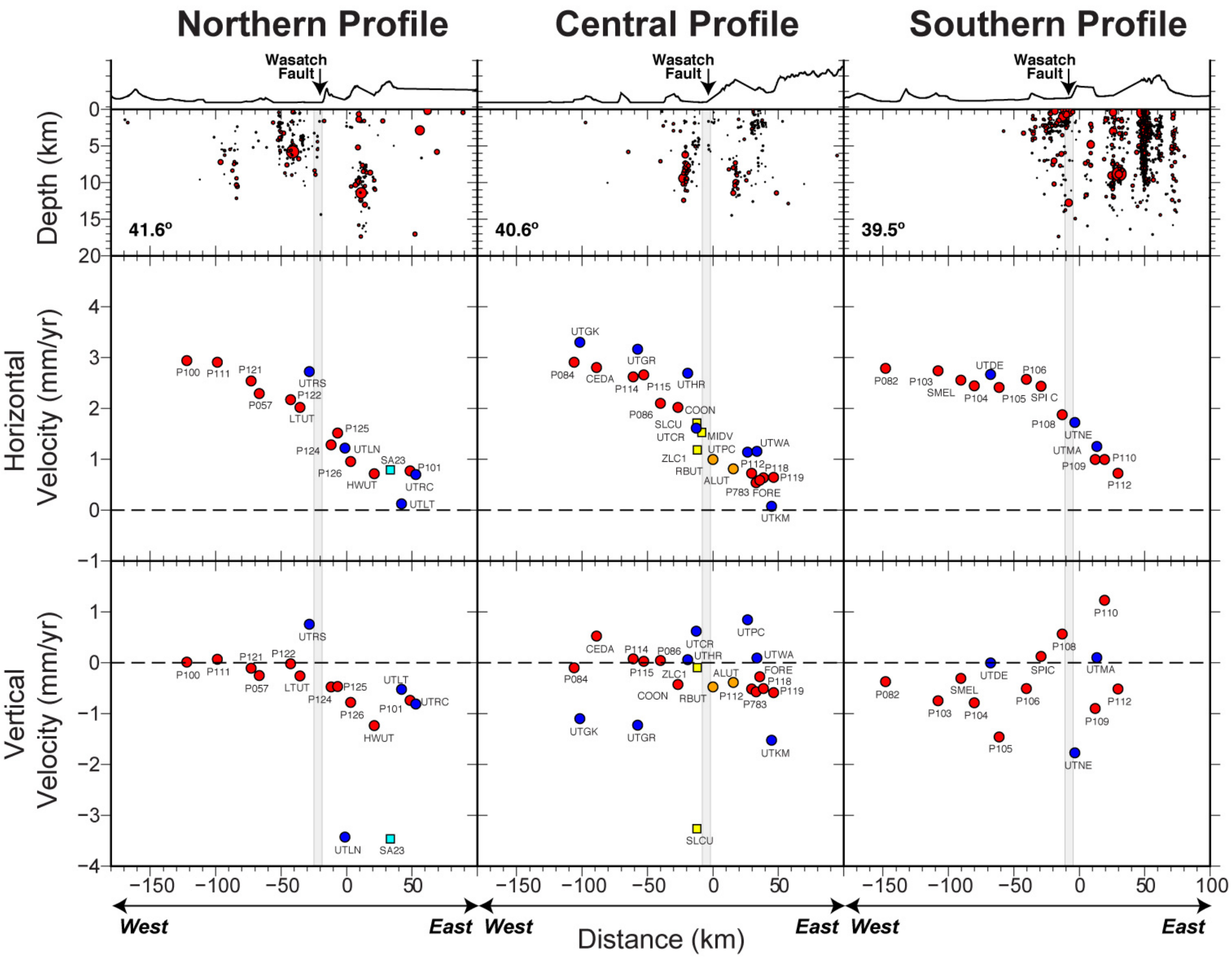

Figure 2. *Profiles of topography, earthquakes, GPS horizontal velocity magnitudes, and GPS vertical velocities. Profiles are taken on east-west cross-sections at 41.6º N., 40.6º N., and 39.5º N., and earthquakes within ±10 km of the profile are projected into the cross-section plane. Earthquakes were obtained from the ANSS catalog. The location of the Wasatch fault zone is marked with an arrow in the topographic cross-section and a gray box in the other cross-sections. GPS stations in the northern profile sample primarily the Brigham City and Collinston segments (see figure 1). GPS stations in the central profile are sample extension across the Salt Lake City segment, while stations in the southern profile measure the Nephi and Levan segments.*

The following is a PDF version of the authors' PowerPoint presentation.

Kinematics of the Wasatch Fault Zone from GPS Measurements, Block Modeling, and Fault Modeling

C. M. Puskas
UNAVCO

R. B. Smith
University of Utah

W.-L. Chang
National Central University, Taiwan

G. Blewitt
University of Nevada, Reno

C. DuRoss
USGS

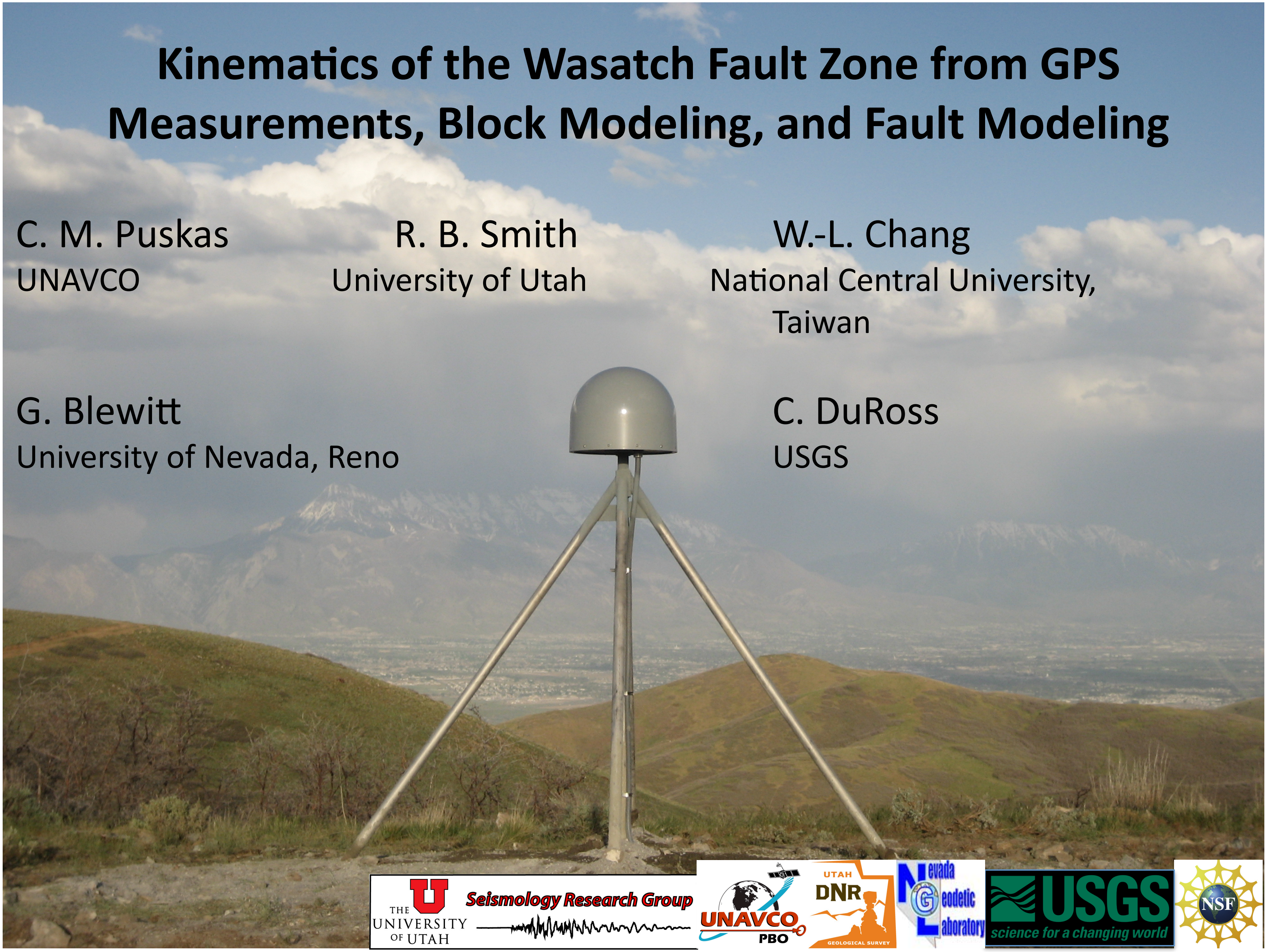

2000-2014 Earthquakes

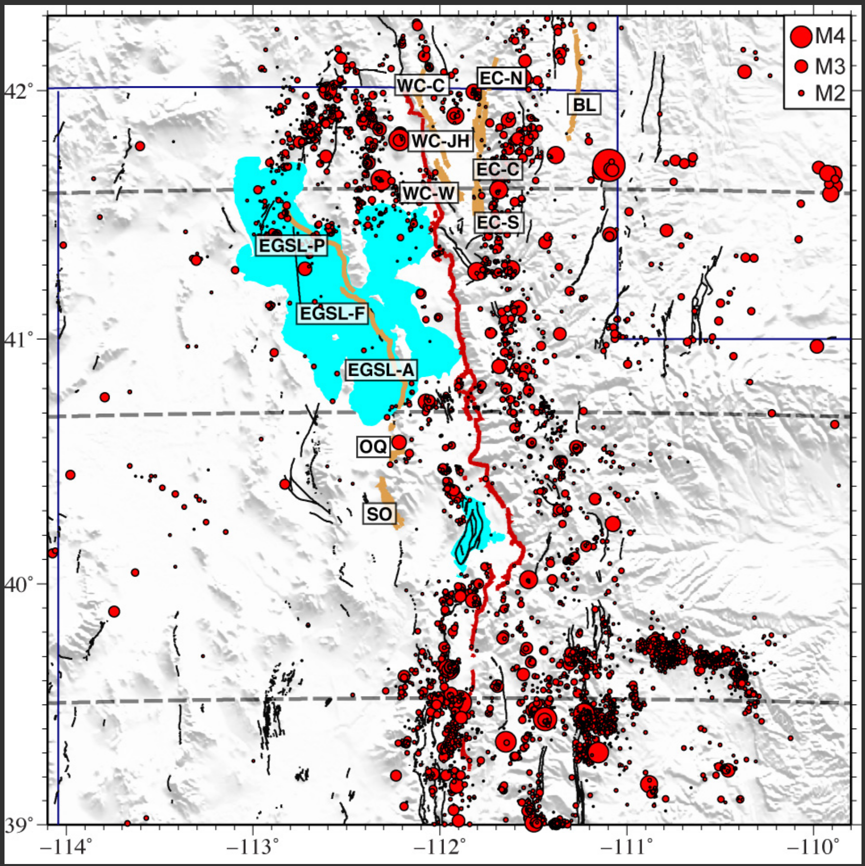

ANSS

Paleoseismic History

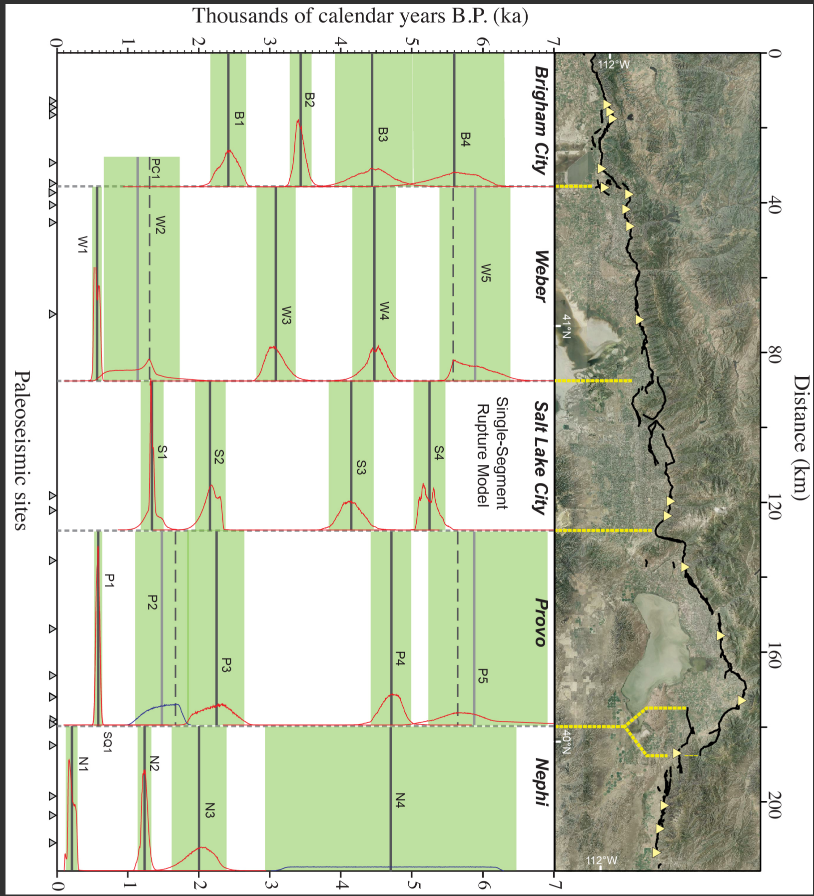

(DuRoss et al., 2011)

- Multiple large normal faults in Wasatch Front
- Seismically active
  - Largest historic event: M6.6 March 12, 1934 Hansel Valley earthquake
  - 4-5 events identified for each Wasatch segment in last 6000 years

Prehistoric Earthquakes Identified for Wasatch Fault

EQ Ref #	Segment Ref #	Age (yrs)	DAge (2-s)	SRL (km)	DSRL (2-s)
E1	N1	206	86	43	11.5
E2	P1	576	48	59	11.5
E3	W1	561	68	56	6.5
E4	W2	1137	641	65	8.5
E5	N2	1234	96	43	11.5
E6	S1	1343	162	40	6.5
E7	P2	1479	378	59	11.5
E8	N3	2004	388	43	11.5
E9	P3	2240	406	59	11.5
E10	S2	2160	215	40	6.5
E11	B1	2417	256	36	6
E12	W3	3087	275	56	6.5
E13	B2	3430	153	36	6
E14	B3	4452	543	36	6
E15	W4	4471	303	36	13
E16	S3	4147	315	40	6.5
E17	P4	4709	285	59	11.5
E18	N4	4699	1768	43	11.5
E19	S4	5250	221	40	6.5
E20	B4	5603	660	36	6
E21	P5	5888	1002	59	11.5
E22	W5	5891	502	56	6.5

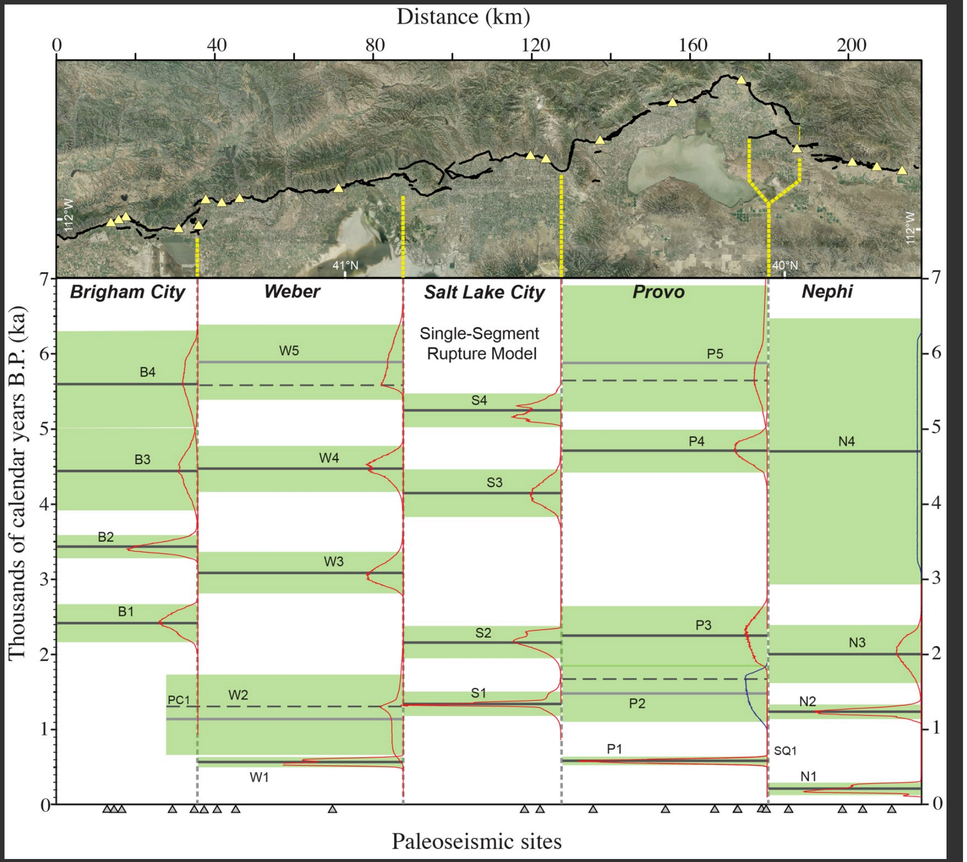

(DuRoss et al., 2011)

Other Prehistoric Earthquakes

Fault Name	Segment Name	Segment Length (km)	Age Range	Closest Wasatch Segment
Hansel Valley		11	78 (1934 M6.6)	Collinston
EGSL	Antelope Island	35	355-797	Weber
EGSL	Antelope Island	35	5936-6406	Weber
EGSL	Fremont Island	30	2939-3385	Weber
N. Oquirrh		21	4800-7900	Salt Lake City
S. Oquirrh		24	1300-4830	Salt Lake City
West Cache	Clarkston	21	3600-4000	Clarkston
West Cache	Wellsville	20	4400-4800	Brigham City
East Cache	Central	17	4300-4600	Brigham City

(Hansel Valley: Doser, 1989; EGSL: Dinter and Pechmann, 2011; Oquirrh: Olig et al., 2011; West Cache, East Cache: Lund, 2005)

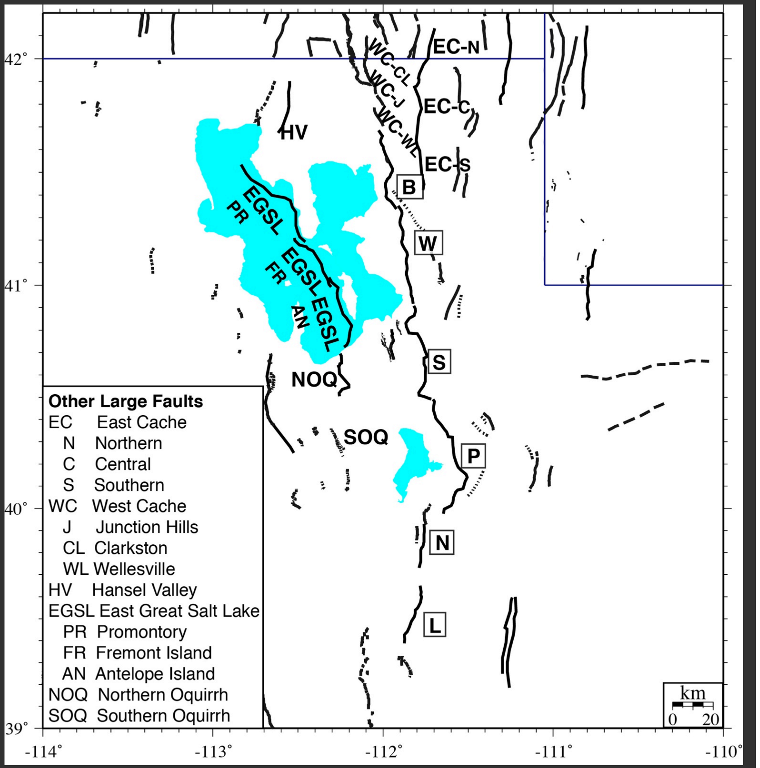

Intermountain Seismic Belt

Strain Rate Magnitudes from Expanded PBO Processing

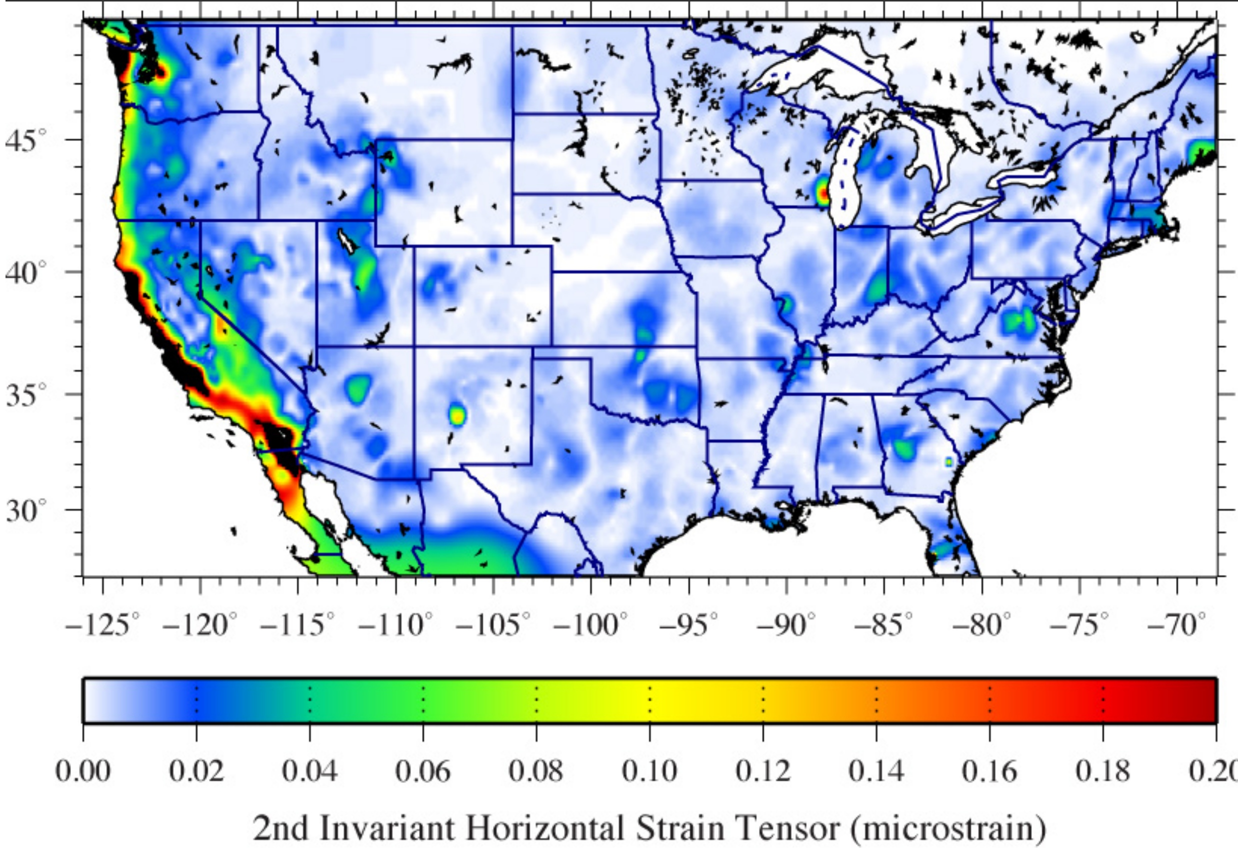

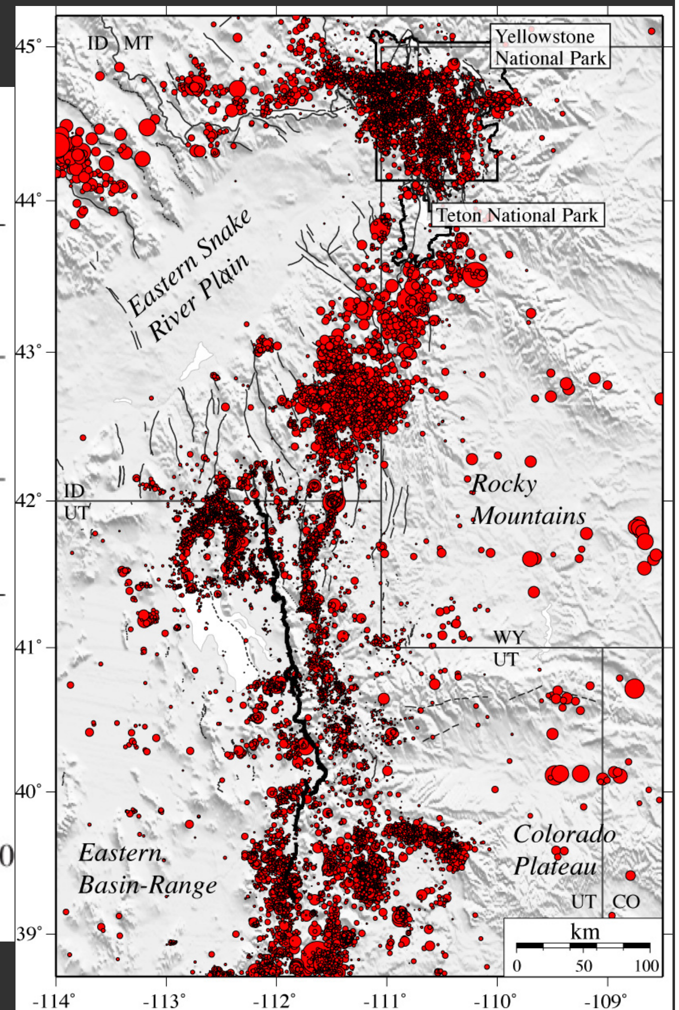

- Locally high strain rates
  - Eastern Boundary of Basin-Range
  - Deformation correlates with Intermountain Seismic Belt

GPS Station Velocities

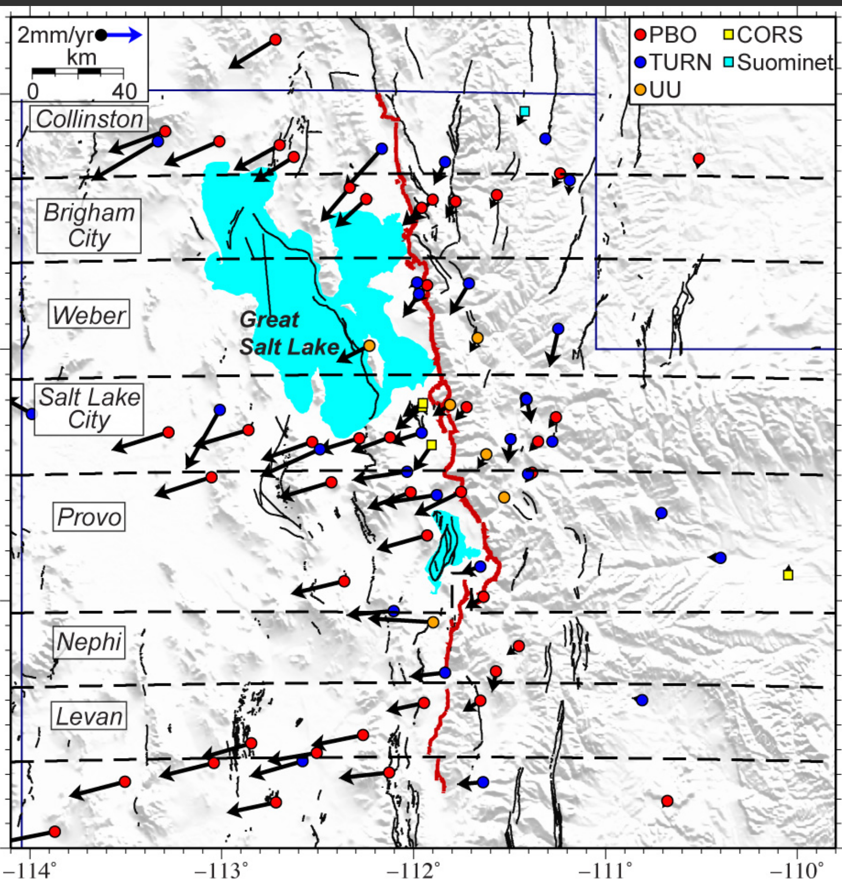

Velocities across E-W Profiles

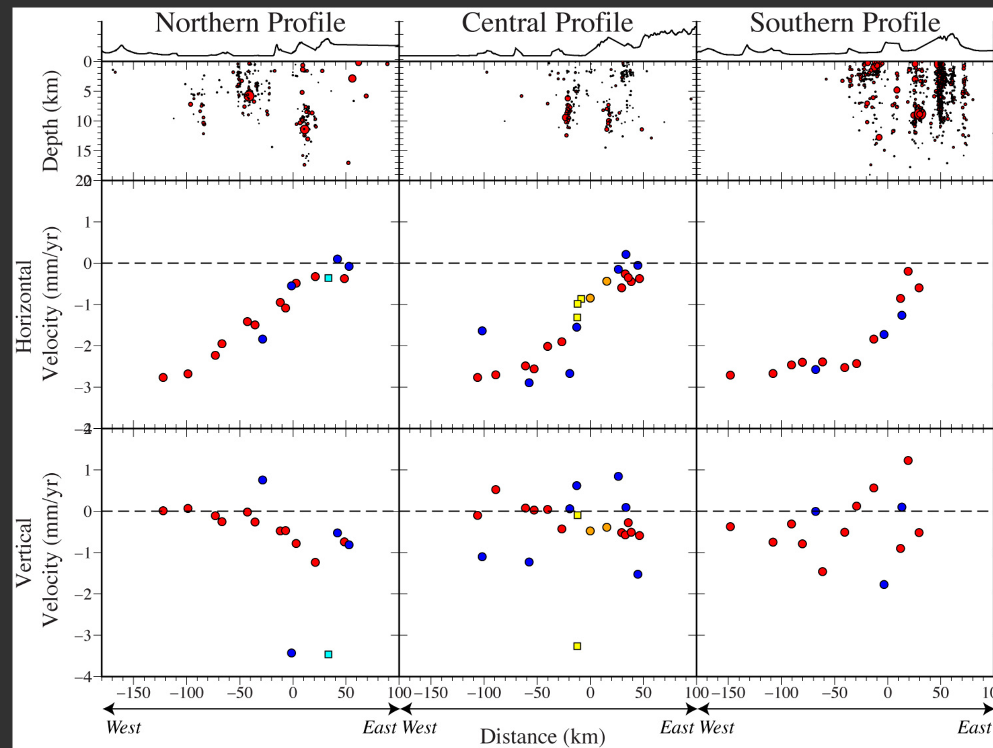

- GPS stations record ~3 mm/yr westward motion across fault zone

- GPS stations from multiple networks record deformation
  - Largest network: Plate Boundary Observatory (PBO)
  - Backbone network established by University of Utah (UU)
  - Extra stations from private Utah Reference Network (TURN)
    TURN data only available through University of Nevada - Reno

Quality Analysis:

1. Visual inspection of time series
2. Examine QA parameters produced by UNR
3. Check velocity maps for outliers
4. Check signal-to-noise ratio, multipaths

- Identify nonlinear velocities
- Stations operating < 2 years

Position Time Series

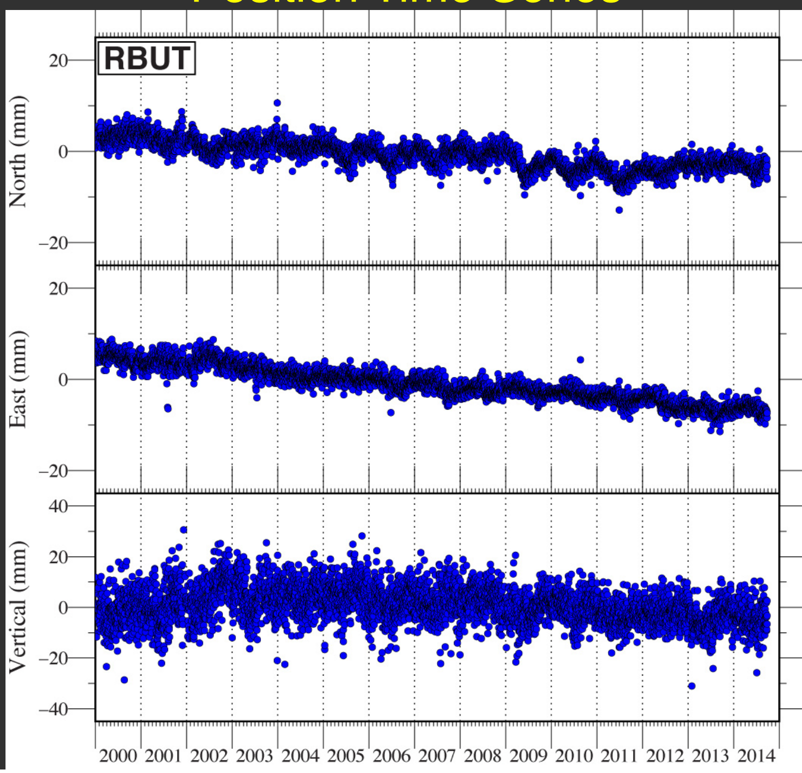

UNR QA Parameters

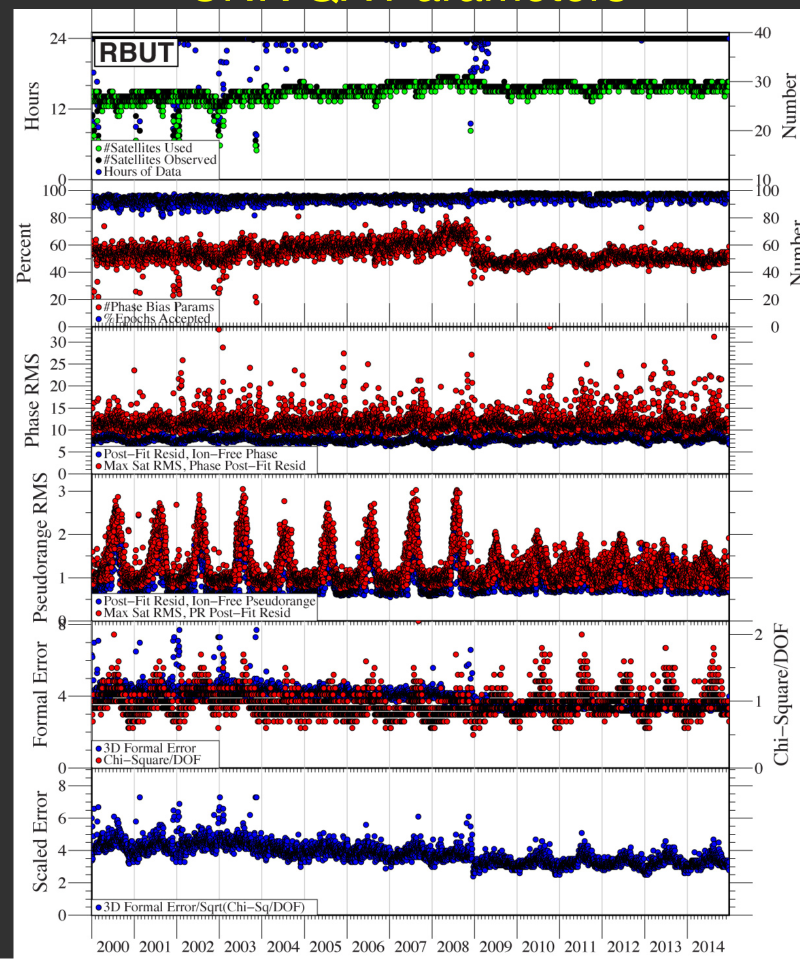

Quality Analysis continued:

- Don't use nonlinear/short/discontinuous time series
- Edit time series if bad quality can be attributed to bad equipment
  - Apply only to longer time series
- Compile list with usable horizontal components but nonlinear vertical

Multipath and SNR

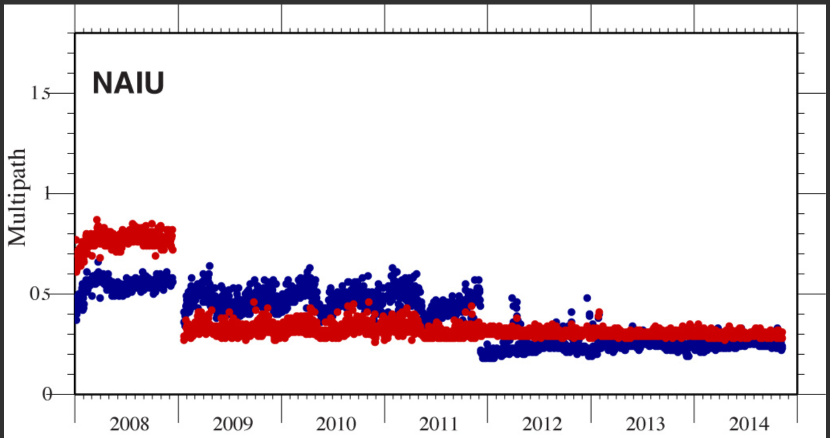

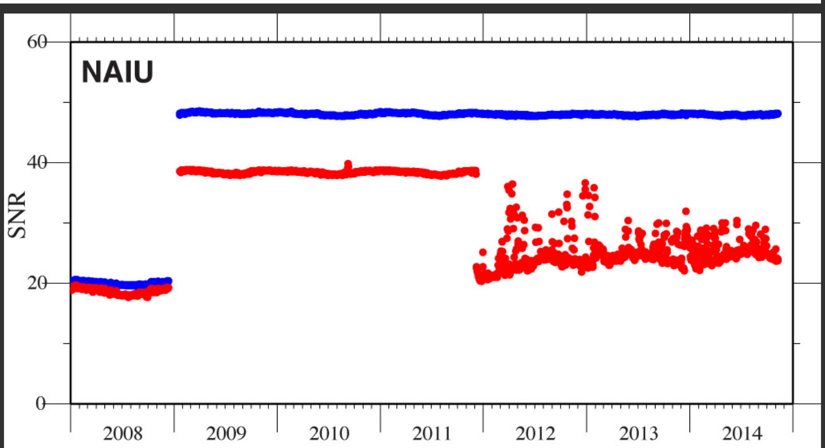

Position Time Series

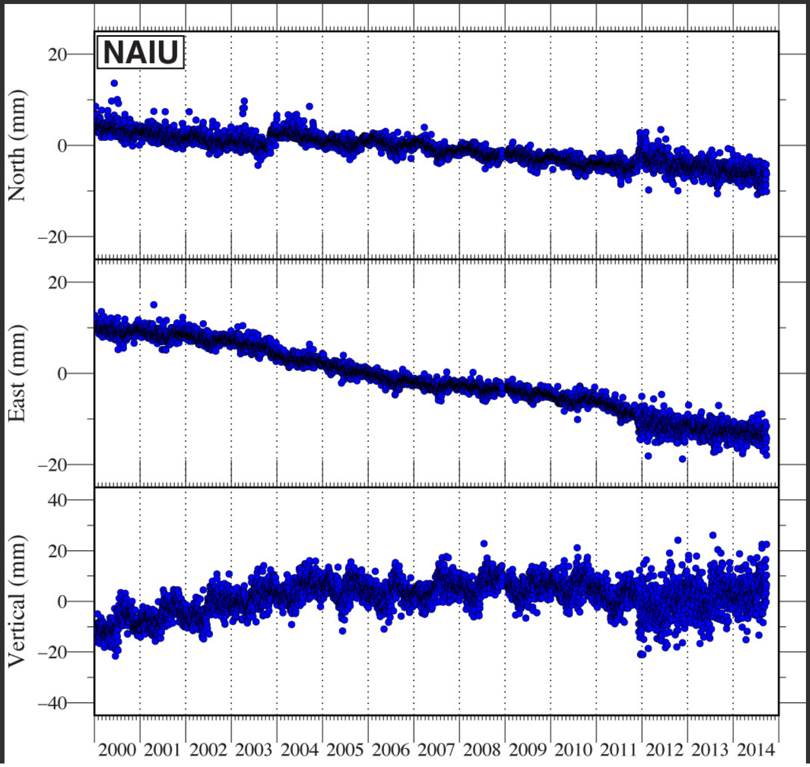

Example: LTUT

- Bad antenna prior to 2007
- Large seasonal variations
- Use only post-2007 data to determine station velocity

UNR QA Parameters

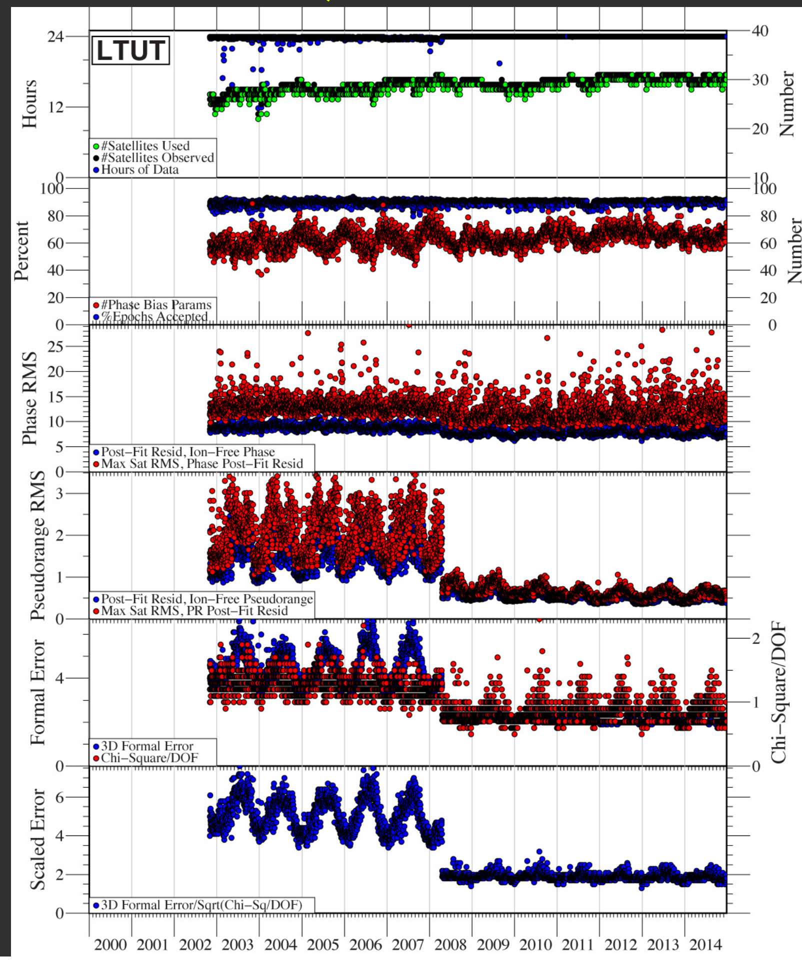

Position Time Series

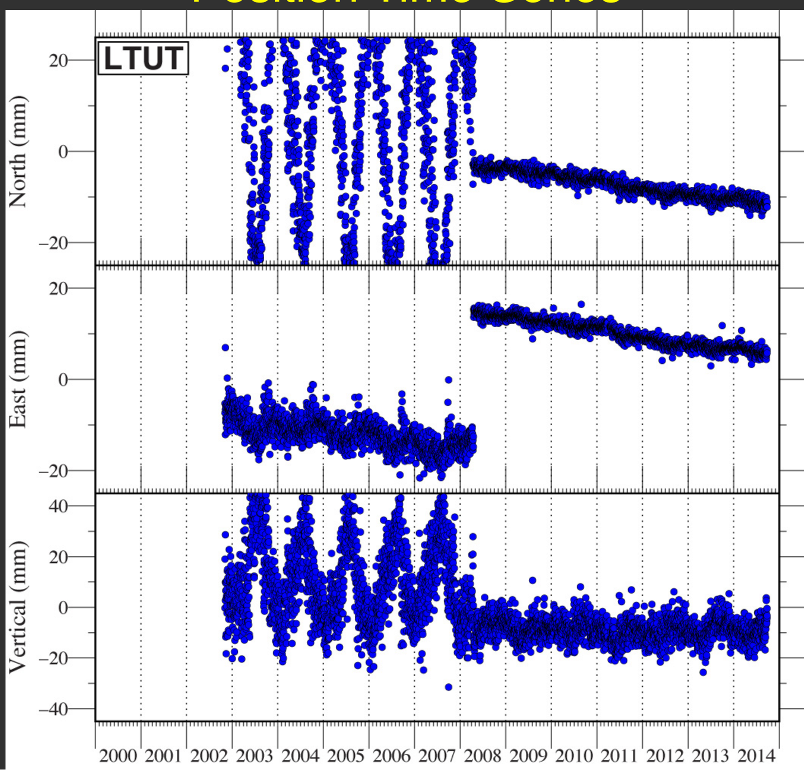

Hydrologic Loading

- Water stored in snow, soil, vegetation
  - Mass derived from land surface models
  - Calculate surface displacements

- Seasonal signal
  - Seasonal amplitudes vary depending on annual precipitation

Seasonal Surface Loading

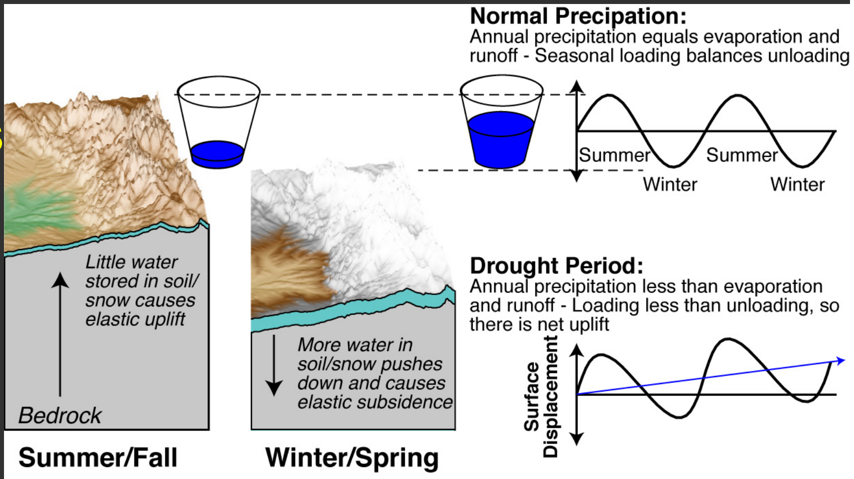

Position Time Series

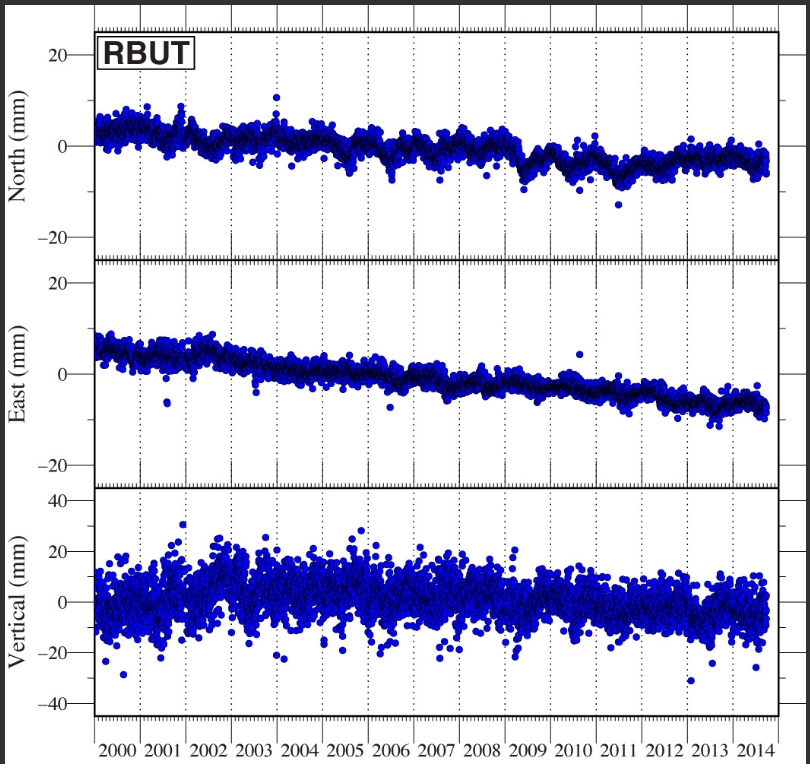

Hydrologic Loading Model

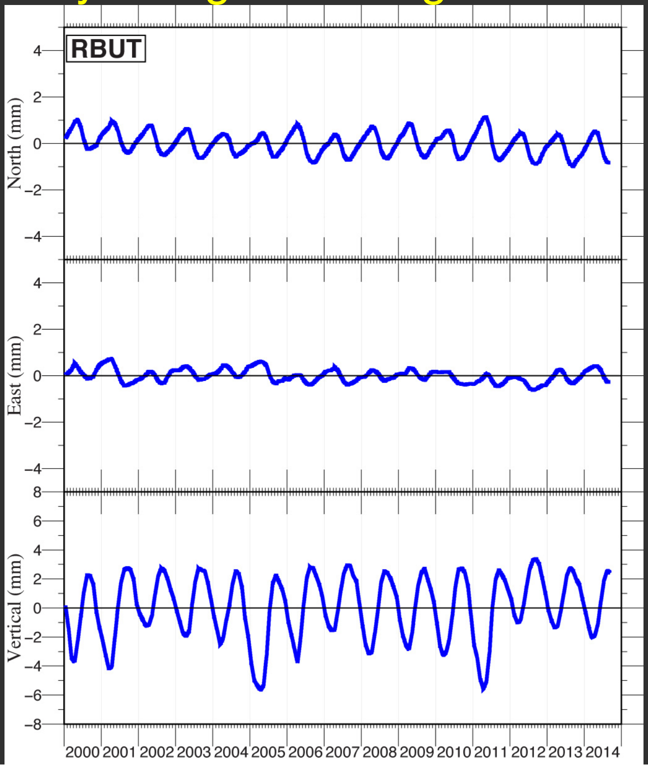

Great Salt Lake Loading

- Water volume obtained from Loving et al. (2000)
  - Lake surface levels vary ~10 ft for 2000-2014
  - Most volume in western basins
  - Water density different for north & south lake halves

Lake Levels 2000-2014

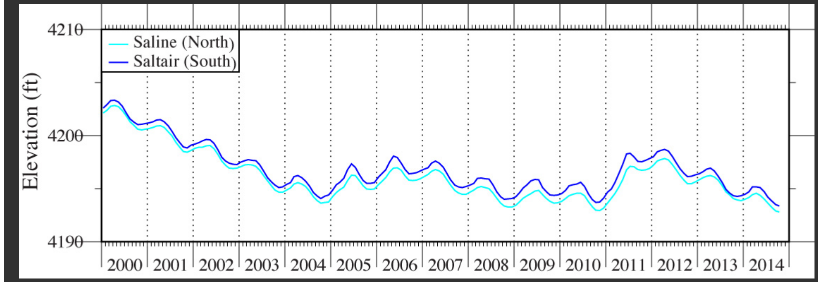

- Modeled displacements up to 3 mm
  - Compare with 10-20 mm variations in GPS time series

Lake Loading Model

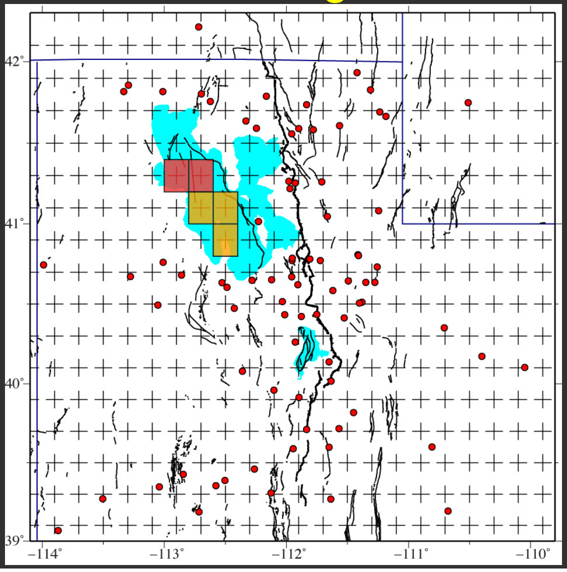

Position Time Series

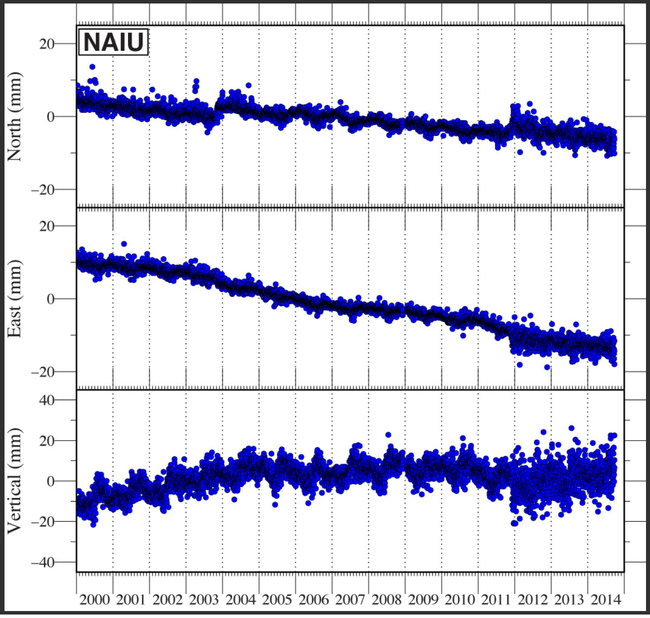

Lake Loading Displacements

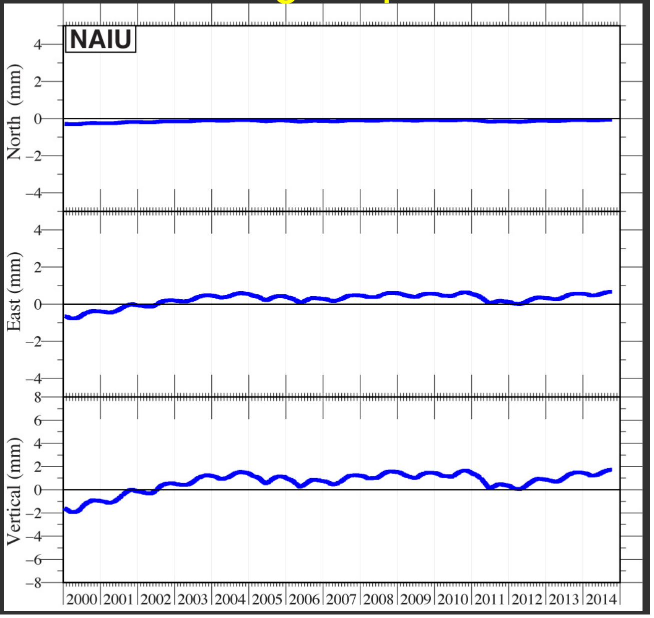

Original Time Series

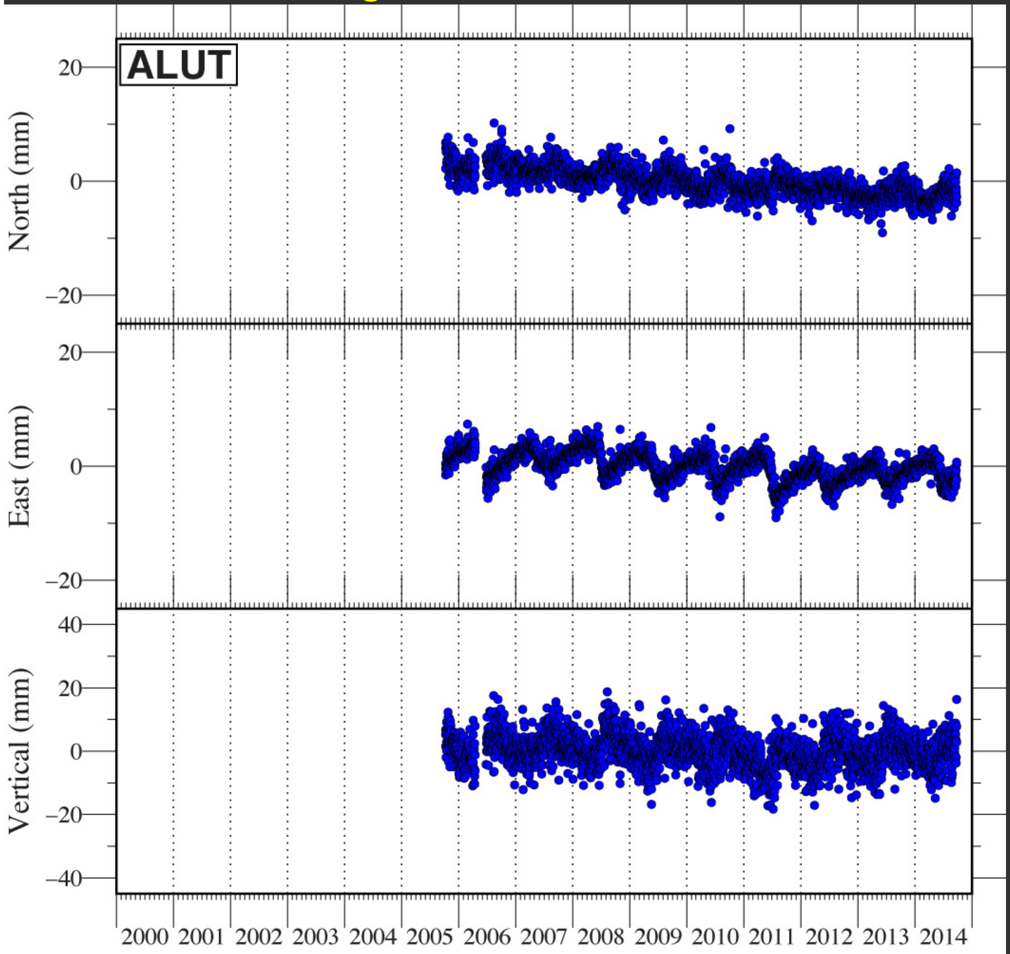

Residuals – Velocity, Seasonal Removed

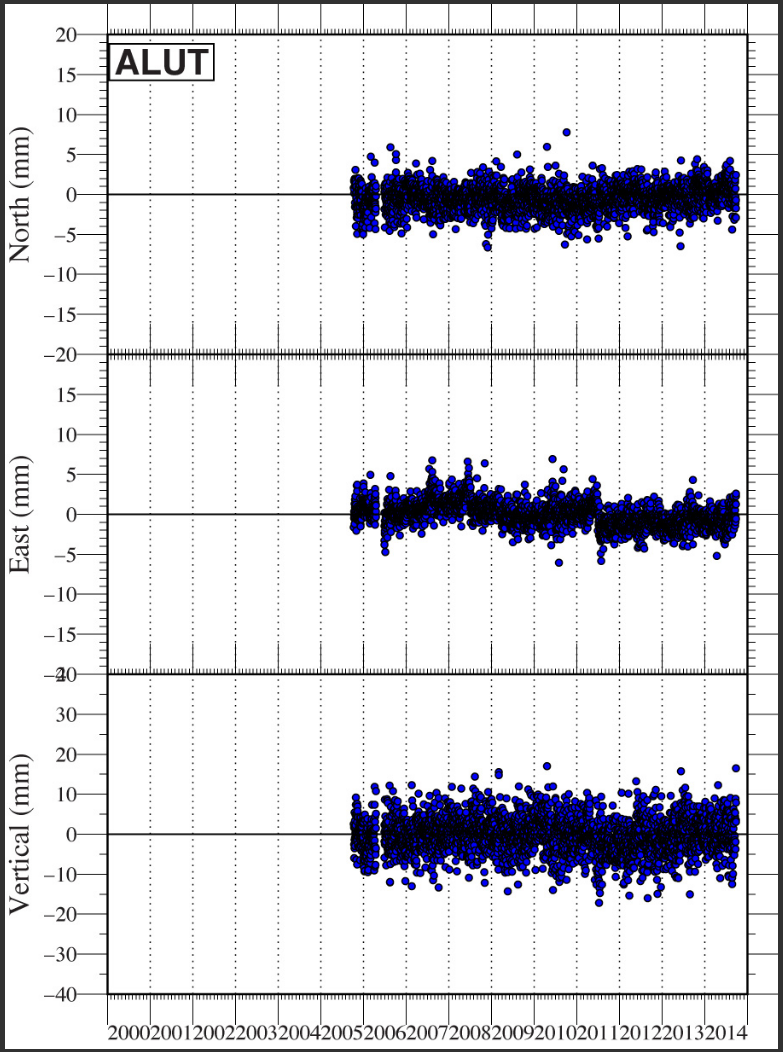

- Velocity calculated as slope of time series components
  - Filter seasonal signal
  - Fix offsets
  - Fit post-seismic decay (in case of earthquake)
  - Fitting code from Langbein (2004) and Langbein and Johnson (1997)

NAIU original velocities:
VE = -1.53 mm/yr
VN = -0.86 mm/yr
VU = 0.81 mm/yr

Accounting for GSL+hydro loading:
VE = -2.03 mm/yr
VN = -0.89 mm/yr
VU = 0.66 mm/yr

UTDE original velocities:
VE = -2.59 mm/yr
VN = -0.64 mm/yr
VU = 2.08 mm/yr

Accounting for hydro loading:
VE = -2.8 mm/yr
VN = -0.46 mm/yr
VU = 1.2 mm/yr

Original vs. Hydrologically Corrected Velocities

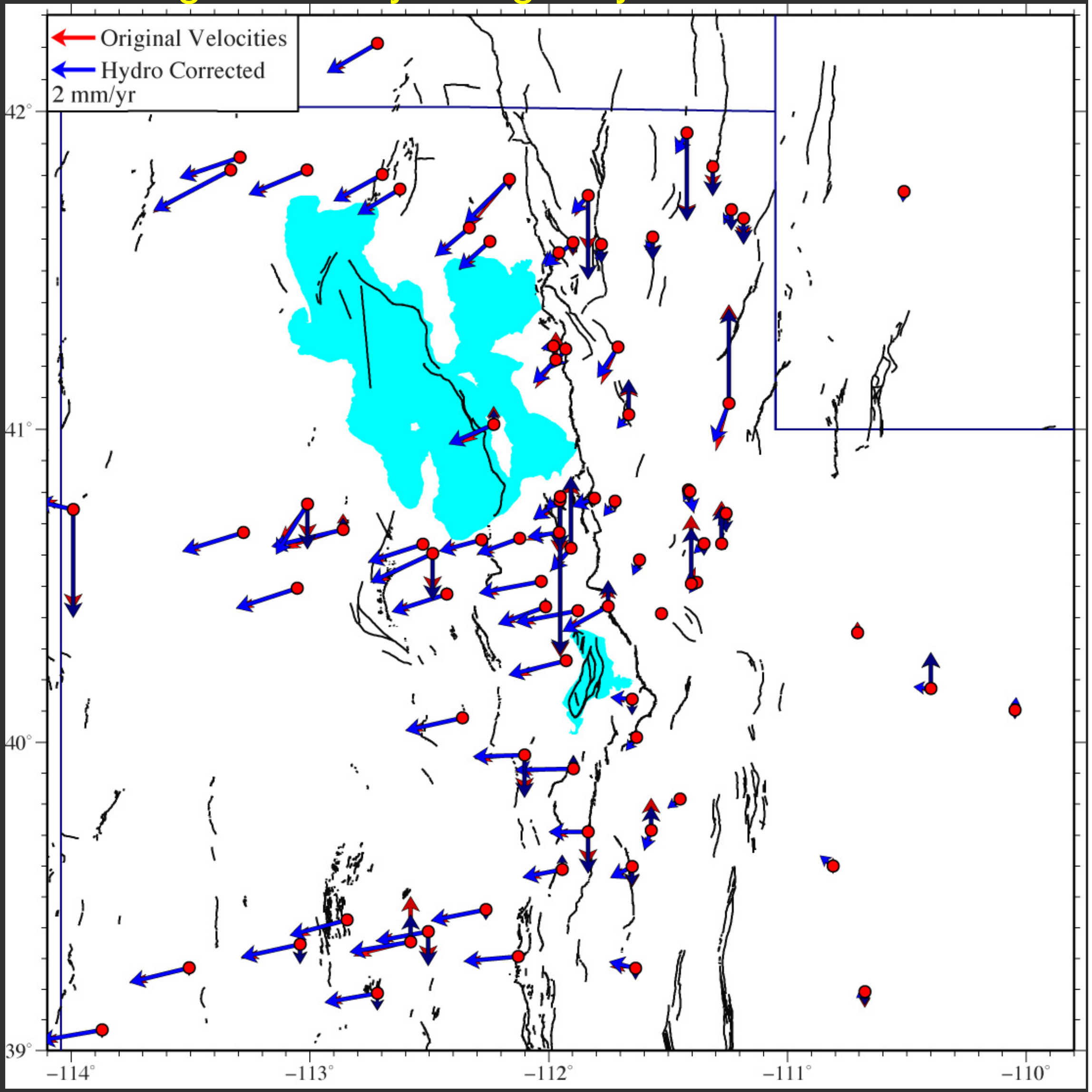

UTDE was operational from 2011-2013 – more affected by seasonal variations

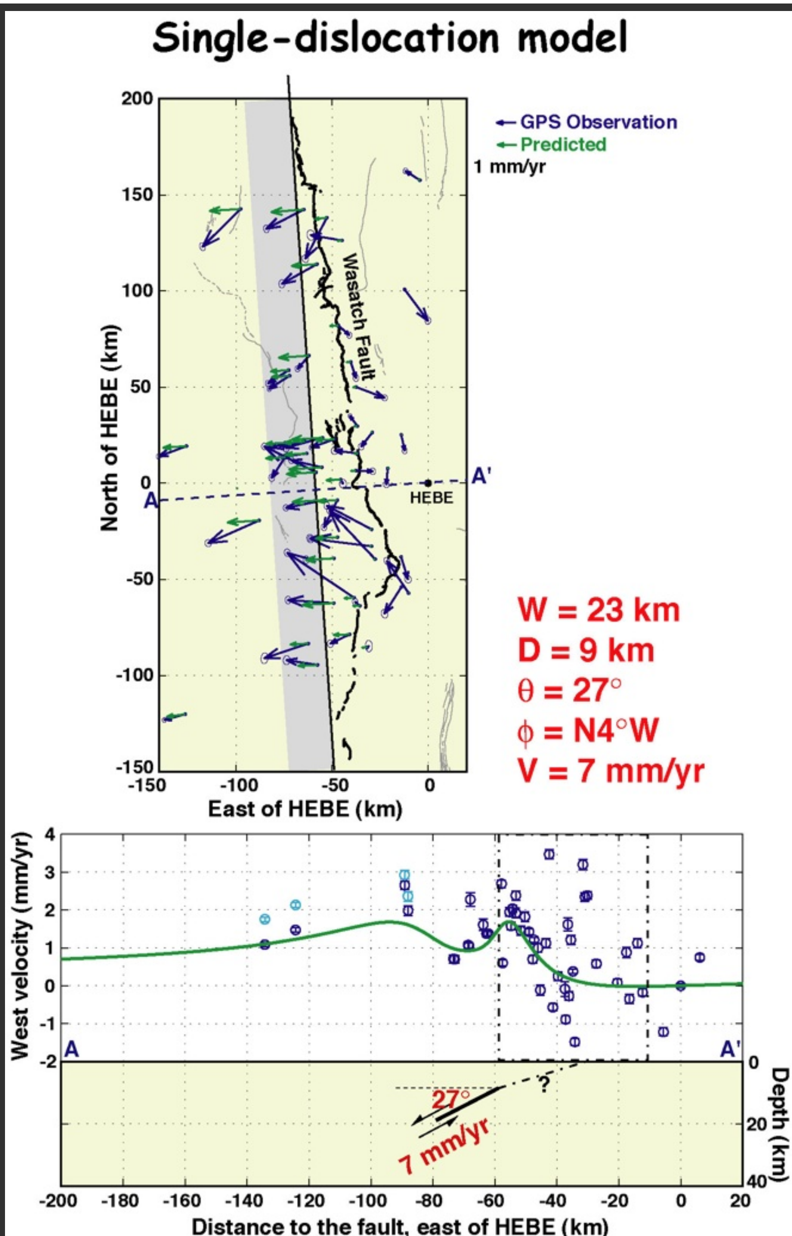

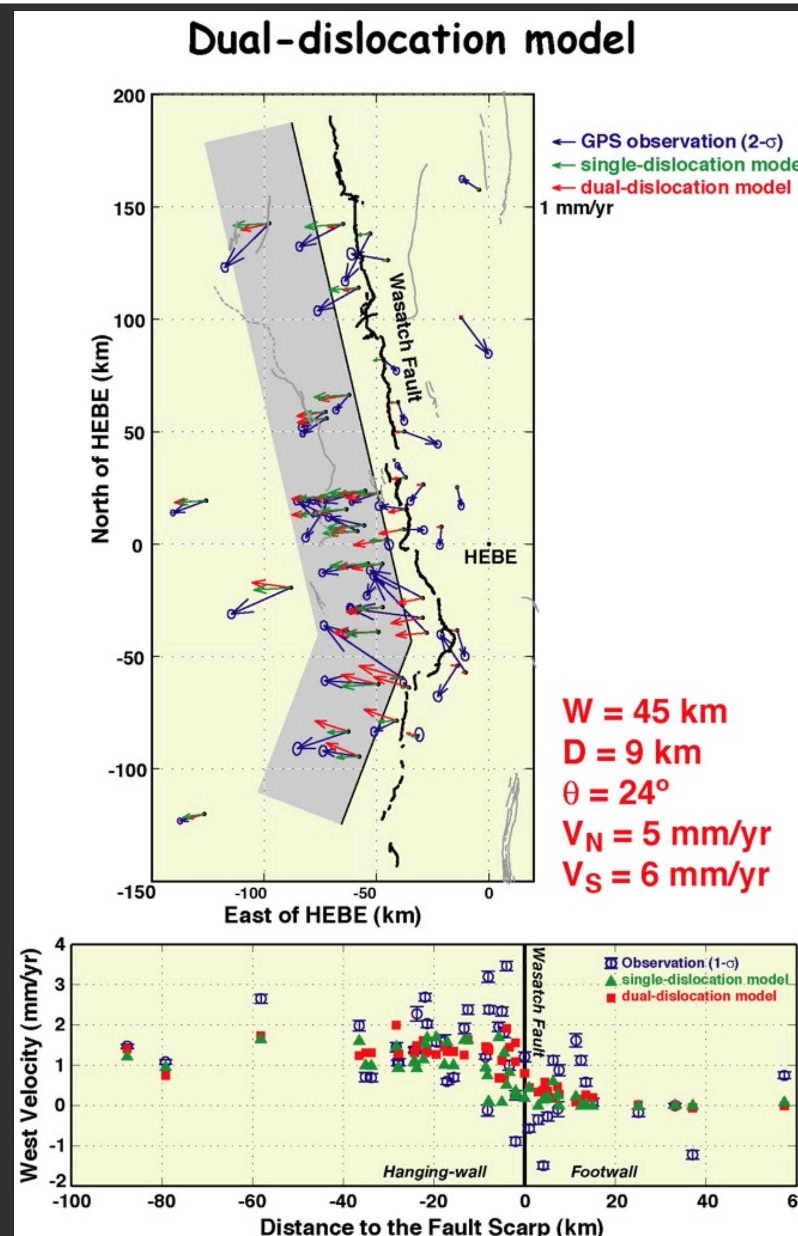

- Older dislocation models based on campaign GPS data
- Did not account for block motions

Block Motions

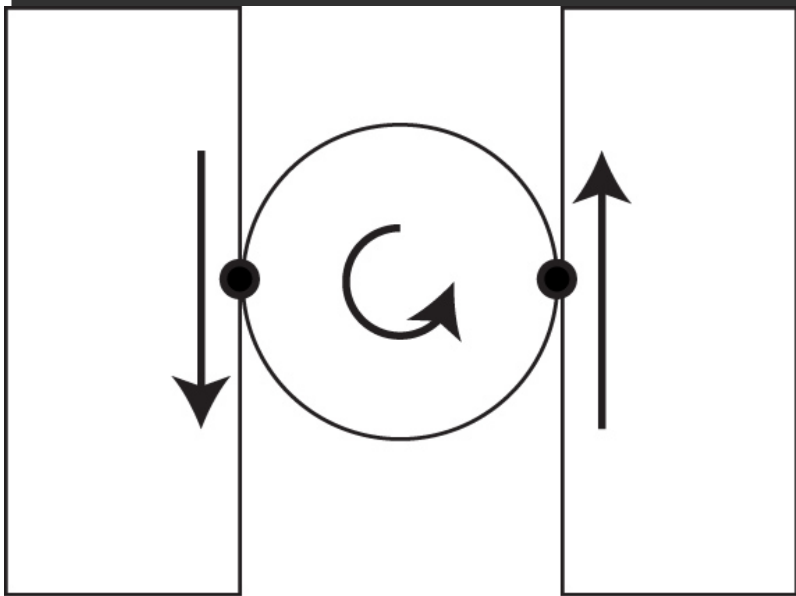

Fault Loading Schematics

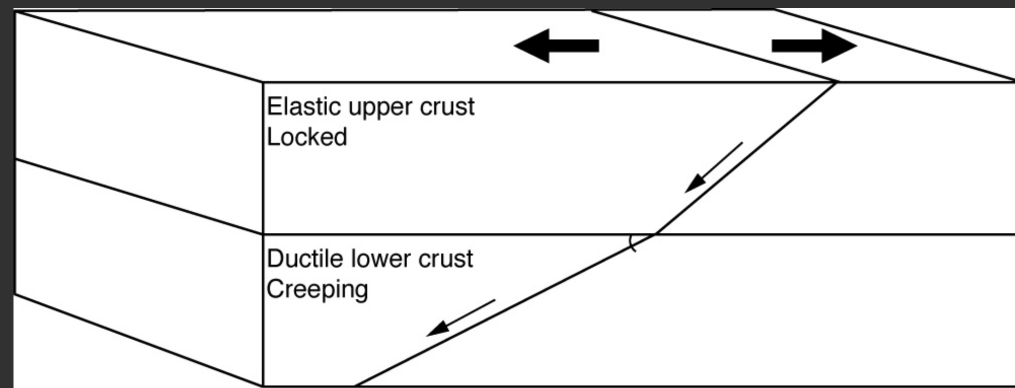

- Observed deformation = block motion + fault loading

- Locked fault will slow down deformation
  - Observed rates < block rates

- Solve for block motions directly if station in rigid interior (Savage et al., 2001)
  - Assume intermediate blocks accommodate motion between larger blocks

GPS Stations in Basin-Range and East Utah

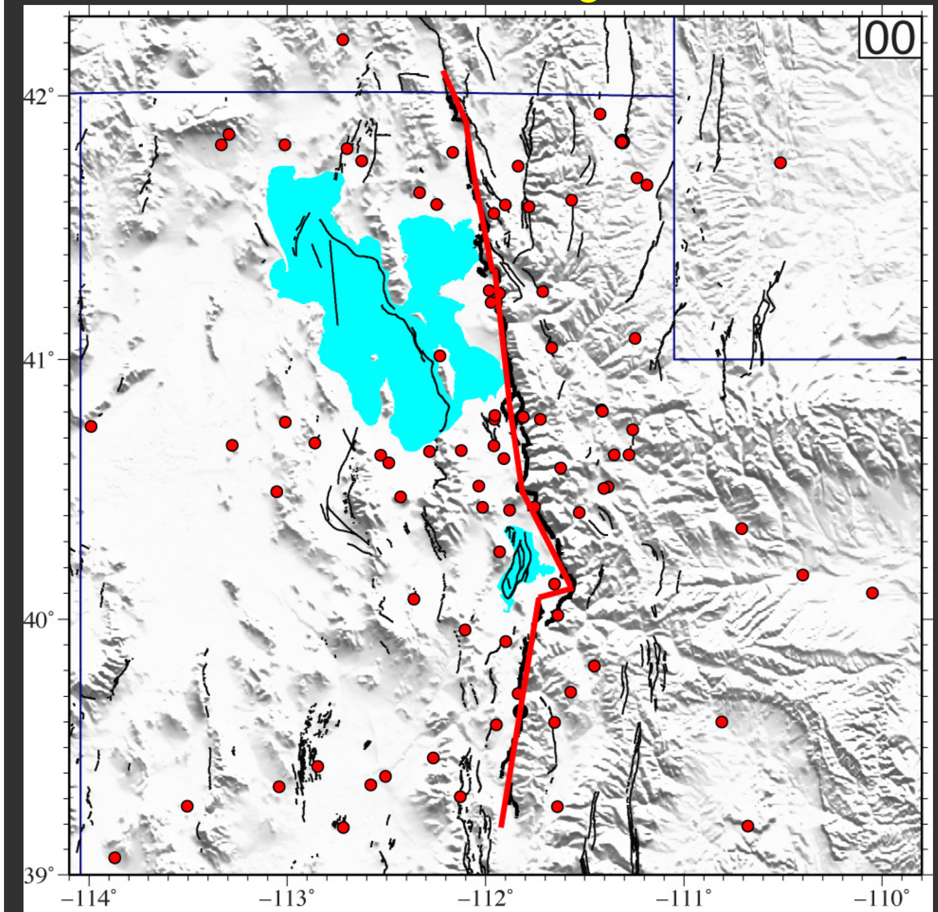

Block Interior GPS Station

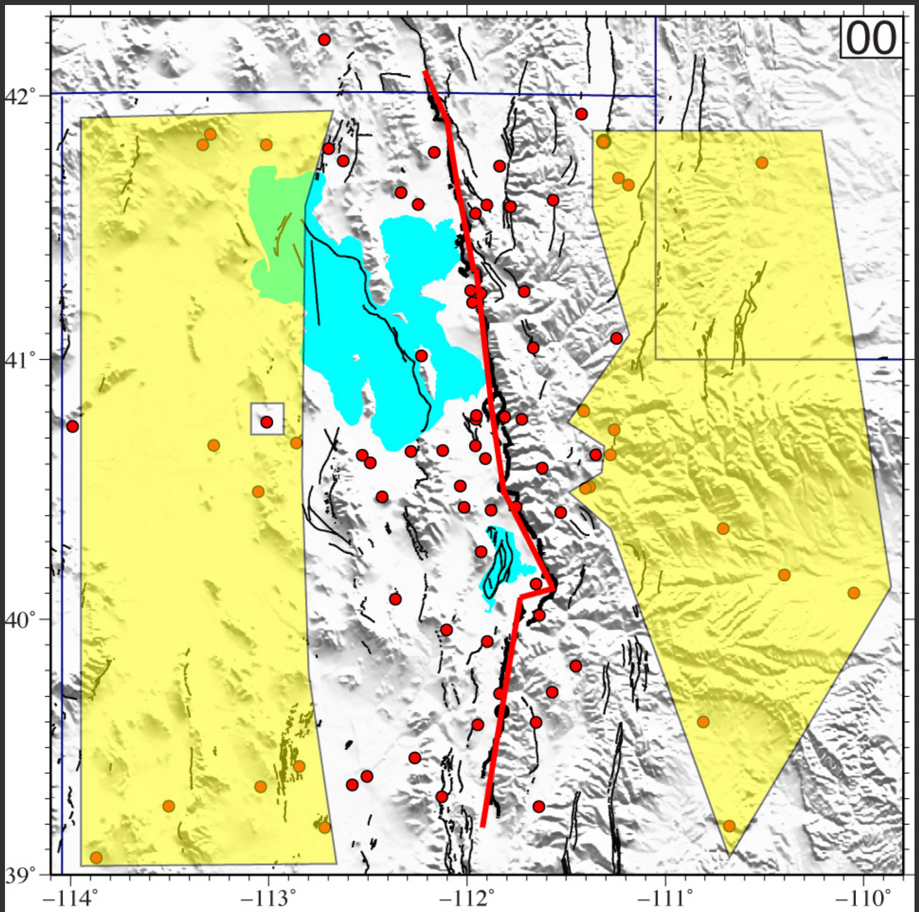

- Basin-Range and Eastern Utah are chosen as large blocks
- Solve for rotation of EUT block
  - Apply rotation to all stations in study area (get local reference frame)
- Solve for BR block rotation
  - Solve for other block motions based on boundaries between EUT & BR

Original Velocities

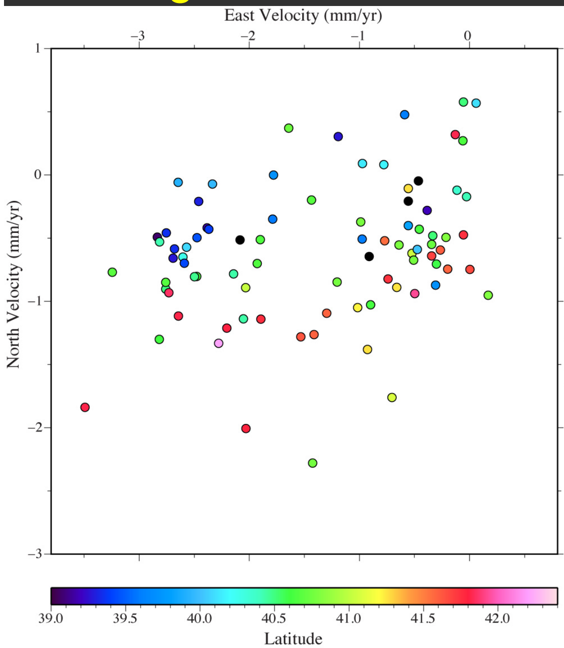

Rotated Velocities

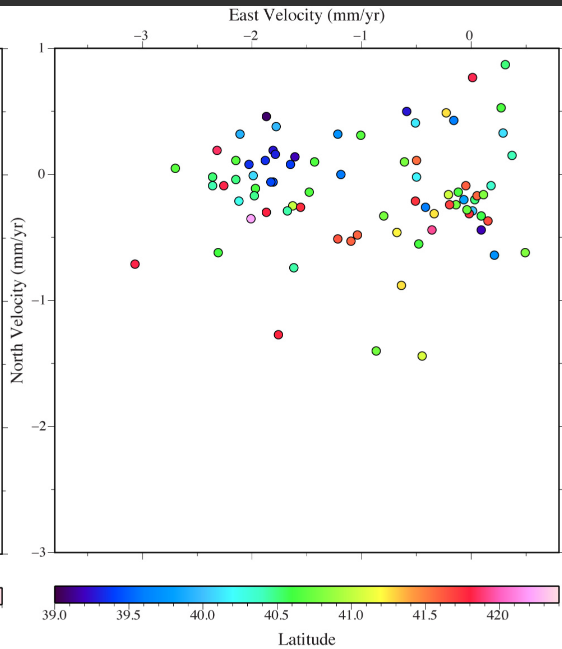

EUT-fixed Strain Rates/Velocity Map

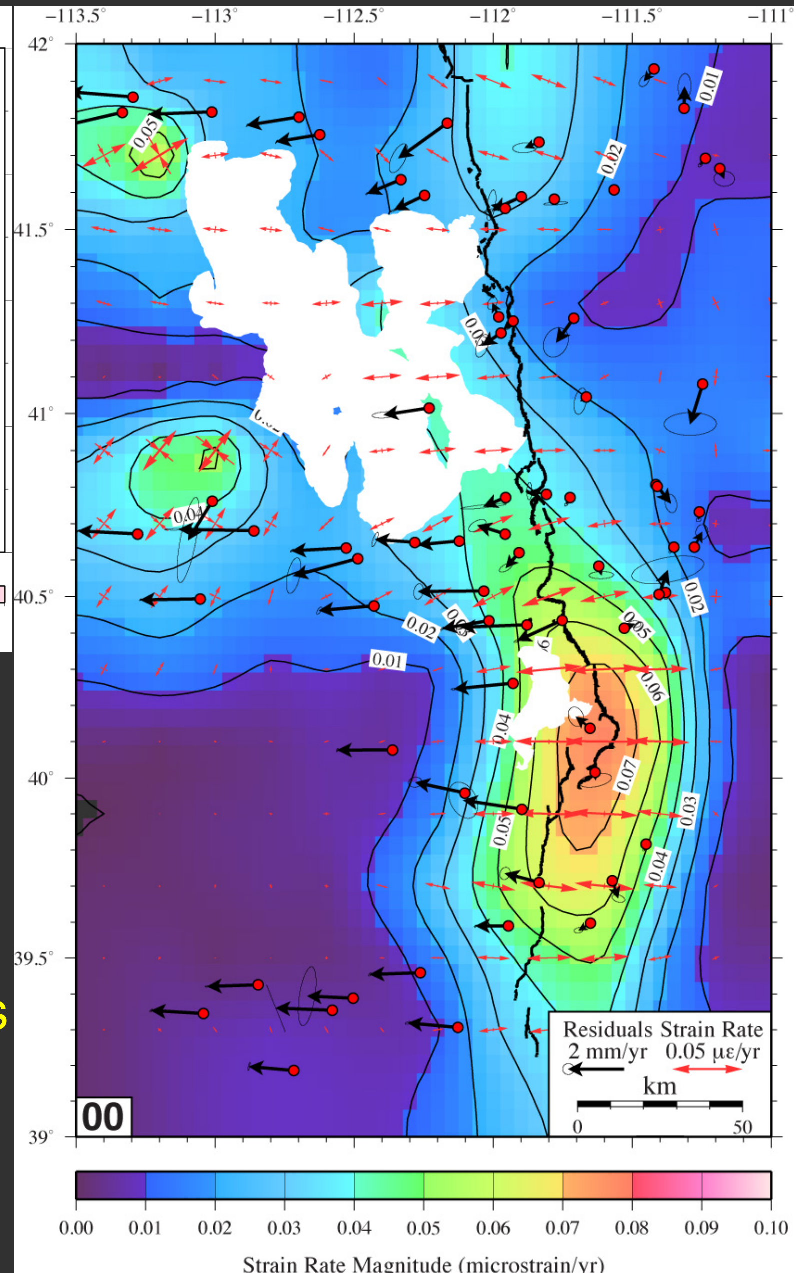

- Velocities tend to higher to the south
- Rotation reduces north component velocities
- Highest strain rates at Provo/Nephi segments

Many Possible Block Combinations

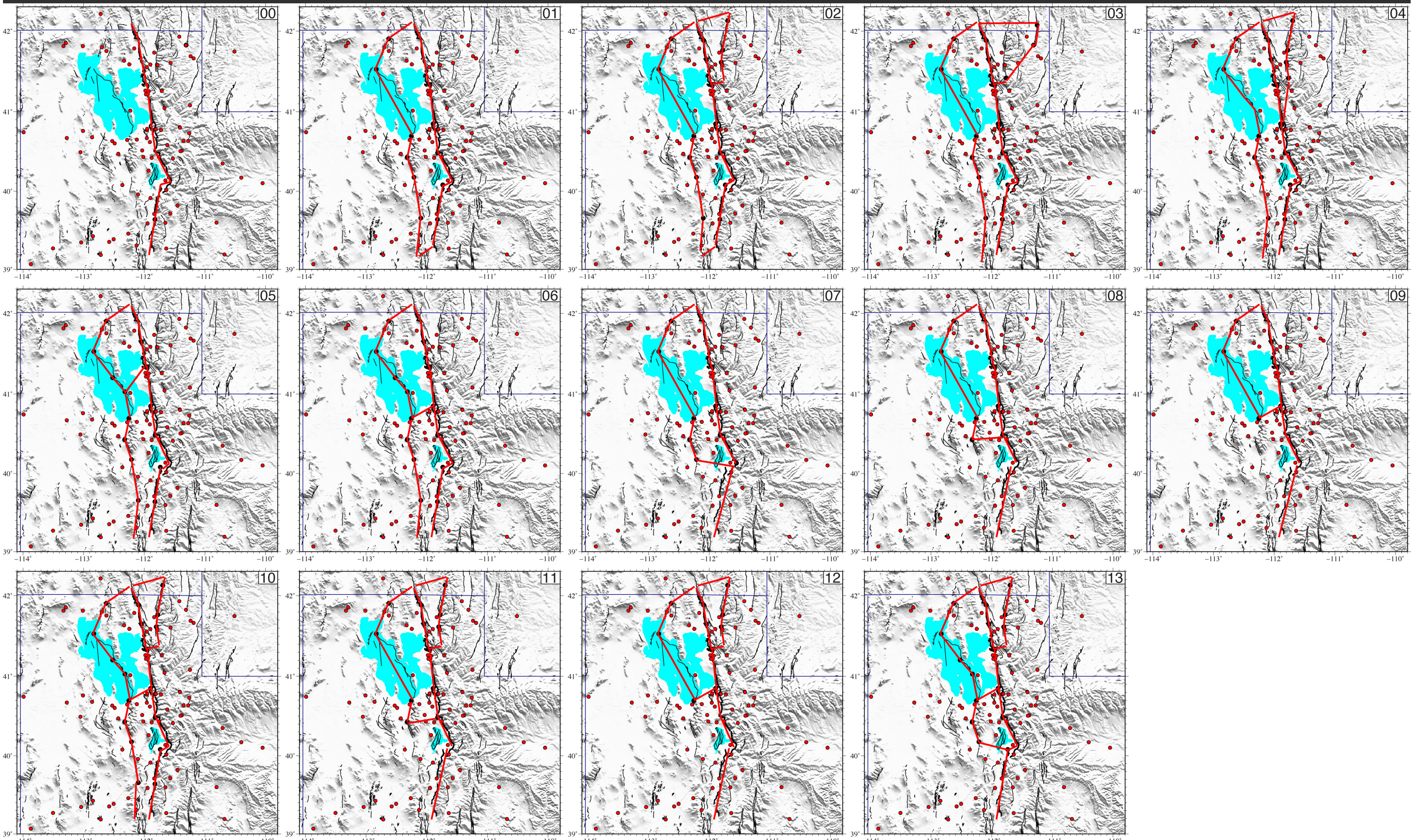

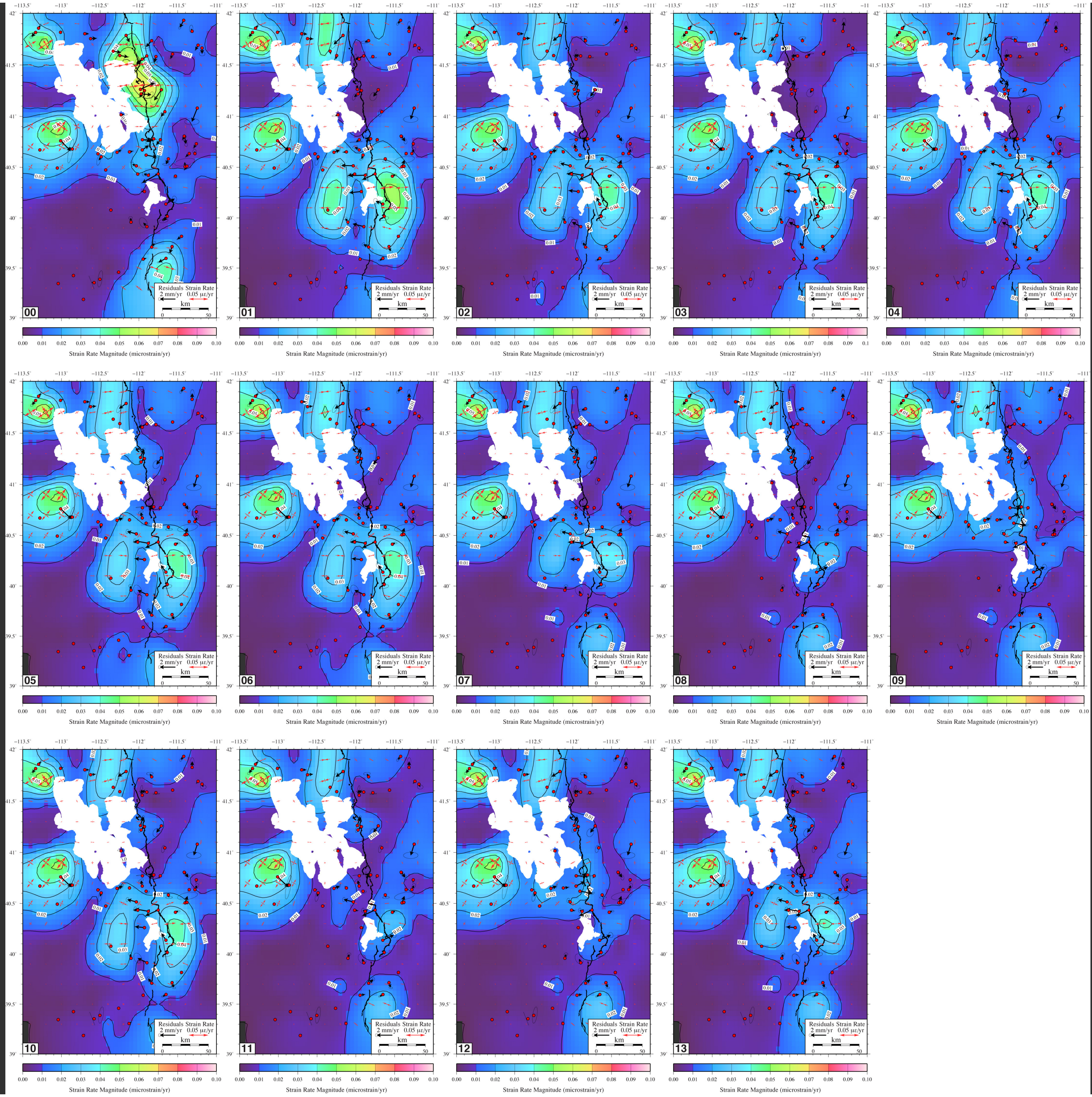
00
01
02
03
04
05
06
07
08
09
10
11
12
13
Residuals Strain Rate
2 mm/yr 0.05 με/yr
km
Strain Rate Magnitude (microstrain/yr)

Strain Rate Magnitude from Block Combinations

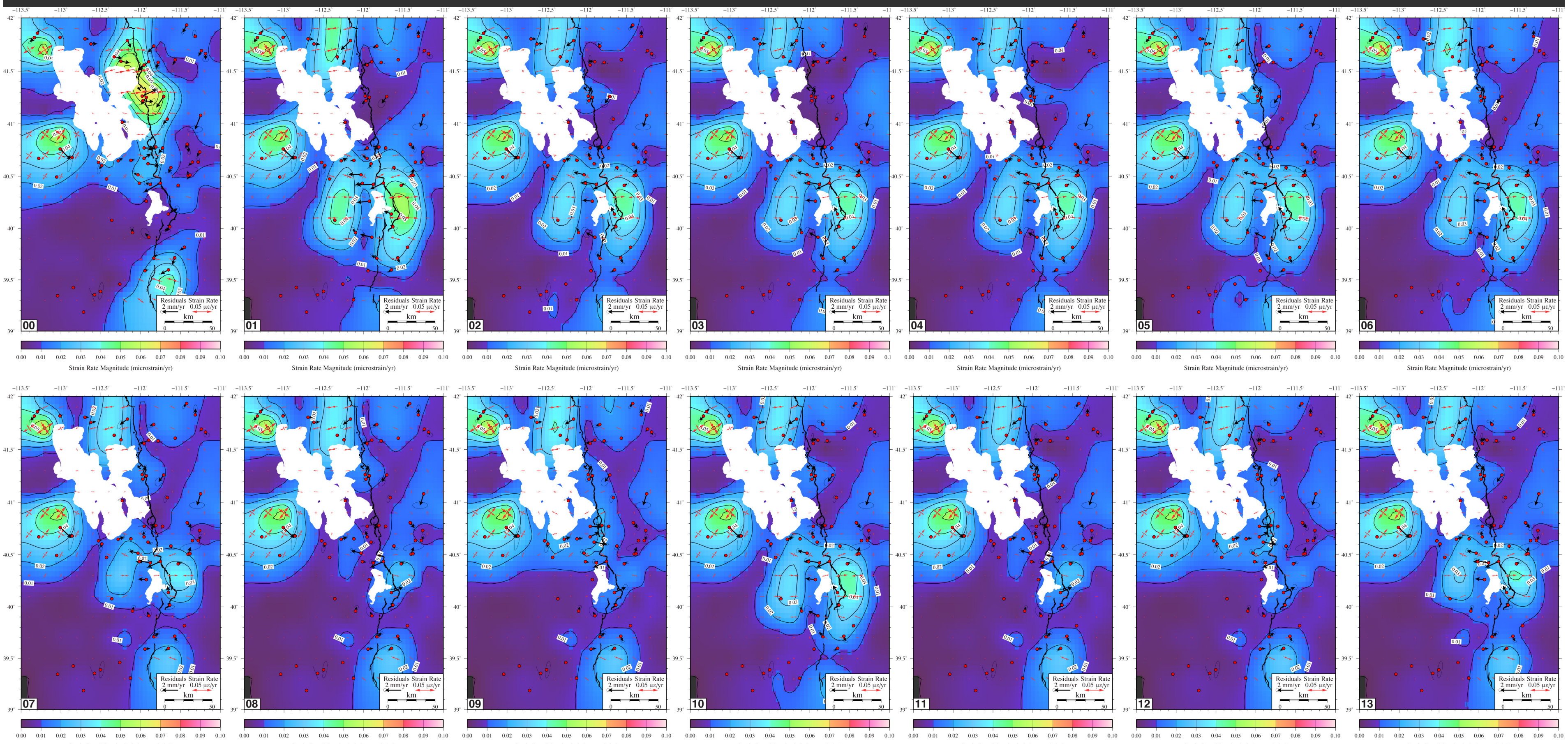

Model Criteria:

- Minimize c^2 for observed-block velocities
- Minimize strain rate magnitudes
- Produce reasonable velocity profiles

Best-Fit Model – Minimum c^2

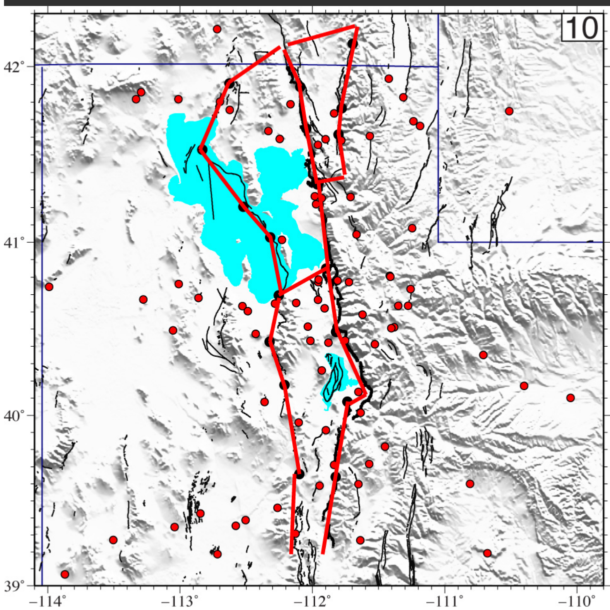

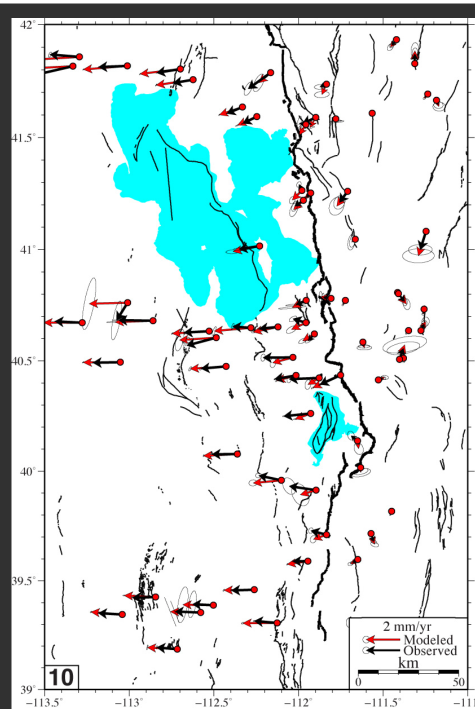

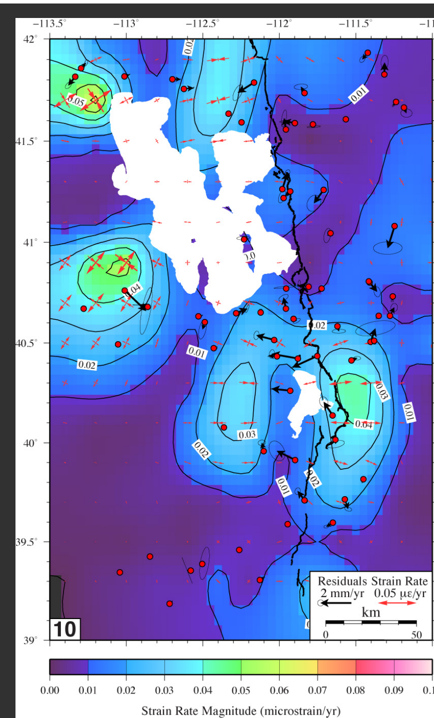

Best-Fit Model – Minimum Strain

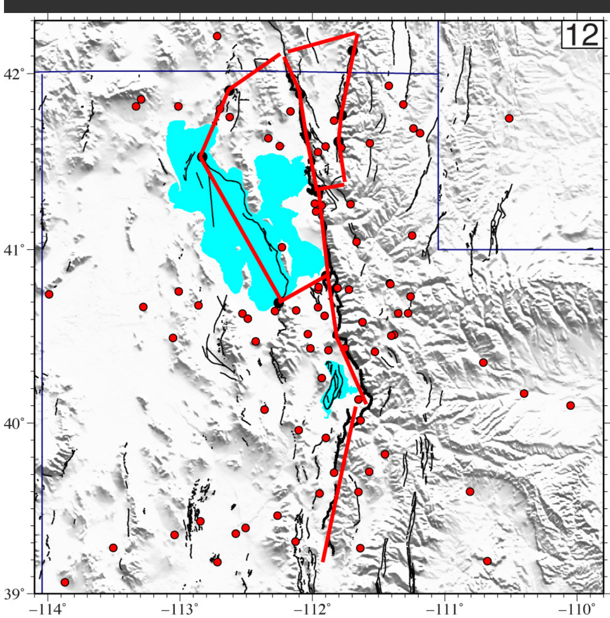

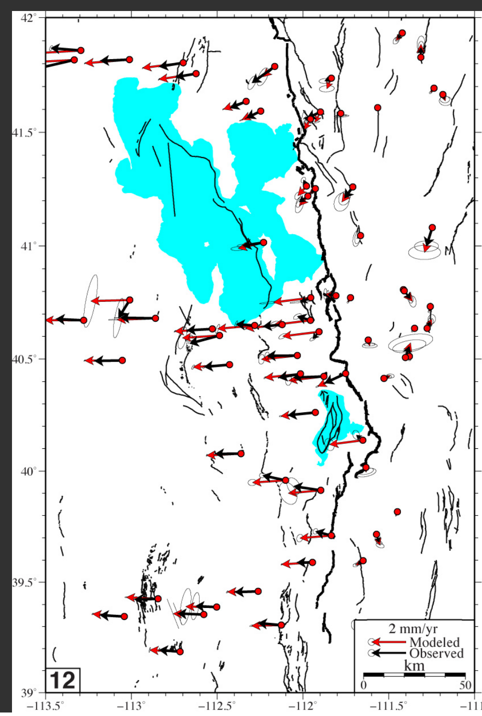

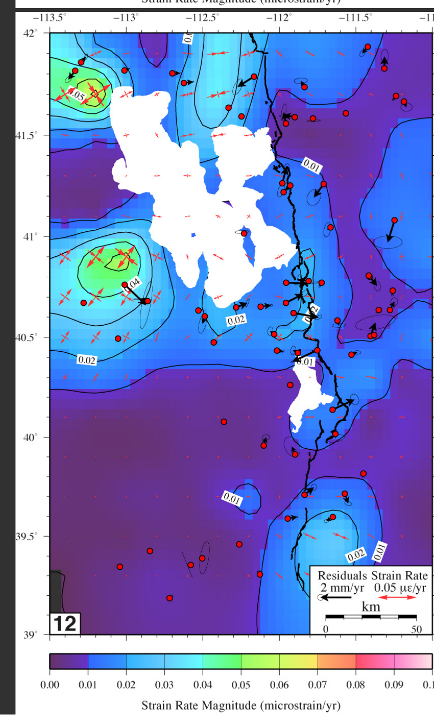

Best-Fit Model – Minimum c^2

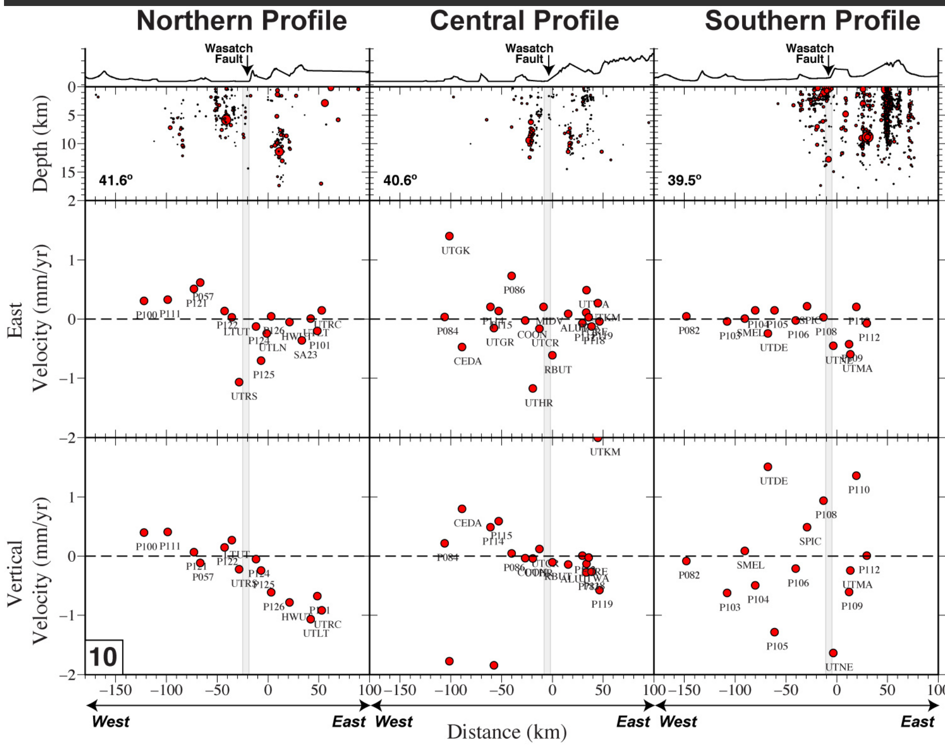

Best-Fit Model – Minimum Strain

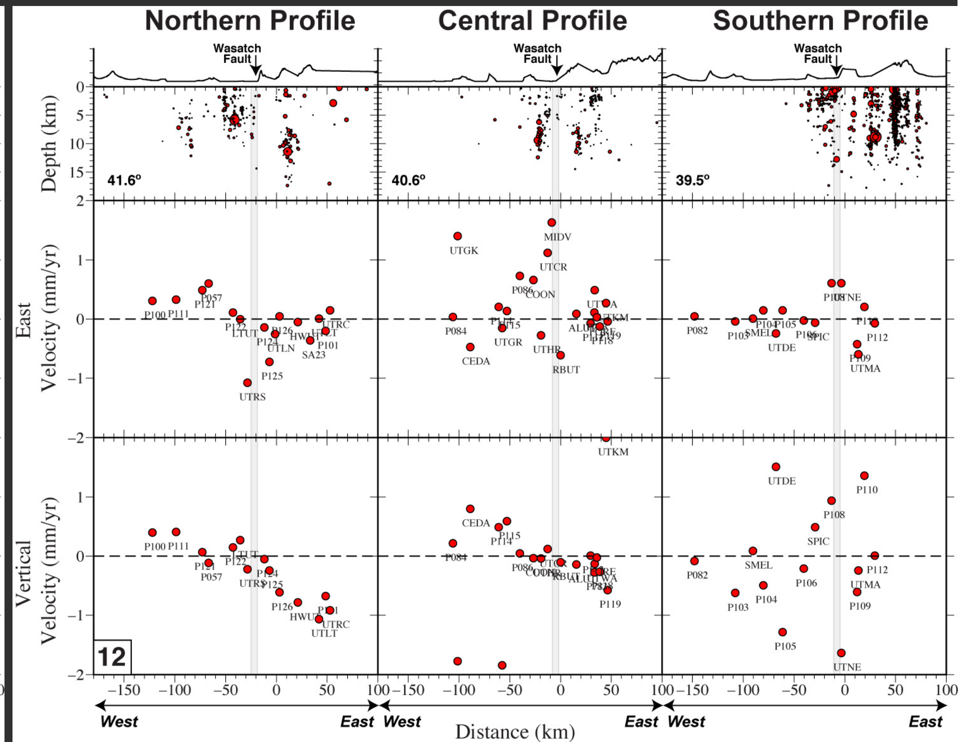

- Minimum c2 model has horizontal velocities < 1 mm/yr
- Minimum strain model has 2-mm/yr jump at central Wasatch/EUT boundary
- Horizontal profiles show observed-block velocities
- Vertical deformation not affected by block motions
  - Noisier, more outliers

Best-Fit Model – Minimum c^2

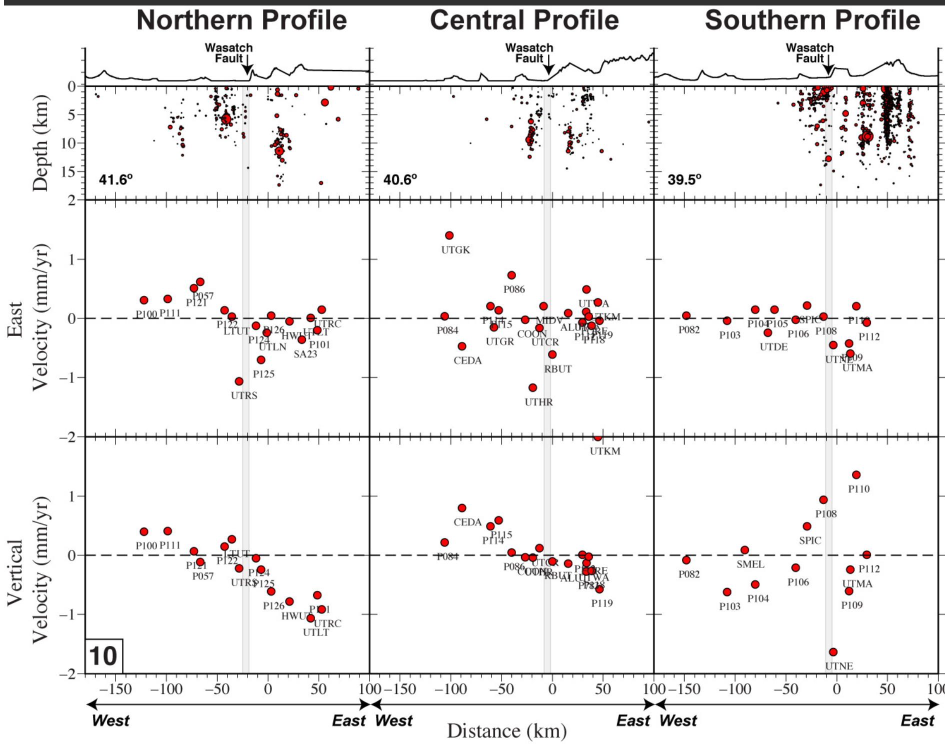

Best-Fit Model – Minimum Strain

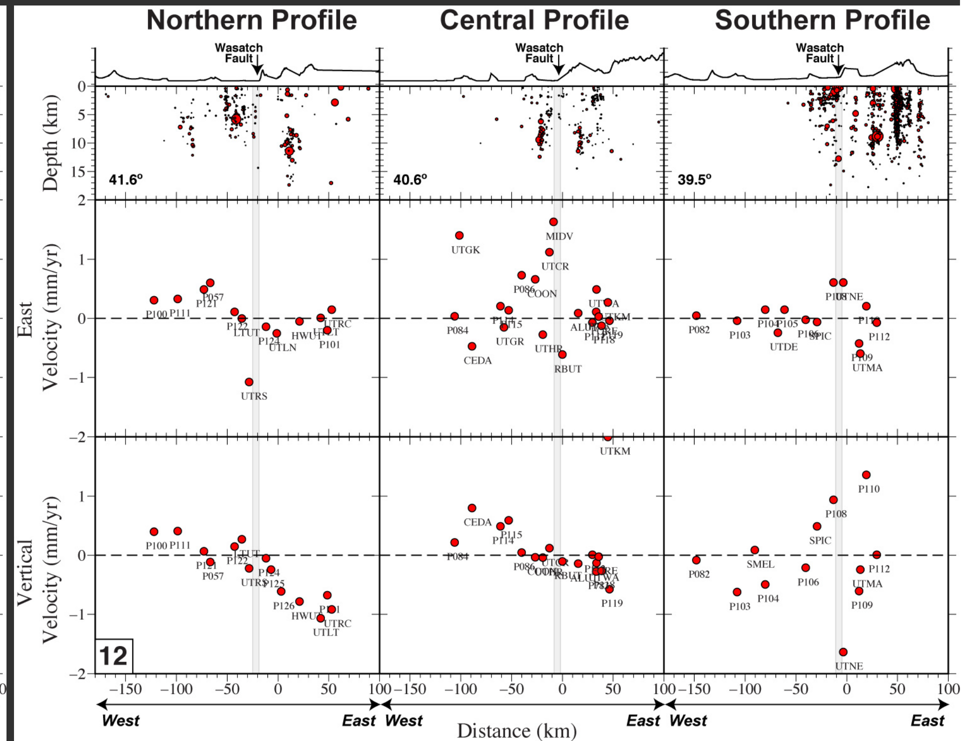

Cleaned profiles remove outliers/bad/dubious velocities

Okada Dislocation – Planar Fault

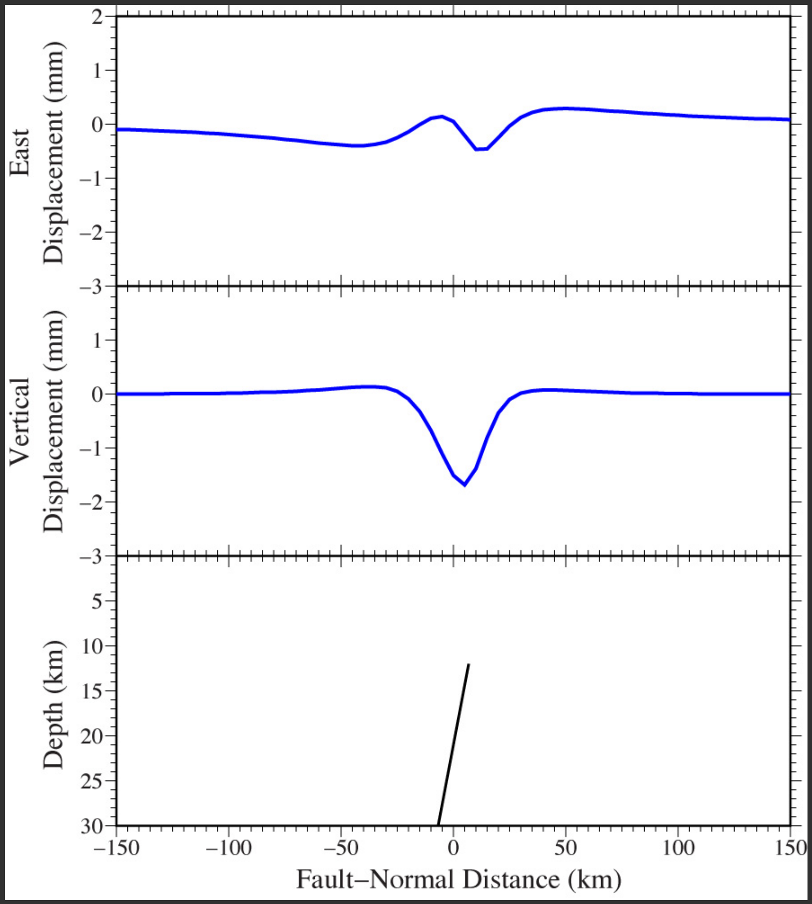

Okada Dislocation – Listric Fault

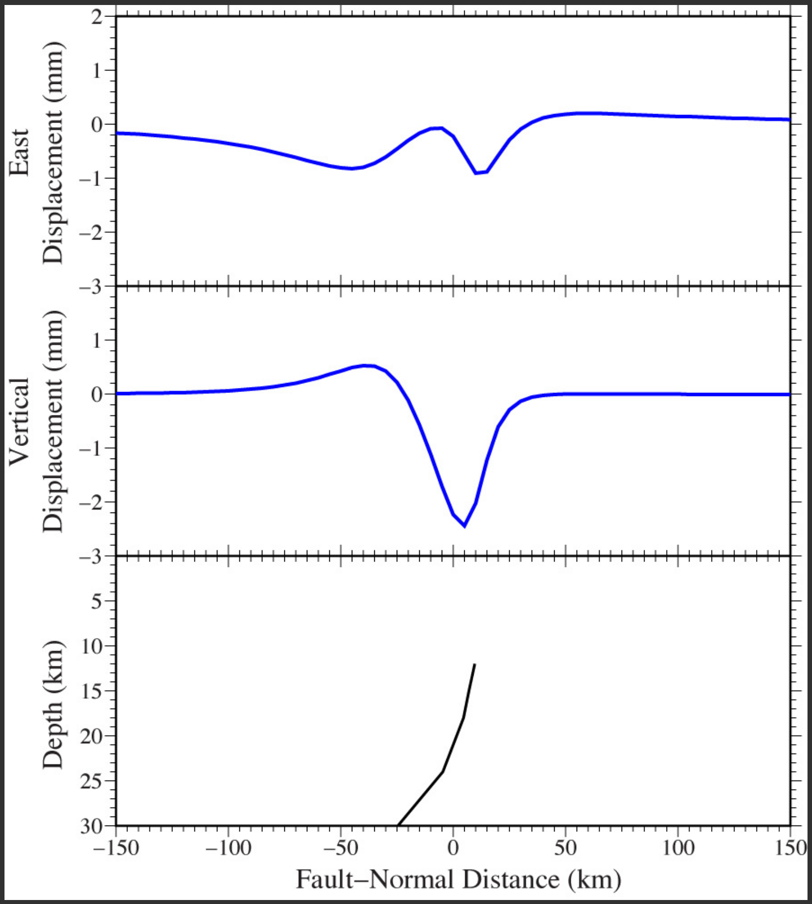

- Listric and planar faults have similar deformation patterns
- Listric faults produce larger surface offsets for given slip rate

Parallel Planar Faults, Equal Dislocations (5 mm)

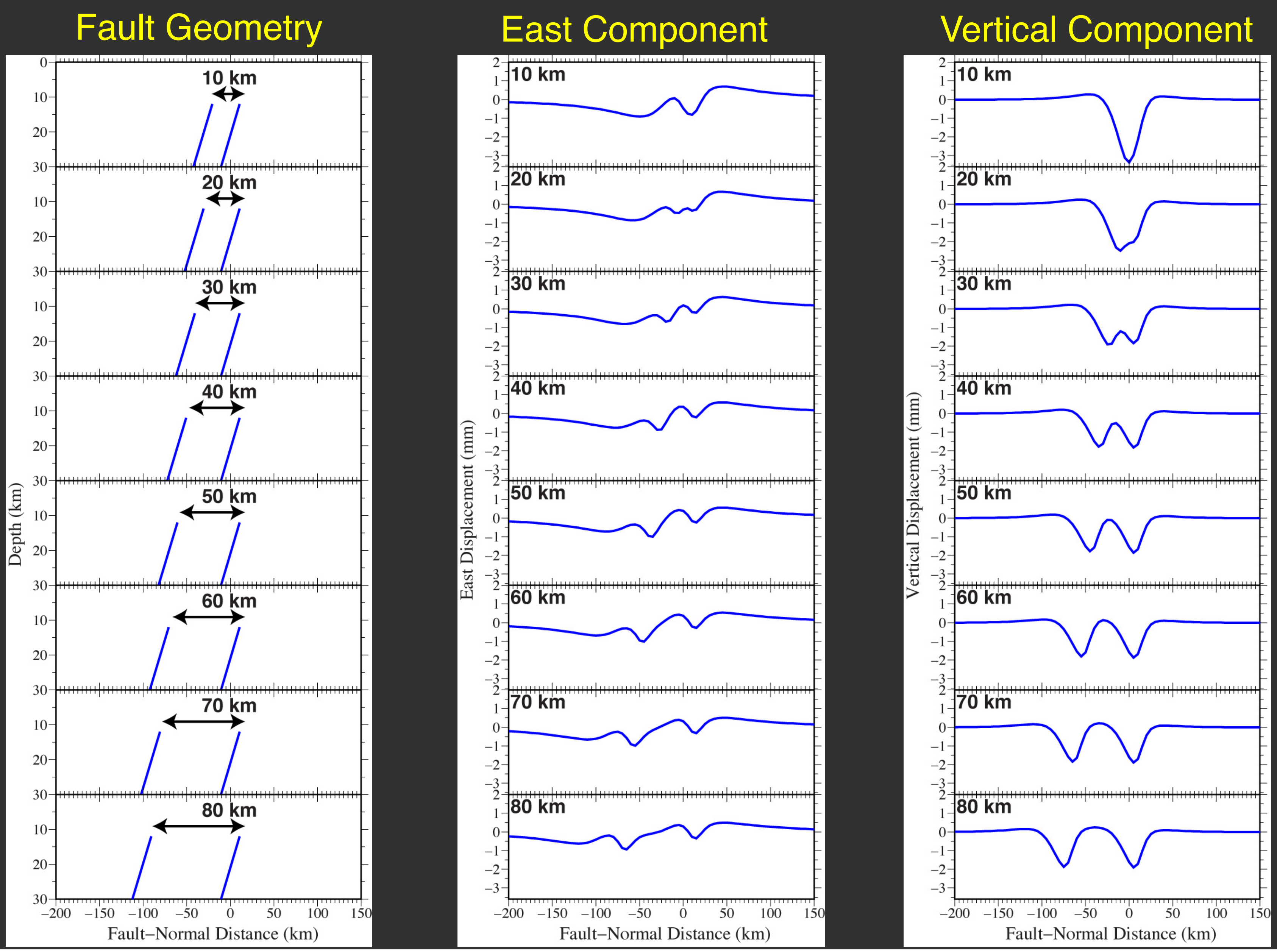

Parallel Planar Faults, Unequal Dislocations (2&5 mm)

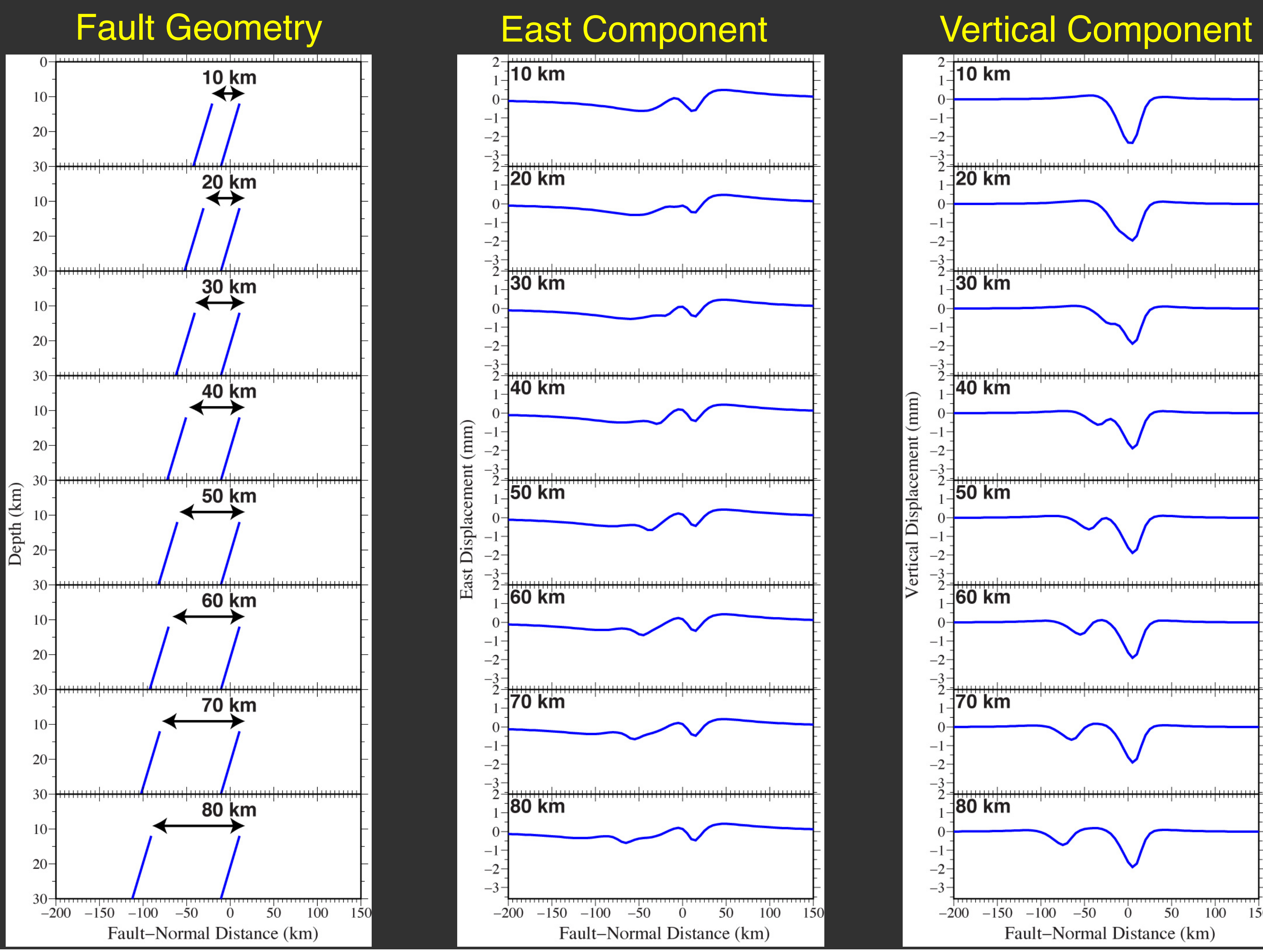

Block Residuals

Okada Dislocations

Best-Fit Model – Minimum c^2

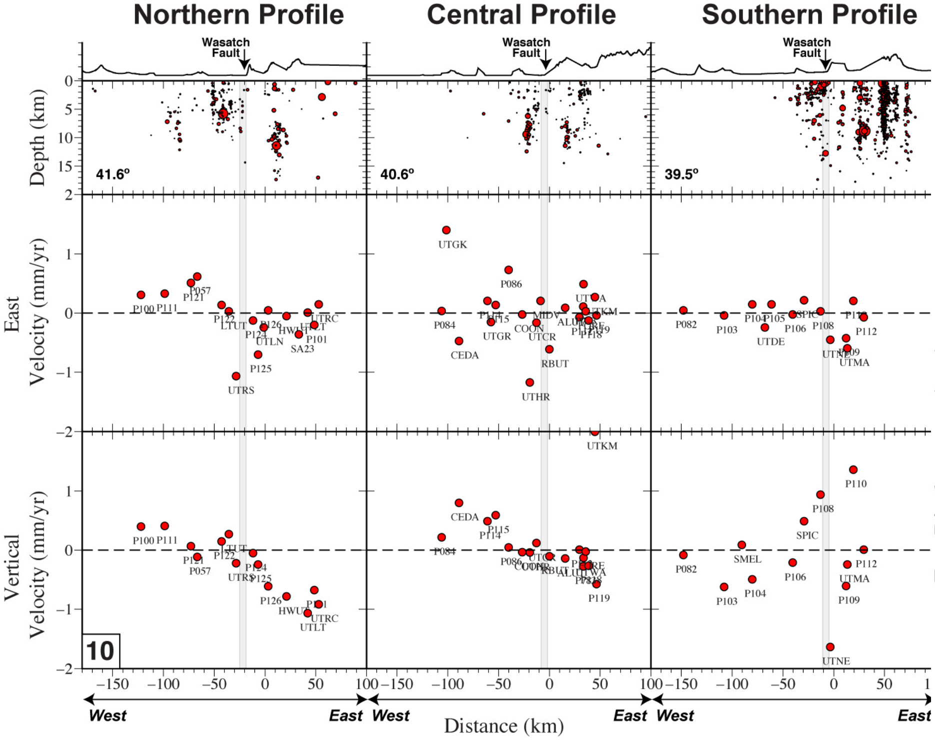

East Component

Vertical Component

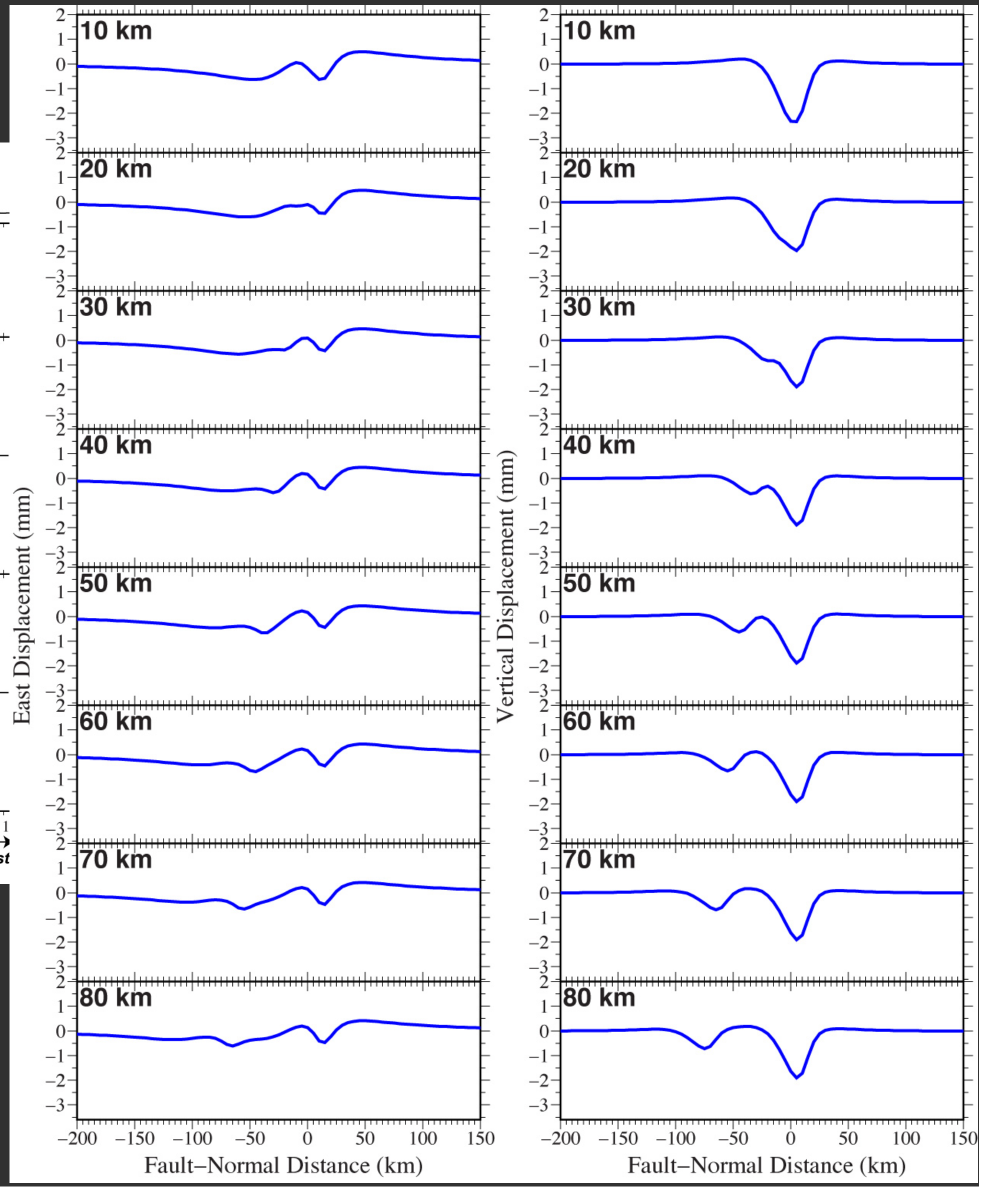

Conclusions

- Strain partitioned across multiple faults to north of Salt Lake Valley
  - Wasatch block
  - Cache Valley block
  - Additional blocks possible, difficult to determine

- Possible Wasatch block in Salt Lake/Provo Valleys

- Possible direct Basin-Range/Eastern Utah boundary in Salt Lake/Provo Valleys
  - Best two models disagree

- Fault slip rates difficult to model from block residuals
  - Vertical velocities will be required to constrain loading models
  - More GPS QC work required


Questions?

Stable North America Basin and Range

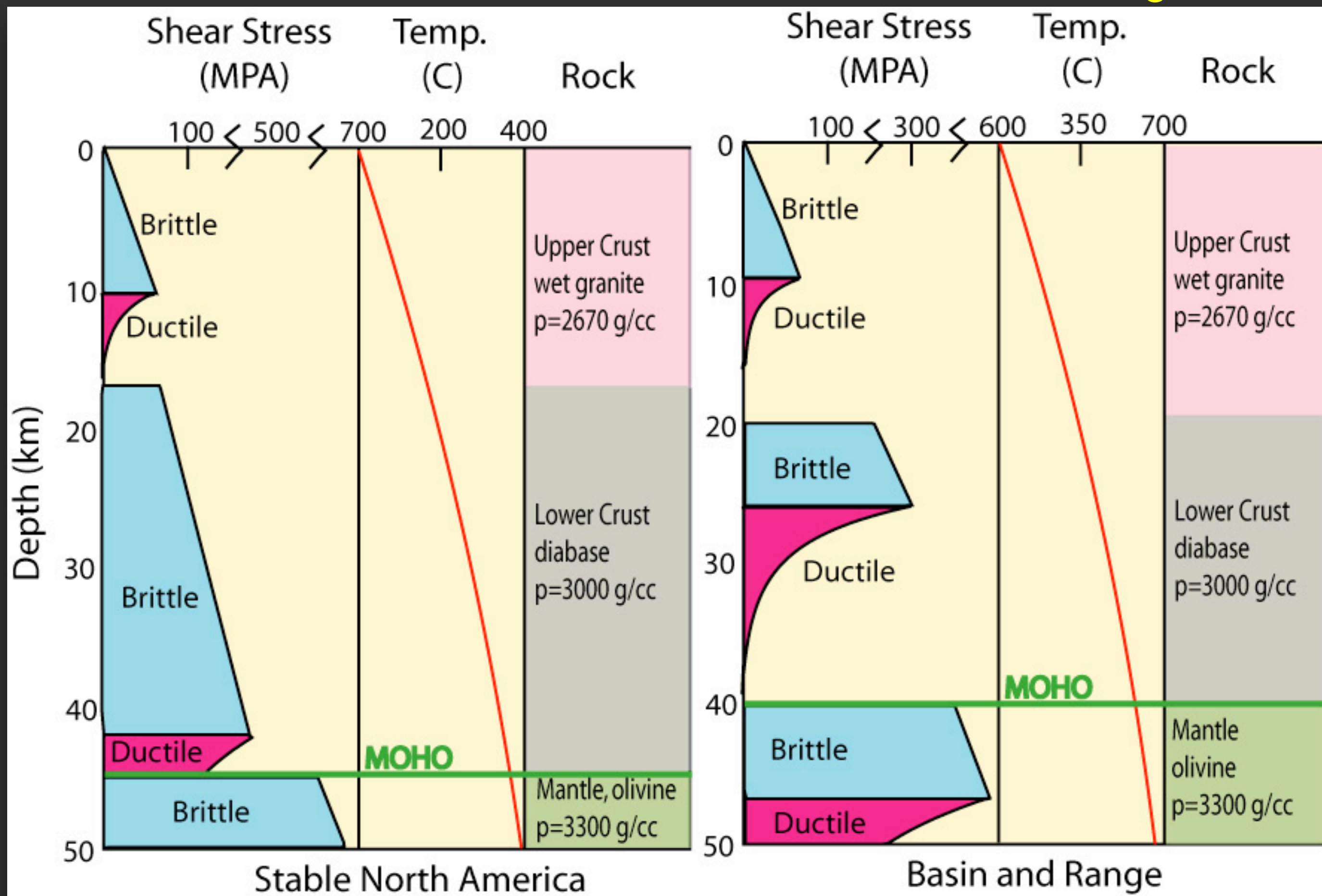

Technical Session 7 – Using Geodesy to Characterize Seismic Hazard in the Basin and Range Province

Moderator: Bill Hammond, University of Nevada, Reno

Fault Slip Rates in the Western Great Basin from Geodetic and Geologic Data: *Bill Hammond, Corné Kreemer, Jayne Bormann, and Geoff Blewitt, University of Nevada, Reno*

InSAR Analysis of the 2008 Reno-Mogul M4.7 Earthquake Swarm—Implications for Seismic Hazard in the Western Basin and Range: *John Bell, Nevada Bureau of Mines and Geology; Falk Amelung, University of Miami; and Christopher Henry, Nevada Bureau of Mines and Geology*

The Geodetic Strain Rate Field for the Colorado Plateau and Southern Basin and Range: *Corné Kreemer, Geoffrey Blewitt, and William Hammond, Nevada Bureau of Mines and Geology; and James Broermann and Richard A. Bennett, University of Arizona*

Update of Deformation Rates in the Snake River Plain: *Suzette Payne, Idaho National Laboratory; Robert King, Massachusetts Institute of Technology; and Robert McCaffrey, Portland State University*

Geodetic Constraints on Kinematics and Strain Rates in the Northern Basin and Range: *Rebecca Bendick, Dylan Schmeelk, Yelebe Birhanu, and Cody Bomberger, University of Montana*

FAULT SLIP RATES IN THE WESTERN GREAT BASIN FROM GEODETIC AND GEOLOGIC DATA

Bill Hammond, Corné Kreemer, Jayne Bormann, and Geoff Blewitt
Nevada Bureau of Mines and Geology (Nevada Geodetic Laboratory)
and Nevada Seismological Laboratory
University of Nevada, Reno MS178
Reno Nevada, 89557
Senior author email address: whammond@unr.edu

Since Basin and Range Province Seismic Hazard Summit II approximately one decade ago (Utah Geological Survey, 2005), substantial progress has been made in the measurement, modeling, and interpretation of active crustal deformation in the western Basin and Range Province. Slip rates are a key input into the analytical framework used by the U.S. Geological Survey (USGS) to construct the National Seismic Hazard Maps that portray the probability of damaging shaking from earthquakes (Petersen and others, 2014). This presentation summarizes recent advances and active research in geodetic measurements that constrain fault slip rates, improving our understanding of the distribution of seismic hazard in Nevada and eastern California.

A primary factor in the improvement of measurement precision has been the expansion of GPS networks across the western Great Basin and Sierra Nevada. This period saw expansion of both the National Science Foundation EarthScope Plate Boundary Observatory continuous network and the semi-continuous Mobile Array of GPS for the Nevada Transtension (MAGNET) network operated by the University of Nevada, Reno. Time series have gotten longer and reduced the uncertainties of rates, patterns, and style of active crustal strain. MAGNET now covers the entire Walker Lane from south to north and much of the adjoining Basin and Range Province, touching southern Oregon, southern Utah, and western Arizona. The time series are now long enough at most stations to estimate rates of crustal motion to within a few tenths of a mm/yr, sufficient to resolve details of the crustal deformation field. In addition to improvements in network coverage, there have been concurrent improvements in the integration of data from other GPS networks, completeness of databases, consistency of metadata, and realization and alignment to reference frames that have improved the processing of GPS data and enhanced resolution.

We combine GPS data with geologic data on the geometry of active crustal faults to develop fault-scale to near-Province-scale block models to estimate fault slip rates in the complex transtensional environment of the western Great Basin. We will discuss key conclusions derived from models of the northern Walker Lane (Hammond and others, 2011), Mohawk Valley/Grizzly Valley/Honey Lake fault systems (Bormann, 2013), central Walker Lane (Bormann, 2013), and insights gleaned from a synoptic model that extends across the entire Walker Lane (Bormann and others, 2013).

Additionally, we present a new block model of slip rates on faults in and around Las Vegas, Nevada, constrained by the new velocity field presented in this publication (Kreemer and others, 2015) that includes recent data from the continuous networks and the densified MAGNET network. The velocity field has a gradual east-west gradient in westward velocity, of ~0.7 mm/yr between -114° and -115° longitude, crossing Las Vegas. We include in our model a block whose boundaries follow the Frenchman Mountain, Eglington, and Decatur faults, the active structures nearest to Las Vegas, and estimate slip rates on these faults that are kinematically consistent with the regional deformation pattern between the southern Walker Lane, Basin and Range, and Colorado Plateau. These faults have slip rates of <0.2 mm/yr in the Quaternary Fault and Fold Database of the United States (USGS and Nevada Bureau of Mines and Geology, 2006). Our estimates, based on our preliminary model from GPS geodesy (figure 1) are 0.26+/-0.34 mm/yr (normal) for the Frenchman Mountain fault and 0.29+/-0.32 mm/yr normal for the Eglington fault. These rates are consistent with average rates on active normal faults in the central Nevada Basin and Range (where e.g., the Wells, Nevada, **M** 6.0 earthquake occurred in 2008). While these rates are an order of magnitude smaller than slip rates in the southern Walker Lane to the west (e.g., the Northern Death Valley and Black Mountain fault systems) their proximity to Las Vegas can impact hazard for this urban area.

Despite the advances in constraining deformation rates, and a broad and frequent agreement between geologic and geodetic fault slip rates, there are still features of the deformation field that are not perfectly understood. Examples of complexities include (1) the presence of non-tectonic deformation signals associated with large active magmatic sources, e.g., Long Valley, California (Chacko and others, 2014), (2) long lasting transients associated with viscoelastic relaxation after large crustal earthquakes, (e.g., the early to mid-20th century events in the Central Nevada seismic belt), and (3) uncertainty in the pattern of crustal block contiguity where deformation may be more diffuse, complex, or absorbed aseismically by folding structures (Wesnousky and others, 2012). Discrepancies can be exacerbated by other factors including inadequacy of geodetic network coverage, unrecognized uncertainty in geologic rates, over simplification of fault structures in geodetic block models, or changes in block motions over time. An example of a disagreement in the central Walker Lane is the apparent dominance of shear deformation in geodetic results where the neotectonic record had found relatively little shear deformation (Wesnousky and others, 2012). However, continued investigation has recently found new evidence for strike-slip deformation that can help narrow the gap (Dong and others, 2014). In this presentation, we will discuss the different classes of disagreement between geologic and geodetic data, the challenges in reducing these uncertainties, and how they impact uncertainties of slip rates.

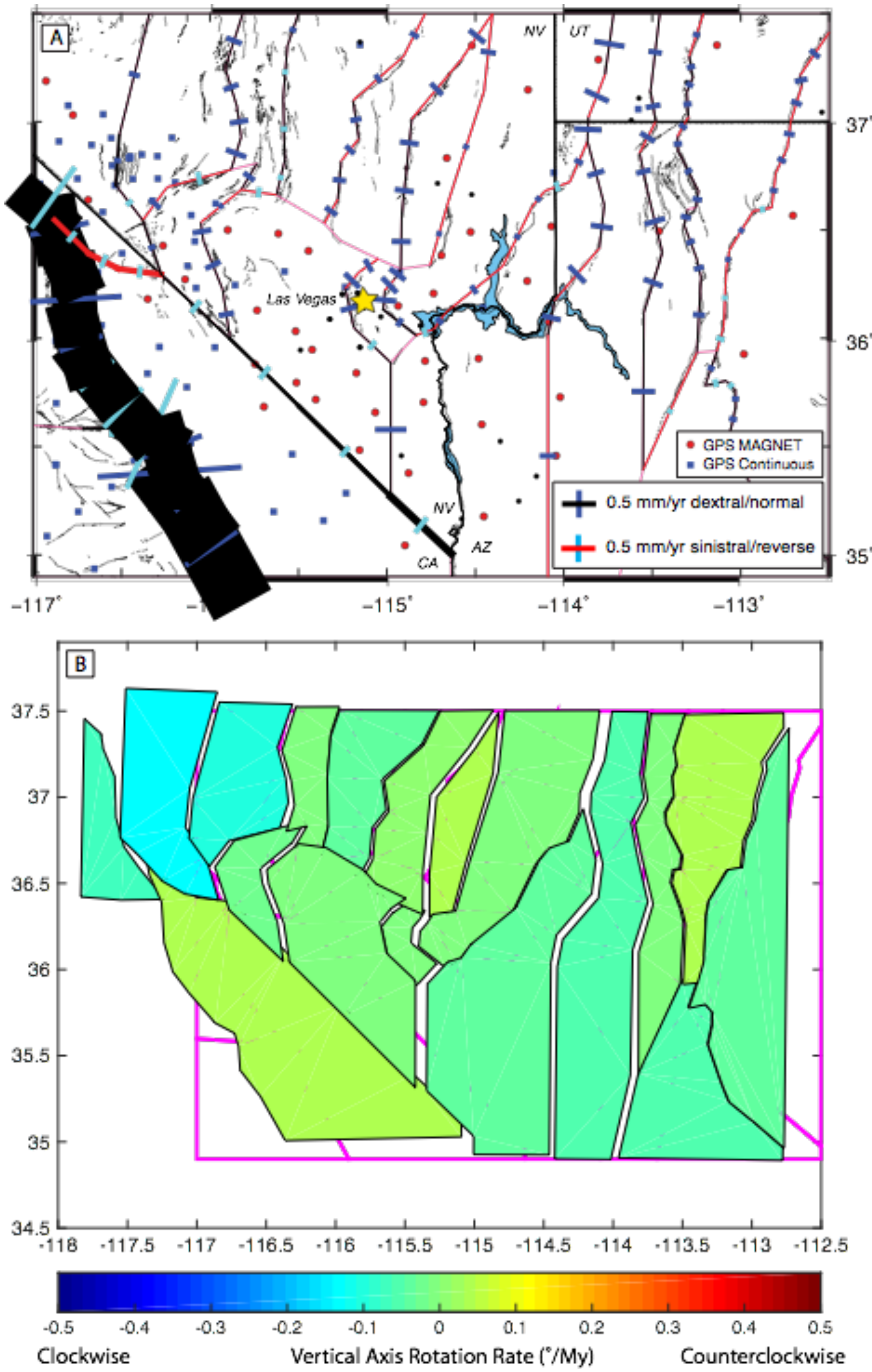

Figure 1. *Preliminary block model of slip rates and block rotations in the region including and surrounding Las Vegas, Nevada. (A) Fault slip rates where thickness of black (red) lines indicate rate of dextral (sinistral) slip, and length of blue (cyan) fault-crossing bars indicates rate of normal (reverse) sense of slip. The thick black line on the southwest side of the model is the Death Valley-Black Mountain fault system. (B) Block rotations and translations with color scale that indicates rate and sign of local vertical axis component spin.*

REFERENCES

Bormann, J., Hammond, W.C., Kreemer, C., Blewitt, G., and Jha, S., 2013, A synoptic model of fault slip rates in the Eastern California shear zone and Walker Lane from GPS velocities for seismic hazard studies [abs.]: Seismological Research Letters v. 84, no. 2, p. 274.

Bormann, J., 2013, Constraints on shear strain accommodation in the northern Walker Lane and the geometry of normal fault ruptures through geodetic and geologic observation: University of Nevada, Reno, Ph.D. dissertation, 150 p., August, 2013.

Chacko, R., Hammond, W.C., and Blewitt, G., 2014, Magmatic-tectonic interactions Implications for seismic hazard assessment in the Long Valley caldera region: Presented at 2014 Fall Meeting, American Geophysical Union, San Francisco, Calif., Dec. 15-19, Abstract G31A-0407.

Dong, S., Ucarkus, G., Wesnousky, S.G., Maloney, J., Kent, G., Driscoll, N., and Baskin, R., 2014, Strike-slip faulting along the Wassuk Range of the northern Walker Lane, Nevada, *in* The Origin and Evolution of the Sierra Nevada and Walker Lane Theme Issue: Geosphere, v.10, no.1, p. 40-48, do:10.1130/GES00912.1.

Hammond, W.C., Blewitt, G., and Kreemer, C., 2011, Block modeling of crustal deformation of the northern Walker Lane and Basin and Range from GPS velocities: Journal of Geophysical Research, v. 116, B04402, doi:10.1029/2010JB007817.

Kreemer, C., Blewitt, G., Hammond, W.C., Bormann , J., and Bennett, R.A., 2015, The geodetic strain rate field for the Colorado Plateau and southern Basin and Range, *in* Lund, W.R., editor, Proceedings of the Range Seismic Hazard Summit III: Utah Geological Survey Miscellaneous Publication 15-5 (this volume).

Petersen, M.D., Zeng, Y., Haller, K.M., McCaffrey, R., Hammond, W.C., Bird, P., Moschetti, M., Shen, Z., Bormann, J., and Thatcher, W., 2014, Geodesy- and geology-based slip-rate models for the Western United States (excluding California) National Seismic Hazard Maps: U.S. Geological Survey Open-File Report 2013–1293, 86 p., http://pubs.usgs.gov/of/2013/1293/.

Utah Geological Survey, Lund, W.R., editor, 2005, Western States Seismic Policy Council, Proceedings Volume of the Basin and Range Seismic Hazard Summit II: Utah Geological Survey Miscellaneous Publication 05-2, 505 p., http://ugspub.nr.utah.gov/publications/misc_pubs/MP-05-2.pdf.

U.S. Geological Survey and Nevada Bureau of Mines and Geology, 2006, Quaternary fault and fold database for the United States, accessed November 29, 2014, online, http//earthquakes.usgs.gov/regional/qfaults/.

Wesnousky, S., Bormann, J., Kreemer, C., Hammond, W.C., and Brune, J., 2012, Neotectonics, geodesy and seismic hazard in the northern Walker Lane of western North America—Thirty kilometers of crustal shear and no strike-slip?: Earth and Planetary Science Letters, v. 329-330, p. 133–140, doi:10.1016/j.epsl.2012.02.018.

The following is a PDF version of the authors' PowerPoint presentation.

Fault Slip Rates in the Western Great Basin from Geodetic and Geologic Data

Bill Hammond, Corne Kreemer,
Jayne Bormann, Geoff Blewitt
Nevada Geodetic Laboratory
Nevada Bureau of Mines and Geology
University of Nevada, Reno
whammond@unr.edu

Nevada Geodetic Laboratory
nbmg
NEVADA
National Science Foundation
WHERE DISCOVERIES BEGIN
earthscope
NASA
USGS
science for a changing world

- What is geodesy?

- Strain Accumulation…and Release. The seismic cycle.

This Talk

- Where we are in measurement of active crustal deformation in the western Great Basin. Networks. Processing. Data products.

- Tectonic context for faults in the BRP.

- Slip rates on active faults. How we get them. Uncertainties.

MAGNET*

* the Mobile Array of GPS for Nevada Transtension

- 388 Stations and Still Growing
- Semi-continuous observation strategy
- 1100 km aperture
- Spans Basin and Range NSEW

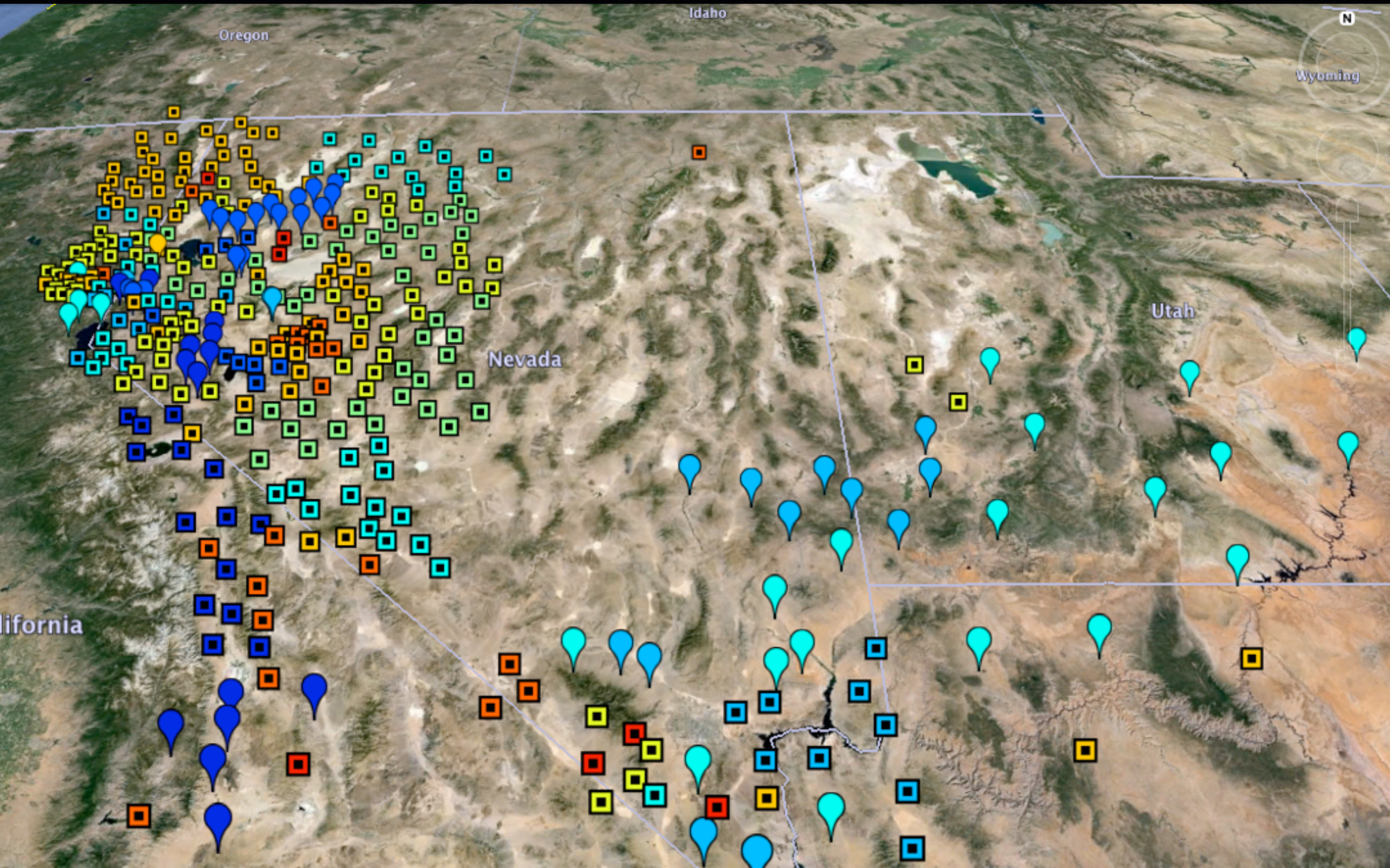

Combining Networks To Optimize
Measurement of Crustal Deformation

Semi-continuous occupation strategy
UNR's MAGNET: Mobile Array of GPS for Nevada Transtension.
Inexpensive. Flexible. Improved geographic coverage.

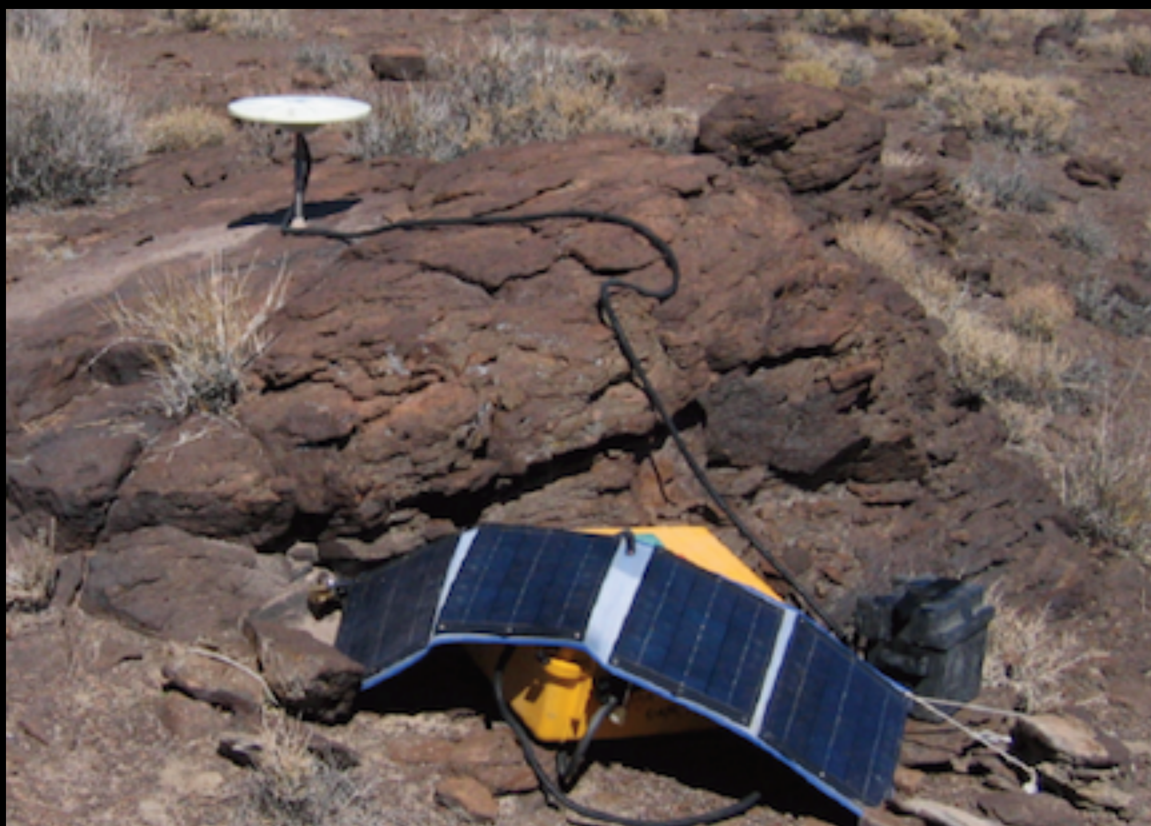

Continuous GPS Stations
e.g. EarthScope Plate Boundary Observatory
BARD, EBRY, SCIGN, etc.
Continuous occupation
Temporally complete time series
Better constraint on transient deformation

Data Processed at NGL/UNR with
GIPSY/OASIS using mega-network approach
results posted at *http://geodesy.unr.edu*

MAGNET* Plus Other Continuous GPS Stations

EBRY, BARGEN, PBO, CORS, BARD, Regional Networks

* the Mobile Array of GPS for Nevada Transtension

http://geodesy.unr.edu

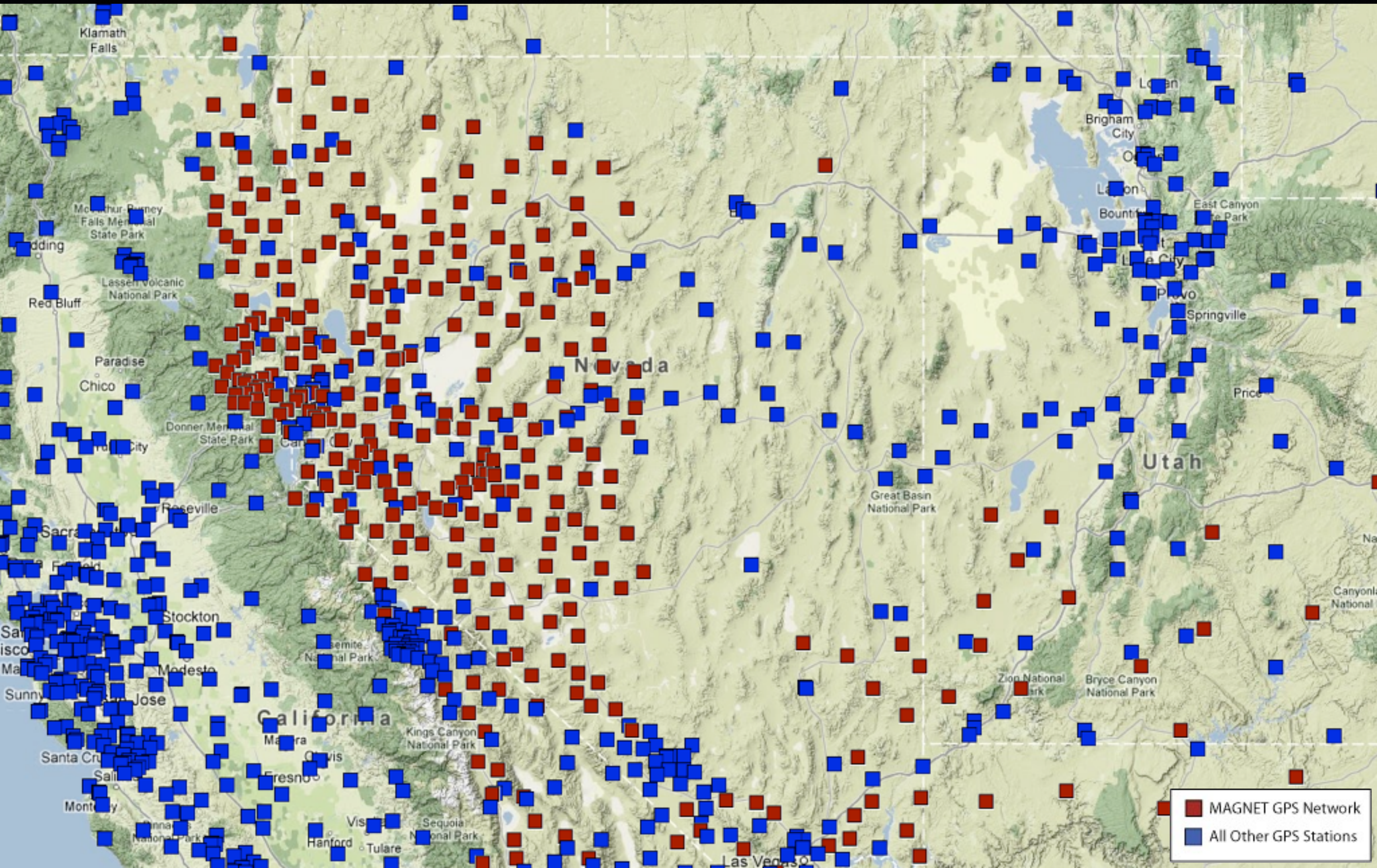

MAGNET* Plus Other Continuous GPS Stations

EBRY, BARGEN, PBO, CORS, BARD, Regional Networks

* the Mobile Array of GPS for Nevada Transtension

http://geodesy.unr.edu

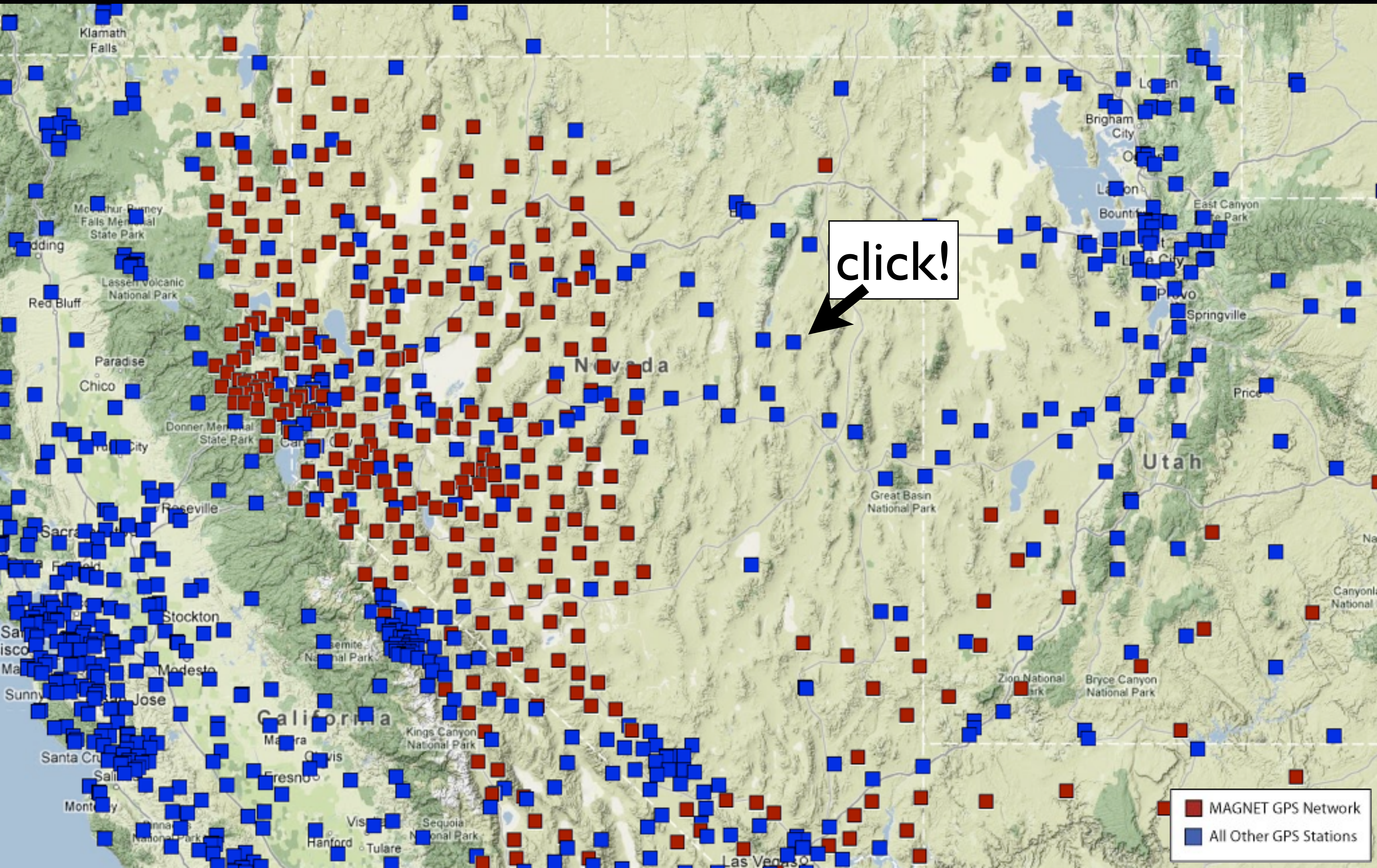

NGL providing GPS solutions online for <u>>12,800 stations</u>

- Processing and time series generation done using GIPSY/OASIS software by Geoff Blewitt
- Graphic and text files.
- Available via http and ftp.
- Interactive map browsing and text listings of stations.
- Global distribution of stations.
- IGS2008 and North America (NA12) reference frames.

Low latency products available:
- >8000 stations with 5 minute solutions next day
- >2000 stations with 5 minute solutions every hour.

- See the shape of the Great Basin every 5 minutes.

- Useful for rapid earthquake information.
- details: http://geodesy.unr.edu/gps/ngl.acn

NGL providing GPS solutions online for >12,800 stations

• Processing and time series generation done using GIPSY/OASIS software by Geoff Blewitt
• Graphic and text files.
• Available via http and ftp.
• Interactive map browsing and text listings of stations.
• Global distribution of stations.
• IGS2008 and North America (NA12) reference frames.

Low latency products available:
• >8000 stations with 5 minute solutions next day
• >2000 stations with 5 minute solutions every hour.

• See the shape of the Great Basin every 5 minutes.

• Useful for rapid earthquake information.
• details: http://geodesy.unr.edu/gps/ngl.acn

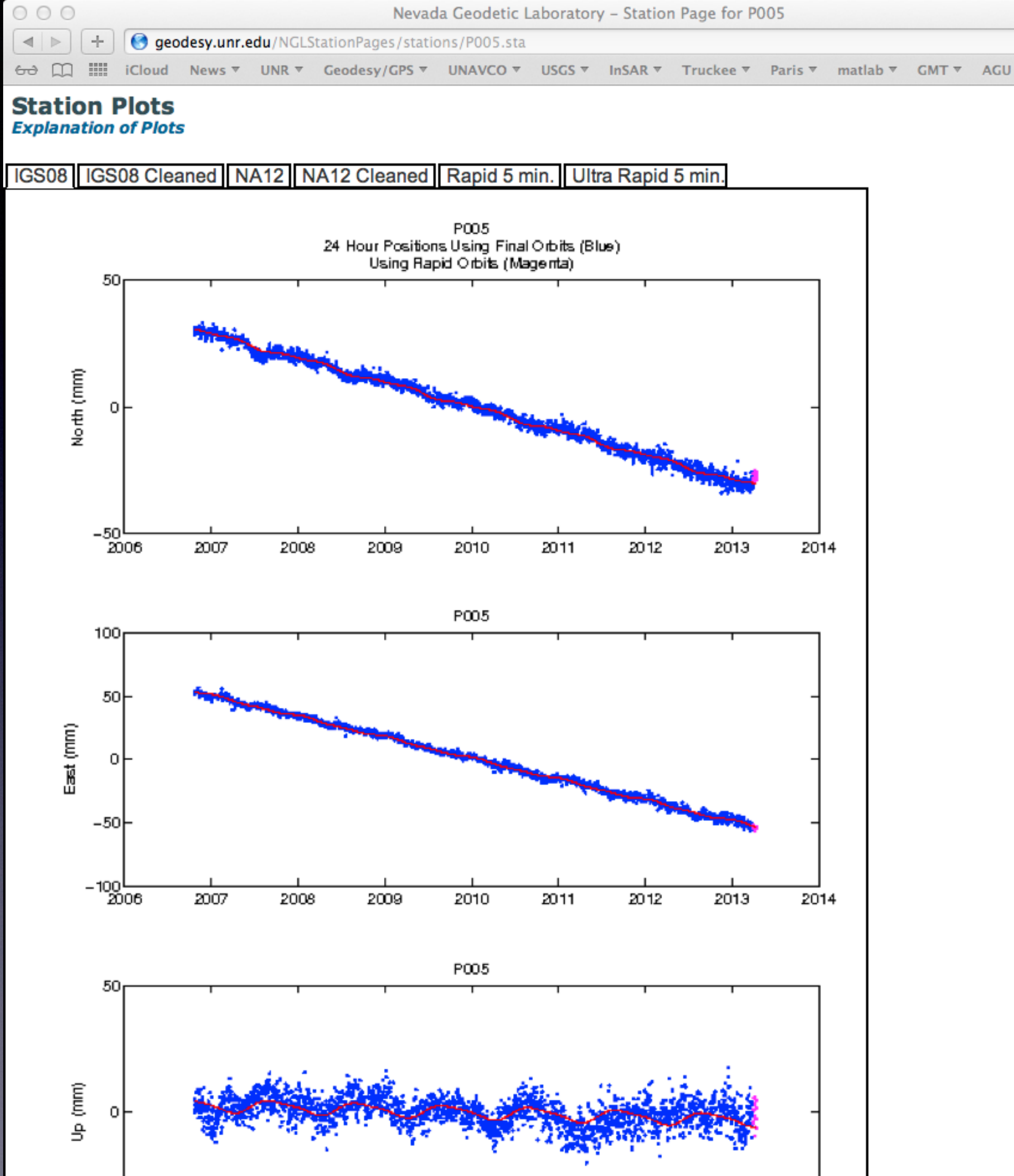

NGL providing GPS solutions online for <u>>12,800 stations</u>

- Processing and time series generation done using GIPSY/ OASIS software by Geoff Blewitt
- Graphic and text files.
- Available via http and ftp.
- Interactive map browsing and text listings of stations.
- Global distribution of stations.
- IGS2008 and North America (NA12) reference frames.

Low latency products available:
- >8000 stations with 5 minute solutions next day
- >2000 stations with 5 minute solutions every hour.

- See the shape of the Great Basin every 5 minutes.

- Useful for rapid earthquake information.
- details: http://geodesy.unr.edu/gps/ngl.acn

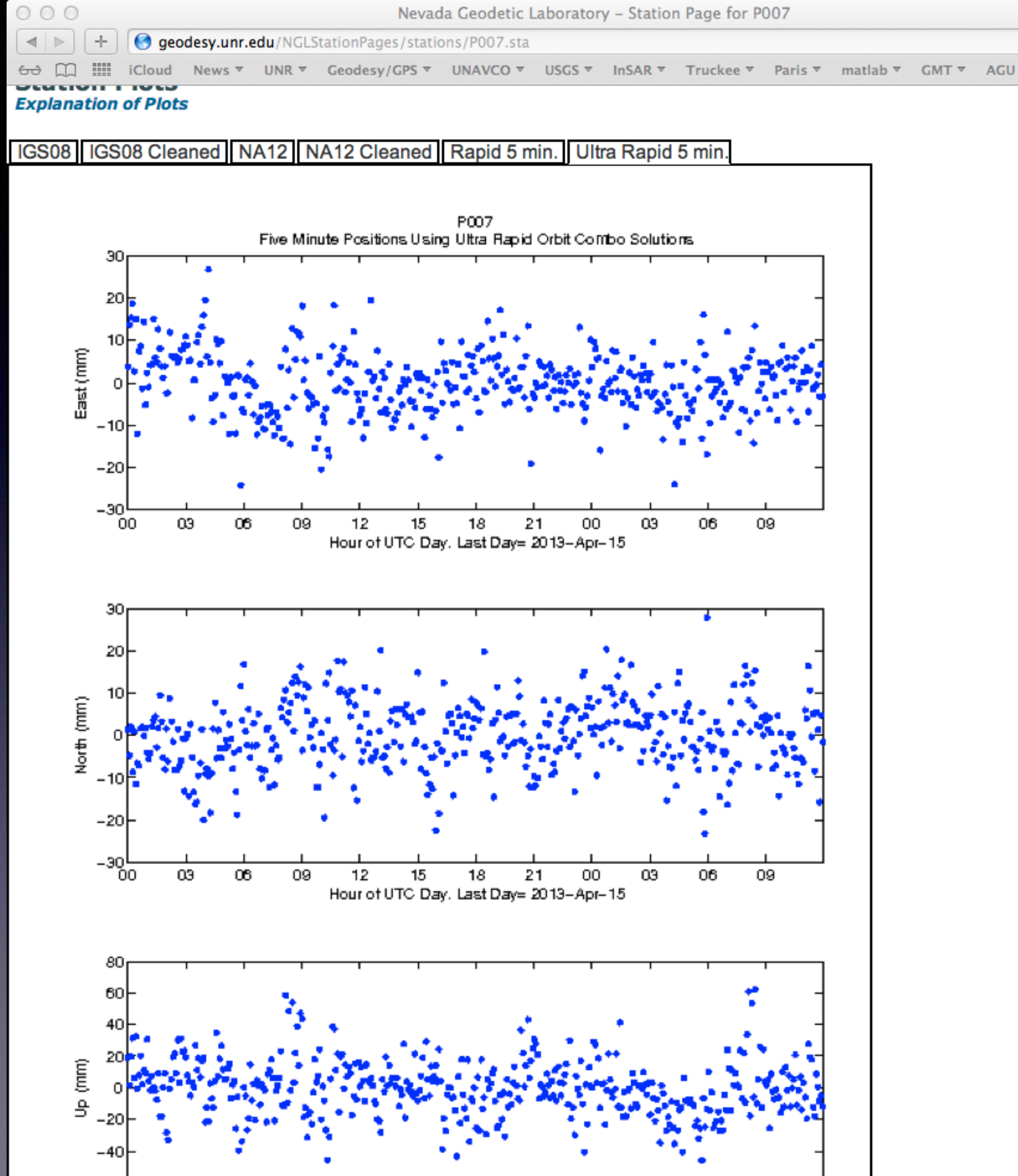

Strain Rate Map

- Portrays intensity of deformation rate with color (red=fast / blue=slow)
- Strain rates show high correlation with seismic hazard maps
- Kreemer et al., 2012 NBMG map number 178 (free online! modest charge for printing)
- Rapidly deforming zone covers Walker Lane and more

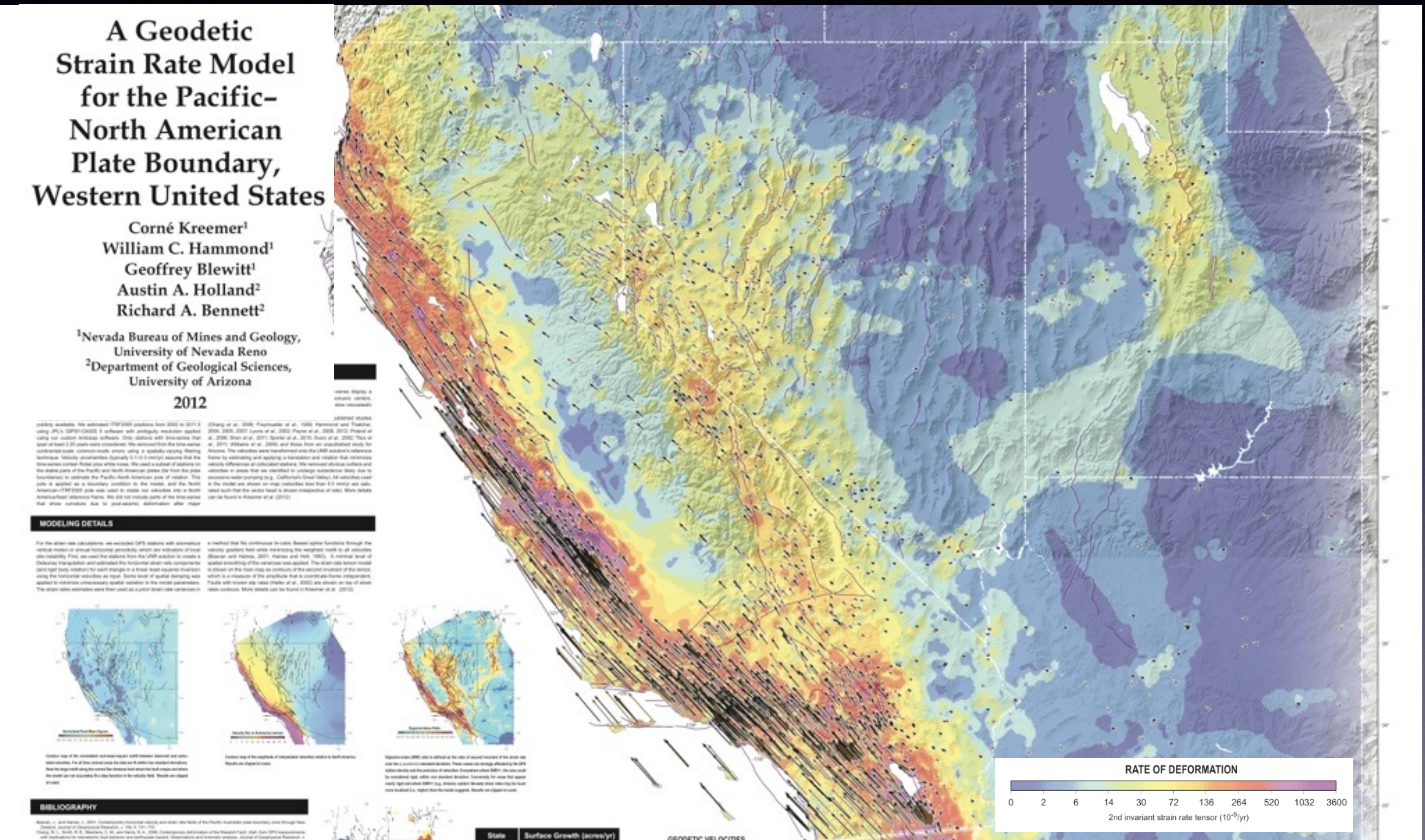

Pacific/North America Plate Boundary

• Rotated view, Pacific motion "up" in figure in Mercator projection around the Pacific/North America pole of rotation

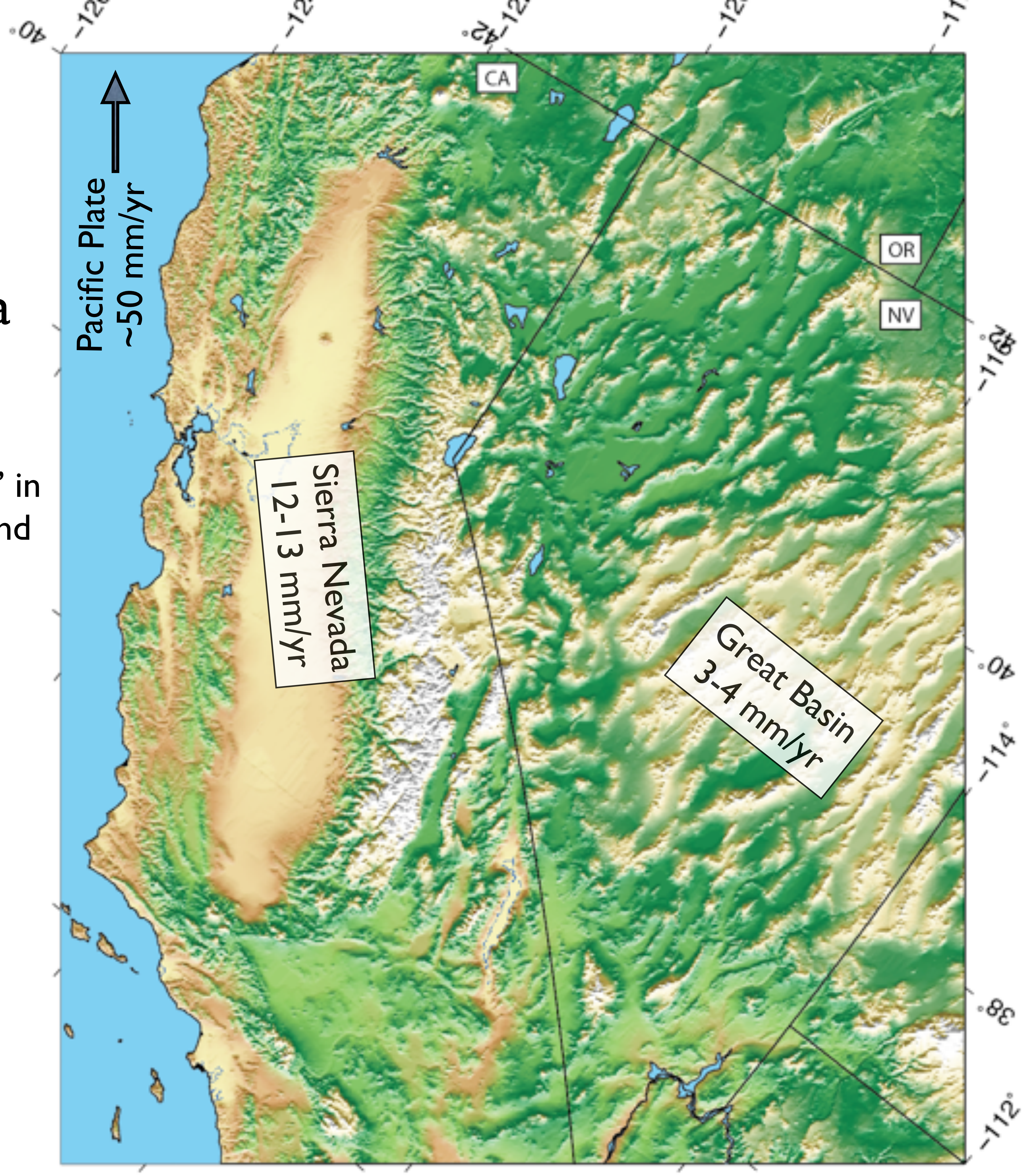

Basin and Range GPS Velocity in North America <u>Reference Frame</u>

- Rapid deformation across the San Andreas system.
- Sierra Nevada/Great Valley microplate translates ~// to PA plate with counterclockwise rotation.
- Northern Basin and Range towards Pacific Northwest experiences clockwise rotation.
- Northern Walker Lane occupies region where sign of vertical axis rotation changes.
- Still some big gaps in coverage.

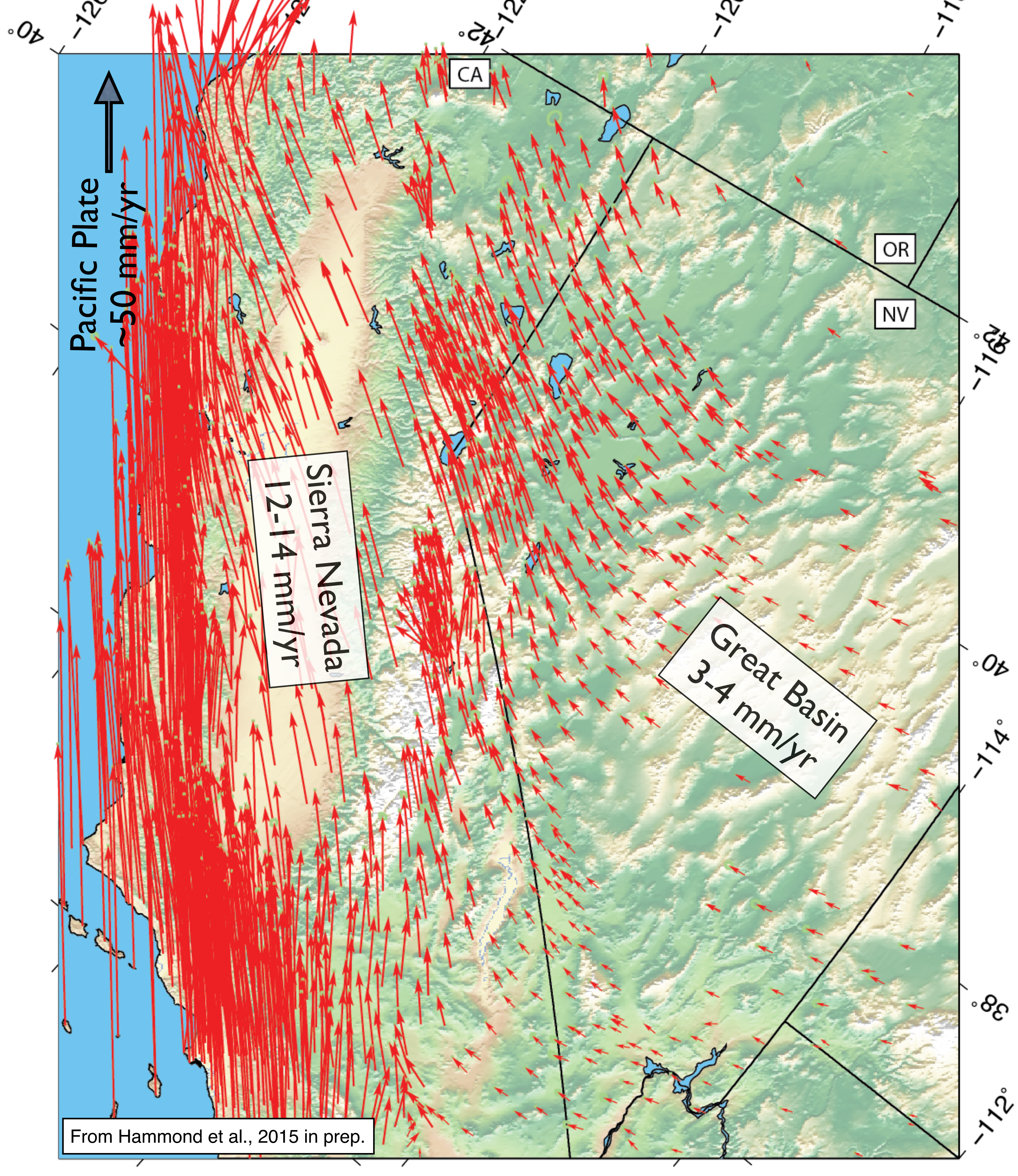

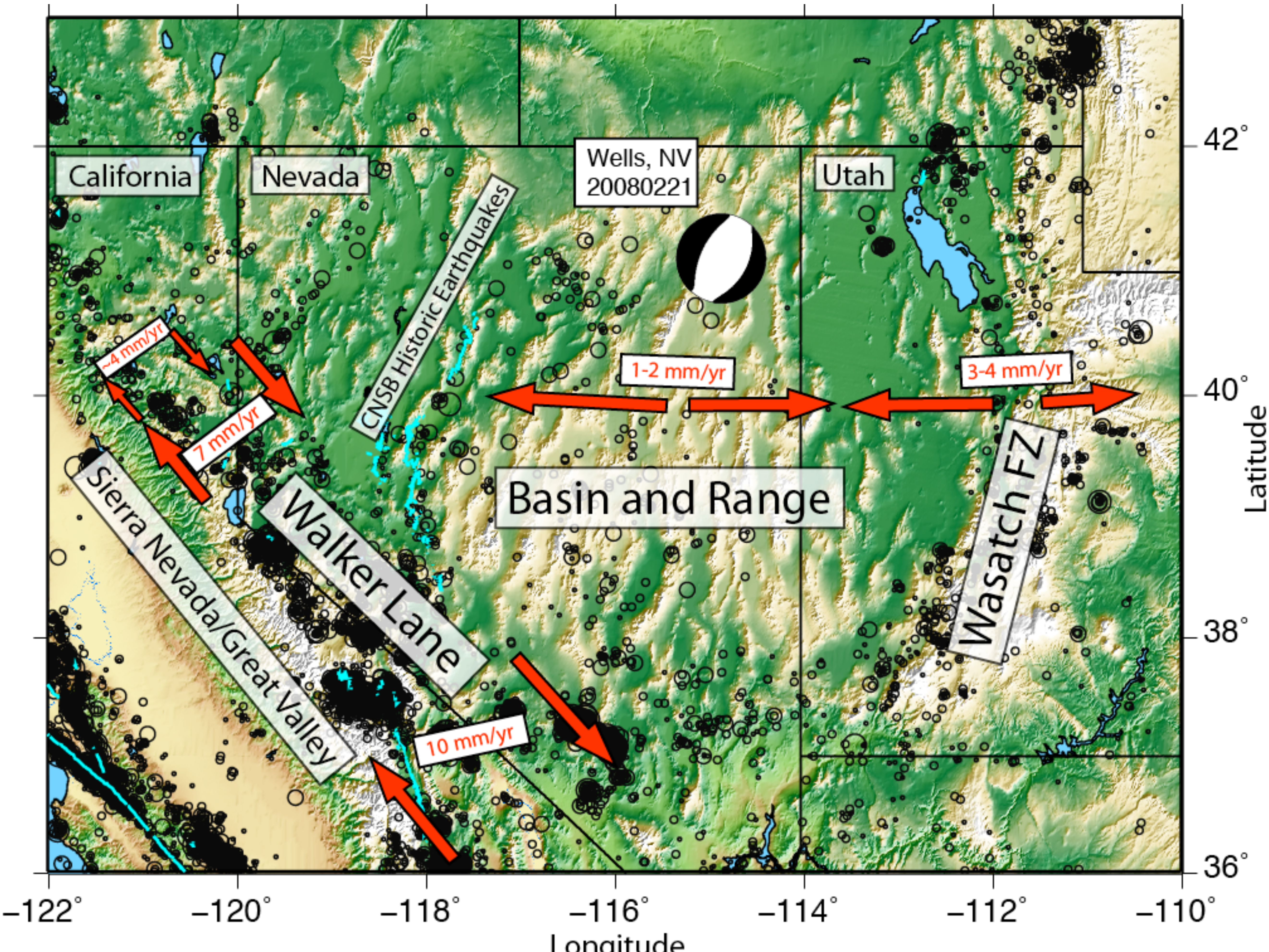

California
Nevada
Wells, NV
20080221
Utah
CNSB Historic Earthquakes
~4 mm/yr
7 mm/yr
1-2 mm/yr
3-4 mm/yr
Basin and Range
Wasatch FZ
Walker Lane
Sierra Nevada/Great Valley
10 mm/yr
42°
40°
38°
36°
Latitude
−122°
−120°
−118°
−116°
−114°
−112°
−110°
Longitude

Contours of Velocity Magnitude from Strain Rate Map

- Velocity contours widen to the north, more focused to the south. Reveals highest strain rates are west near Sierra Nevada and in southern Walker Lane.

- Changes in rates begin to increase well east of the traditional boundary of the walker lane, near the east edge of MAGNET, where contours get extra wiggly.

- Contours crossing north end of Great Valley attributable to SNGV running into northern California, causing contraction. SNGV not completely rigid on north end. Hard to see that in visual inspection of velocities.

- Deformation east of 3 mm/yr contour is low but non-zero.

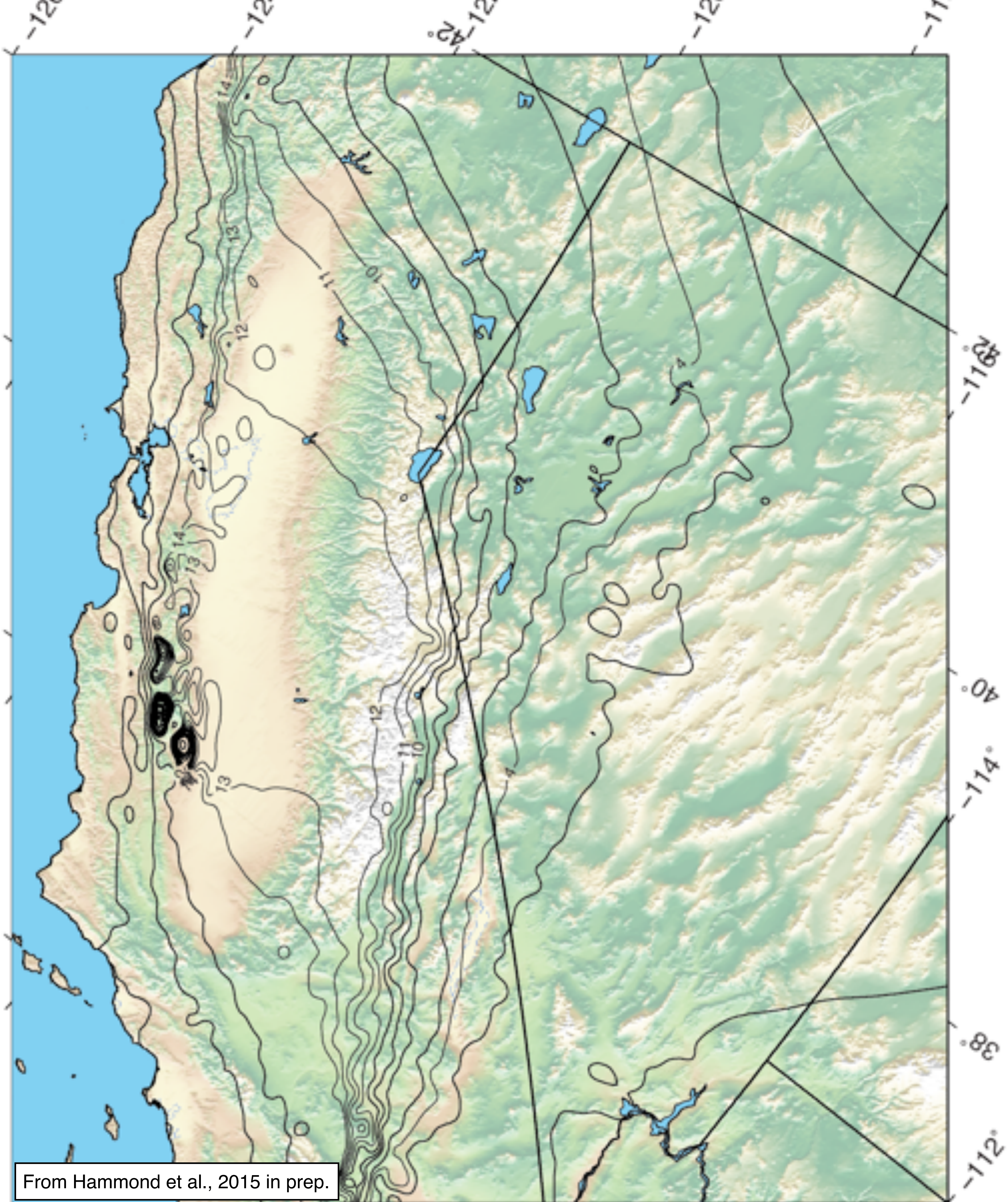

From Hammond et al., 2015 in prep.

Magnitude of Strain Rate (2nd Tensor Invariant)

red=fast deformation
blue=slow deformation

- Tensor strain rate from velocities focussed in Walker Lane.

- Highest strain rates to the west, near Sierra Nevada range front.

- Geodetic Walker Lane includes Tahoe, or Sierra Nevada range front.

Coverage weak in northwest, velocity contours smoother, strain rate lower. Reason for apparent termination of WL?

- East NV deforms slowly but significantly.

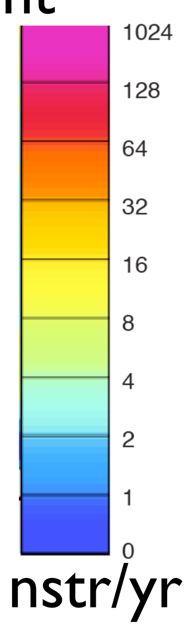

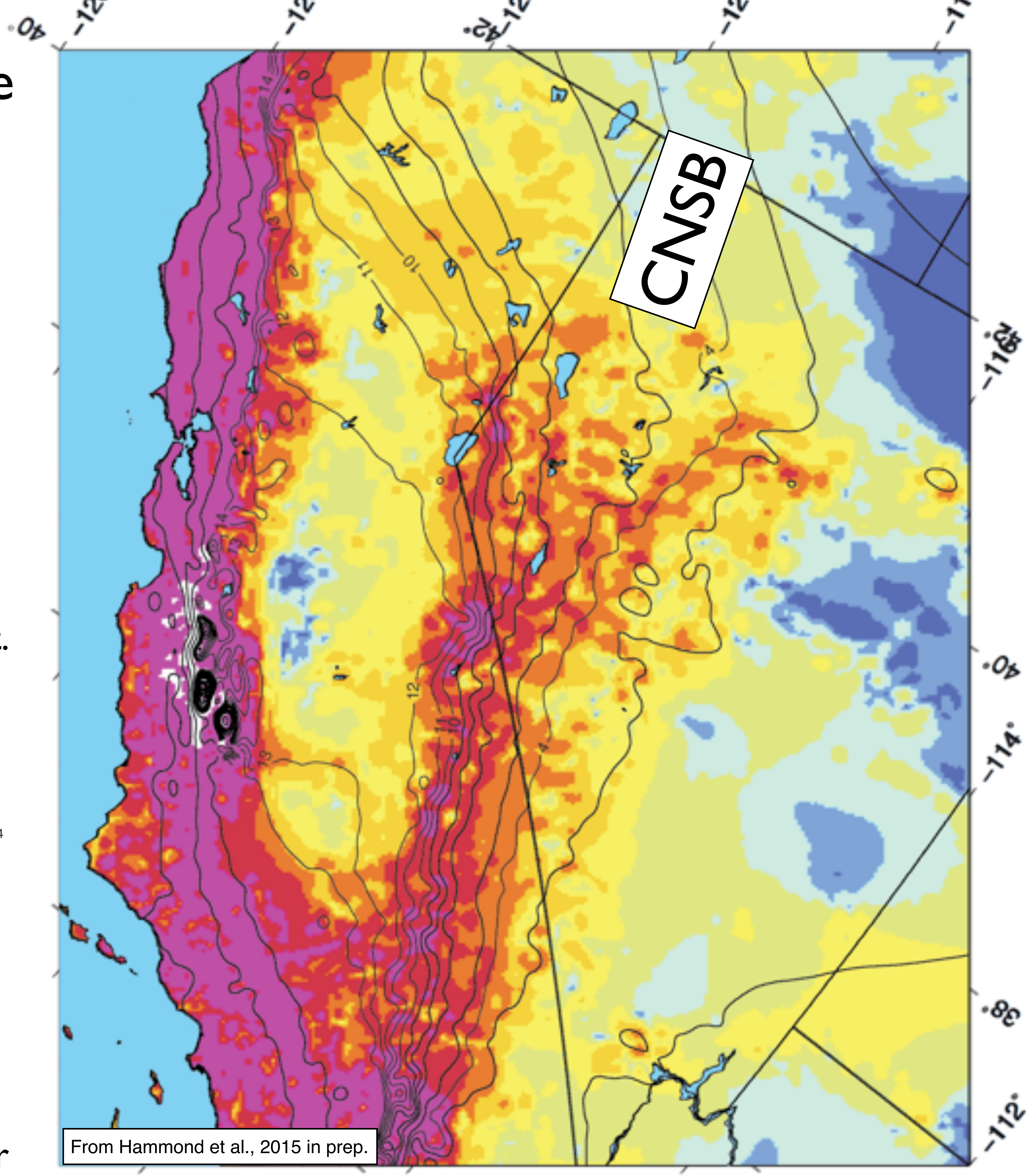

Magnitude of Strain Rate (2nd Tensor Invariant)

red=fast deformation
blue=slow deformation

• Tensor strain rate from velocities focussed in Walker Lane.

• Highest strain rates to the west, near Sierra Nevada range front.

• Geodetic Walker Lane includes Tahoe, or Sierra Nevada range front.

Coverage weak in northwest, velocity contours smoother, strain rate lower. Reason for apparent termination of WL?

• East NV deforms slowly but significantly.

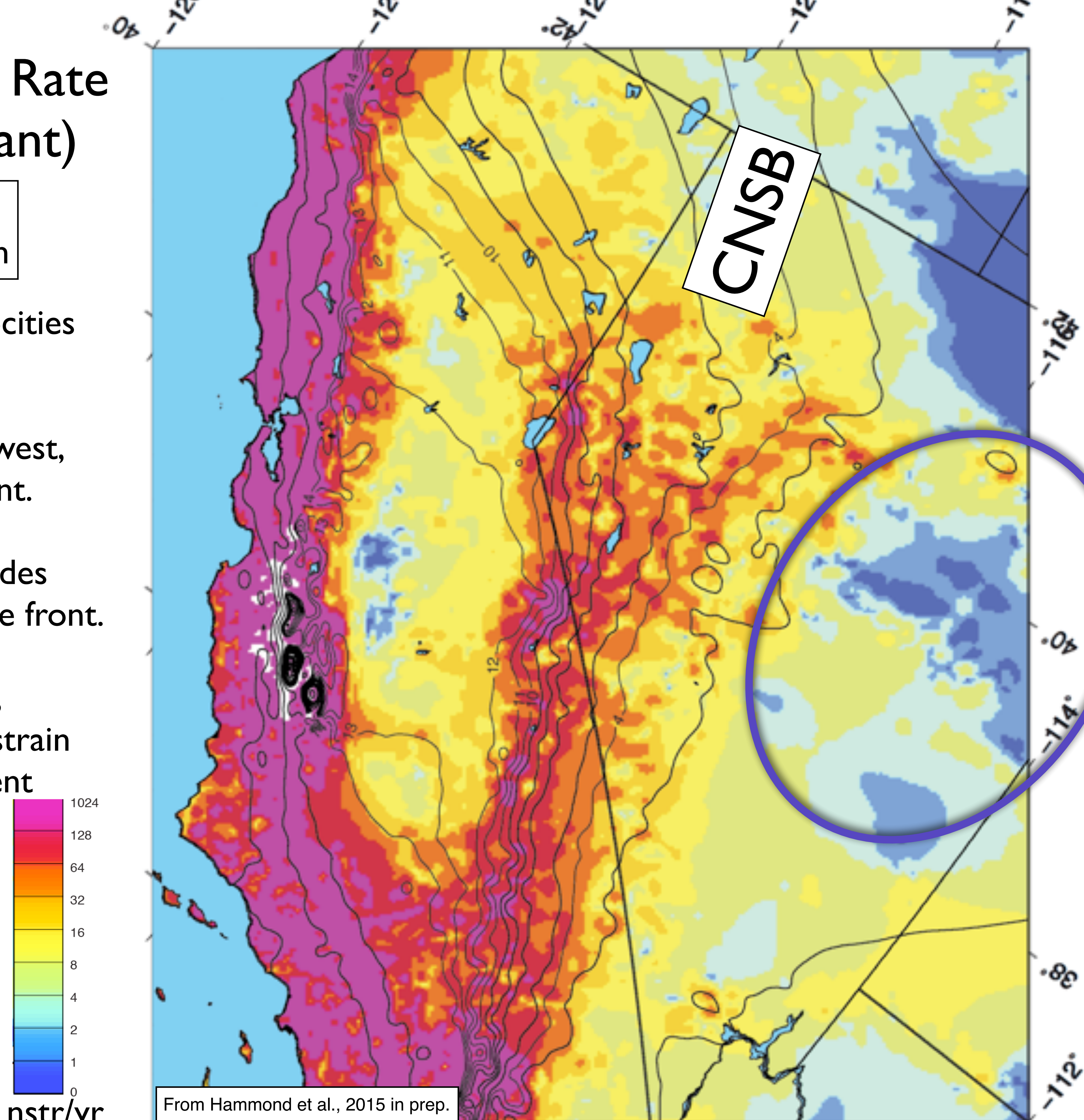

Significant Shear Strain to NV/UT Border

- Slow but not Dead
- Shear Not Uniaxial
- Constant Not Episodic

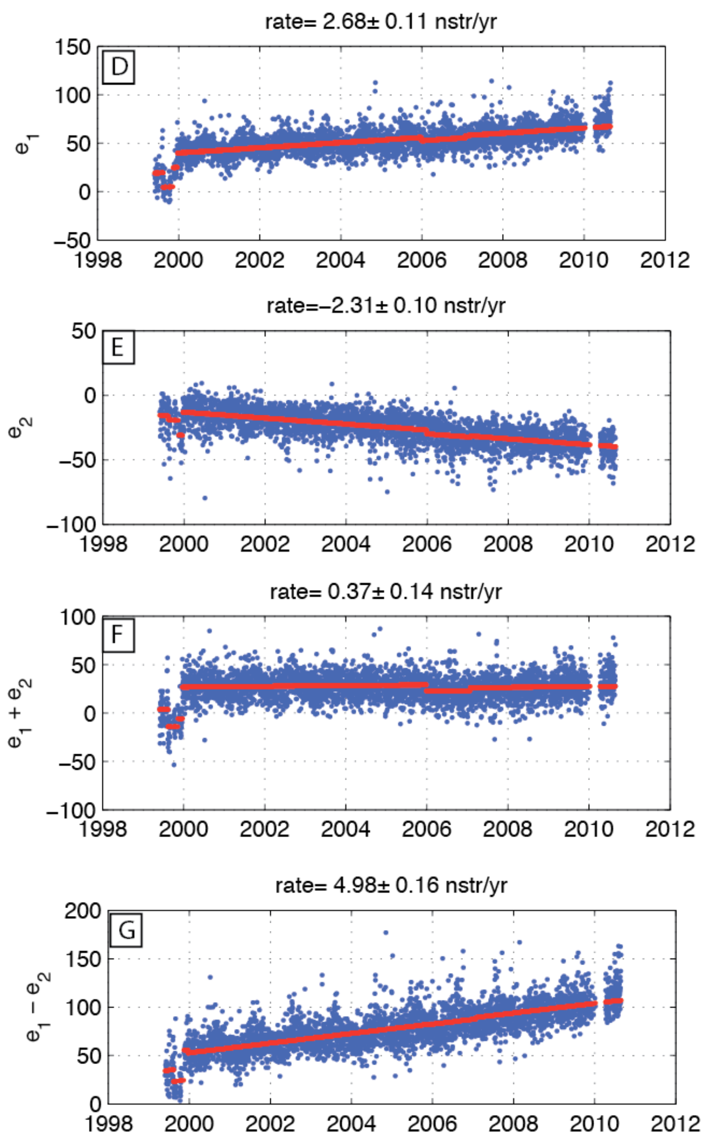

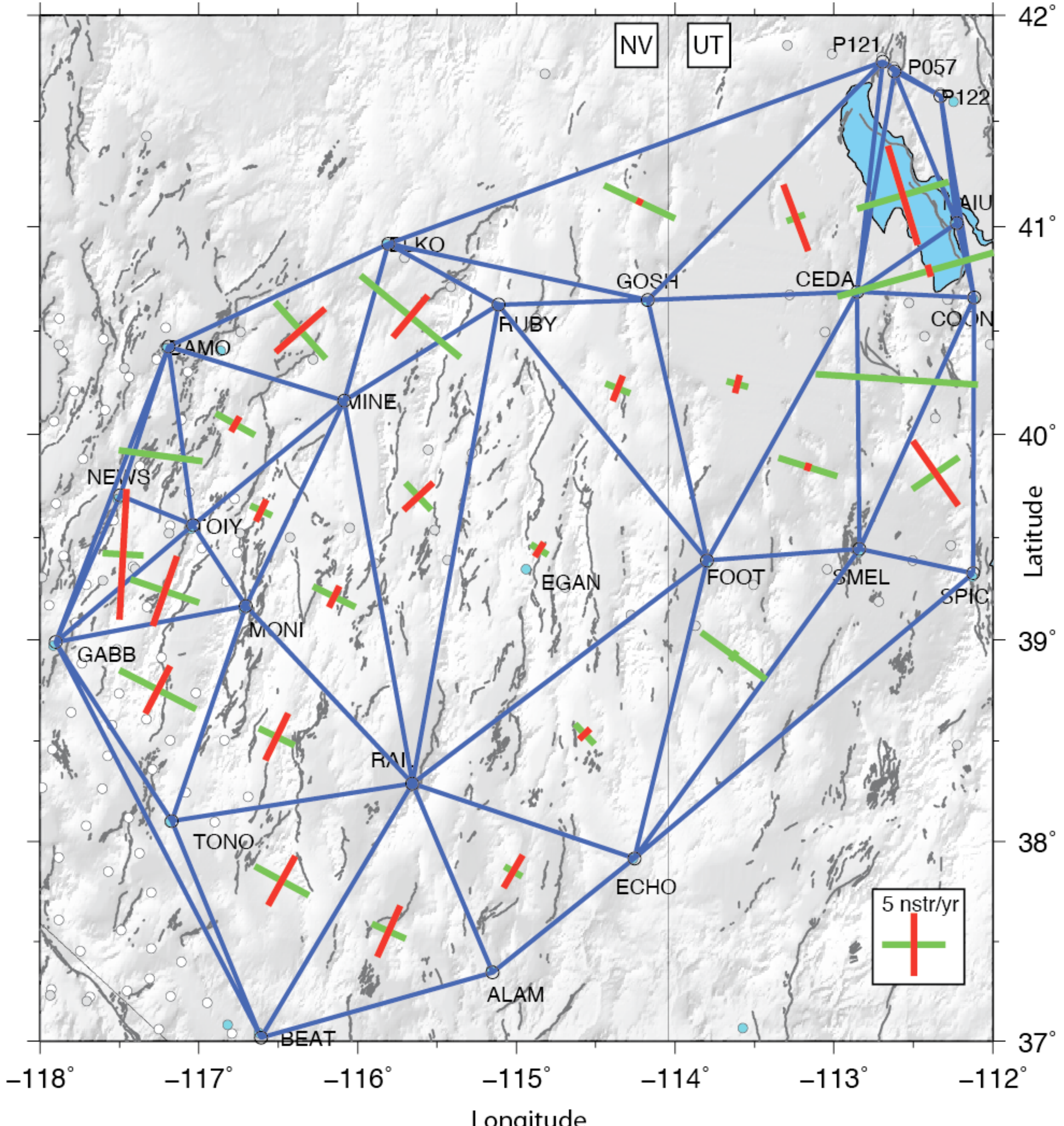

- No Microplates.
- Average system 0.1-0.2 mm/yr
- Great Basin Deforms Everywhere and All the Time

From Hammond et al., 2014 JGR

Dilatational Strain Rate
Net Area Growth
Proto-Rifting

Not change in color scale!
red=net extension
blue=net contraction

- Area growth implies rifting of the lithosphere in the Walker Lane.
- Dilatation harder to image than shear because it is much slower than shear rate. Small difference between two large principal strain rates.
- Viscoelastic relaxation in Central Nevada causes transient dilatation.
- Contraction on flanks characteristic of transient.
- Strain in east NV present but hard to image with this technique.

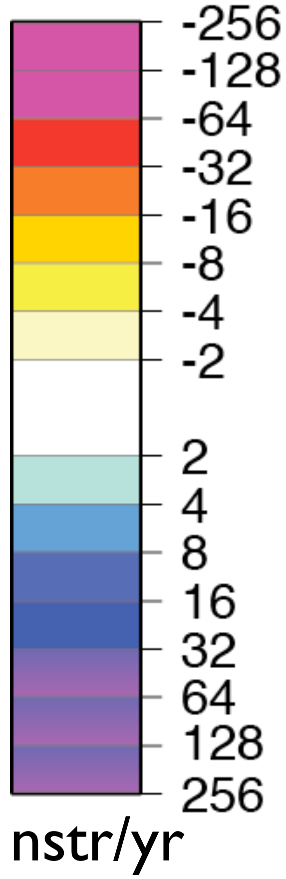

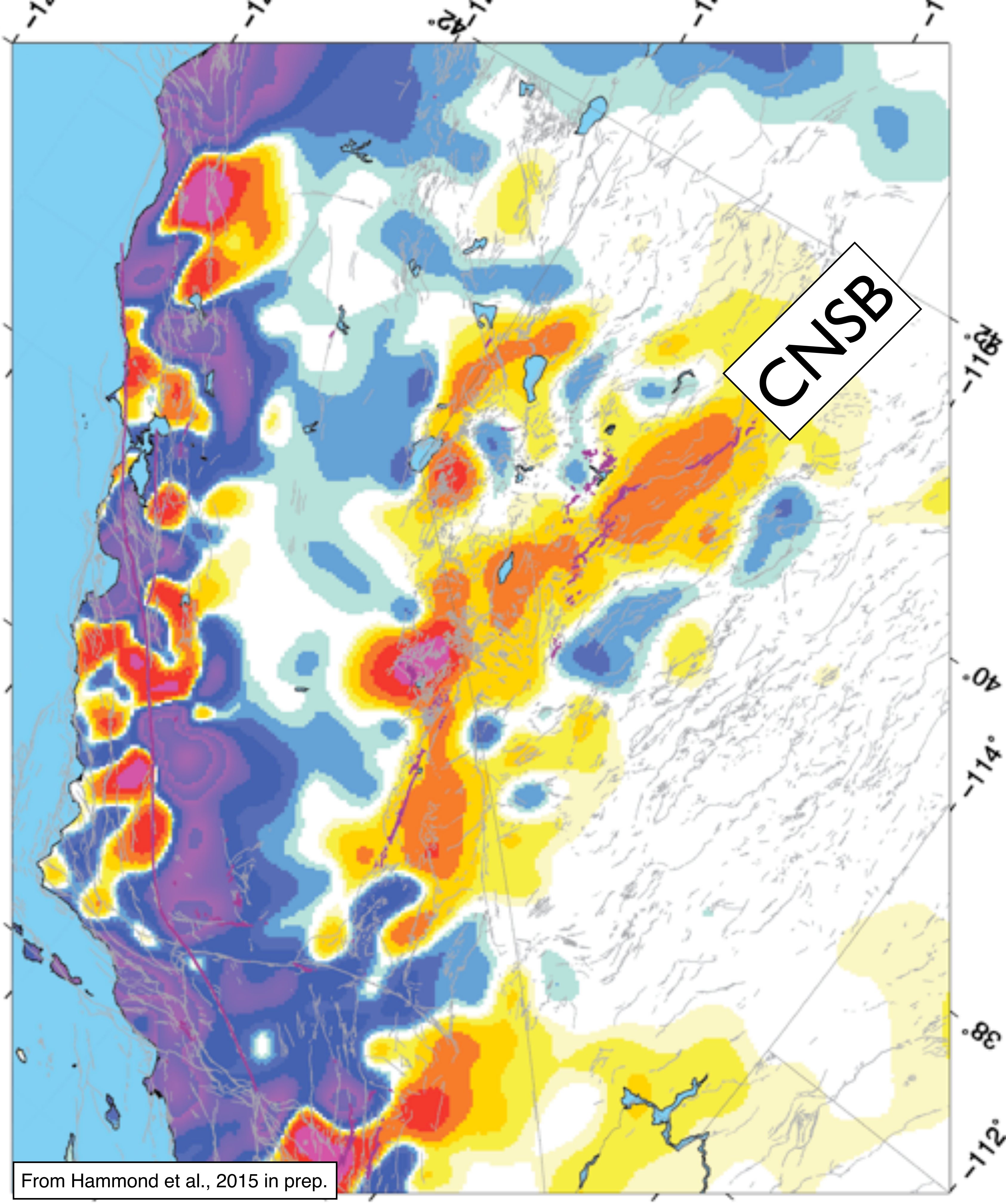

Dilatation Anomaly at CSNB Correlated with Pattern of Vertical Motion Measured with GPS

Dilatation Observed in Horizontal GPS Velocities

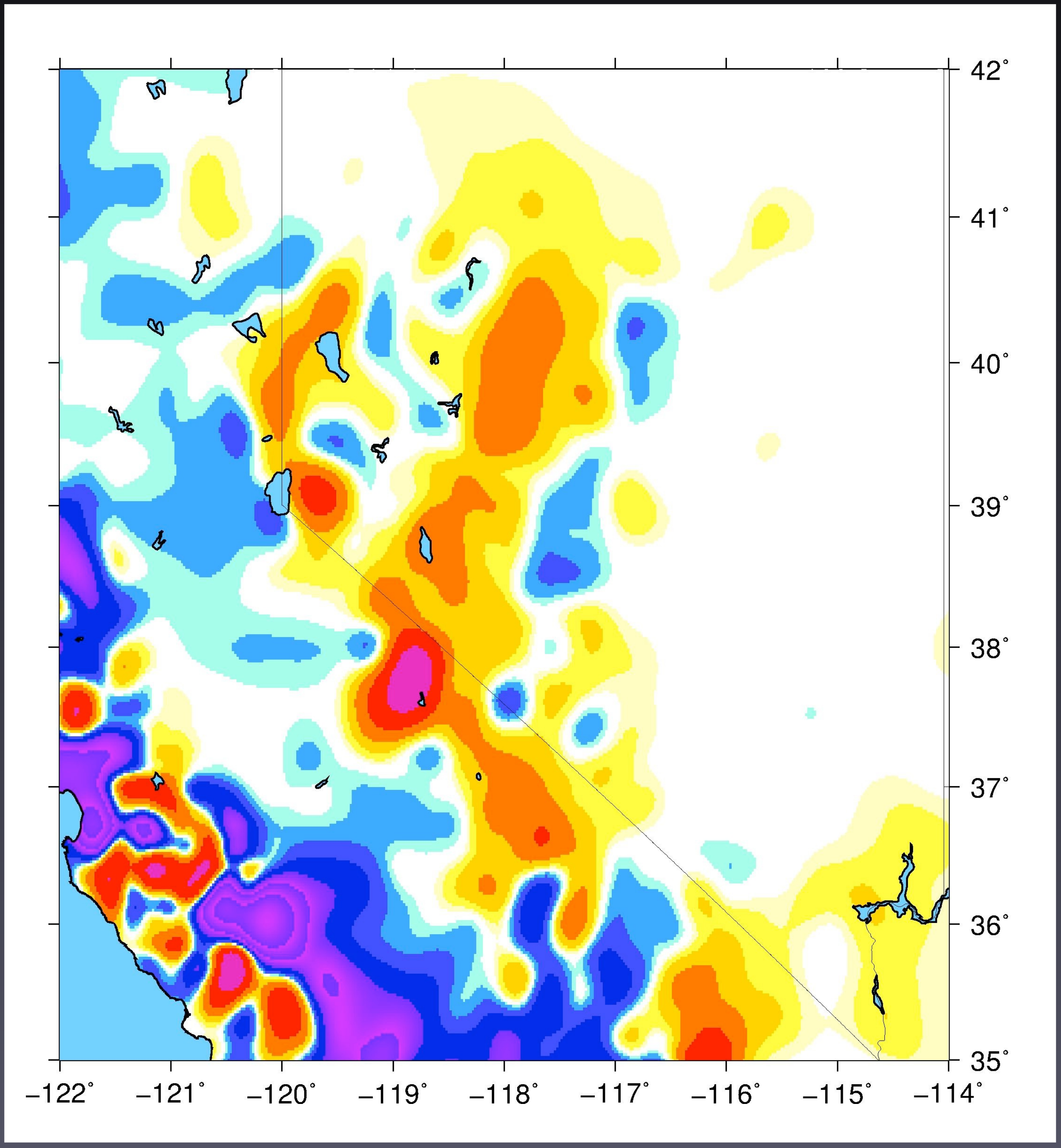

From Kreemer et al., 2012 Strain Rate Map

Vertical GPS Rates Interpolated Using Kriging

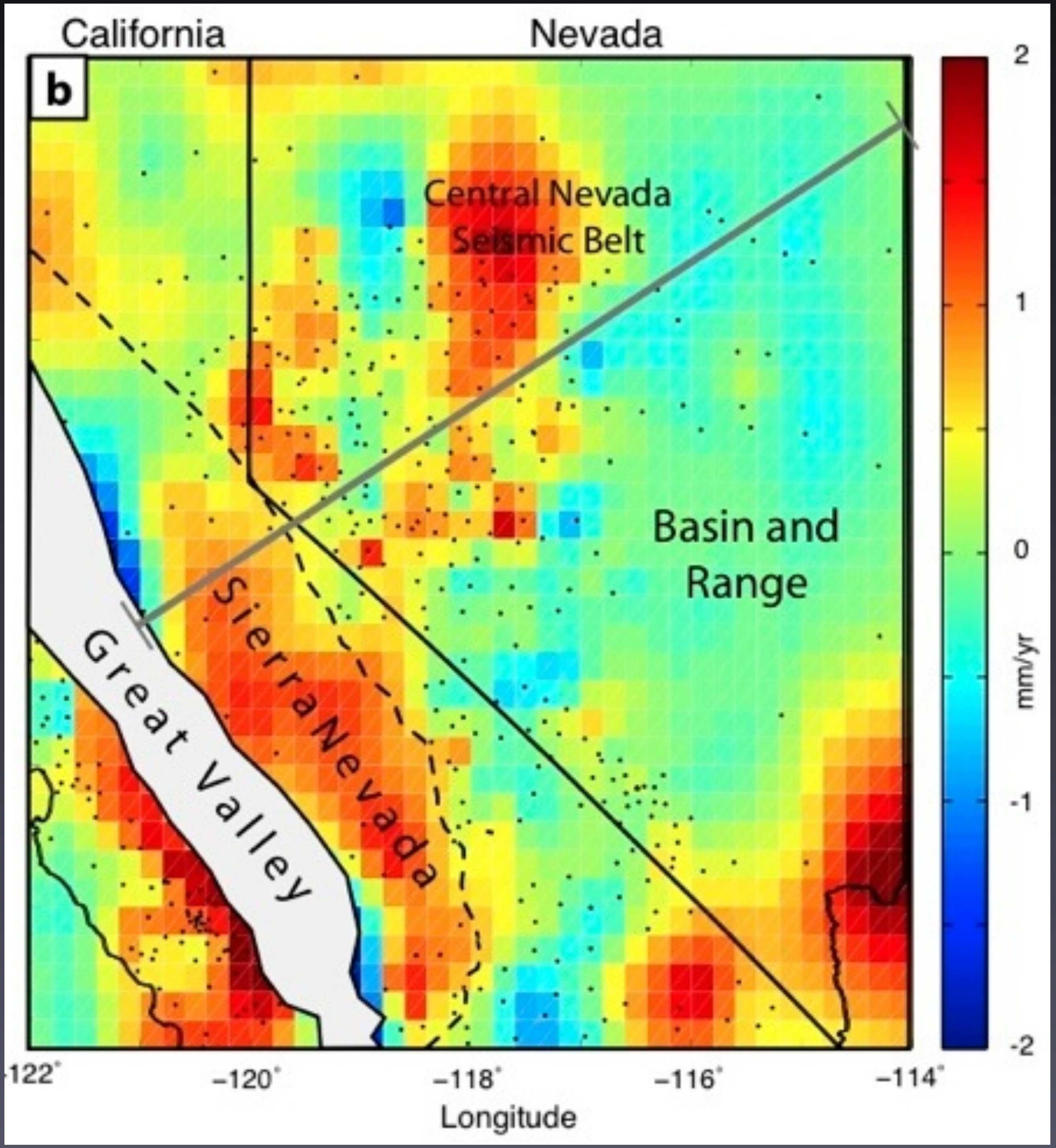

From Hammond et al., 2012 (Geology)

Dilatation Anomaly at CSNB Correlated with Pattern of Vertical Motion Measured with GPS

Dilatation Observed in Horizontal GPS Velocities

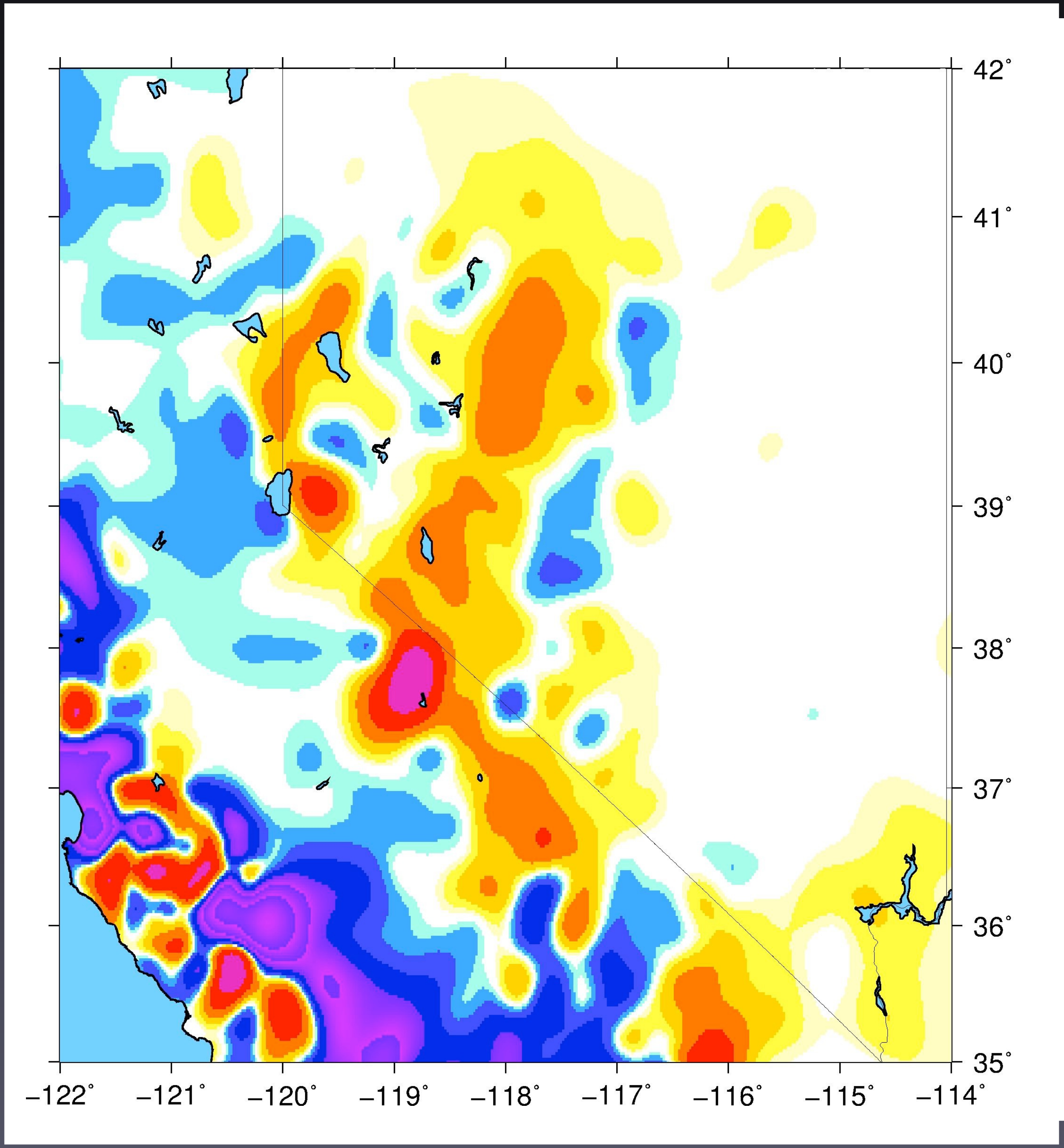

From Kreemer et al., 2012 Strain Rate Map

Viscoelastic Postseismic Relaxation Model

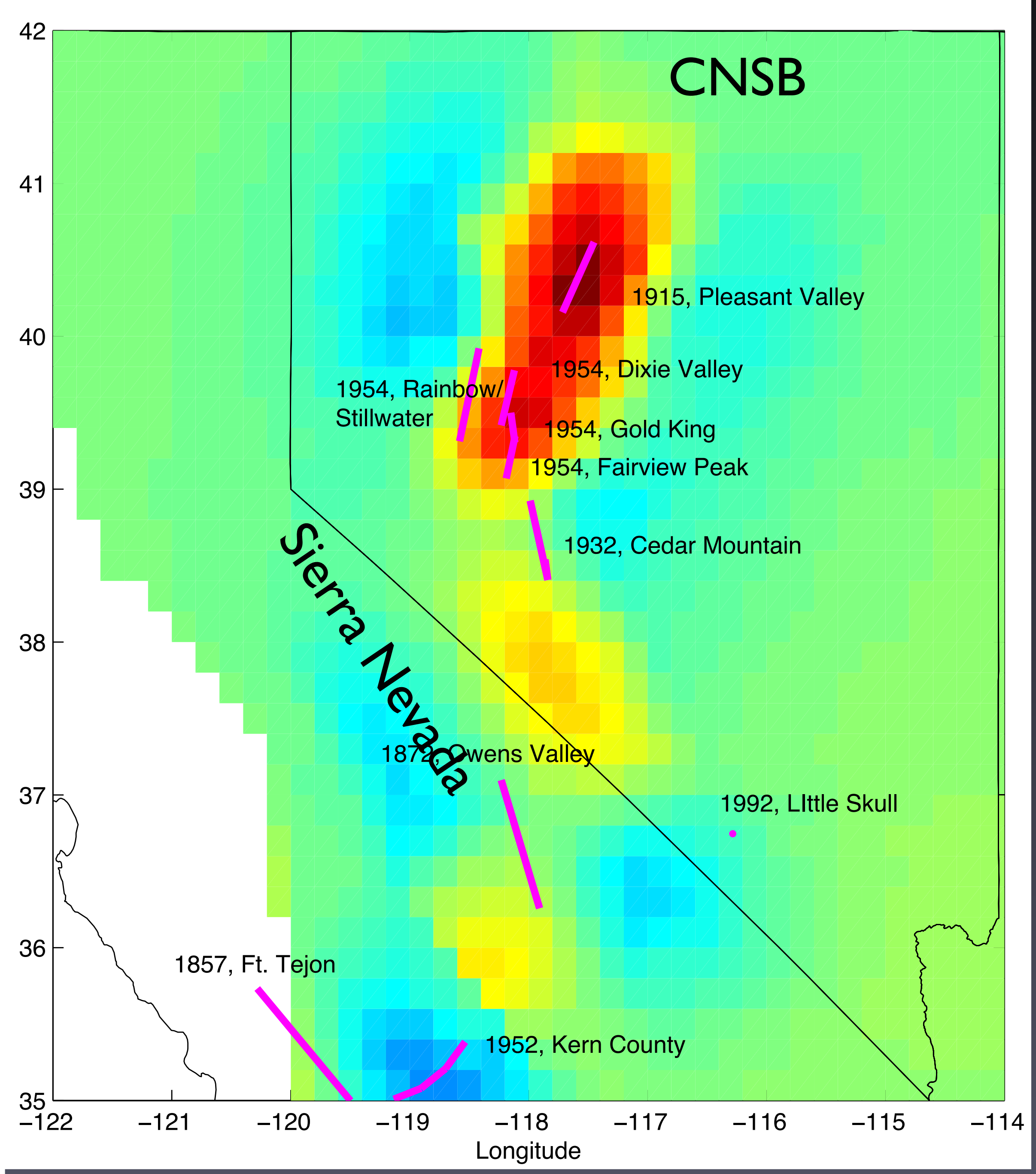

Modeled with VISCO1D (Pollitz, 1997)
with Maxwell viscoelastic rheology

Block Models

The Northern Walker Lane

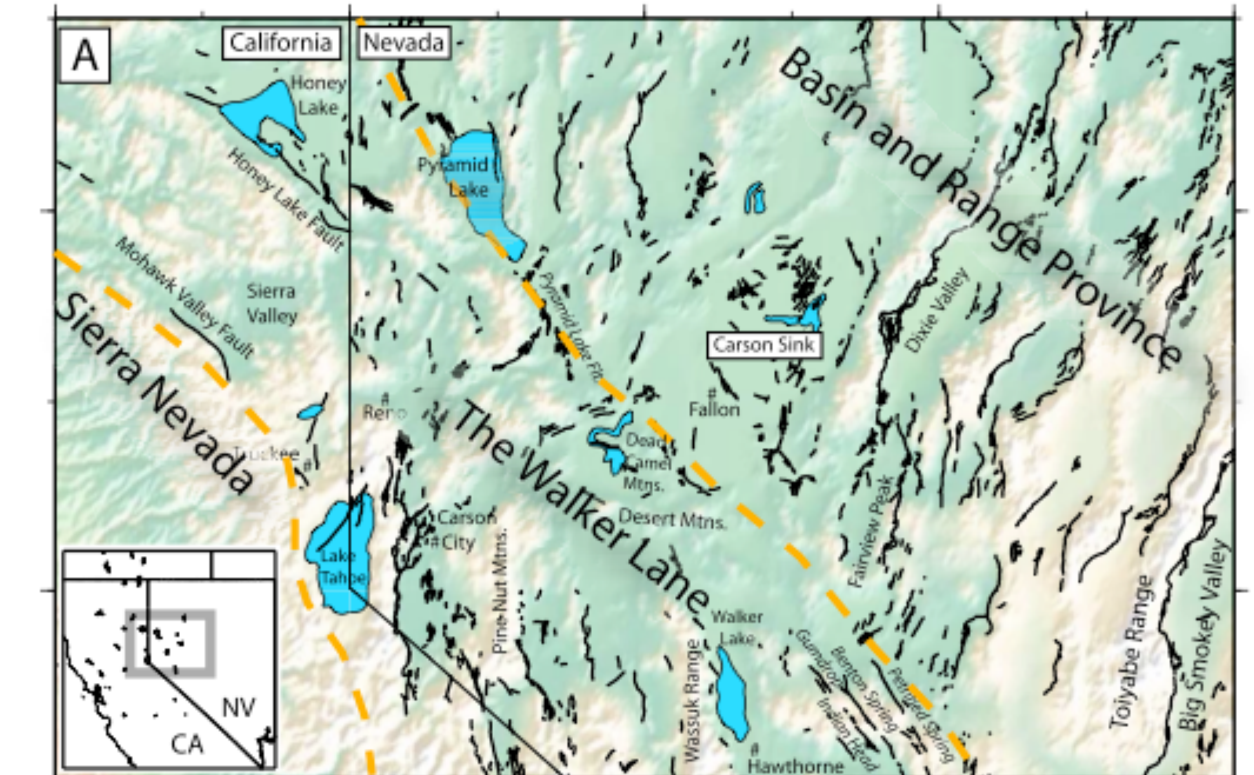

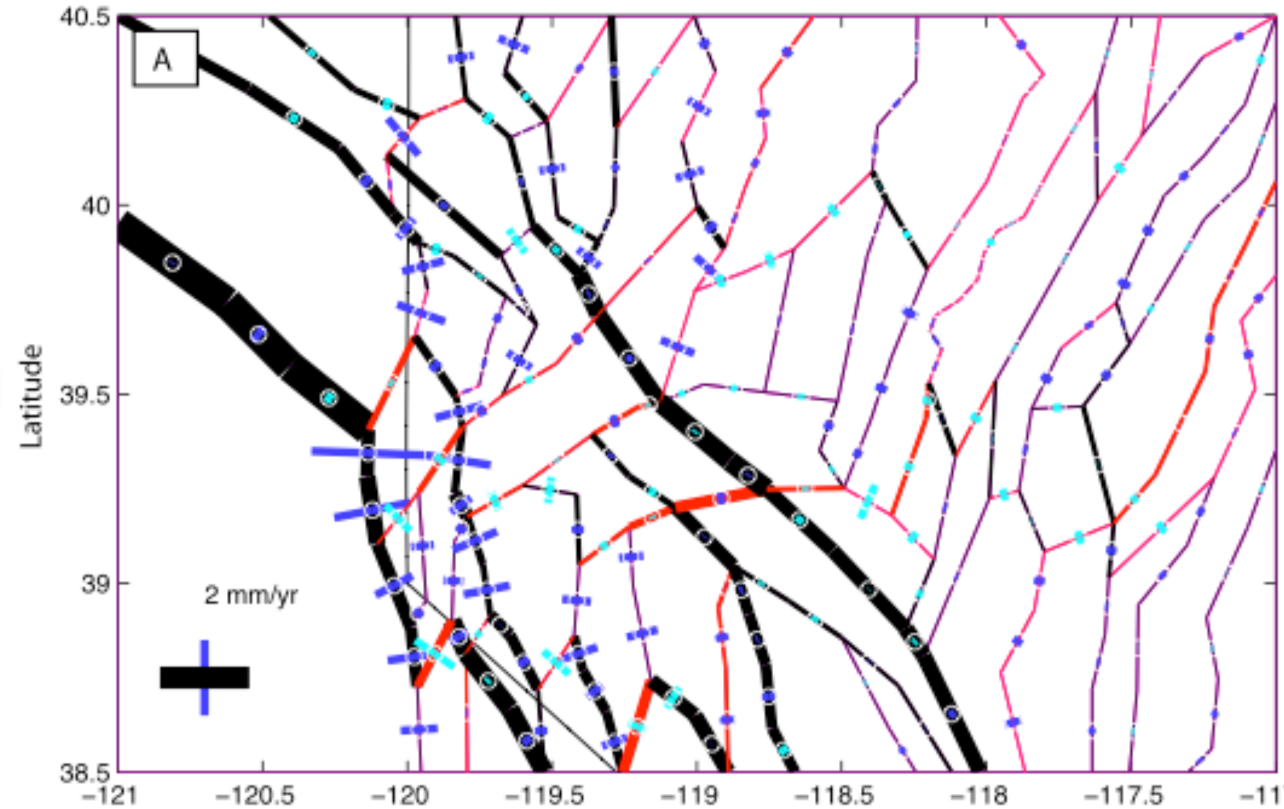

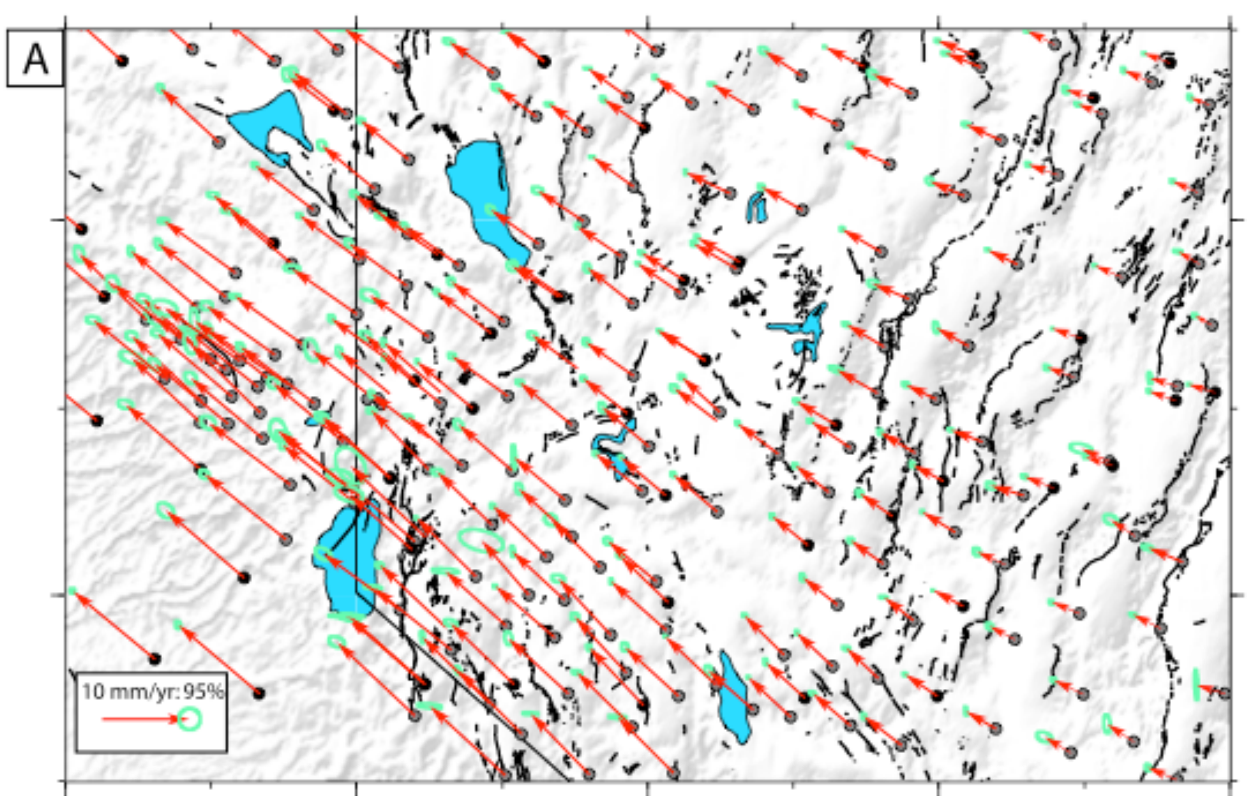

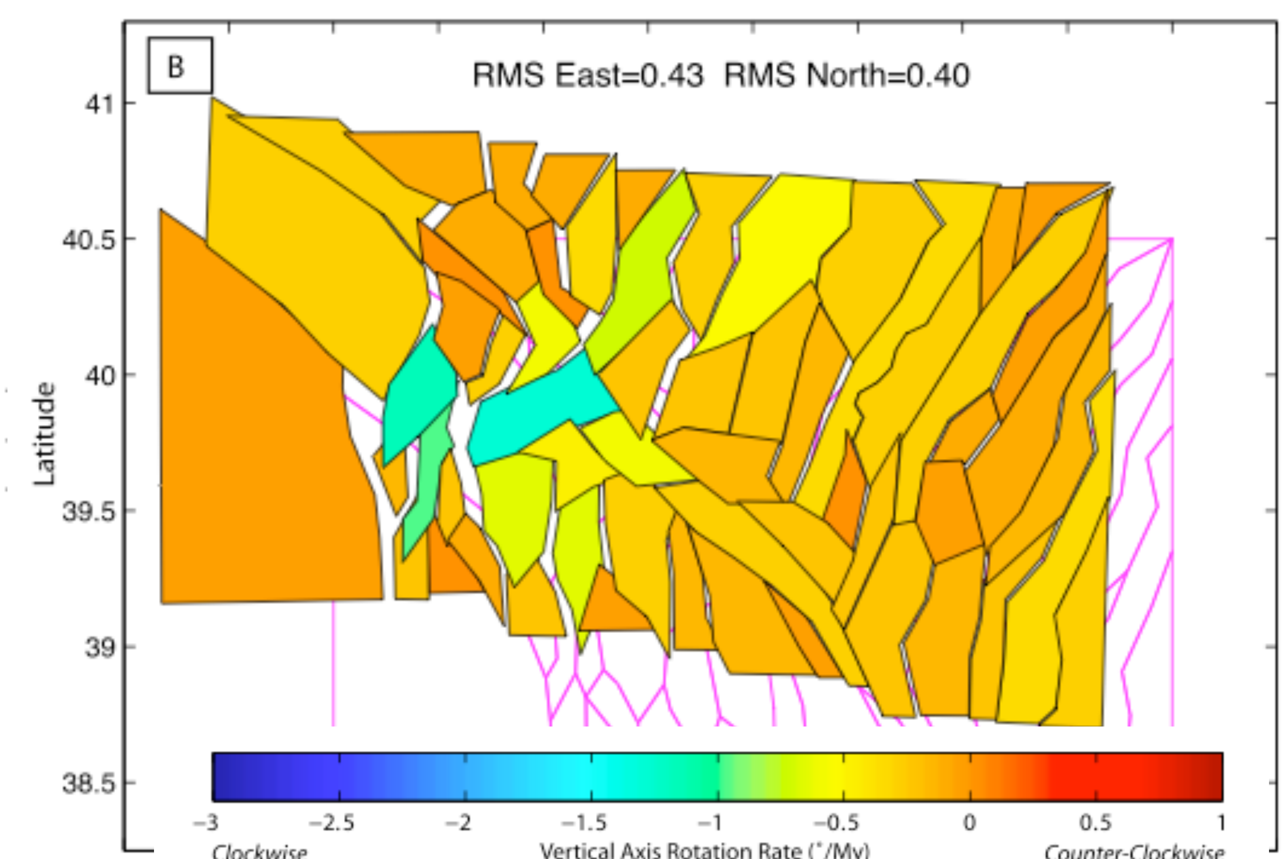

From Hammond et al., 2011 JGR

Geologic vs. Geodetic Slip Rates

Global Major Plate Boundaries

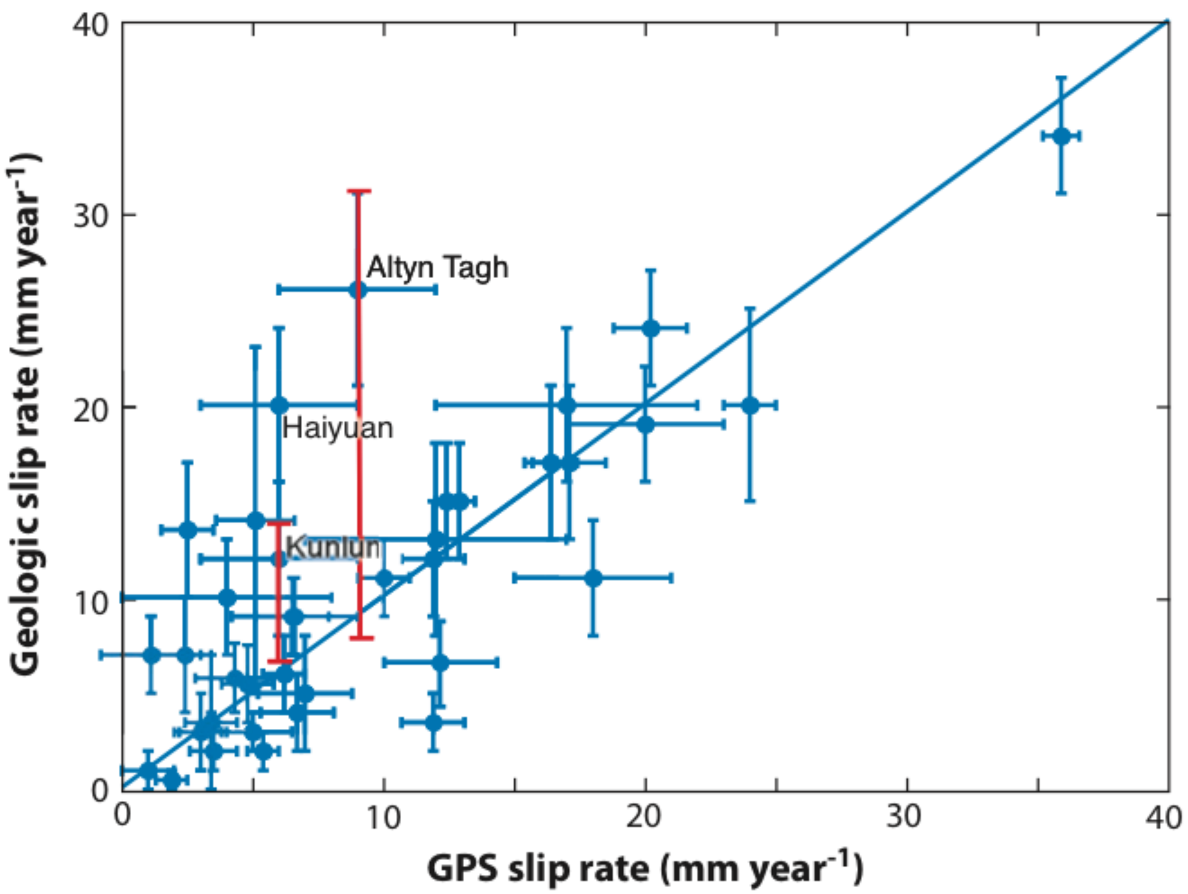

Thatcher, 2009 Ann. Rev. Earth Planet. Sci.

Northern Walker Lane

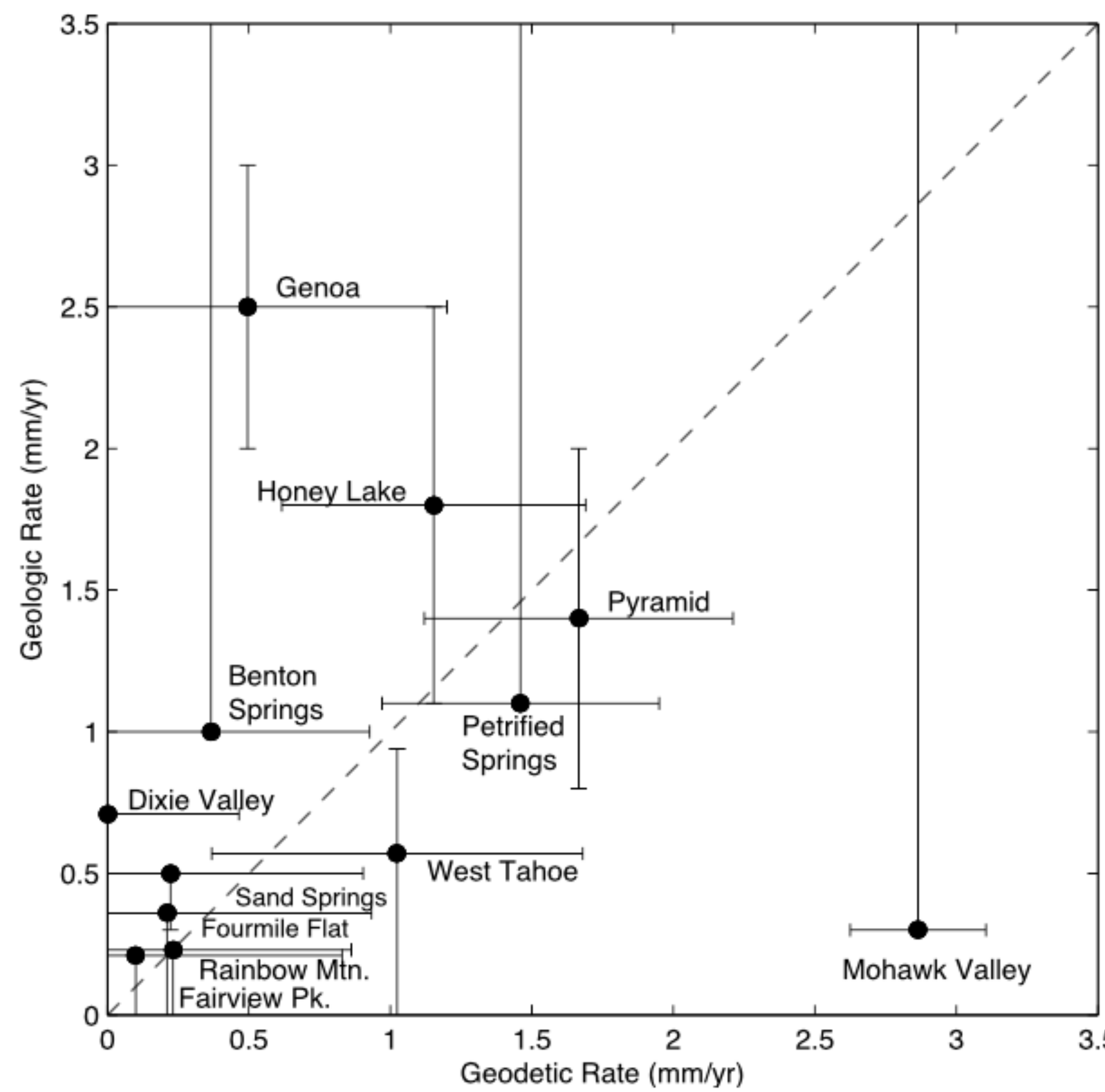

Take a Long Walk Across the Walker Lane

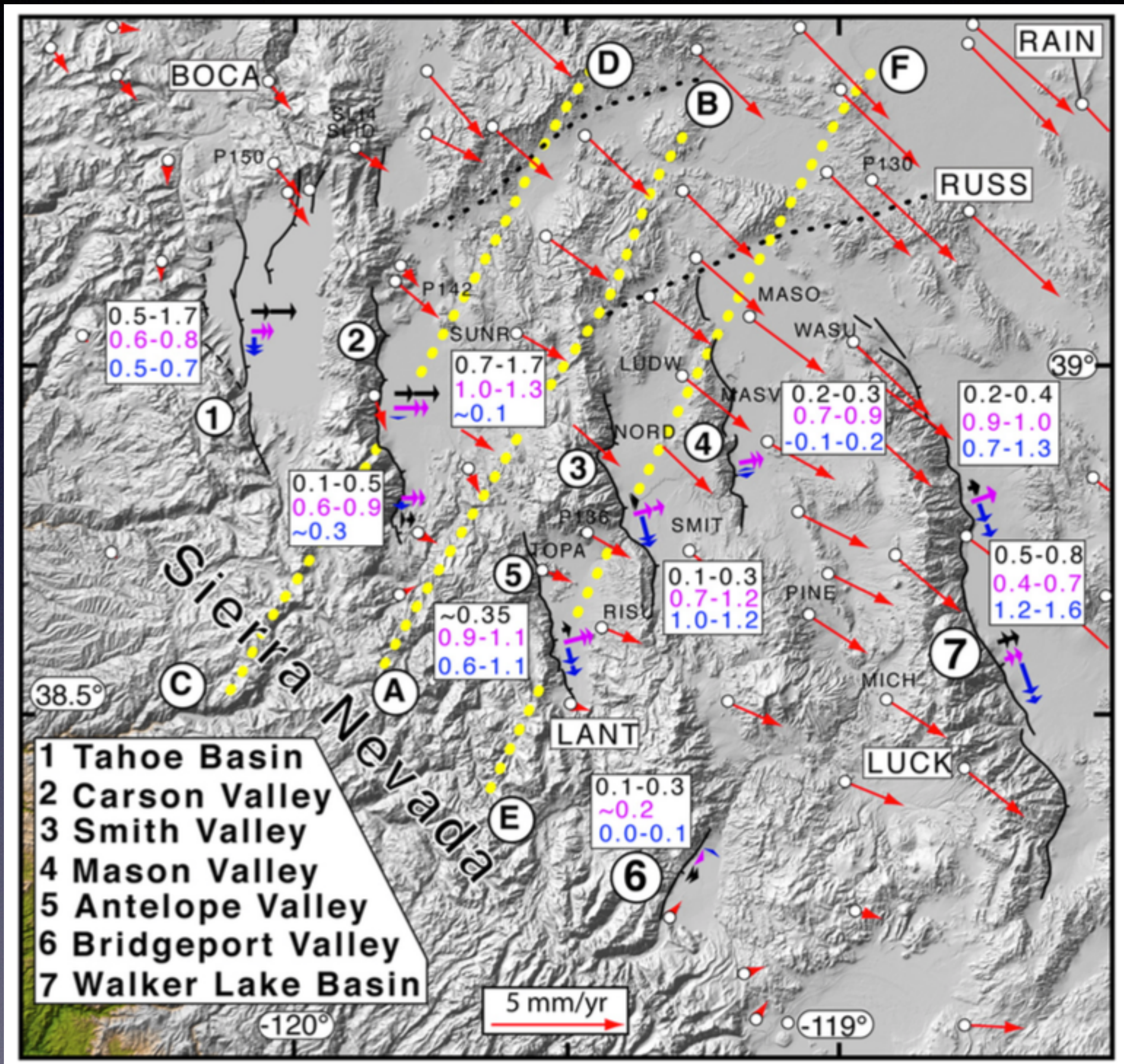

Wesnousky et al., 2012. EPSL

- GPS in *Sierra Nevada Reference Frame* (red vectors) show clearly the shear and tearing.
- Well developed faults can be crossed, or not crossed in transects.
- Detailed comparison with geologic slip rates in at each fault (boxes with numbers). Rates agree in extension direction. *Strike slip is mostly absent in geologic slip rates.*
- Where'd it go? Recently more strike slip found in basins, see e.g. Dong et al., 2014 study of Wassuk.
- Strike slip strain release could be pervasively missing in geologic datasets. Geodesy suggests strike slip could be more likely than normal slip. Owen's Valley waiting to happen?

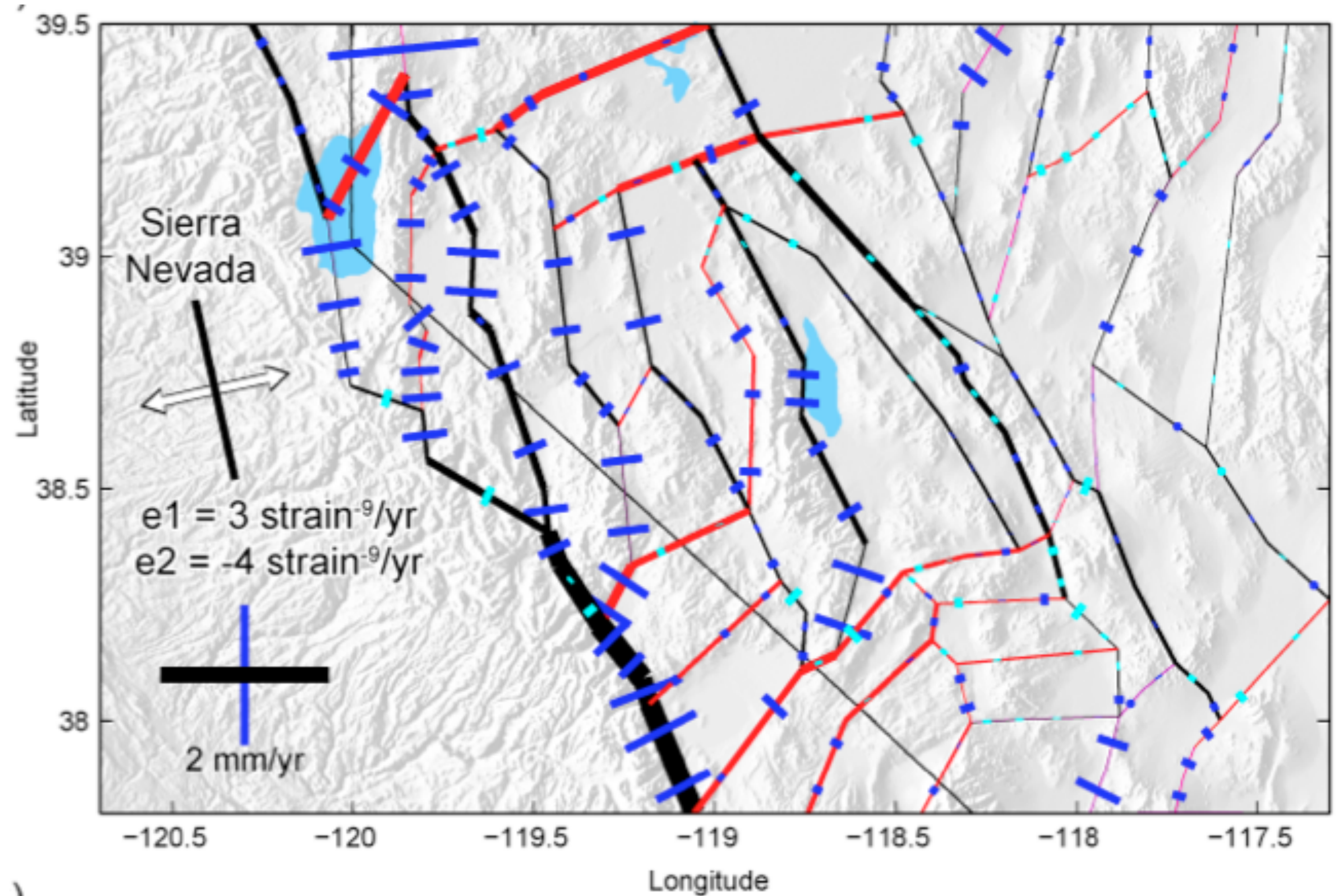

Central Walker Lane

from Jayne Bormann 2013, Ph.D. Diss.

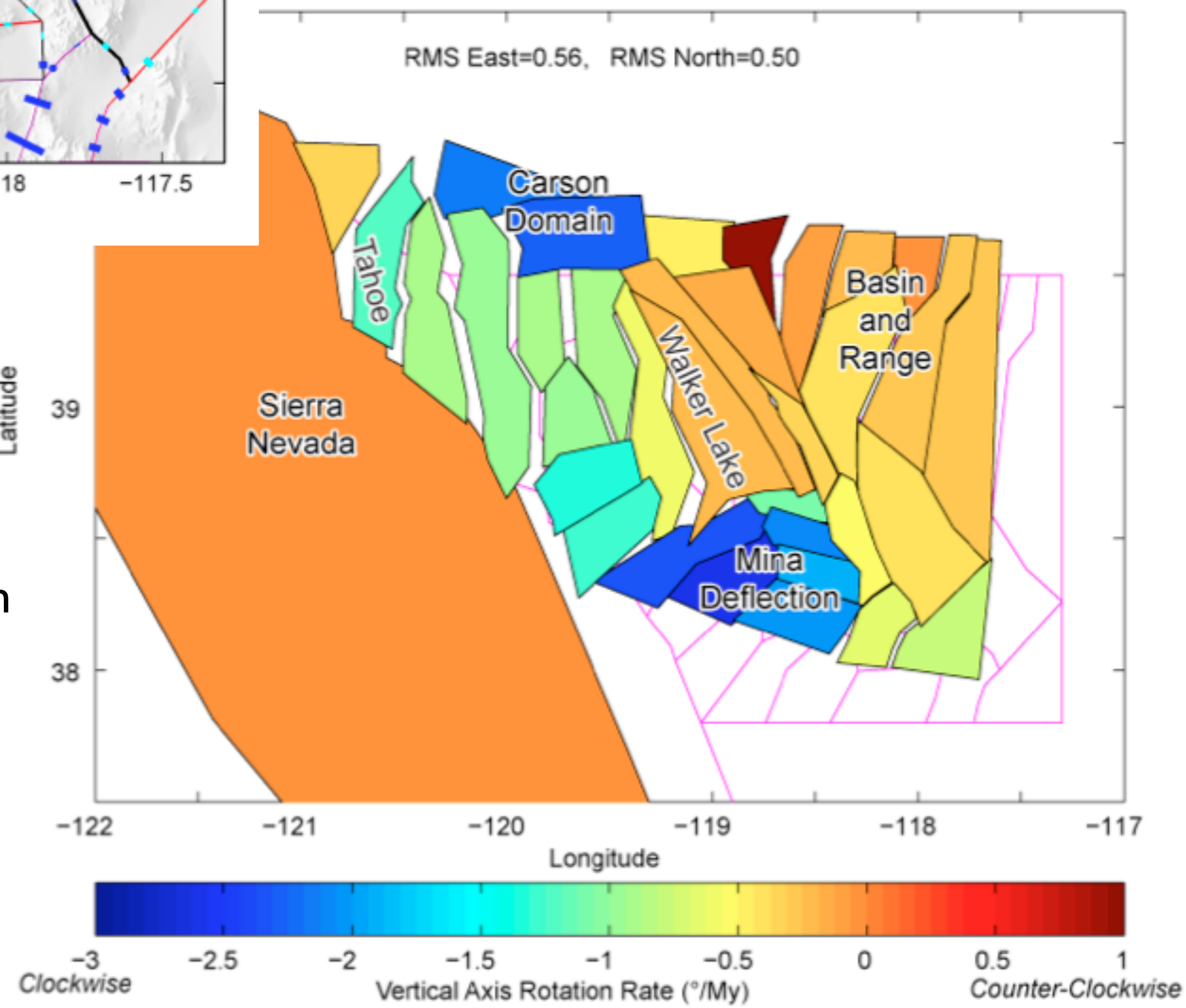

- Estimate rotation rates, fault slip rates from GPS velocities and fault geometries.
- Rotation and slip rate style domains.
- Shear through Tahoe, Carson, Smith Mason Valleys, Walker basin
- Bormann model shows Deformation cannot be accommodated via normal faulting alone, even with block rotations allowed.

Mohawk Valley, Honey Lake, Grizzly Valley

- GPS suggests dextral slip rates of 2.2+/-0.2 mm/yr for Mohawk Valley, 1.1+/-0.4 mm/yr for the Honey Lake Fault.
- Using block models we tested for slip on the Grizzly Valley Fault, a concealed structure exhibiting Quaternary activity (see Gold et al., 2014 JGR)
- Result: GPS data do not require, but allow for slip on the GVF of up to 1.4+/-0.5 mm/yr of slip on this fault. Max slip on GVF reduces Mohawk Valley to 1.6 and HLF to 0.7 mm/yr.
- But introducing the GVF does not explain the mismatch between geologic and geodetic slip rate on Mohawk Valley.

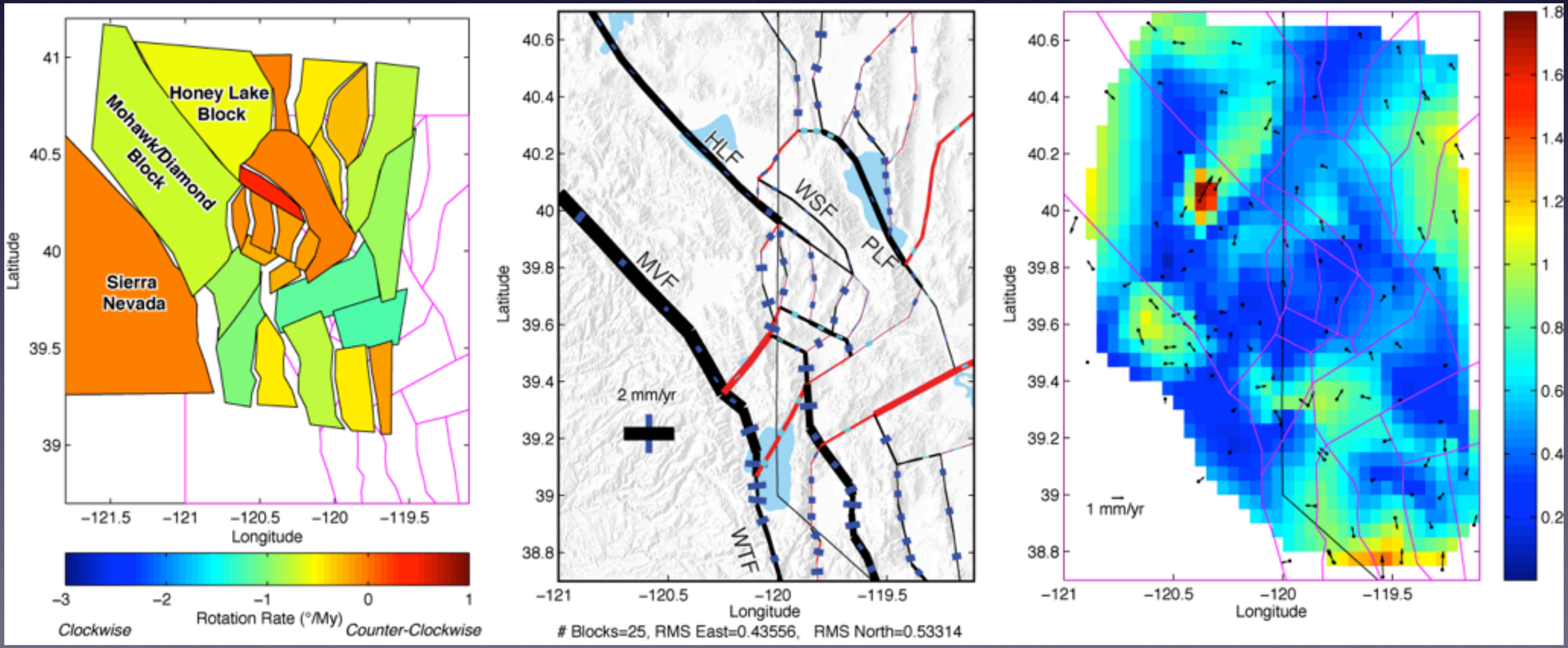

Motion of Blocks Slip Rates Misfit to Data

Mohawk Valley, Honey Lake, Grizzly Valley

- GPS suggests dextral slip rates of 2.2+/-0.2 mm/yr for Mohawk Valley, 1.1+/-0.4 mm/yr for the Honey Lake Fault.
- Using block models we tested for slip on the Grizzly Valley Fault, a concealed structure exhibiting Quaternary activity (see Gold et al., 2014 JGR)
- Result: GPS data do not require, but allow for slip on the GVF of up to 1.4+/-0.5 mm/yr of slip on this fault. Max slip on GVF reduces Mohawk Valley to 1.6 and HLF to 0.7 mm/yr.
- But introducing the GVF does not explain the mismatch between geologic and geodetic slip rate on Mohawk Valley.

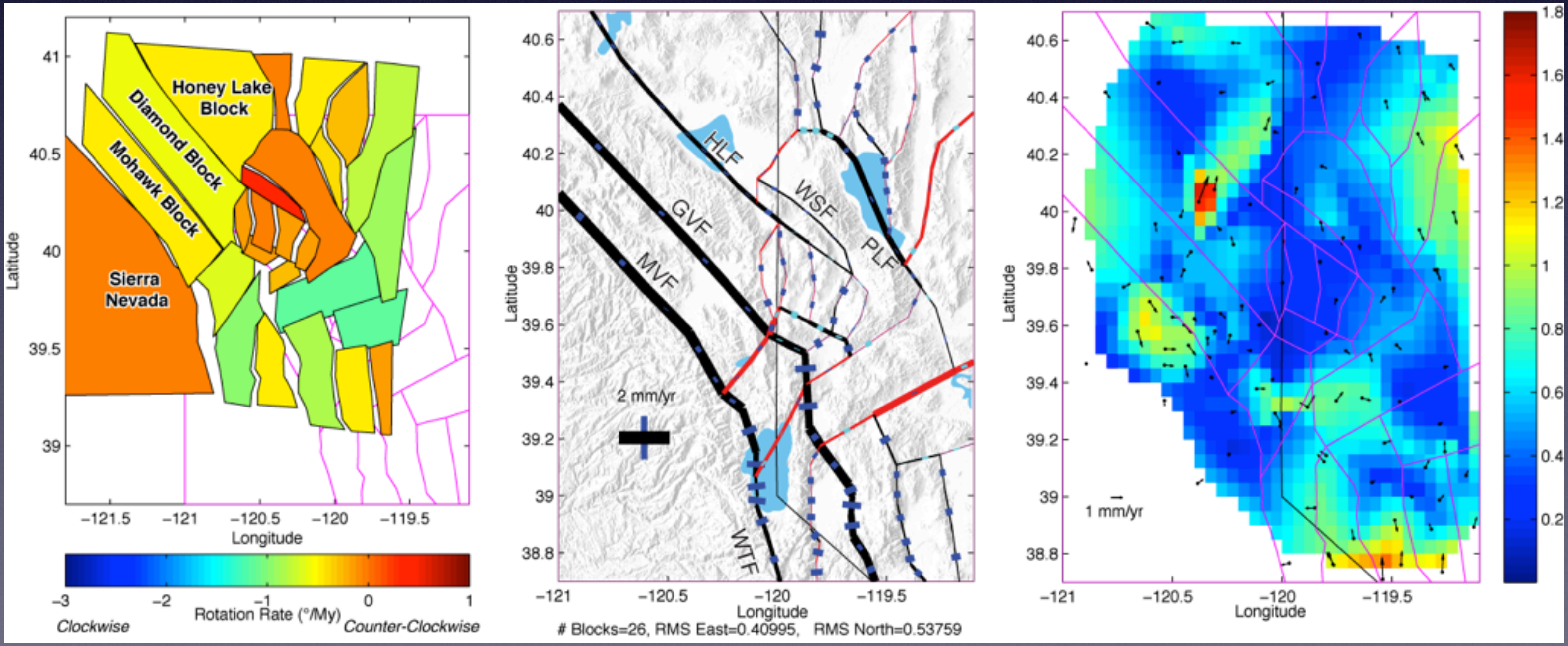

Motion of Blocks Slip Rates Misfit to Data

The New GPS Data Reduce Uncertainties in Slip Rates

Hammond and Thatcher, 2007 uncertainty bounds

Bormann et al., uncertainty bounds

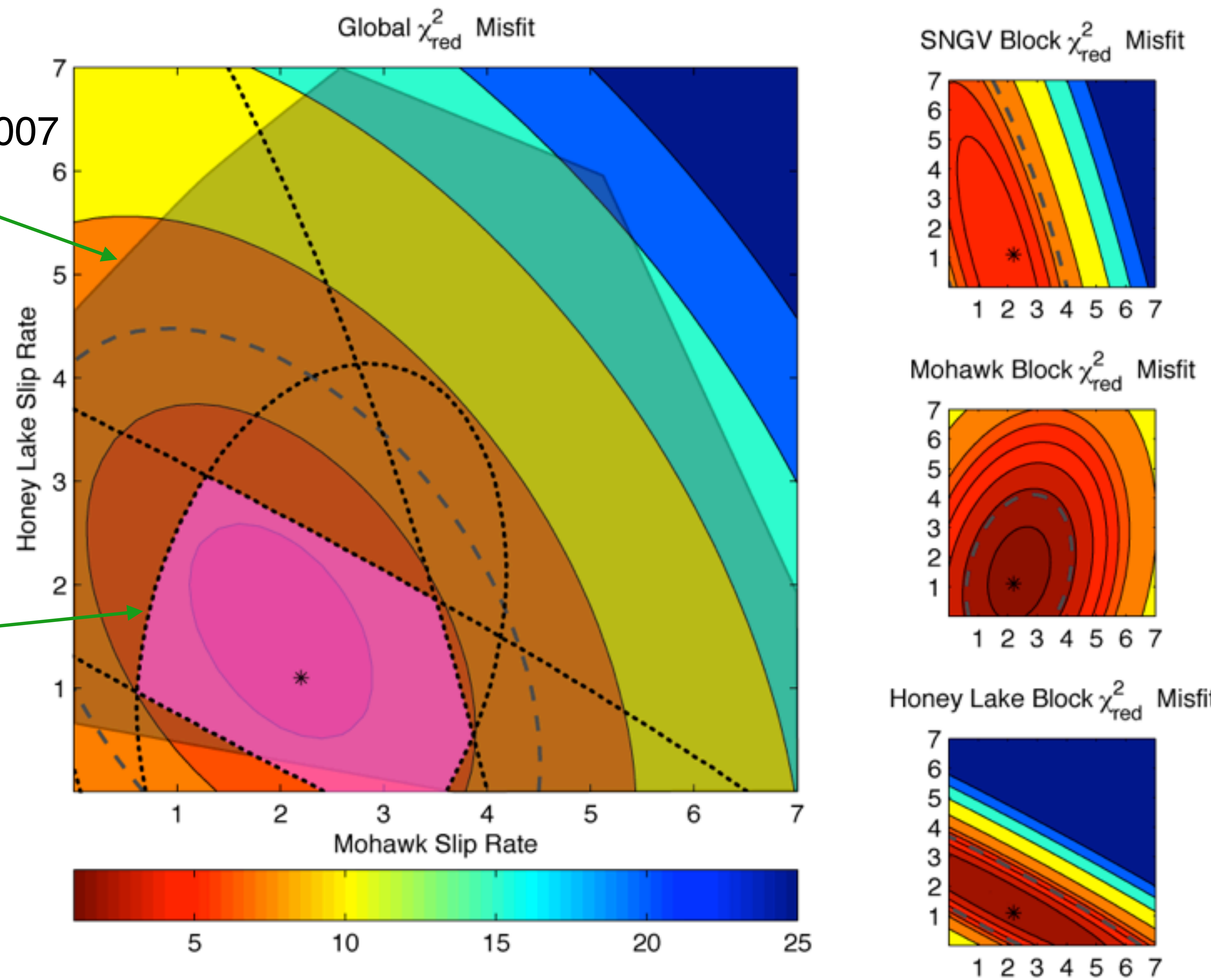

Preliminary Walker Lane Scale Block Model

- Rotational domains (Carson, Mina Deflection, Mojave)
- Left lateral slip rate domains
- Largest slip rates near east/west edges of Walker Lane
- Rotation rates between -2 to 1°/Myr
- Significant but slow strain rates east of Walker Lane

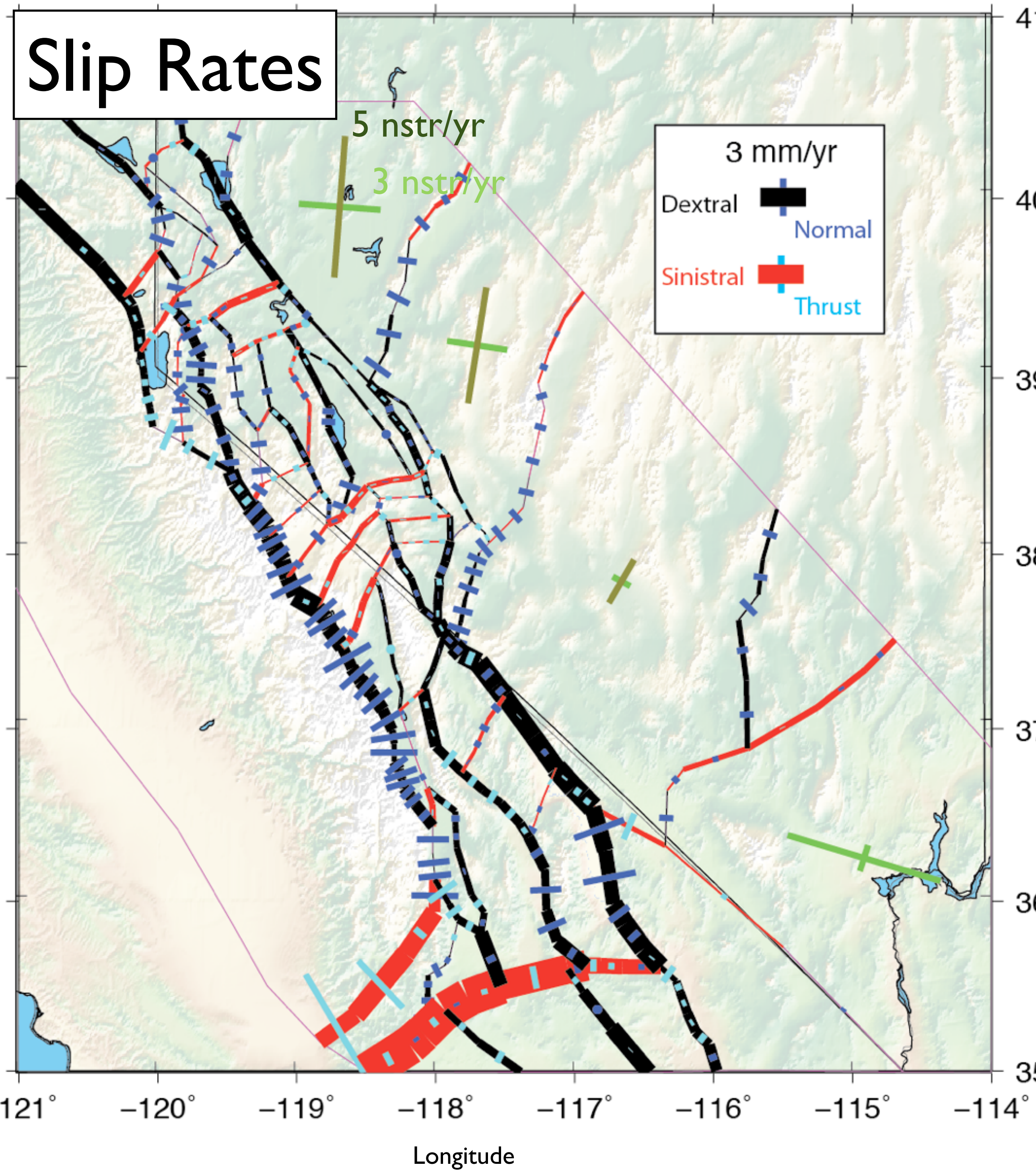

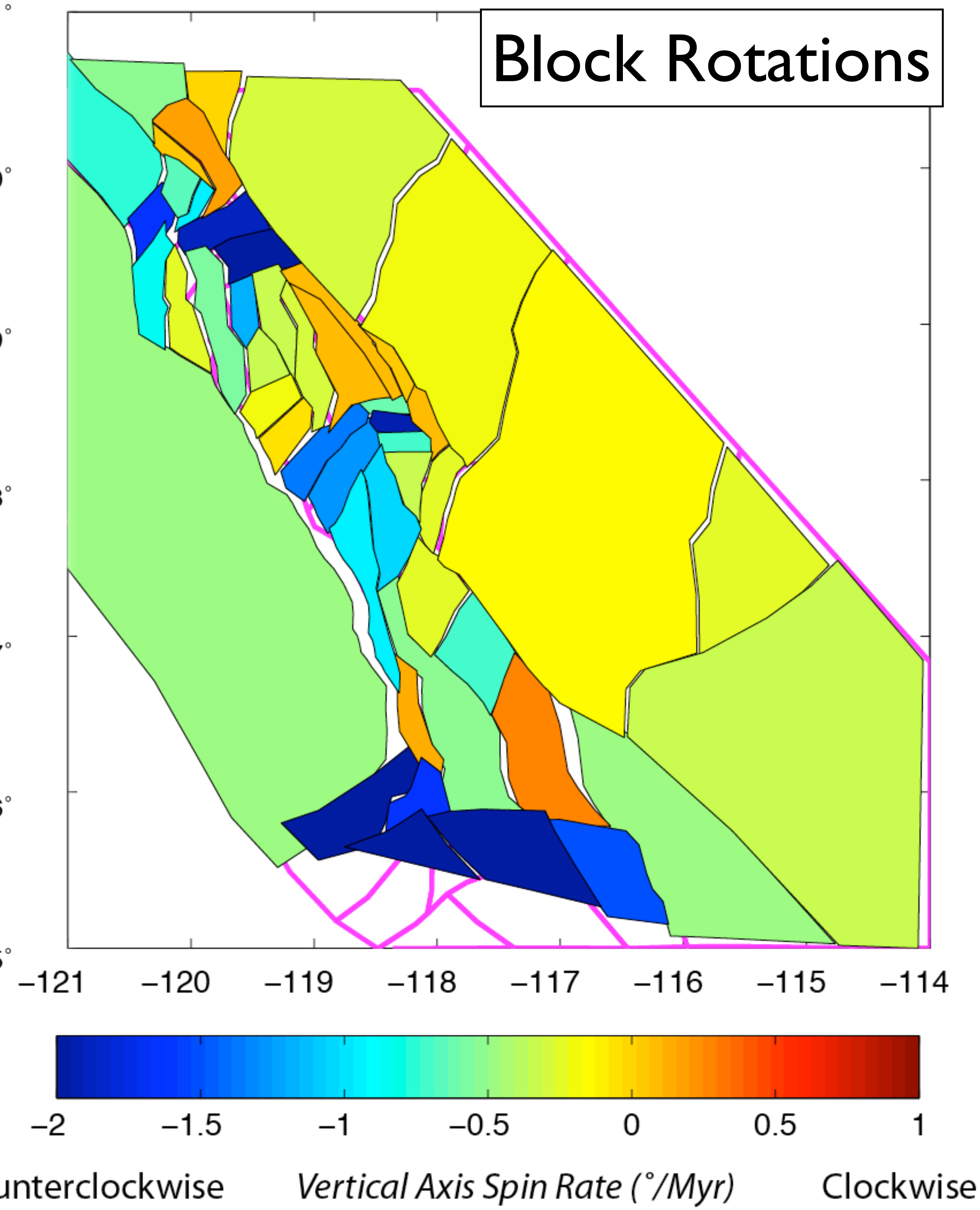

Las Vegas: Densification of GPS Coverage with MAGNET

- Collaboration between the UNR and University of Arizona (with J. Broermann and R.Bennett)
- Complements coverage by EarthScope Plate Boundary Observatory, SCIGN, EBRY GPS networks
- Filling gap between CP and ECSZ
- ~40 new stations surveyed from 2007 to 2014
- Exclude stations with strong perturbations from hydro signals, e.g. in Las Vegas Valley.

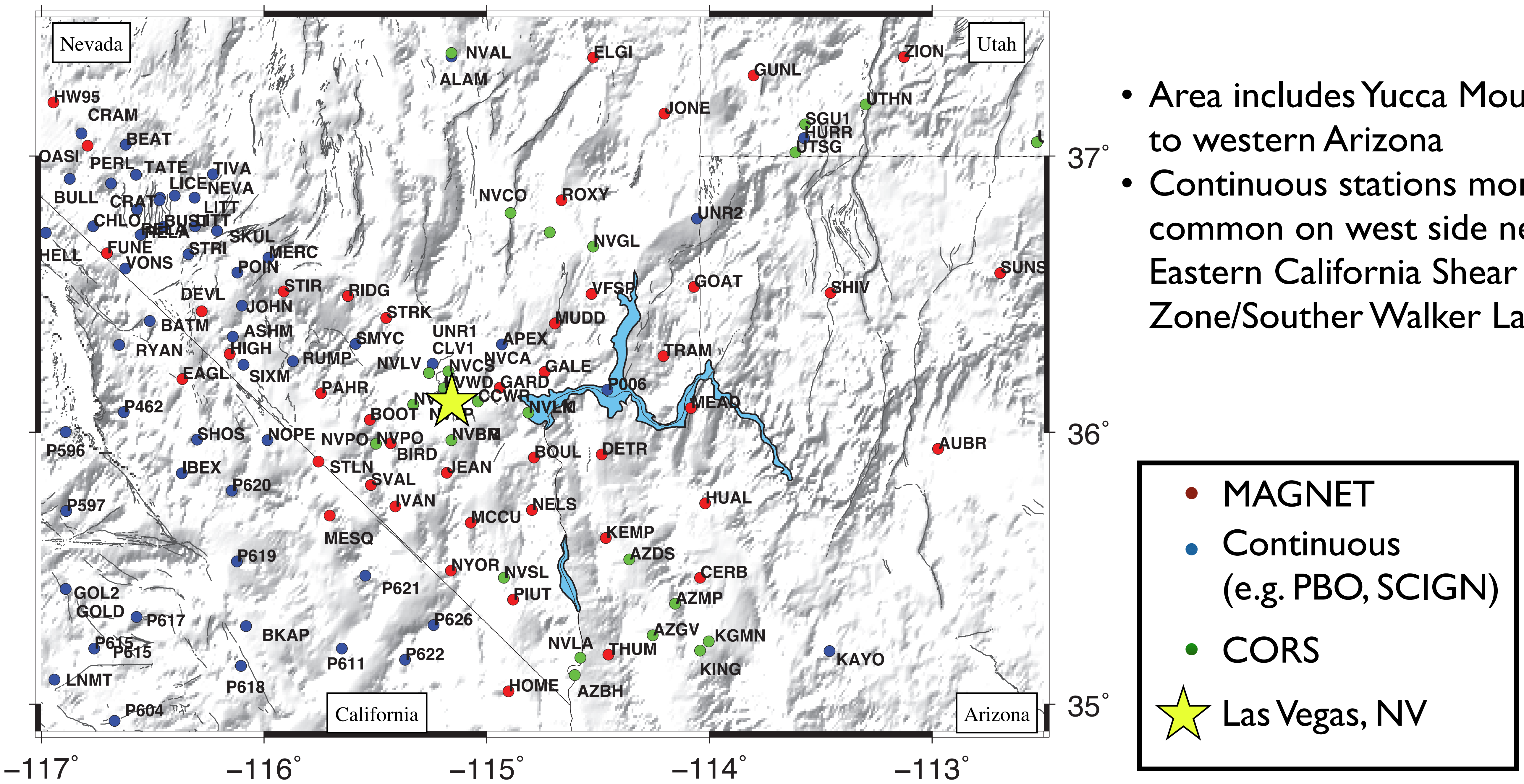

- Area includes Yucca Mountain to western Arizona
- Continuous stations more common on west side near Eastern California Shear Zone/Souther Walker Lane

Velocities in North America Reference Frame

- NA12 Reference Frame (Blewitt et al. 2013)
- Uncertainties including power law noise (explored using CATS and Hector softwares Williams et al., 2003, Bos et al., 2012)
- Gradual increase of west and north velocity from east to west
- Rotation of azimuths northwest closer to ECSZ/Walker Lane

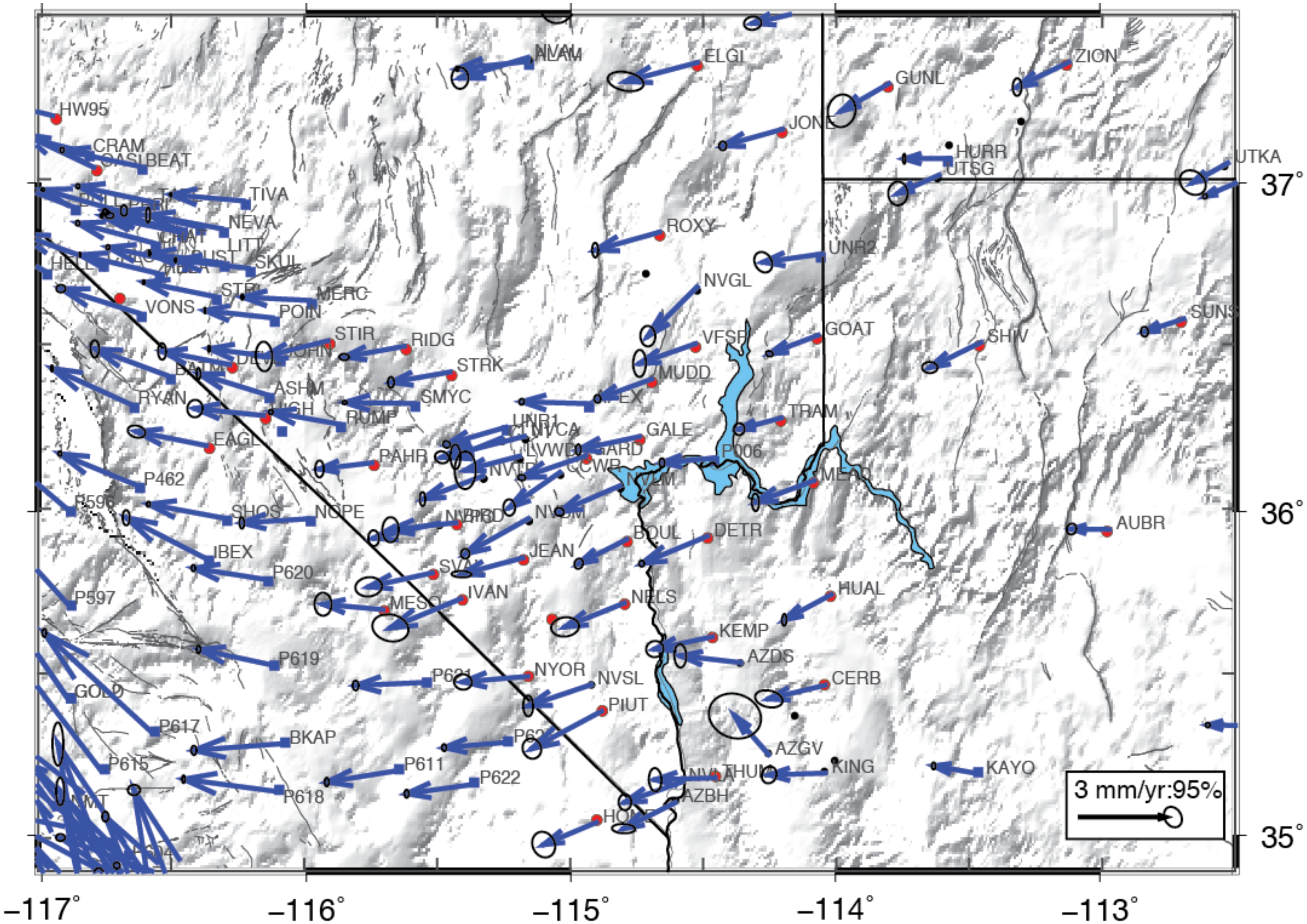

Velocities in North America Reference Frame

- NA12 Reference Frame (Blewitt et al. 2013)
- Uncertainties including power law noise (explored using CATS and Hector softwares Williams et al., 2003, Bos et al., 2012)
- Gradual increase of west and north velocity from east to west
- Rotation of azimuths northwest closer to ECSZ/Walker Lane

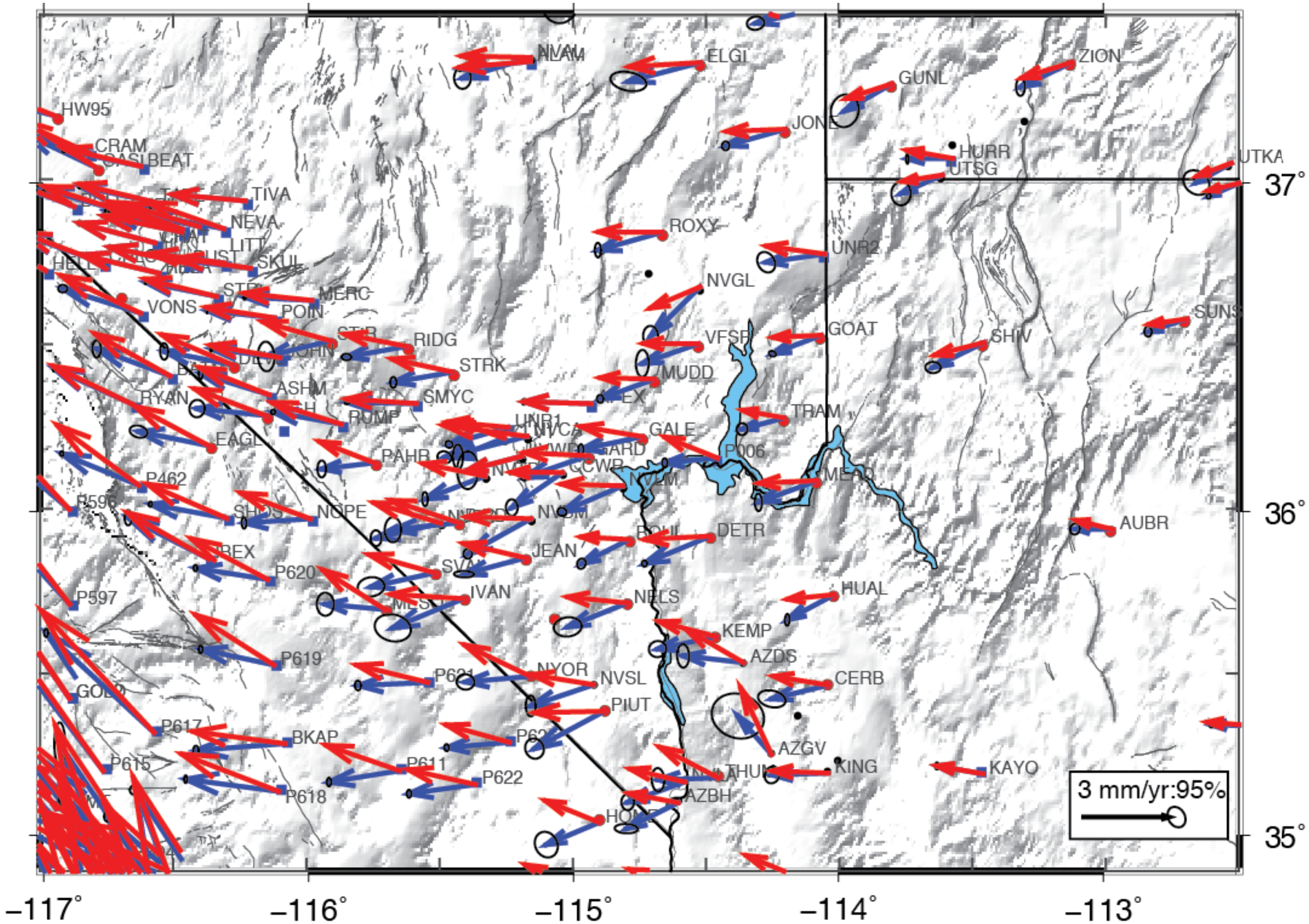

Correction for postseismic

- Increases north component of velocity, changing sign of component for most of southern Nevada
- Rotates velocity azimuths CW
- Correction is *smooth* so has relatively little effect on individual slip rates
- Velocity profile shows Las Vegas Valley lies within zone of north velocity gradient

Velocities in North America Reference Frame

- NA12 Reference Frame (Blewitt et al. 2013)
- Uncertainties including power law noise (explored using CATS and Hector softwares Williams et al., 2003, Bos et al., 2012)
- Gradual increase of west and north velocity from east to west
- Rotation of azimuths northwest closer to ECSZ/Walker Lane

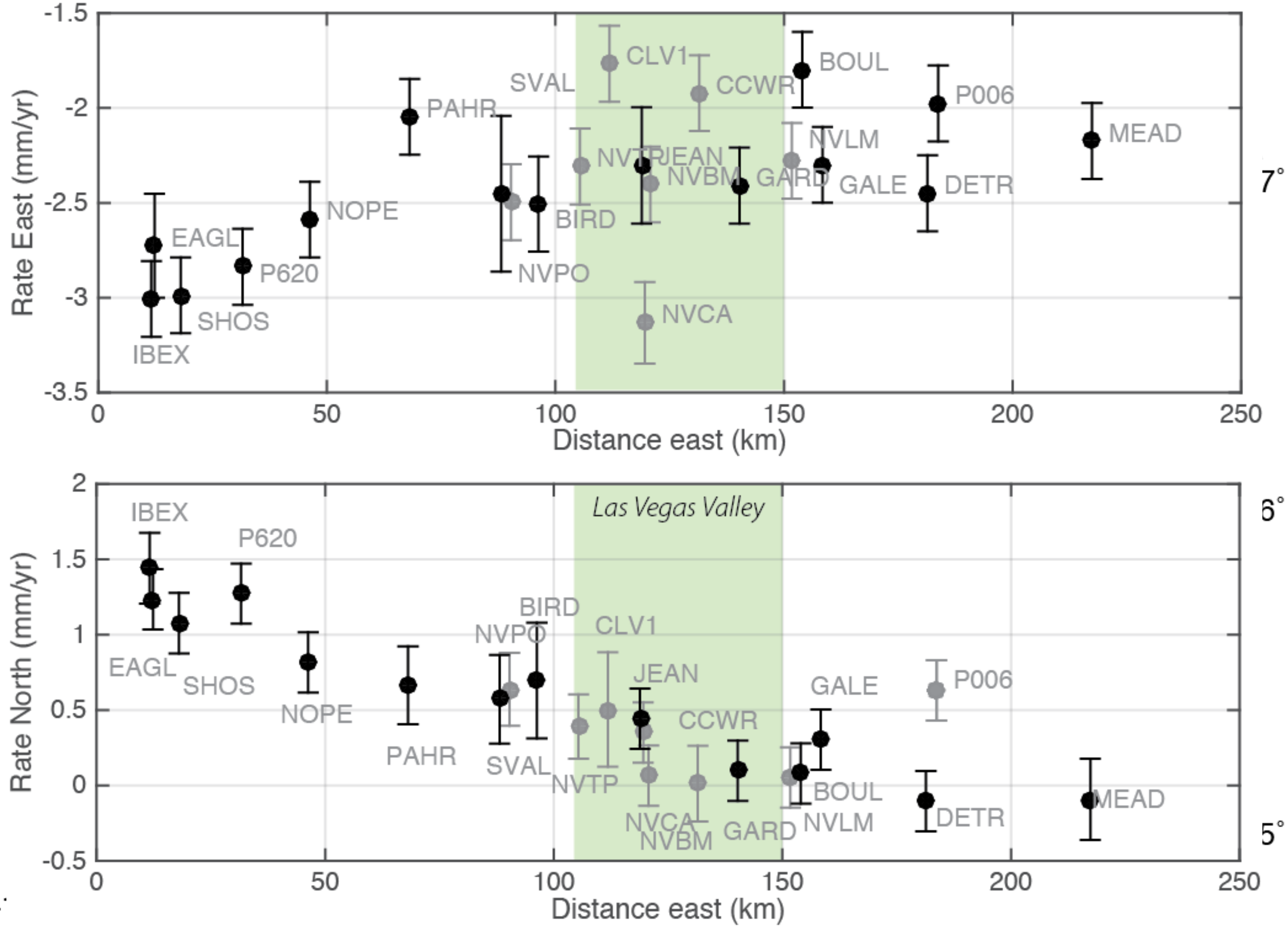

Correction for postseismic

- Increases north component of velocity, changing sign of component for most of southern Nevada
- Rotates velocity azimuths CW
- Correction is *smooth* so has relatively little effect on individual slip rates
- Velocity profile shows Las Vegas Valley lies within zone of north velocity gradient

Block Model: Slip Rates and Rotation Rates Constrained by GPS

in transition from Colorado Plateau to Eastern California Shear Zone

Slip Rates

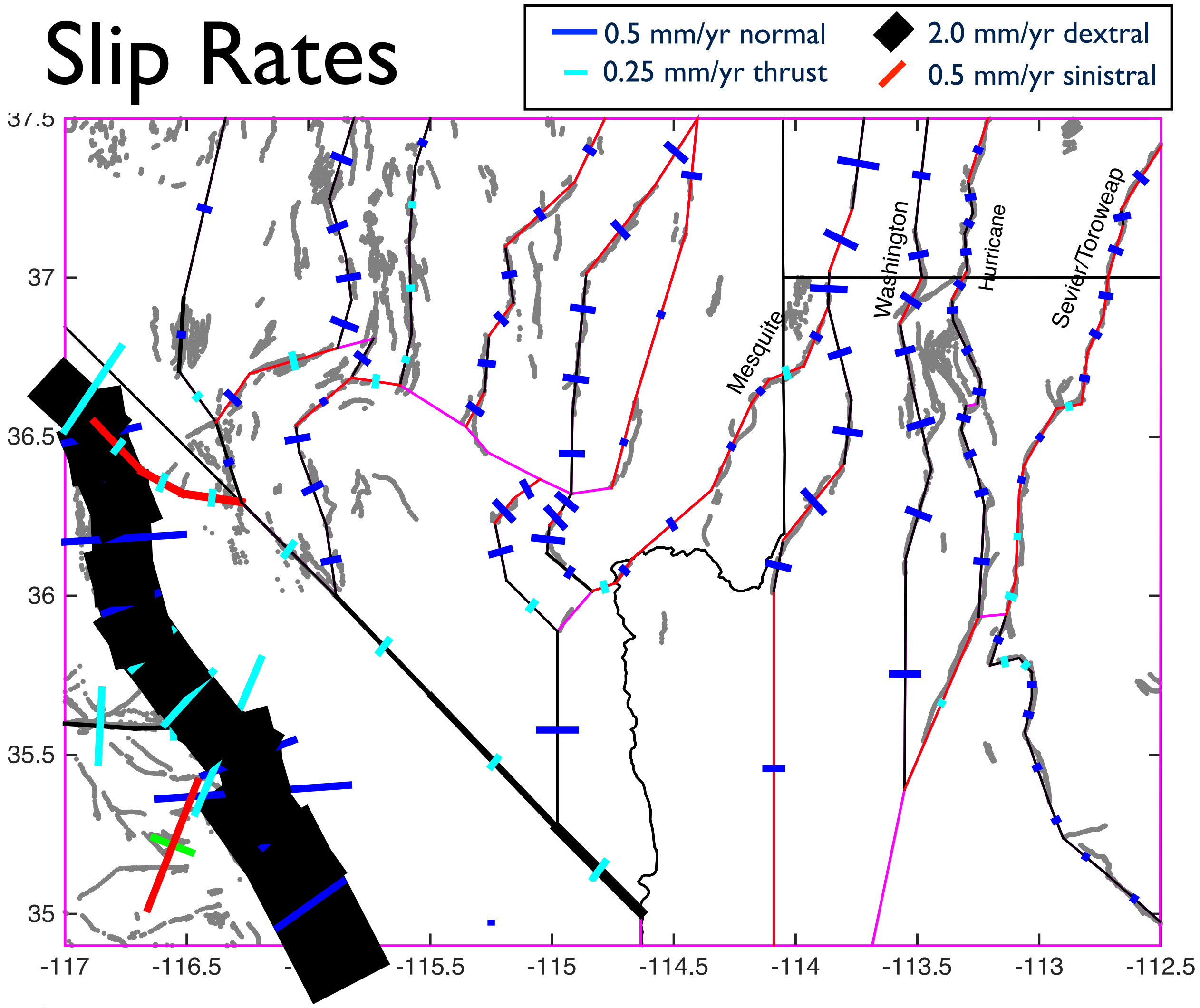

Block Rotations

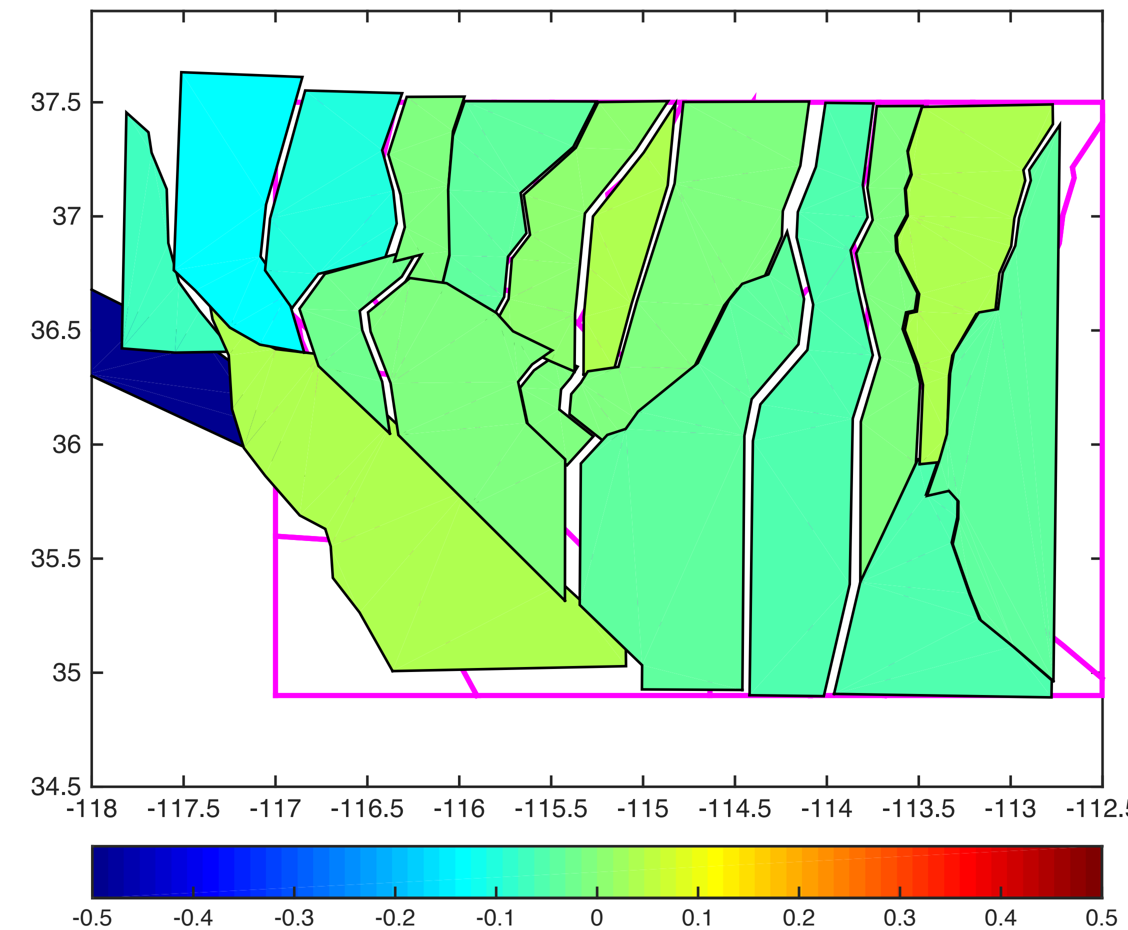

Las Vegas, NV

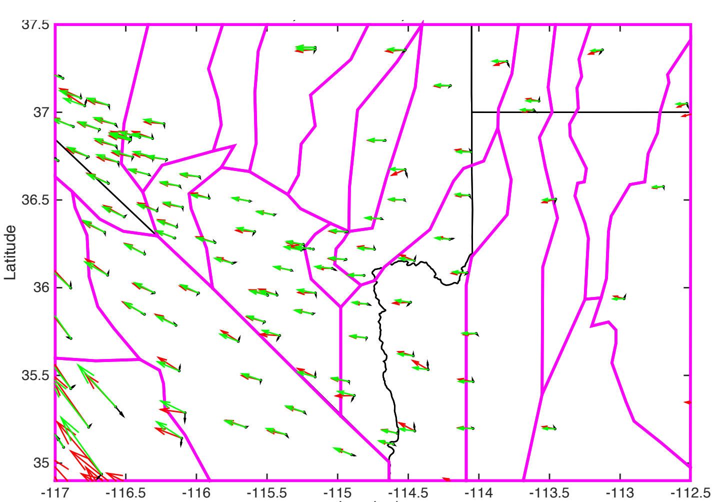

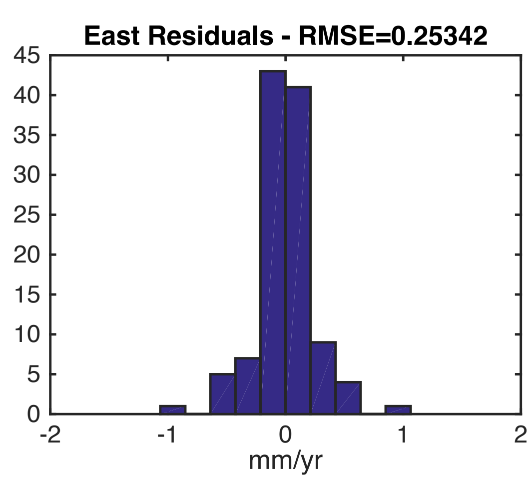

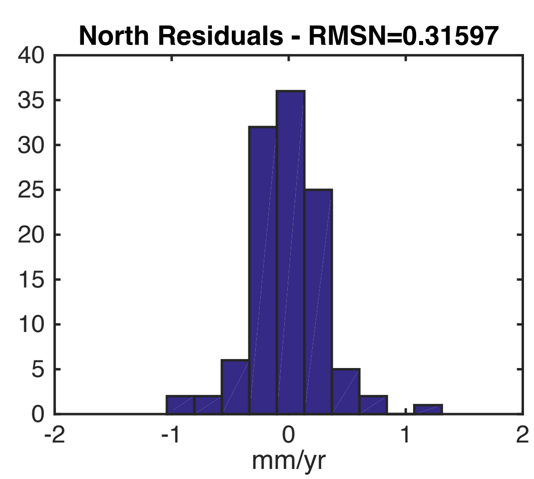

- Regularization to minimize vert. axis rotation + slip rates
- 0.3 mm/yr RMS residual
- Deformation distributed
- LV part of broad pattern of normal extension
- minor sinistral slip on NE striking faults

Block Model: Slip Rates and Rotation Rates Constrained by GPS

in transition from Colorado Plateau to Eastern California Shear Zone

Slip Rates

0.5 mm/yr normal
0.25 mm/yr thrust
2.0 mm/yr dextral
0.5 mm/yr sinistral

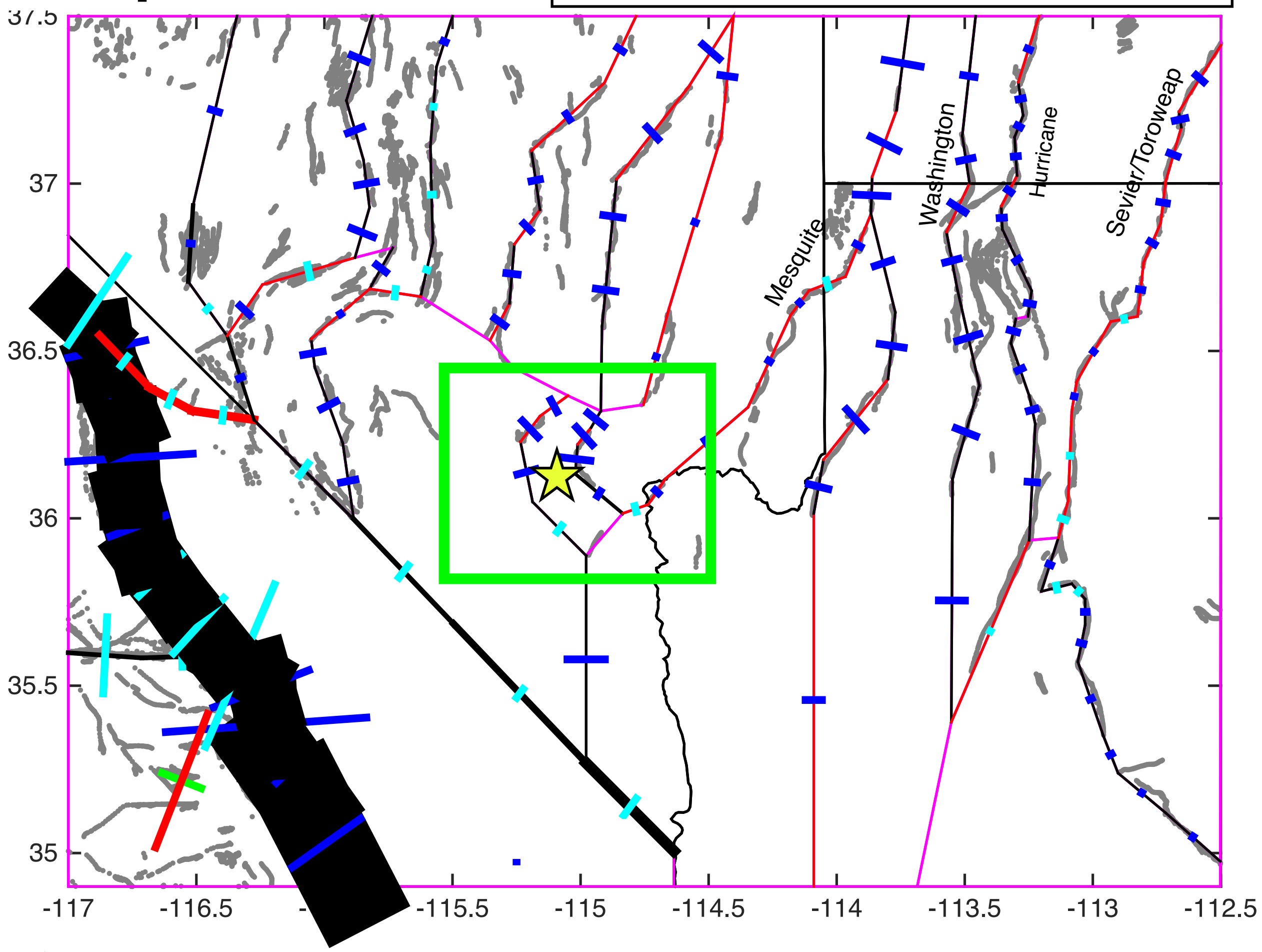

Block Rotations

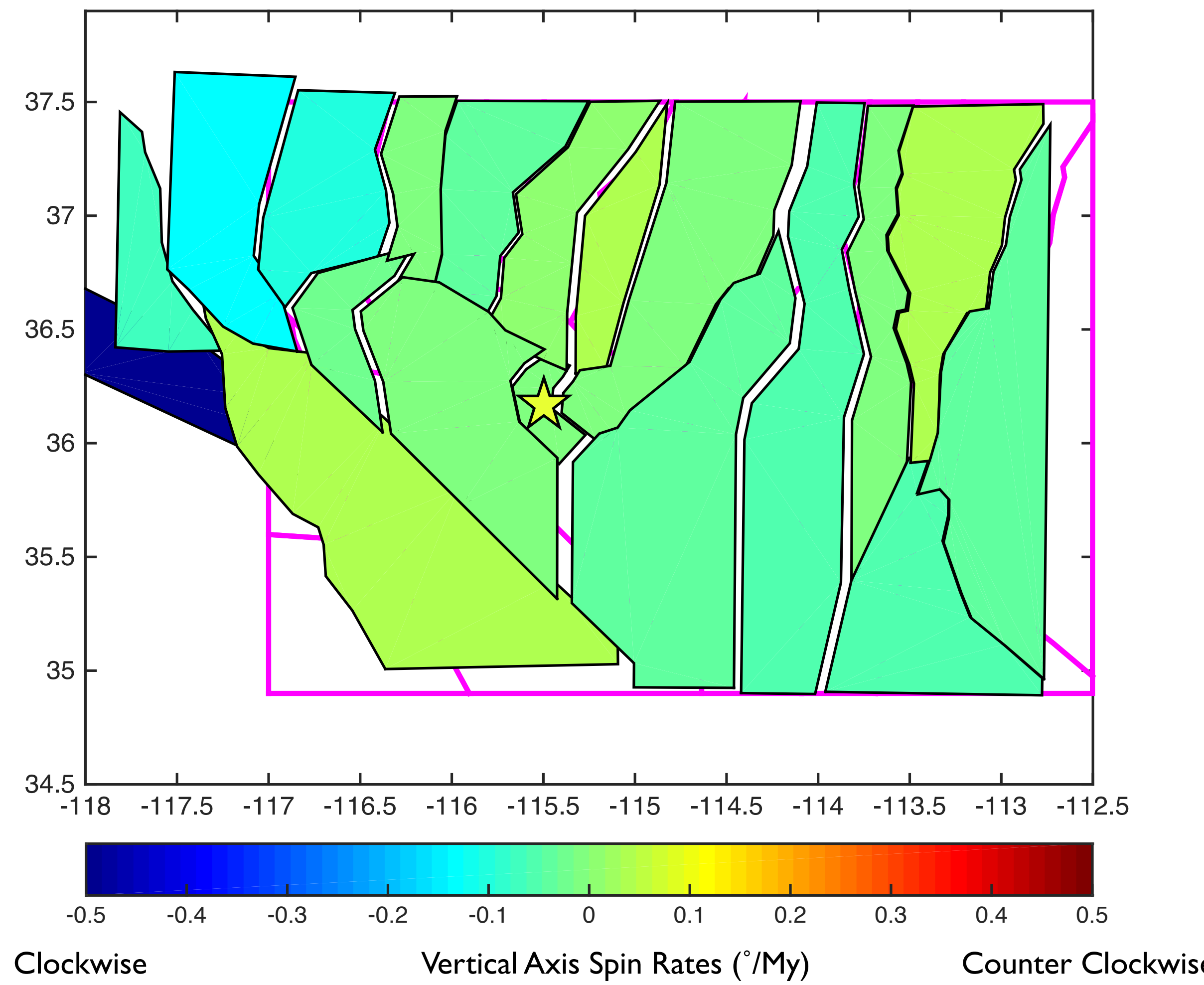

Las Vegas, NV

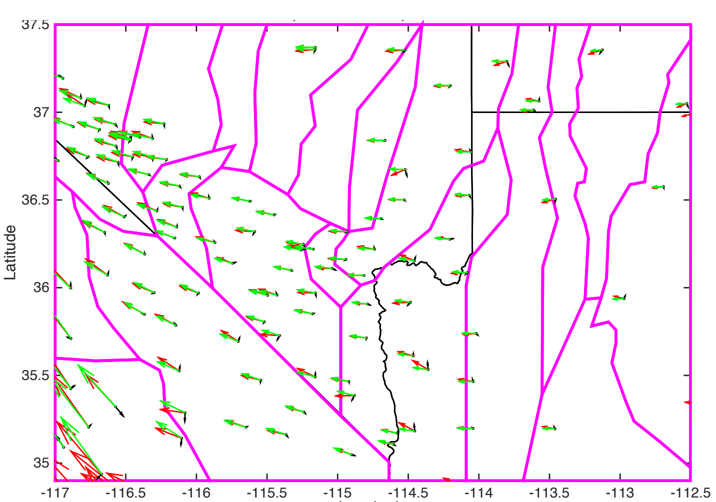

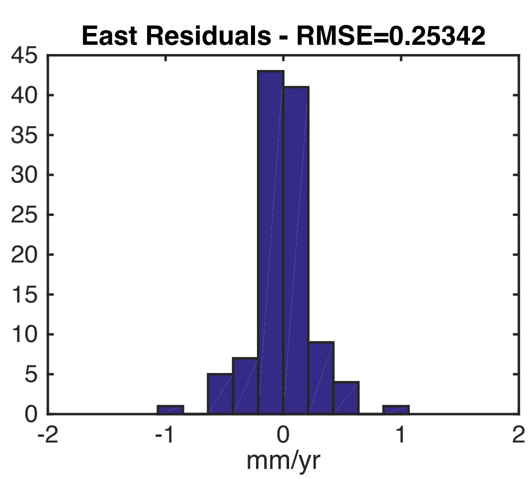

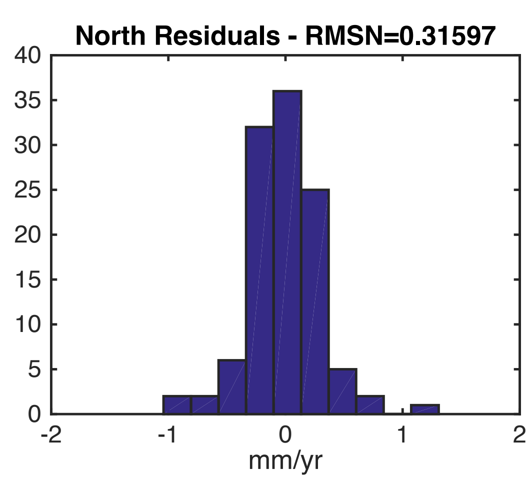

- Regularization to minimize vert. axis rotation + slip rates
- 0.3 mm/yr RMS residual
- Deformation distributed
- LV part of broad pattern of normal extension
- minor sinistral slip on NE striking faults

Slip Rates on Faults Near City of Las Vegas, NV

- Model has rates similar to others in Basin and Range
- 0.2-0.3 mm/yr for each set, range based on variability owing to fault strike
- Predominantly normal in style though some dextral for sections that strike northwest
- Integrated budget of 0.4 - 0.6 mm/yr extension across all of Las Vegas Valley system.
- Rates are best estimates, individual rates could differ, but budget must be honored

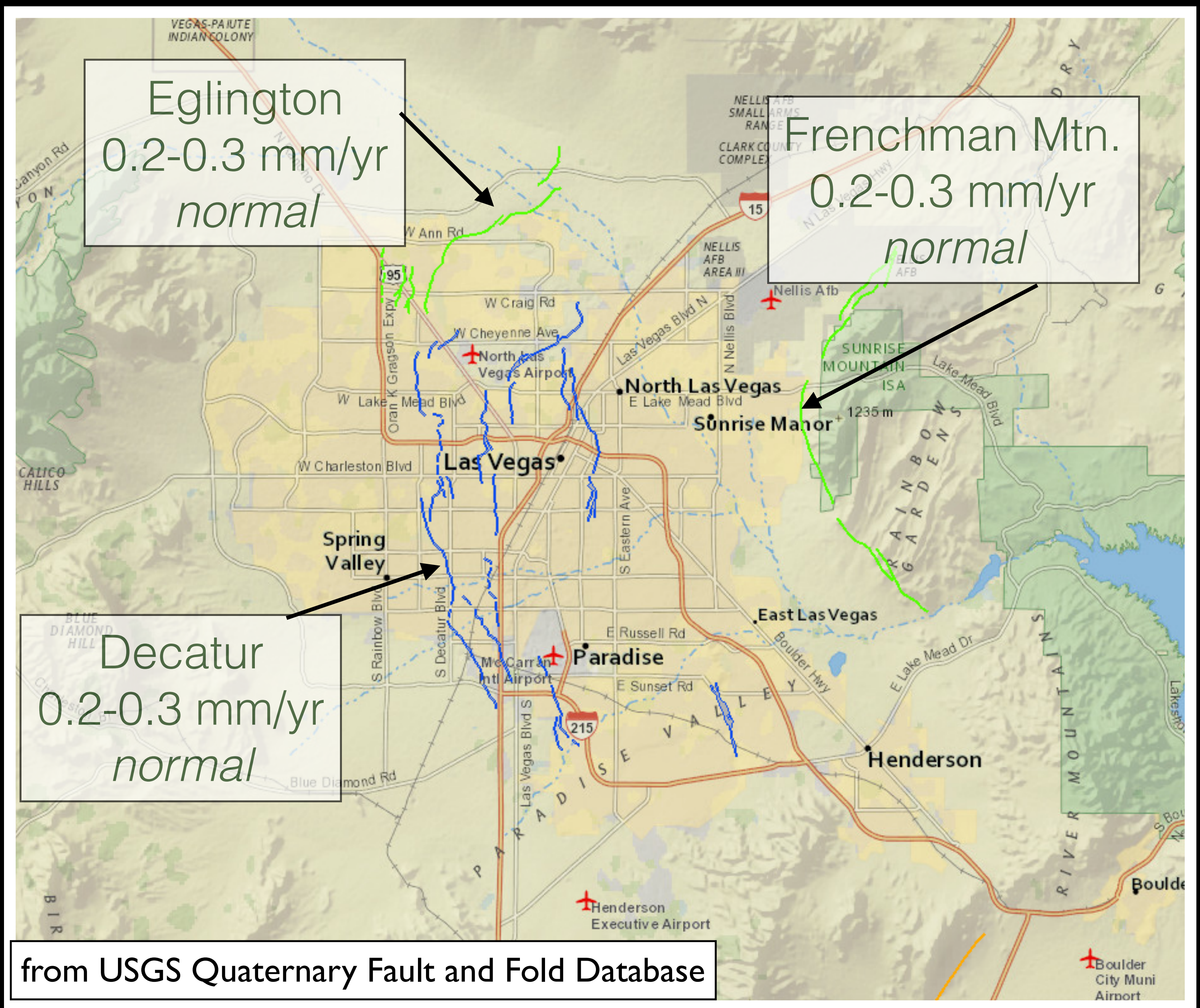

from USGS Quaternary Fault and Fold Database

Eglington Fault 0.2 -0.3 mm/yr normal

Frenchman Mountain 0.2-0.3 mm/yr normal

Decatur Fault 0.2-0.3 mm/yr normal

- Complex but modeled as single system
- Mapped, though not well studied
- Probably tectonic, 1-2 m scarps cutting late Pleistocene fans
- USGS assigns Class B <0.2 mm/yr
- No paleoseismic studies

Dextral slip accommodated elsewhere, e.g. Las Vegas Valley shear zone to the north, Stateline Fault to southwest slips 0.4 - 0.8 mm/yr.

Thoughts on Disagreements Between Geologic and Geodetic Data

Agreements are more common that disagreements…
(*Somewhat amazing given how differently the measurements are made*.)
We don't learn much when we all agree. Disagreements are opportunities.

Recognize Multiple *Classes of Disagreement*

Type A. Individual differences attributable to undocumented uncertainties in:
Geodetic results
Limitations from modeling strategy (e.g. wrong block geometry), unaccounted for transient deformation (from e.g. postseismic relaxation), bad network geometry, etc.
Geologic results
e.g. Biases from low sample size in paleoearthquake event studies, fault complexities in presence of multiple strands, etc.

Type B. Systematic differences across systems of faults/tectonic provinces. e.g.:
- Missing shear strain/strike slip deformation in Central Walker Lane
- Shear strain in eastern Basin and Range from

Geodesy good at *budgets across systems of faults*

Type C. Real Differences. Not all slip rates should agree.
These are change in slip rate over time that result from changes in adjacent block motions for a significant length of geologic time, e.g. greater than several seismic cycles. The Earth Can Do This.


Questions?

INSAR ANALYSIS OF THE 2008 RENO-MOGUL M 4.7 EARTHQUAKE SWARM: IMPLICATIONS FOR SEISMIC HAZARD IN THE WESTERN BASIN AND RANGE

John W. Bell[1], Falk Amelung[2], and Christopher D. Henry[1]
[1] Nevada Bureau of Mines and Geology, University of Nevada, Reno, Nevada
[2] Rosenstiel School of Marine and Atmospheric Science, University of Miami, Miami, Florida
Senior author email address: jbell@unr.edu

In February, 2008, a swarm of small magnitude (**M** 1–4), shallow (< 2–3 km) earthquakes began near Mogul, Nevada, 10 km west of Reno (Smith and others, 2008; figure 1A, B). The swarm activity increased in intensity and culminated in an **M** 4.7 (M_w 5.0) main event on April 25, 2008. Following the main shock, post-seismic swarm activity continued at a similar rate through August 2008. Focal mechanisms indicated that dextral slip occurred on a concealed northwest-striking fault at the northern end of the Carson Range, the northernmost block of the Sierra Nevada (Smith and others, 2008; figure 1B). The **M** 4.7 earthquake was unusual because it was a strike-slip event that occurred within an extensional domain of the western Basin and Range Province. Published geologic mapping had not identified any major northwest-striking, late Cenozoic structures, or any Quaternary faults that could account for the strike-slip event. In this study, we used InSAR to detect the ground deformation associated with the **M** 4.7 main event. Our results (Bell and others, 2012) showed that InSAR can be successfully used to model small tectonic events, thereby providing new insights into tectonic processes, evolutionary trends, and seismic hazard for the western Basin and Range Province.

The western Basin and Range Province underwent post-mid-Miocene east-west extension followed by transcurrent faulting associated with the development of the Walker Lane, a 700-km-long zone of predominantly northwest-striking dextral faults. The Reno basin is dominated by post-mid-Miocene extension, and is near the boundary with the relatively stable Sierra Nevada and west of the northern Walker Lane (Faulds and Henry, 2008).

To search for ground deformation associated with the Mogul swarm, we processed interferograms using C-band radar data acquired by the European Space Agency Envisat satellite. We processed 26 descending pairs and 12 ascending pairs covering both the main event and the foreshock and aftershock periods. Six best descending and six best ascending unwrapped interferograms were then averaged (stacked) to increase the signal-to-noise ratio. Although no surface rupture was associated with the swarm, consistent and measureable ground deformation signals of up to 2.5 cm were found on interferograms covering the April 25 main event and the aftershock period. We used the University of Miami geodetic modeling program *Geodmod* to model fault source parameters from the InSAR data. The program infers tectonic deformation sources from unwrapped InSAR data using an inverse modeling approach.

The best-fitting model produces synthetic line-of-sight (LOS) deformation lobes closely similar to the deformation data (figures 2A, 2A', 2B, 2B'). Gibbs sampling was conducted with up to 100,000 sample sweeps, and a best-fit fault source model was selected based on comparisons of data-to-model residuals and Gaussian distributions of variable joint probabilities (figure 2C). The preferred model indicates that the swarm was produced by 25–75 cm of strike-slip displacement on a N. 44 W.-striking fault 3.3 km in length, 1–5 km in width, and at a depth of 2.0 km. The model shows that as much as 4 cm of total across-fault dextral offset occurred with up to ±2 cm of total vertical deformation for the combined main and post-seismic events. Two continuous GPS stations, which straddled the modeled fault, also showed similar displacements totaling 4 cm for the swarm (Blewitt and others, 2008).

Our InSAR results indicate that part of the ground deformation was post-seismic, in agreement with continuous GPS data (Blewitt and others, 2008). Although we cannot precisely resolve the post-seismic displacement, most of the ground deformation (±2 cm) occurred prior to May 28, followed by ±1 cm of additional LOS change by August 6 (figure 2D). Similar co-seismic and post-seismic deformation patterns indicate that continued slip occurred on the same fault. In addition, the model-derived moment magnitude M_w 5.3 is larger than the instrumental M_w 5.0, and it is also larger than the cumulative moment magnitude of all **M** >3 swarm events (Mw 5.1). The additional moment required to produce the modeled M_w 5.3 would be roughly equivalent to another M_w 5.0 event suggesting that a significant amount of the post-seismic slip was aseismic.

Our modeling results for the 2008 earthquake swarm support the concept that Walker Lane transcurrent dextral faulting is migrating westward into areas of previous extension of the western Basin and Range Province (Dixon and others, 1995; Lee and others, 2001; Stockli and others, 2003). The 2008 Mogul swarm occurred on a newly recognized N. 44 W.-striking fault in a region long regarded as part of the extensional domain of the Sierra Nevada-Basin and Range Province transition zone. No dextral faulting has been previously recognized in the Reno basin. The 2008 fault parallels the principal Walker Lane structures to the east and north. Dextral slip on the N. 44 W. Mogul fault would result from simple shear within the ~N. 40 W. northern Walker Lane strain field (Hammond and Thatcher, 2007).

Superposition of Walker Lane style faulting on the extensional Reno basin mostly reflects northward propagation and westward encroachment of the youngest part of the Walker Lane system (Faulds and others, 2005; Faulds and Henry, 2008). Initiation of a new N. 44 W. Mogul fault may be required because the normal faults of the Reno basin are too oblique to the modern strain field, whereas the initially normal Mohawk and Grizzly Valley faults were reactivated as dextral faults because they align with the strain field. Similar westward stepping of dextral faulting into regions of prior extension began about 3 Ma in the southern Walker Lane (Dixon and others, 1995; Lee and others, 2001; Stockli and others, 2003); there dextral slip has been transferred westward from the N. 40 W. Death Valley fault system to the new N. 10-15 W. dextral Owens Valley fault and parallel White Mountains fault, an initially 12 Ma normal fault reactivated as a right-oblique-slip fault (Stockli and others, 2003). This systematic pattern of migration of dextral faulting into areas of previous extension, indicates that characterization of seismic hazard in the western Basin and Range Province should incorporate this newly recognized earthquake potential.

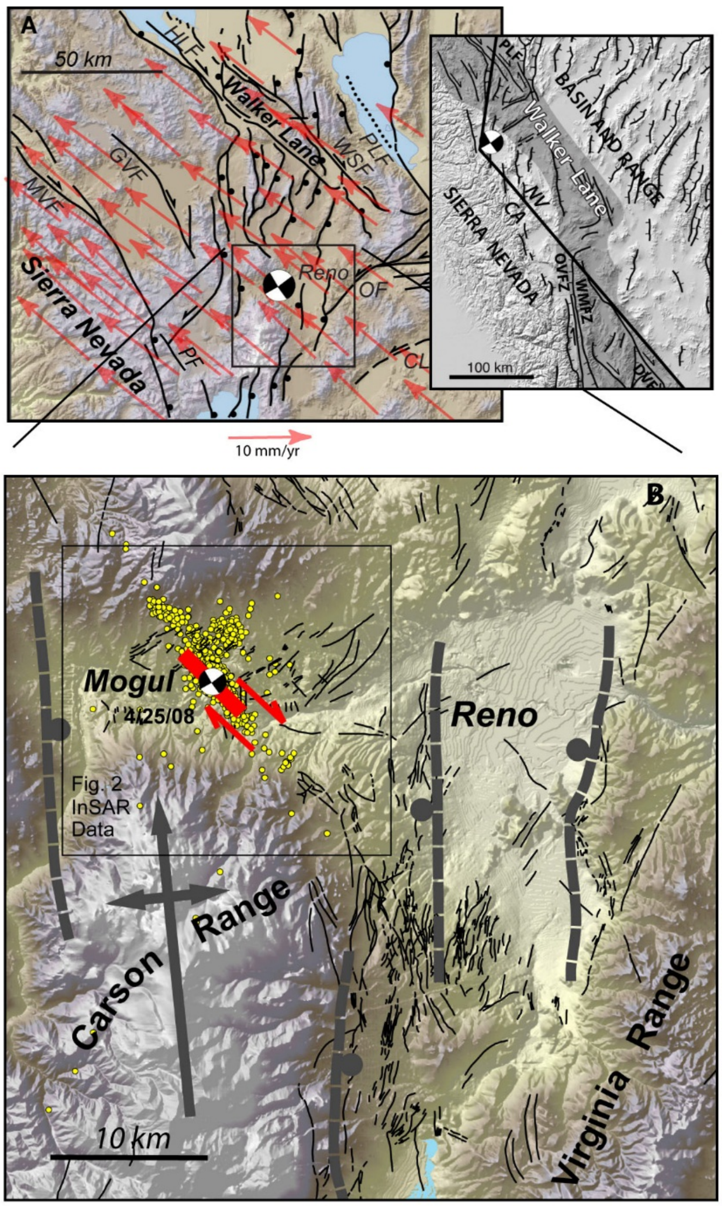

Figure 1. *Structural setting of the 2008 earthquake swarm.*
A. The principal northern Walker Lane faults, Pyramid Lake (PLF), Warm Springs Valley (WSF), and Honey Lake (HLF) faults. Other Walker Lane faults are the sinistral Olinghouse fault (OF) and Carson Lineament (CL). Fault balls indicate downdropped side ….extensional faults.
B. Faults in the Reno basin. Quaternary faults (black); InSAR-derived Mogul fault (red); major extensional faults and plunging extensional anticline of the Carson Range (shaded black). Swarm seismicity (yellow) and focal mechanism from the Nevada Seismological Laboratory.

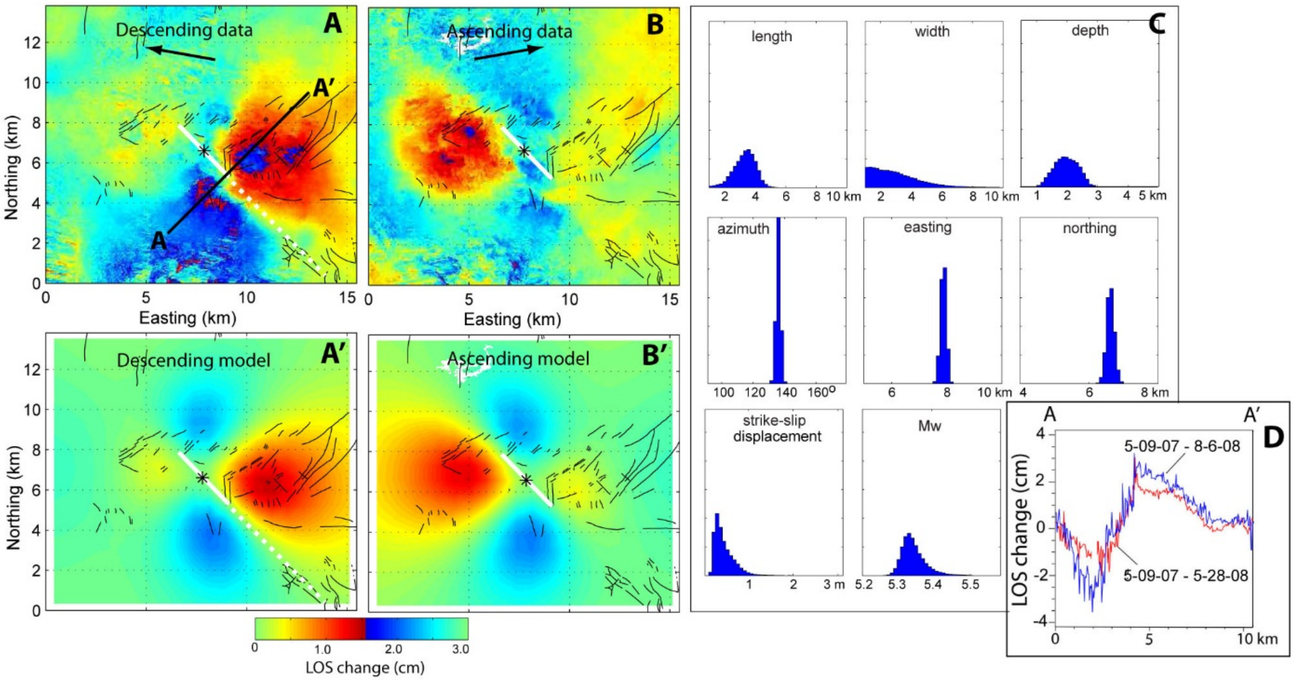

Figure 2. *. Best-fit elastic dislocation fault model for the Mogul earthquake. Quaternary faults shown in black on all figures.*
A-A'. Descending data and model. Modeled fault-slip plane shown in white; possible total extent of fault trace shown as dashed white. Main area of LOS decrease (red lobe) lies to the east of the epicenter.
B-B'. Ascending data and model. Main area of LOS decrease (red lobe) lies to the west of the epicenter.
C. Histograms of joint probability density distributions for fault model parameters derived from Gibbs sampling.
D. Descending InSAR data transect A-A' showing post-seismic LOS change. Red line shows LOS change for first InSAR scene covering main event (5-28-2008); blue line shows additional LOS change on 8-6-2008 InSAR scene.

REFERENCES

Bell, J.W., Amelung, F., and Henry, C.D., 2012, InSAR analysis of the 2008 Reno-Mogul earthquake swarm—Evidence for westward migration of Walker Lane style dextral faulting: Geophysical Research Letters, v. 39, L18306, doi:10.1029/2012GL052795.

Blewitt, G., Bell, J., Hammond, W.C., Kreemer, C., Plag, H., and dePolo, C., 2008, GPS and InSAR monitoring of the Mogul swarm—Evidence for mainly aseismic fault creep with implications for seismic hazard [abs.]: Eos Transactions American Geophysical Union, Fall Meeting, v. 89, no. 53, abstract S53C-03.

Faulds, J.E., and Henry, C.D., 2008, Tectonic influences on the spatial and temporal evolution of the Walker Lane—An incipient transform fault along the evolving Pacific–North American plate boundary, *in* Spencer, J.E., and Titley, S.R., editors, Ores and orogenesis—circum-Pacific tectonics, geologic evolution, and ore deposits: Arizona Geological Society Digest, v. 22, p. 437–470.

Faulds, J.E., Henry, C.D., and Hinz, N.H., 2005, Kinematics of the northern Walker Lane—An incipient transform fault along the Pacific-North American plate boundary: Geology, v. 33, no. 6, p. 505–508.

Dixon, T.H., Robaudo, S., Lee, J., and Reheis, M.C., 1995, Constraints on present-day Basin and Range deformation from space geodesy: Tectonics, v. 14, p. 755–772.

Hammond, W.C., and Thatcher, W., 2007, Crustal deformation across the Sierra Nevada, northern Walker Lane, Basin and Range transition, western United States, measured with GPS, 2000–2004: Journal of Geophysical Research, v. 112, B05411, doi:10.1029/2006JB004625.

Lee, J., Rubin, C.M., and Calvert, A., 2001, Quaternary faulting history along the Deep Springs fault, California: Geological Society of America Bulletin, v. 113, p. 855–869.

Smith, K., von Seggern, D.H., dePolo, D., Anderson, J.G., Biasi, G.P., and Anooshehpoor, R., 2008, Seismicity of the 2008 Mogul-Somersett, West Reno, Nevada earthquake sequence: Eos Transactions, AGU Fall Meeting, v. 89, no. 53, abstract S53C-02.

Stockli, D.F., Dumitru, T.A., McWilliams, M.O., and Farley, K.A., 2003, Cenozoic tectonic evolution of the White Mountains, California and Nevada: Geological Society of America Bulletin, v. 115, p. 788–816.

The following is a PDF version of the authors' PowerPoint presentation.

InSAR Analysis of the 2008 Reno-Mogul M4.7 Earthquake Swarm: Implications for Seismic Hazard in the Western Basin and Range

John Bell[1], Falk Amelung[2], Chris Henry[1]

1) Nevada Bureau of Mines and Geology, University of Nevada, Reno

2) University of Miami, Rosenstiel School of Marine and Atmospheric Science

jbell@unr.edu

with some extra GPS stuff added by Bill Hammond

Mogul Swarm, Reno NV. Initiated February, 2008

- Thousands of earthquakes M <1-4
- Shallow hypocenter most depths < 3 km
- Inside Reno city limits ~9 km from downtown.
- Exciting times. Rattled nerves.
- Main shock M4.7 (4.9?) on April 25, 2008
- Strike slip mechanism, northwest dextral slip.
- Northwest trending locations, plus NE cluster
- No surface rupture

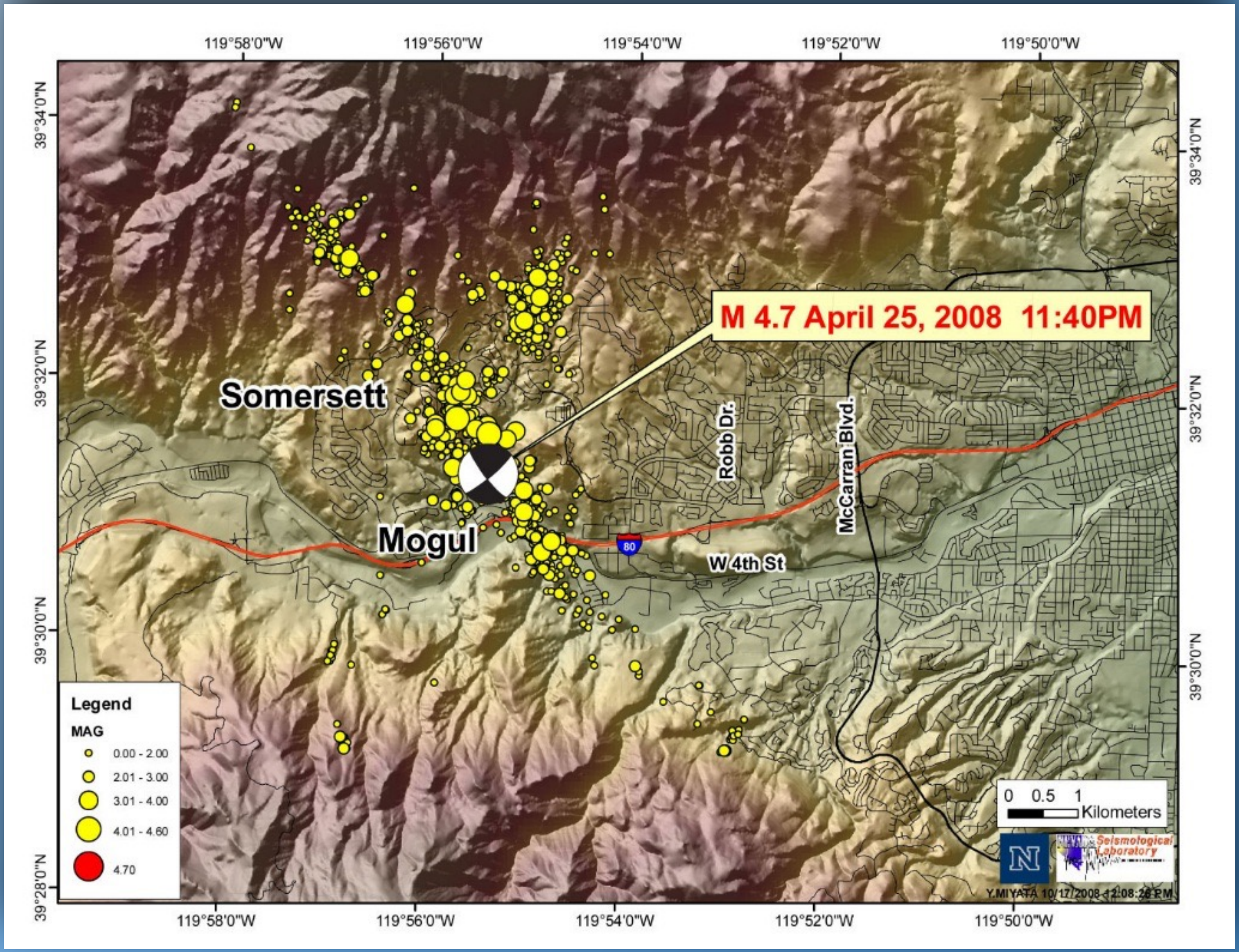

relocations by
Ken Smith, Nevada Seismo Lab

<u>More info at this meeting:</u>
See poster by Christine Ruhl on activity of this and other recent (and ongoing) Nevada swarms.

Mogul Swarm, Reno NV. Initiated February, 2008

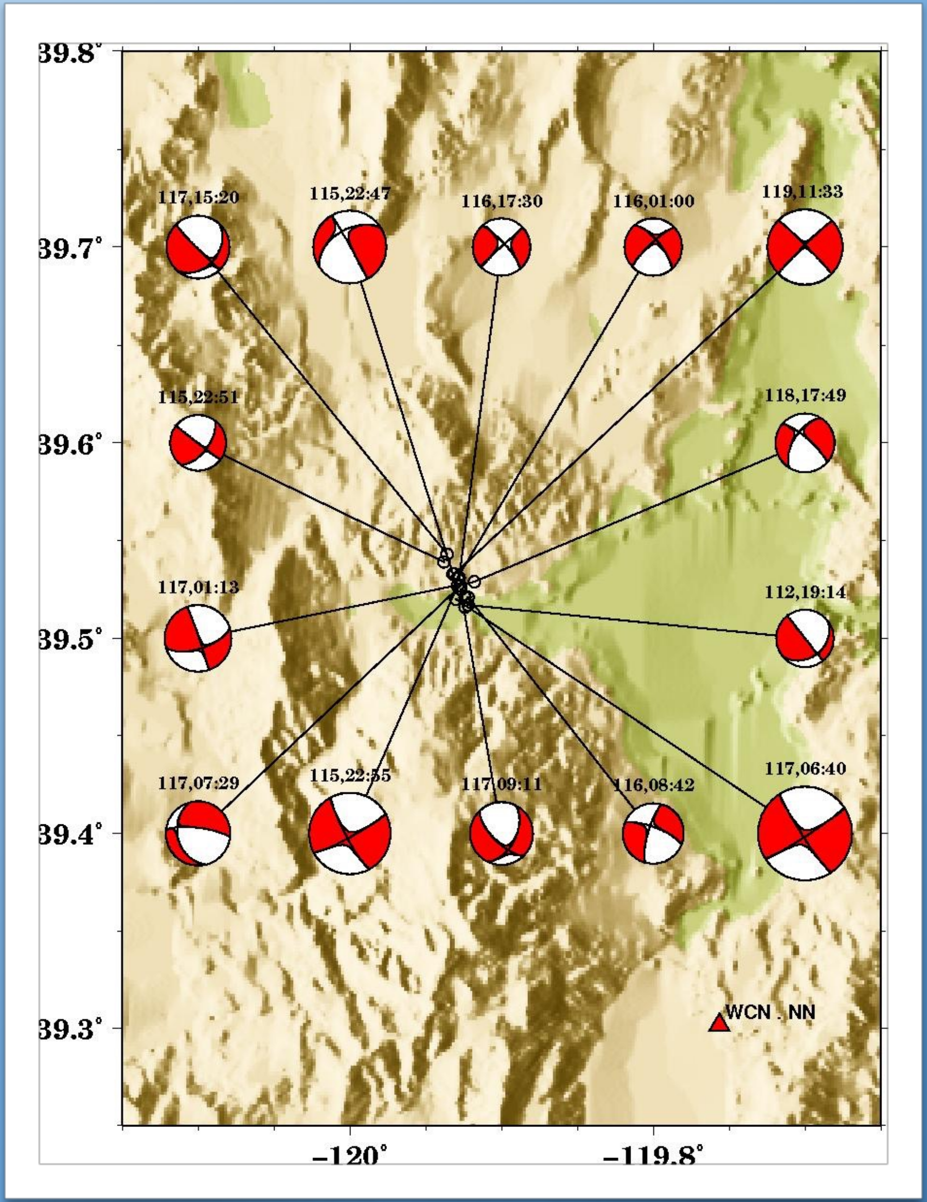

- Most event had strike slip mechanism
- Strike of nodal plane consistent with distribution of locations.

Gene Ichinose

Mogul Swarm, Reno NV. Initiated February, 2008

- Number of Earthquakes/day
- Increasing through day of main shock

- Cumulative number of earthquakes/day
- Events continue for months afterward

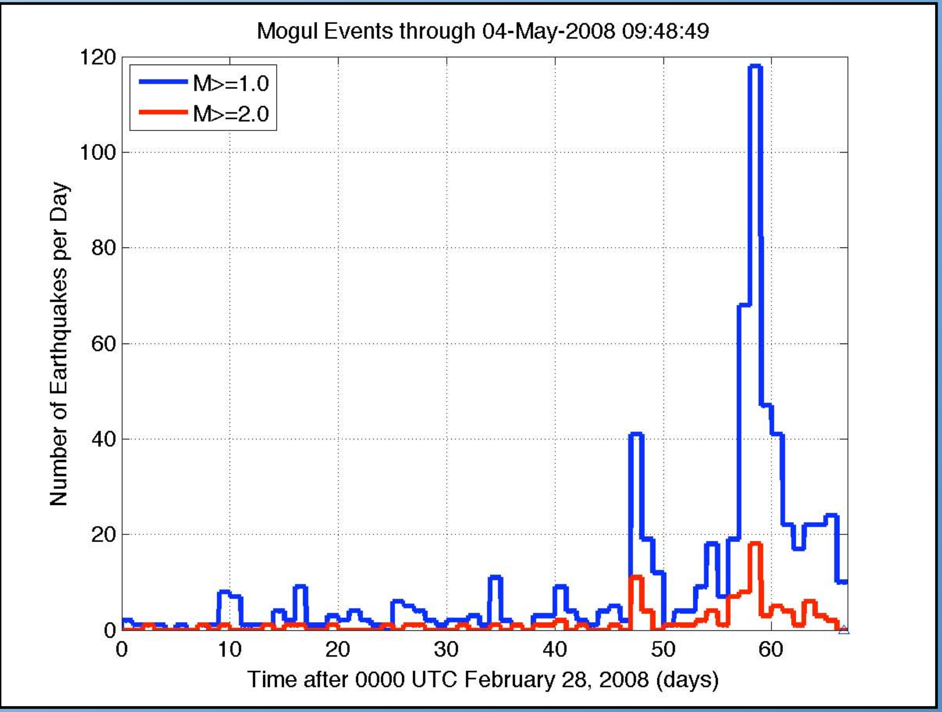

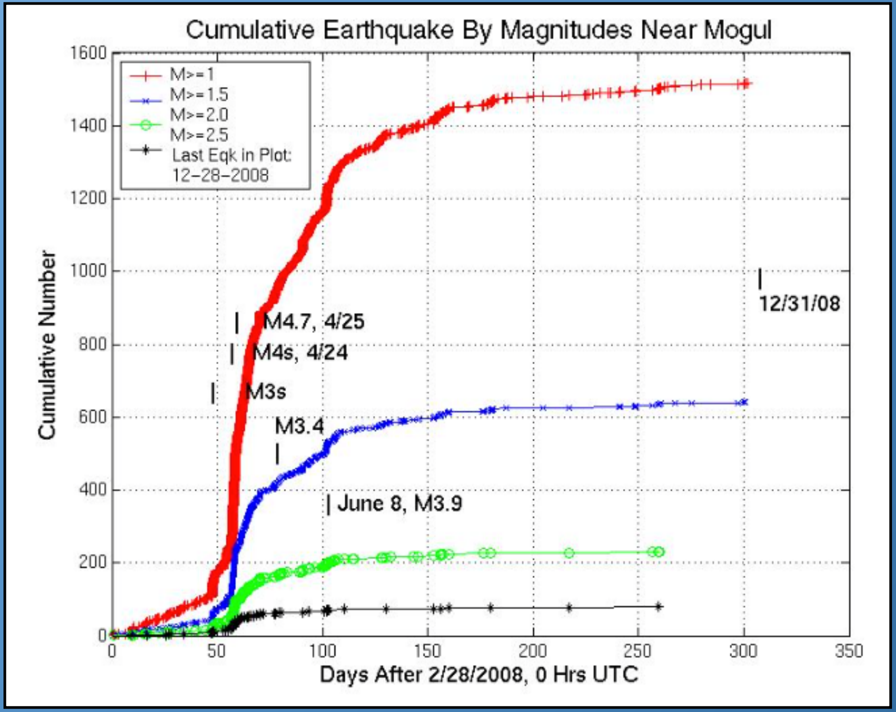

from UNR Seismo Lab.
http://crack.seismo.unr.edu/feature/2008/mogul.html

Damage From Main Shock

Damage From Main Shock

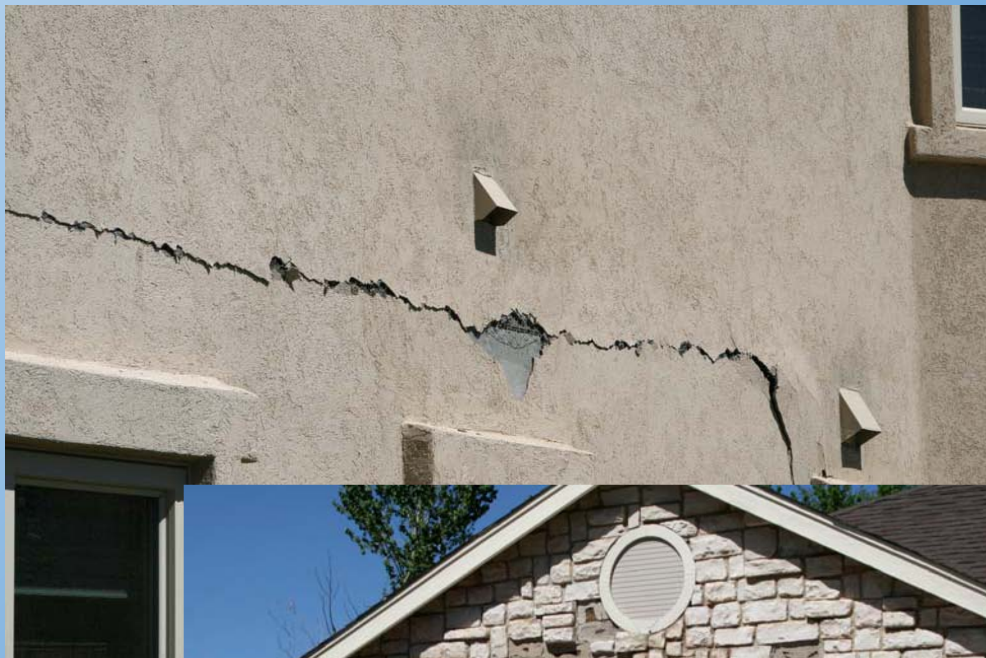

GPS Deployment. MAGNET Stations.

Pre-existing stations:

- MAGNET station RENO
- County library roof continuous station RNO1

- Two more (VRDE, MOGL) rapidly installed **3 days** before main shock
- Got 2 full GPS days of data pre-event.

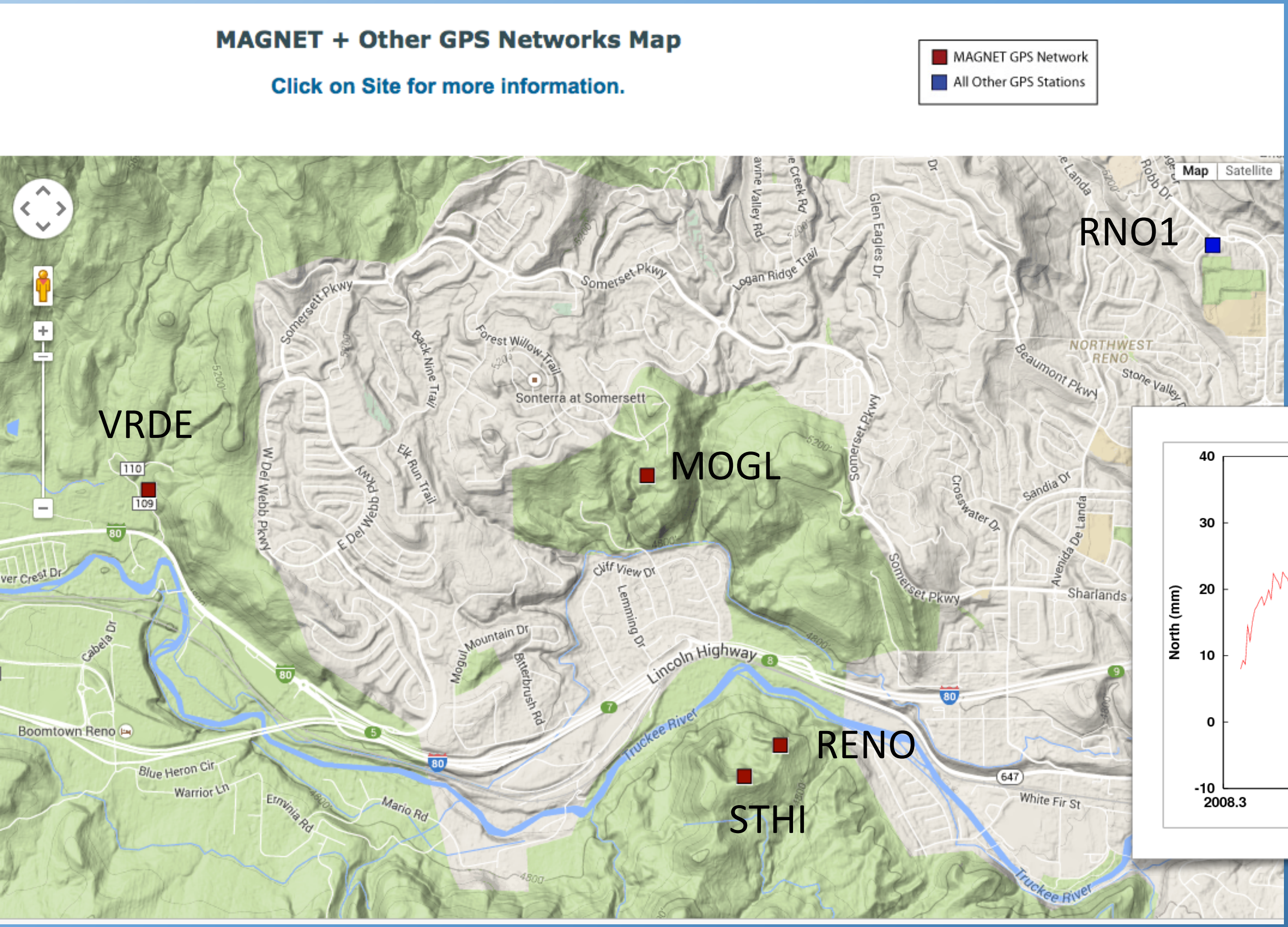

STHI installed as stability check on **RENO** which appeared to be on old landslide. Relative motion was determined to be zero.

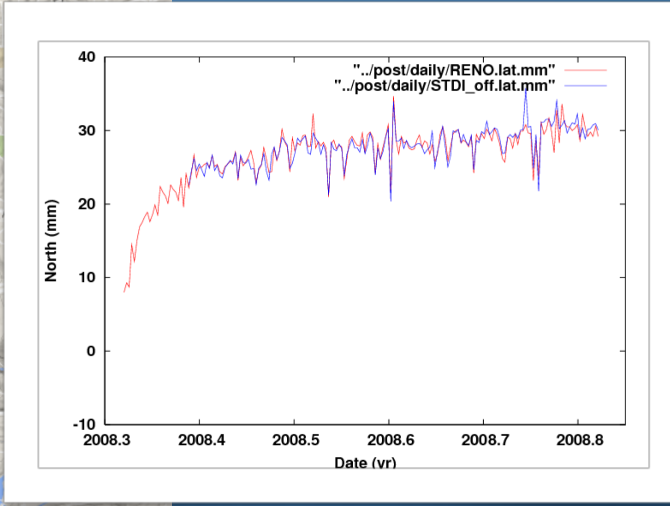

GPS Deployment. MAGNET Stations.

- RENO: Station closest to swarm epicenters
- Postseismic motion near double the coseismic

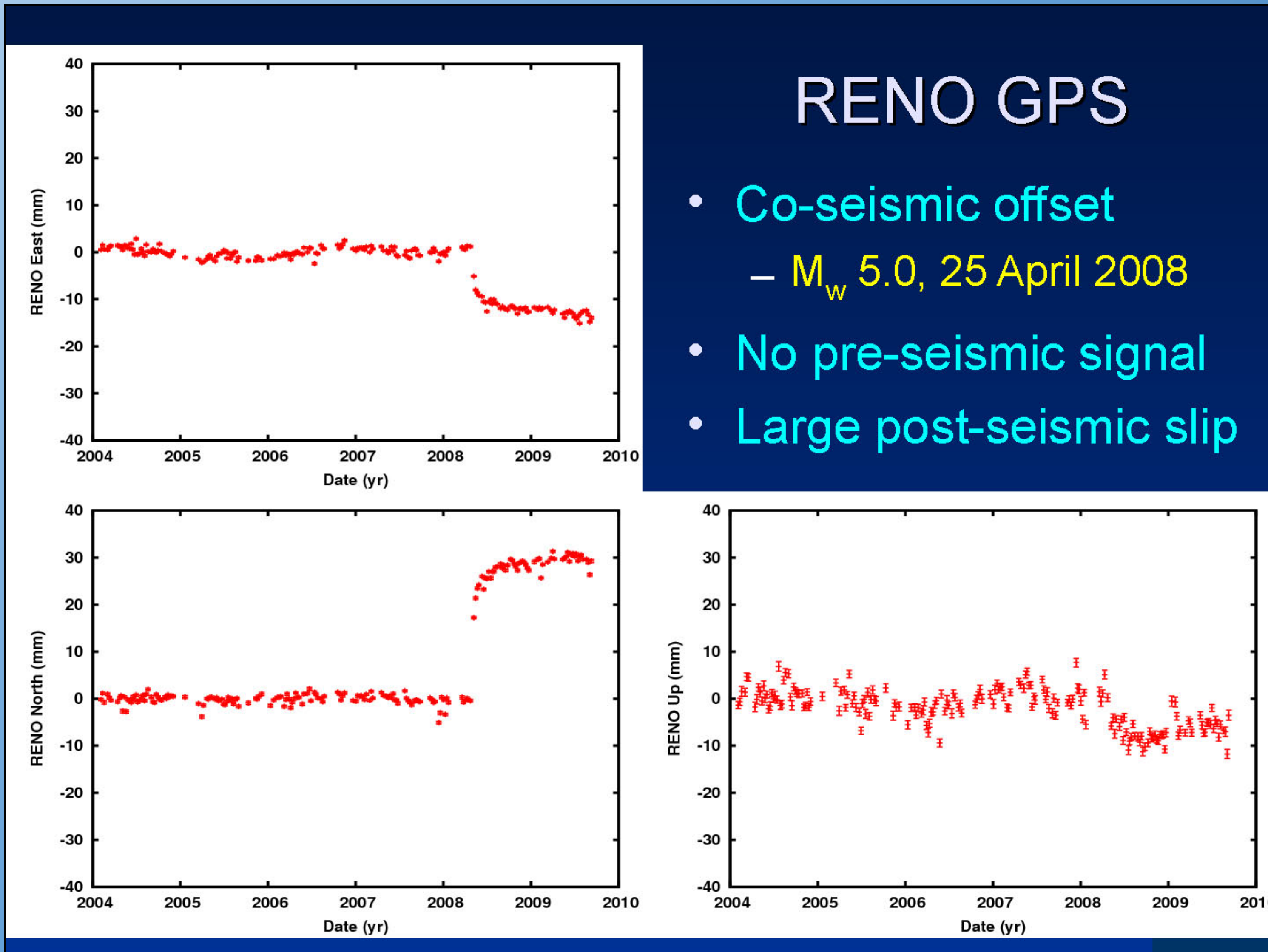

GPS Signals. Co- and Postseismic Motion

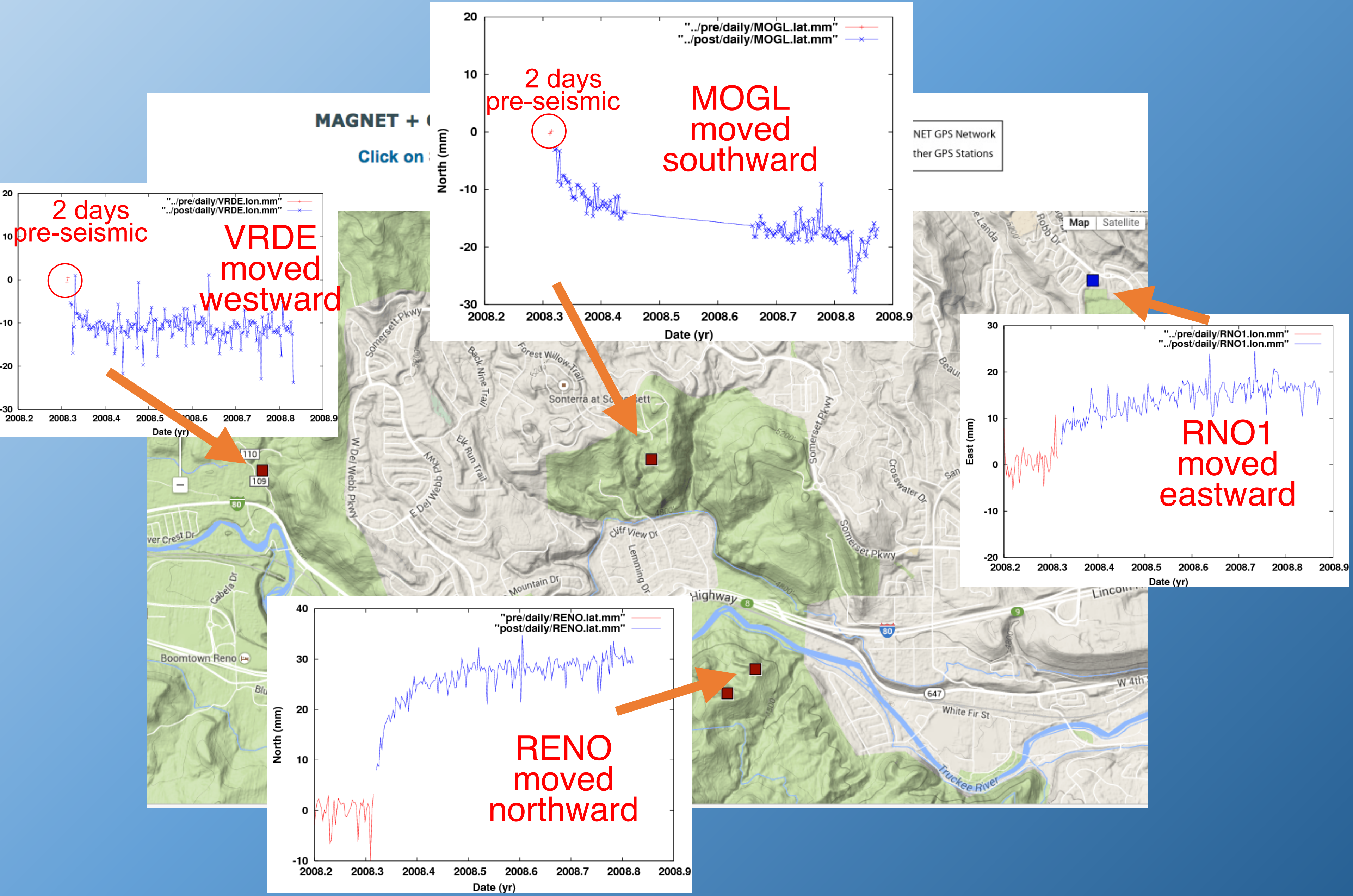

GPS Signals. Co- and Postseismic Motion

- Coseismic moment modeled at M_W=5.0.
- Postseismic motion is double or more than the coseismic. Another $M_{W\sim}$=5.0 or more aseismic.
- Similarities in direction and magnitude of co- and postseismic displacement suggest afterslip.
- Probably in shallow crust along trend outlined by earthquake locations.

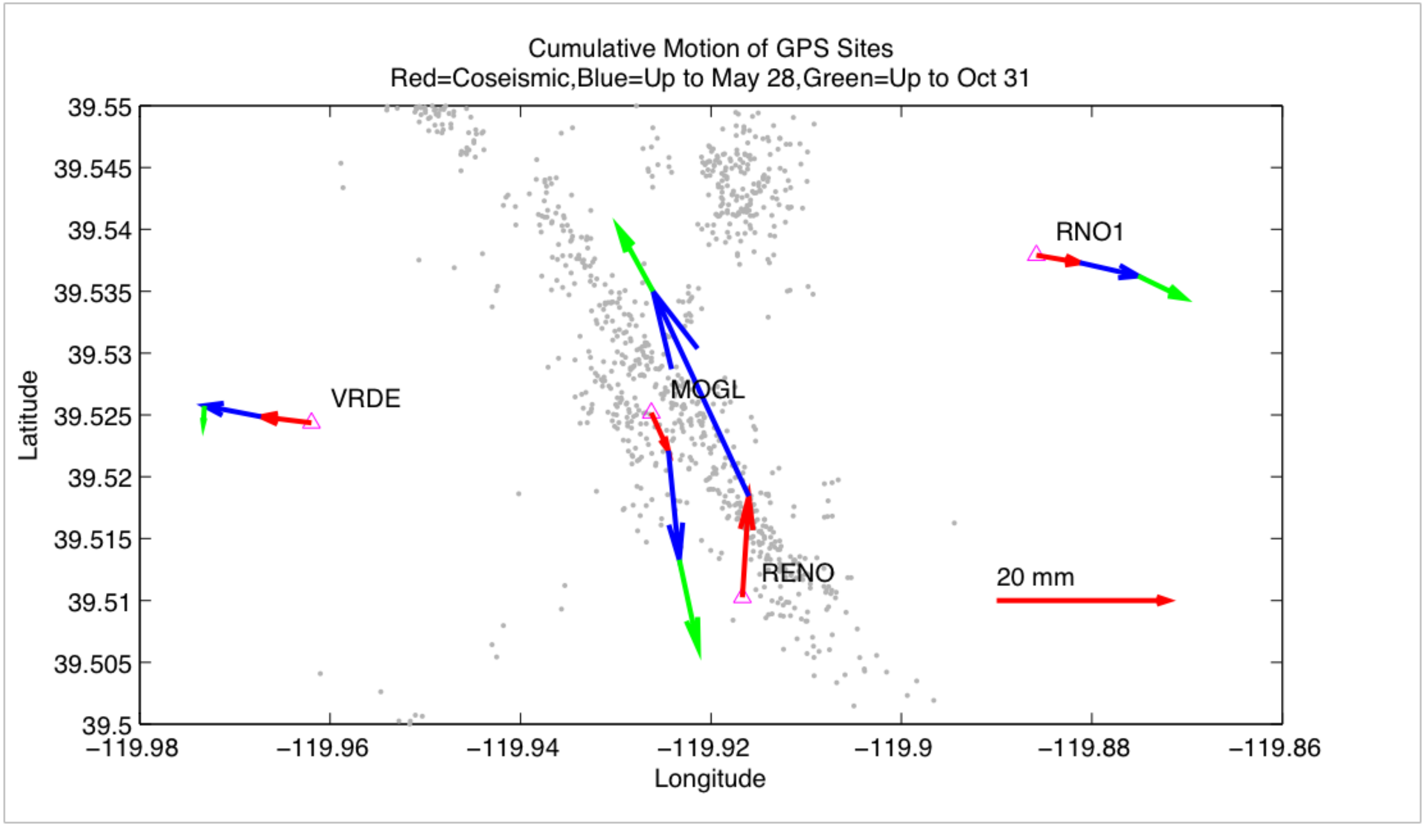

gray = pre main shock earthquake locations

InSAR: Space-Based Radar Interferometry

One Example Interferogram

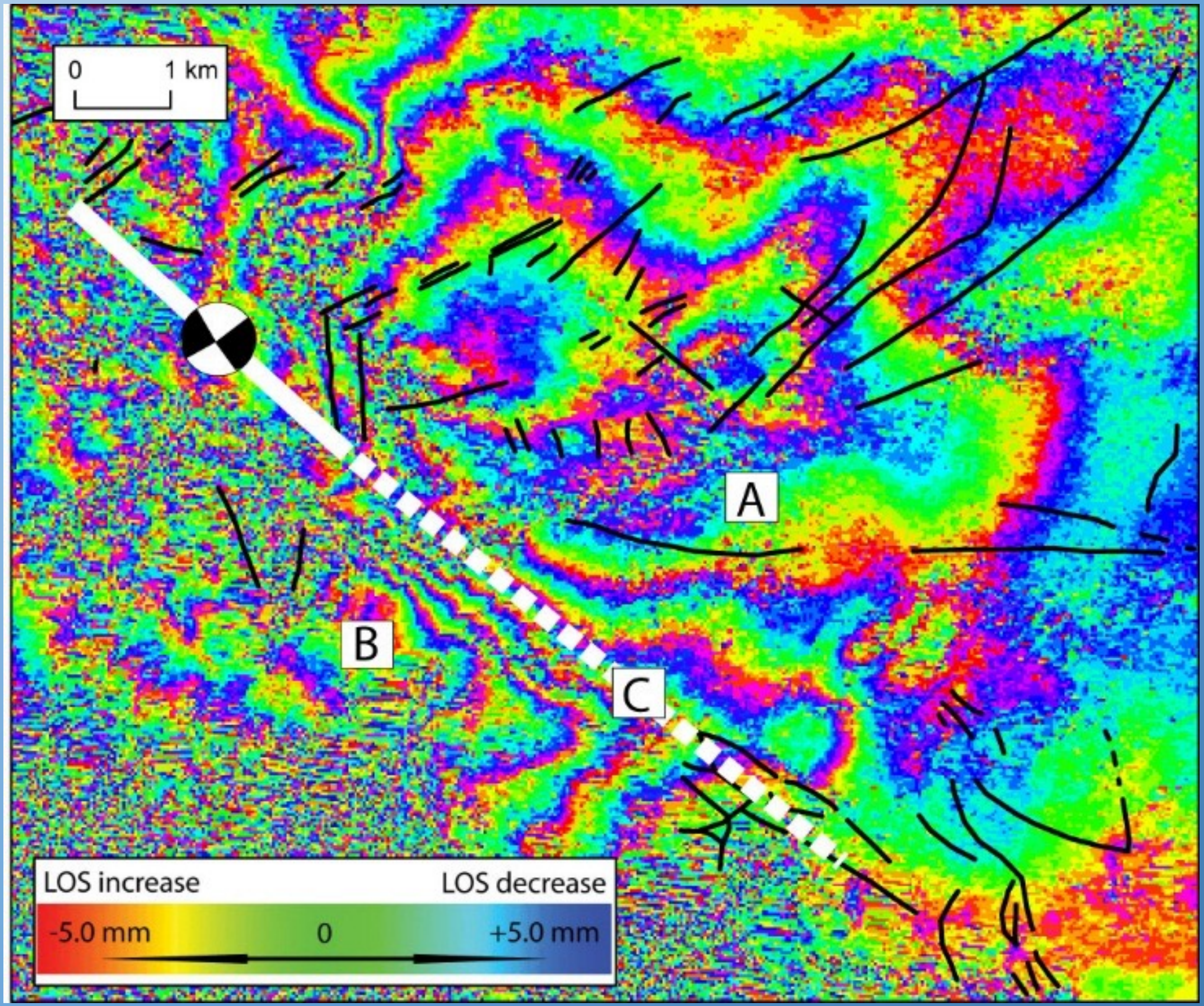

- InSAR provides more geographically complete image of deformation.
- C-Band Envisat Data from ESA
- Each color scale cycle is a "fringe". About 2.8 cm of deformation in satellite line of sight.
- Ascending (took best 6 of 12 pairs) and Descending (took best 6 of 26 pairs). Two look angles see motion in two directions. Better for resolving vertical vs horizontal motion.
- Return time of satellite roughly monthly so time resolution not as fine as GPS.
- More difficult to resolve co- vs. postseismic deformation.

InSAR: Space-Based Radar Interferometry

- Unwrapped phase. Seeing more than one fringe of deformation.
- Similar to GPS, InSAR sees up to 2.5 cm displacement. Mostly sensitive to vertical, so complementary.
- Lobes of up/down consistent with strike slip on shallow fault, projected into line of site (~23˚ from vertical)
- Modeled with dislocation in an elastic half-space. Find best fitting values for 8 parameters. Dip fixed=90˚.
- Inferred 25–75 cm of dextral slip on shallow 2-4 km x 1-5 km patch.

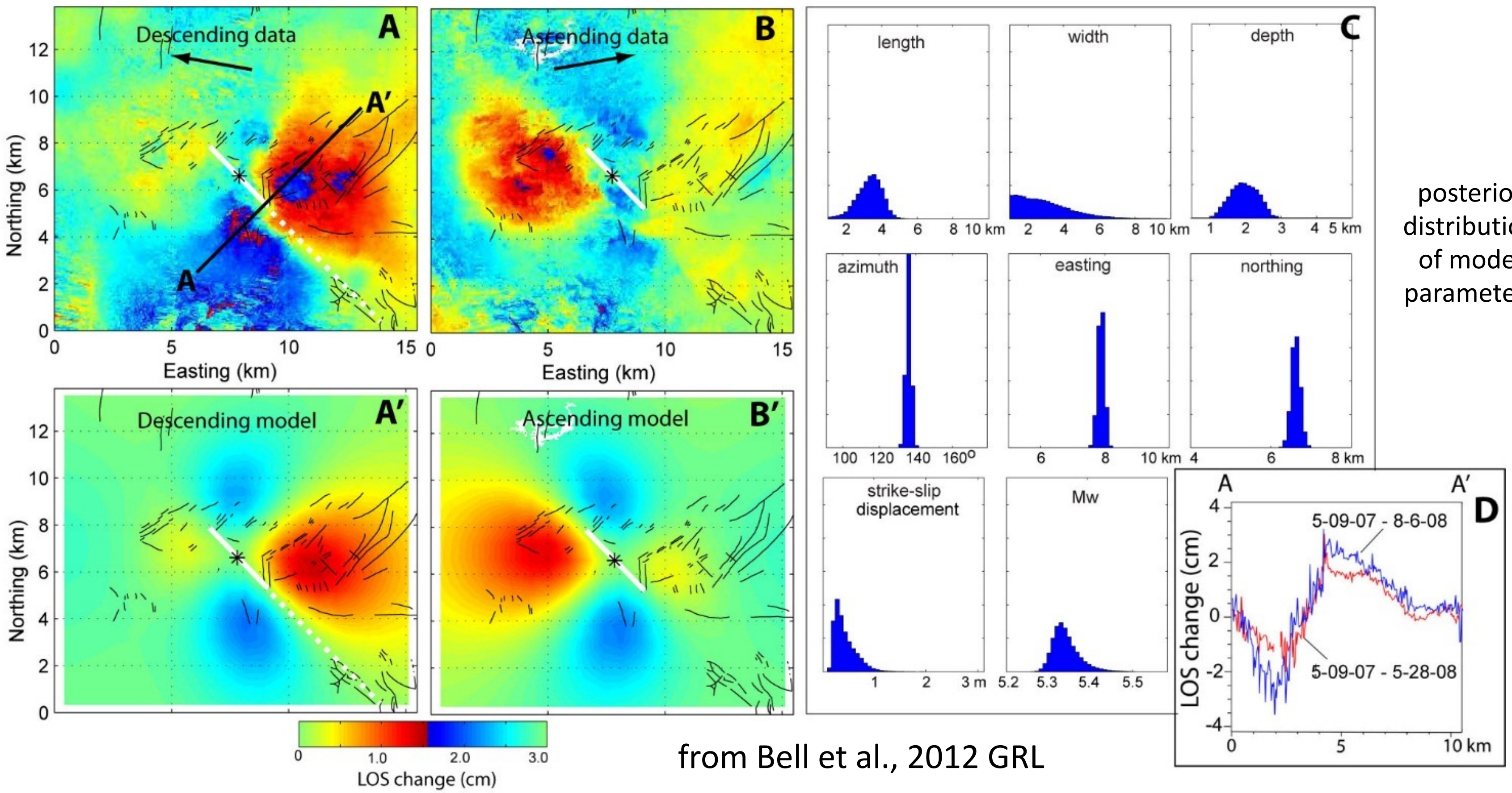

from Bell et al., 2012 GRL

Length (km)	Width (km)	Depth (km)	Strike (azimuth)	Dip	Epicenter easting	Epicenter northing	Displacement	Mw
					95% probability range			
2-4	1-5	1.2-2.5	N42-45W (135-138)	fixed 90°	7.8-8.0	6.5-6.9	0.25-0.75 m	5.3-5.4
					Preferred model			
3.3 ± 0.7	NA	2.0 ± 0.4	N44W ± 1 (136 ± 1)	fixed 90°	7.9 ± 0.1	6.6 ± 0.1	NA	5.32

M_W 5.3-5.4

Preferred M_W 5.32

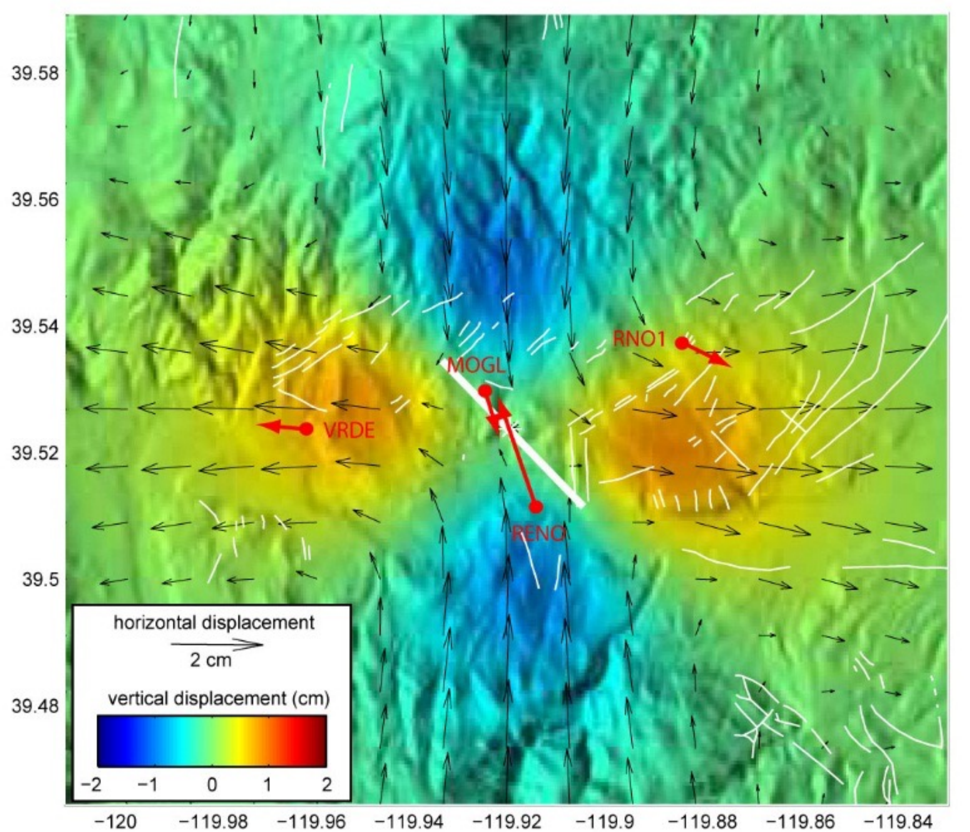

from Bell et al., 2012 GRL

InSAR sees a combination of both co- and postseismic deformation

- Vertical and horizontal displacement from the preferred model (note change in color scale from LOS to vertical now).
- Symmetric lobes of up/down north/south, east/west displacement match GPS-measured displacement.
- InSAR M_W 5.3 larger than seismic M_W 4.9 to 5.0.
- Also bigger than cumulative of all earthquakes in swarm M_W 5.1.

- Typical for swarms in the Basin and Range?
- Many other swarms, but systematic studies have not been performed.

Tectonic Context of Mogul Swarm

- Slip on a previously unrecognized strike-slip fault in the Reno basin, a region of extension-dominated faulting.
- Based on geologic and seismic data this is unexpected.
- Swarm indicates Walker Lane dextral faulting migrating westward to overprint previous extensional structures of the Basin and Range

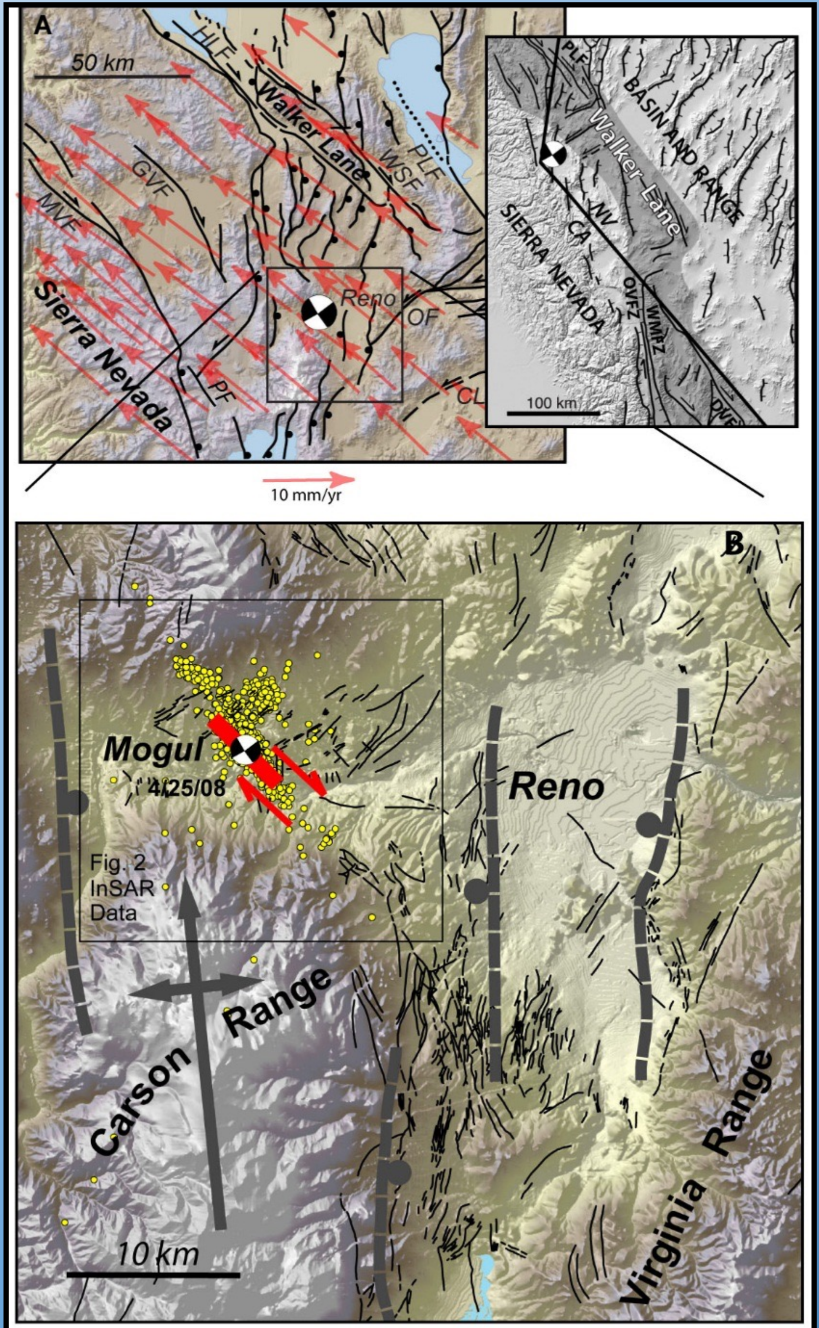

from Bell et al., 2012 GRL

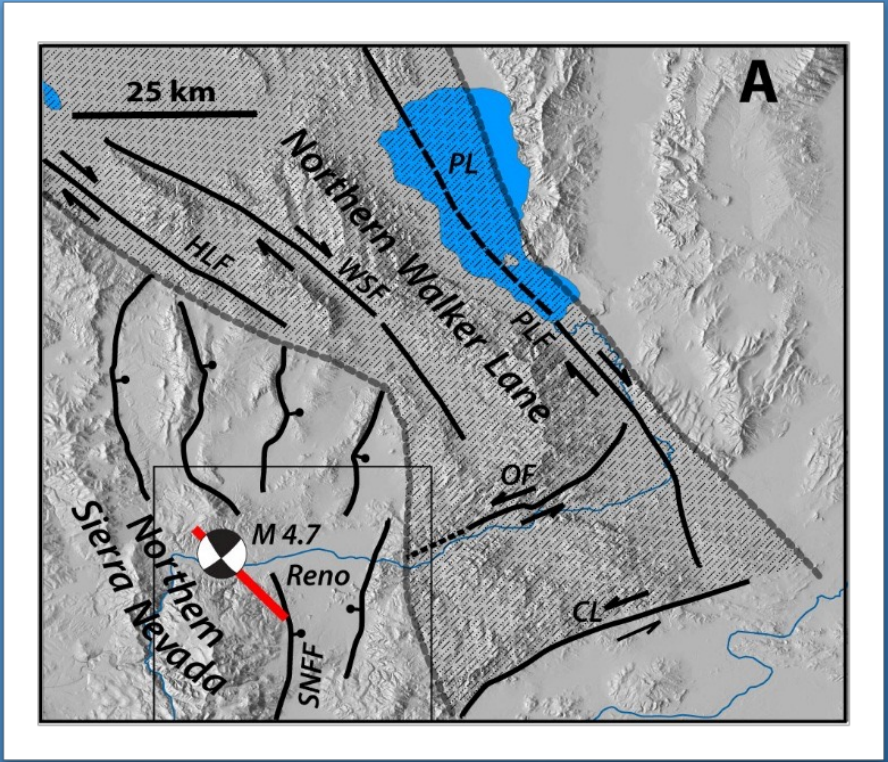

Tectonic Context of Mogul Swarm

- Despite the vigor of swarm, faulting around Mogul area has low displacement and is poorly organized. No recognized through-going strike slip fault.
- To the northwest of Mogul Swarm (in Mohawk Valley, Grizzly Valley and Honey Lake) and east (Pyramid Lake, Olinghouse) there is well recognized dextral shear deformation.
- Direct investigation of Grizzly Valley Fault suggest it is may also be an incipient feature (e.g. Gold et al., 2014).

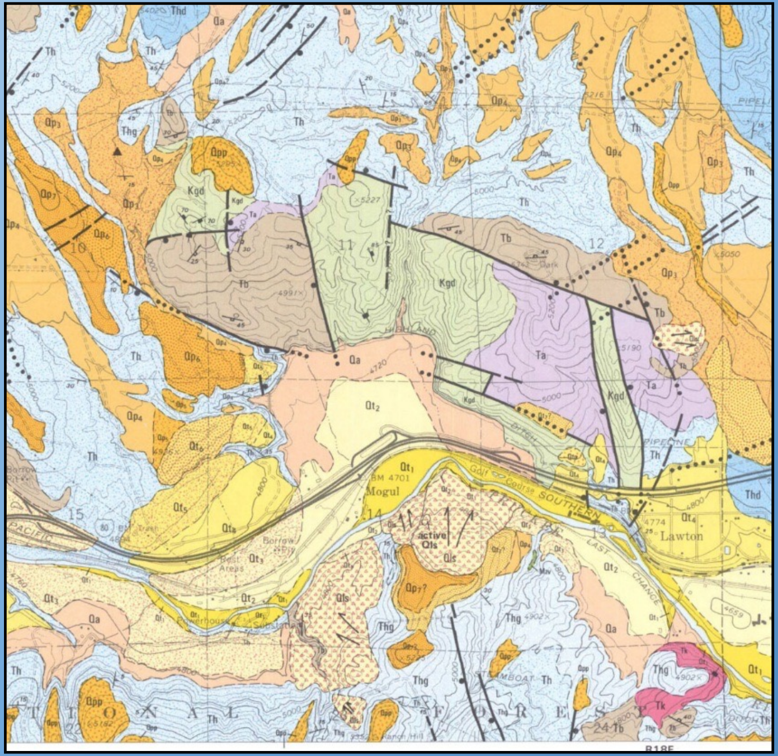

Mogul area

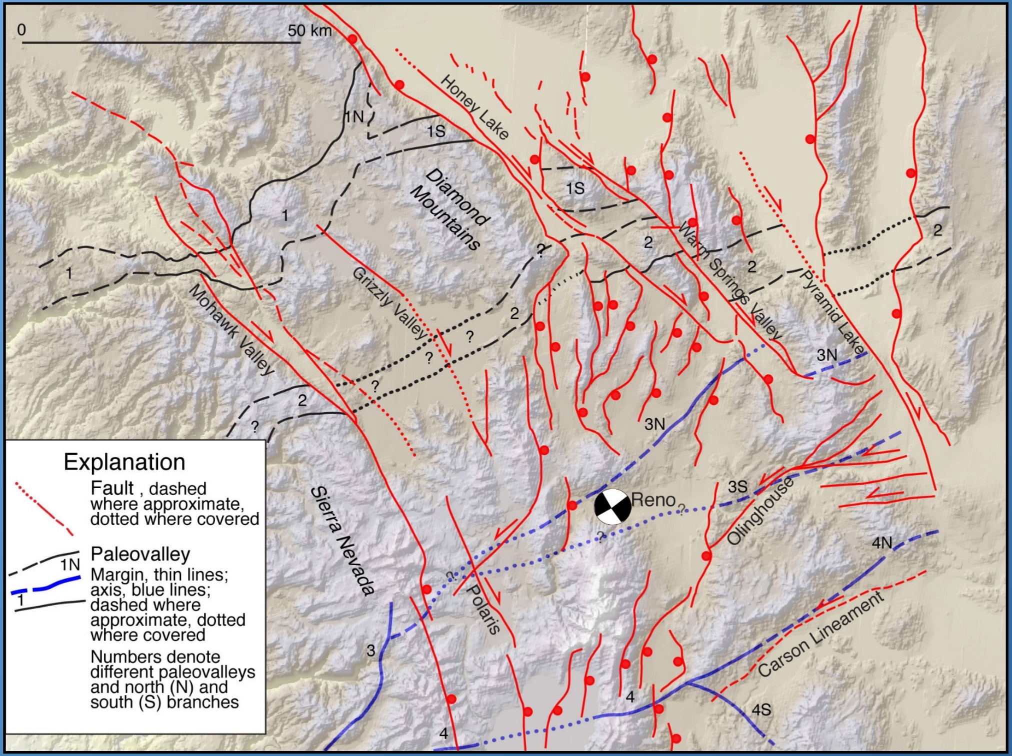

Faults

Tectonic Context of Mogul Swarm

- Based on interseismic deformation from GPS network, dextral slip in Mogul might have been expected.
- Bormann block model predicts dextral slip through a structure passing through west Reno.

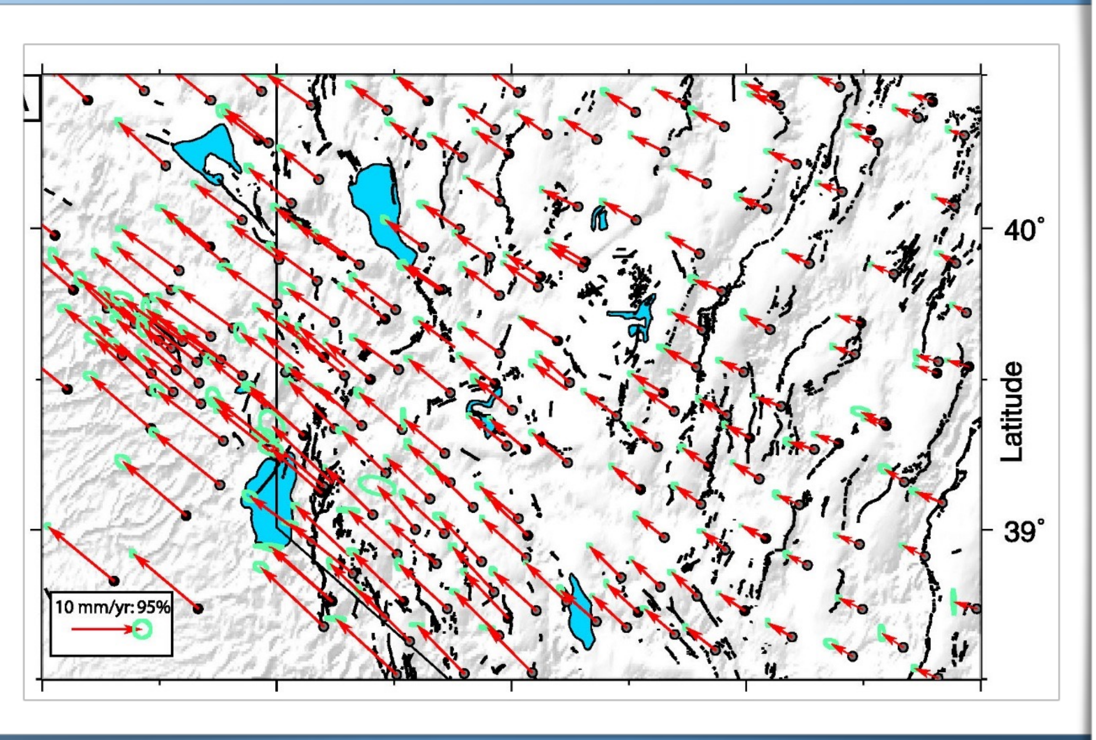

GPS velocities from
Hammond et al 2011 JGR.

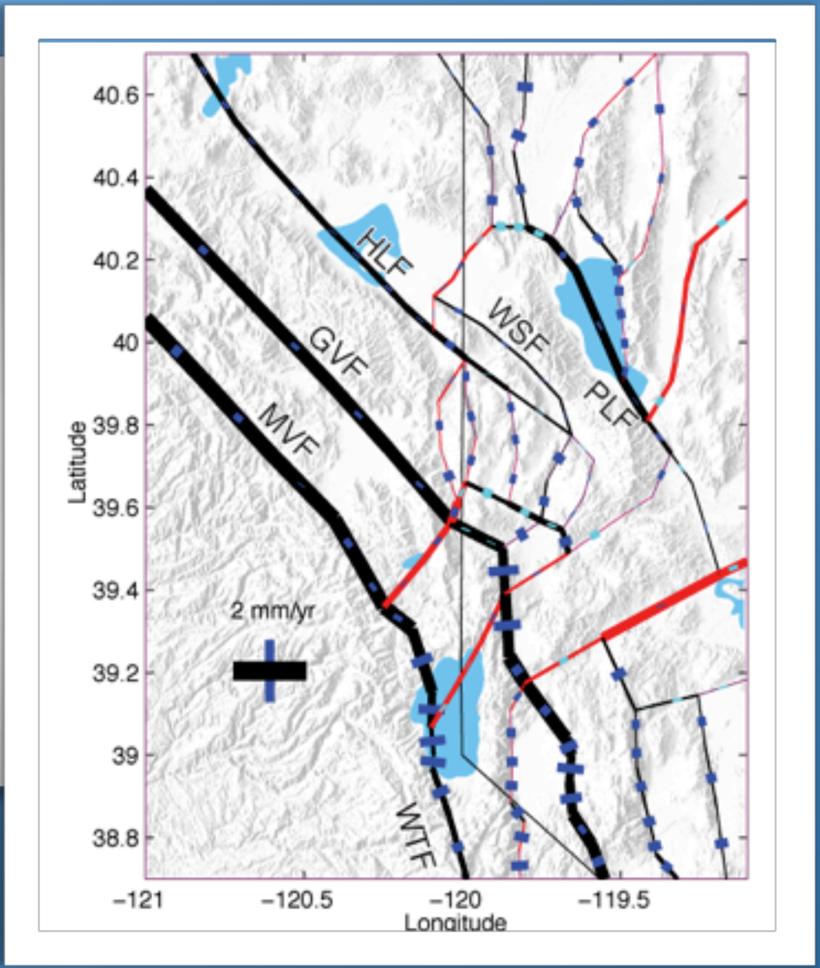

Bormann Block Model

Conclusions

- InSAR data captured details of deformation associated with dextral slip on northwest striking fault during Mogul Swarm main shock and subsequent postseismic afterslip.
- GPS data agree with InSAR in moment calculations and daily observation helps constrain time evolution of the slip.
- Moment of afterslip is equal or greater than coseismic or sum of moment from all events, indicating that there was a significant component of aseismic motion.
- The deformation occurred on unrecognized strike slip fault in Mogul area.
- Slip on this structure is consistent with geodetic measurement of interseismic deformation, but may not have been expected based on geologic observations alone.
- Deformation in Mogul could indicate a westward migration of dextral slip from the Walker Lane into the Reno/Sierra Nevada transition area.

THE GEODETIC STRAIN RATE FIELD FOR THE COLORADO PLATEAU AND SOUTHERN BASIN AND RANGE

Corné Kreemer[1], Geoffrey Blewitt[1], William C. Hammond[1], James Broermann[2], and Richard A. Bennett[2]
[1]Nevada Bureau of Mines and Geology, University of Nevada, 1664. N. Virginia Street, Reno, NV 89557-0178
[2]Department of Geosciences, University of Arizona, 1040 E. 4th Street, Tucson, AZ 85721
Senior author email address: kreemer@unr.edu

The present-day tectonic framework of the Colorado Plateau (CP) and Southern Basin and Range (SBR) region is enigmatic. Except for the Hurricane and Toroweap-Sevier fault zones in the southwestern CP and rift-bounding faults along the Rio Grande Rift (RGR), there are few recognized Quaternary faults. Seismicity is largely concentrated along the CP's western boundary within the northern Basin and Range. Except for the Northern Arizona seismic belt (NASB) in the southwestern CP (east of the Toroweap fault), seismicity is very scarce within the CP, as well as in the SBR and along the RGR. However, there is evidence for past **M** 7+ events in the SBR, including the 1887 **M** 7.5 Sonora earthquake. This earthquake suggests that strain must be accumulating, however slowly (Kreemer and others, 2012). The latter was originally shown by Kreemer and others (2010a) on geodetic grounds. They found that the same zone of ~2.5 mm/yr of extension across the Wasatch fault zone broadens southward, such that the same motion can be found between the RGR and southwestern-most Arizona. A related feature is a WSW-ENE trending, left-lateral shear zone in southern Nevada (i.e., the Pahranagat shear zone), which accommodates up to 1.8 mm/yr of extension (Kreemer and others, 2010b). Motion across the RGR proper is <0.5 mm/yr (Berglund and others, 2012; Kreemer and others, 2010a).

Here, we revisit the geodetic velocity field, in light of many new observations, quantify the associated strain rate field, and discuss the hazard implications. In 2010, as part of the EarthScope Science Program, we installed 34 new continuous GPS stations (CGPS) across the CP's western margin and SBR. This network complements EarthScope's Plate Boundary Observatory as well as other regional networks, including BARGEN, EBRY, and the EarthScope-funded network across the RGR (Berglund and others, 2012). In addition, we have extended UNR's semi-continuous MAGNET network to southern Nevada, so that it now includes the area around Las Vegas and parts of the Pahranagat shear zone.

All data were uniformly processed with GIPSY-OASIS as part of the Nevada Geodetic Laboratory's routine analysis of all CGPS around the world. The daily solutions are transformed into the NA12 frame, which is relative to stable North America and has daily continental-scale common-mode errors removed (Blewitt and others, 2013).

On April 4, 2010, the Mw 7.2 El Mayor-Cucapah earthquake (EMC) struck the southernmost San Andreas fault system. It is now evident that besides causing co-seismic offsets for all sites in our study area, horizontal velocities also significantly changed at the time of the event. These velocity changes can be modeled with a visco-elastic model that has viscosities of 1×10^{20} Pa s and $1 \times 10^{18.5}$ Pa s for the lower crust and upper mantle, respectively. The earthquake slip model was taken from Wei and others (2011). We use the coseismic and postseismic predictions from the PSGRN/PSCMP v.2007 code (Wang and others, 2006) to correct our time-series before analyzing the secular velocities. To develop this model, we assume that the velocities before the EMC earthquake represented long-term crustal motion. These corrections are crucial for our CP-EarthScope stations as we only have data after the EMC. The corrections are also important for our semi-continuous measurements, because for many of those we have only one campaign in 2007, and then a couple of campaigns after the EMC earthquake.

Figure 1 shows the horizontal velocity field in three different reference frames: North America (NA), Colorado Plateau (CP), and Central Great Basin (CGB). The latter two are defined similarly as in Kreemer and others (2010a, b). While both provinces may actually have resolvable strain rates (Kreemer and others, 2010a, 2012; Hammond and others, 2014), the regional velocity fields in these reference frames provide a first-order means to evaluate regional kinematics. We only determined velocities for GPS monuments that are attached to bedrock.

We observe the following relative motions: maximum 1.5 mm/yr across the eastern-most Pahranagat shear zone, 0.7 mm/yr between -115° to -114° W. longitude (encompassing Las Vegas Valley), 0.4 mm/yr across the Hurricane-Toroweap fault zones (just north of Grand Canyon), 1.2 mm/yr across the Hurricane-Sevier faults in southwestern Utah, 0.6 mm/yr across the NASB, negligible motion across the RGR, and gradual increase of up to 3 mm/yr between the RGR and southwestern-most Arizona.

All stations within the CP proper, except those in the area west of the NASB, move as a coherent block around a rotation pole to the north. However, this rigid motion is driven primarily by a very gradual north-to-south increase of the region's westward motion. Given the uncertainties in the velocities, it is possible that part of this can be explained with deformation and, combined with the significant east-west gradient across the SBR, provide an alternative explanation to an independently moving rigid block.

Our results suggest localized strain rates along the CP western margin north of 38° N., distributed strain rates between 36°–38° N. west of -113° W., and increasingly distributed strain rates across the entire width of the SBR south of 36° N.

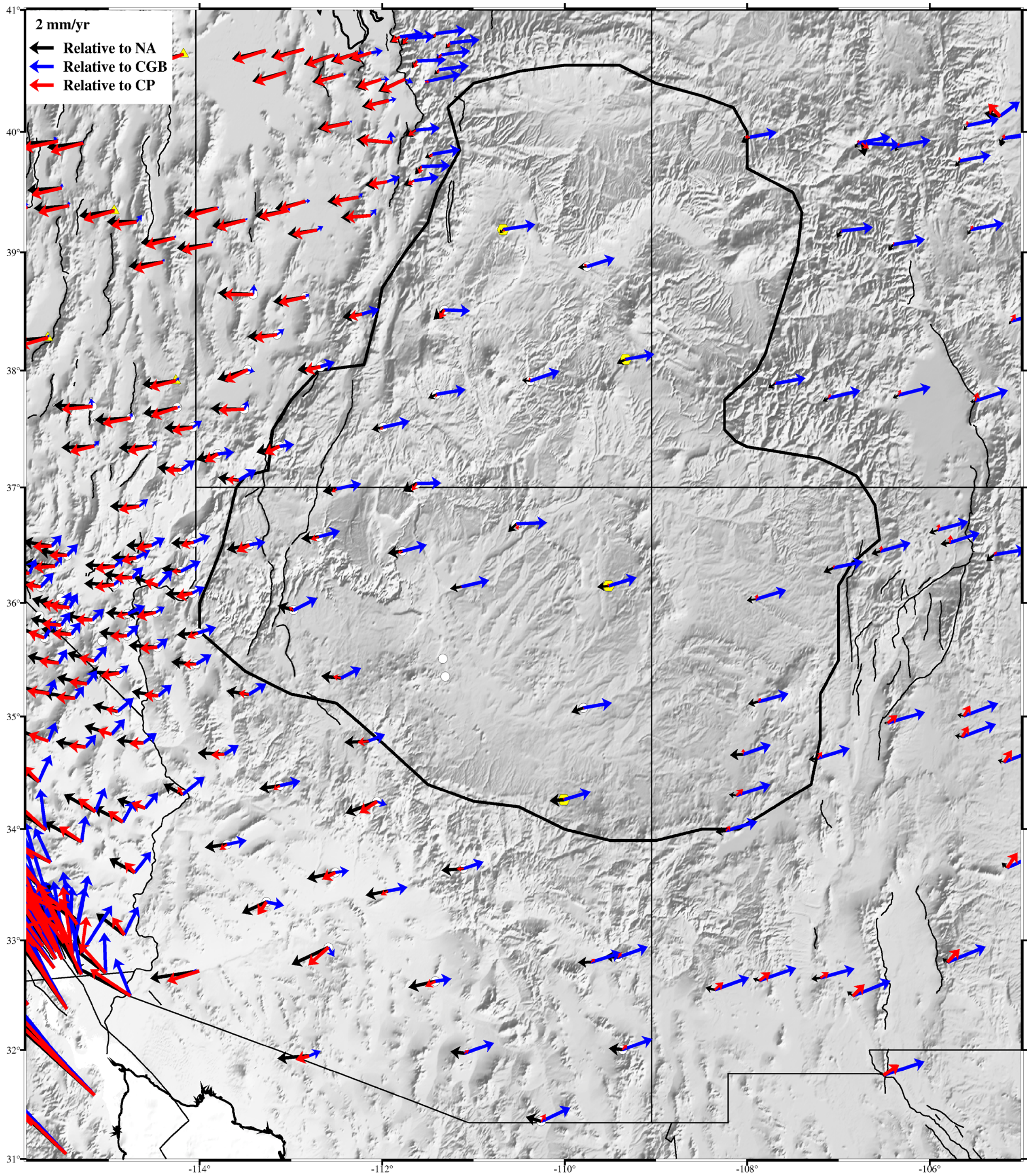

Figure 1. *Horizontal GPS velocity field for the area surrounding the Colorado Plateau (thick outline). Only velocities for bedrock monuments are shown. Results are shown in three different reference frames; North America (NA), Colorado Plateau (CP), and Central Great Basin (CGB). Stations used to define the CP and CGB frame are shown with yellow hexagons and inverted triangles, respectively. Stations installed and operated by us are shown by orange circles. Thin black lines are Quaternary faults with known slip rates.*

REFERENCES

Berglund, H.T., Sheehan, A.F., Murray, M.H., Roy, M., Lowry, A.R., Nerem, R.S., and Blume, F., 2012, Distributed deformation across the Rio Grande Rift, Great Plains, and Colorado Plateau: Geology, v. 40, p. 23–26, doi:10.1130/G32418.1.

Blewitt, G., Kreemer, C., Hammond, W.C., and Goldfarb, J.M., 2013, Terrestrial reference frame NA12 for crustal deformation studies in North America; Journal of Geodynamics, v. 72, p. 11–24, http://dx.doi.org/10.1016/j.jog.2013.08.004.

Hammond, W.C., Blewitt, G., and Kreemer, C., 2014, Steady contemporary deformation of the central Basin and Range Province, western United States: Journal of Geophysical Research, v. 119, p. 5235–5253, doi:10.1002/2014JB011145.

Kreemer, C., Blewitt, G., and Bennett, R.A., 2010a, Present-day motion and deformation of the Colorado Plateau: Geophysical Research Letters, v. 37, L10311, doi:10.1029/2010GL043374.

Kreemer, C., Blewitt, G., and Hammond, W.C., 2010b, Evidence for an active shear zone in southern Nevada linking the Wasatch fault to the Eastern California shear zone: Geology, v. 38, p. 475–478.

Kreemer, C., Hammond, W.C., Blewitt, G., Holland A.A., and Bennett, R.A., 2012. A geodetic strain rate model for the Pacific-North American plate boundary, western United States: Nevada Bureau of Mines and Geology Map 178, scale 1:1,500,000.

Wang, R., Lorenzo-Martin, F., and Roth, F., 2006, PSGRN/PSCMP—a new code for calculating co- and post-seismic deformation, geoid and gravity changes based on the viscoelastic-gravitational dislocation theory: Computers & Geosciences, v. 32, p. 527–541, 2006.

Wei, S. and others, 2011, Superficial simplicity of the 2010 El Mayor-Cucapah earthquake of Baja California in Mexico: National Geoscience, v. 4, p. 615–618, doi:10.1038/ngeo1213.

The following is a PDF version of the authors' PowerPoint presentation.

The Geodetic Strain Rate Field for the Colorado Plateau and Southern Basin and Range

Corné Kreemer

Geoff Blewitt, Bill Hammond

NV Bureau of Mines & Geology
University of Nevada, Reno

Jim Broermann, Rick Bennett

Department of Geosciences
University of Arizona

Outline

What did we know before GPS ?

What did we know from GPS 5 years ago ?

What have we learned since ?

Time-varying velocity/deformation field

Implications for seismic hazard assessment

Regional Seismicity and Faulting

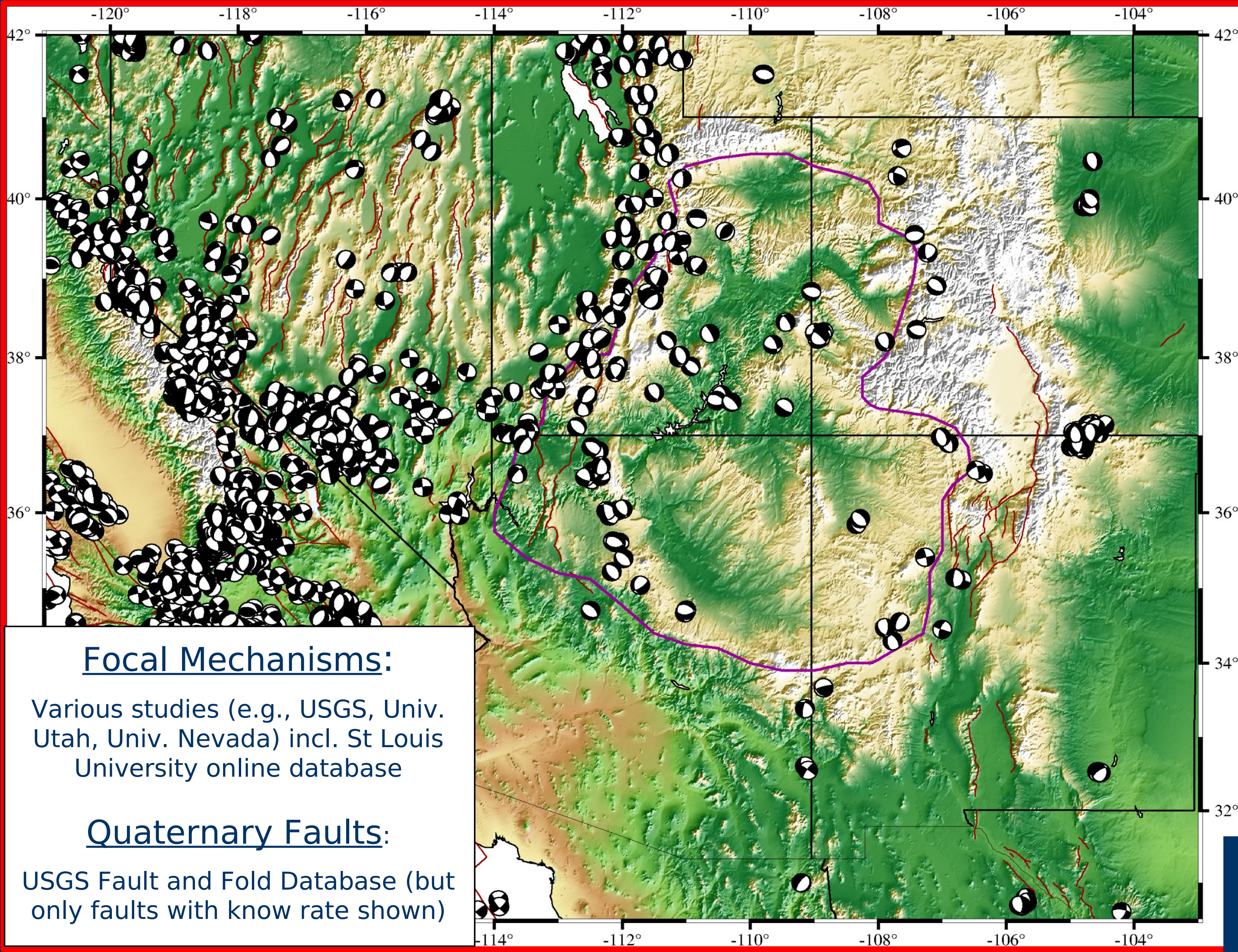

Focal Mechanisms:

Various studies (e.g., USGS, Univ. Utah, Univ. Nevada) incl. St Louis University online database

Quaternary Faults:

USGS Fault and Fold Database (but only faults with know rate shown)

Colorado Plateau's Cenozoic Rotation

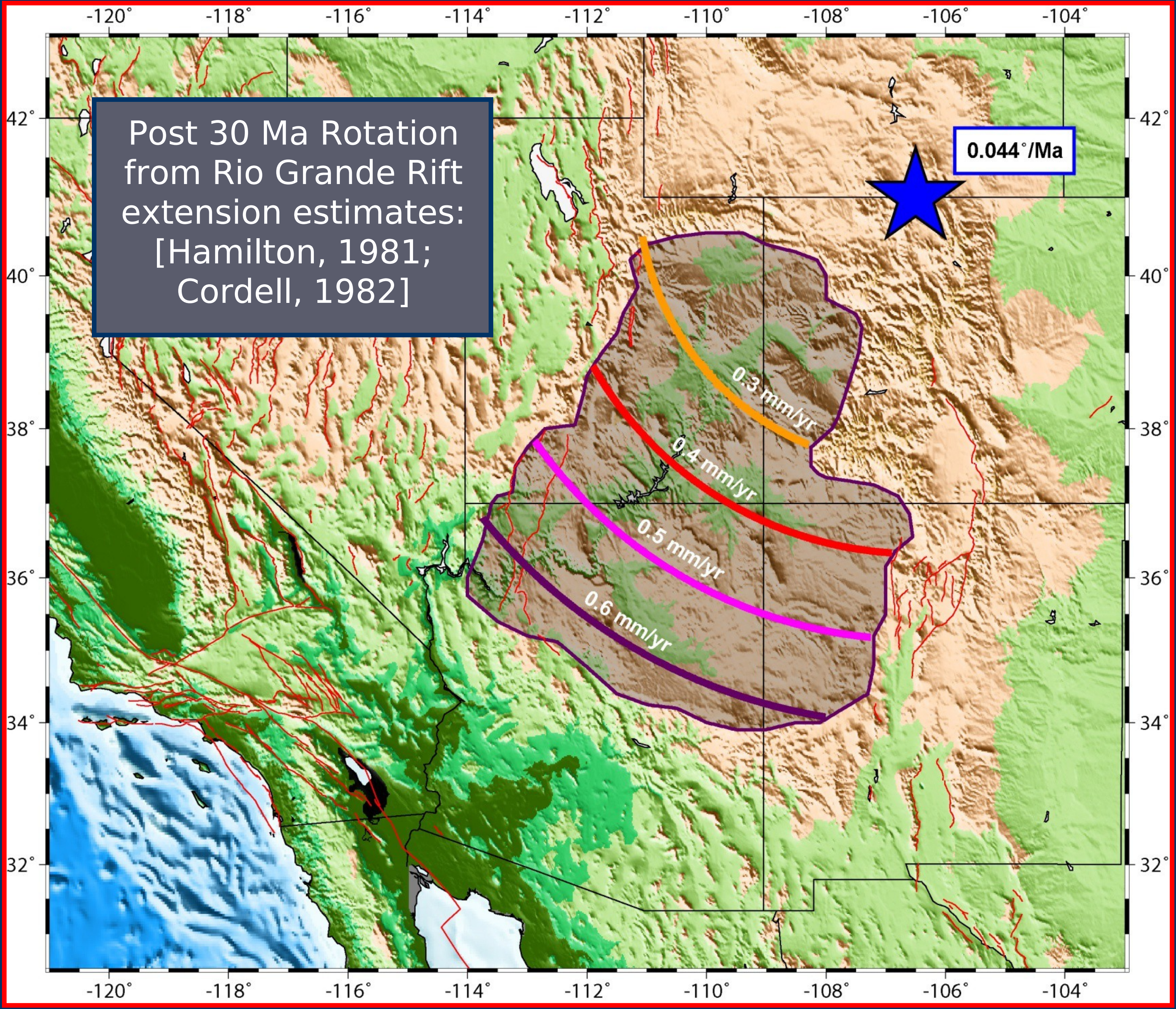

Velocities before EMC (2010)

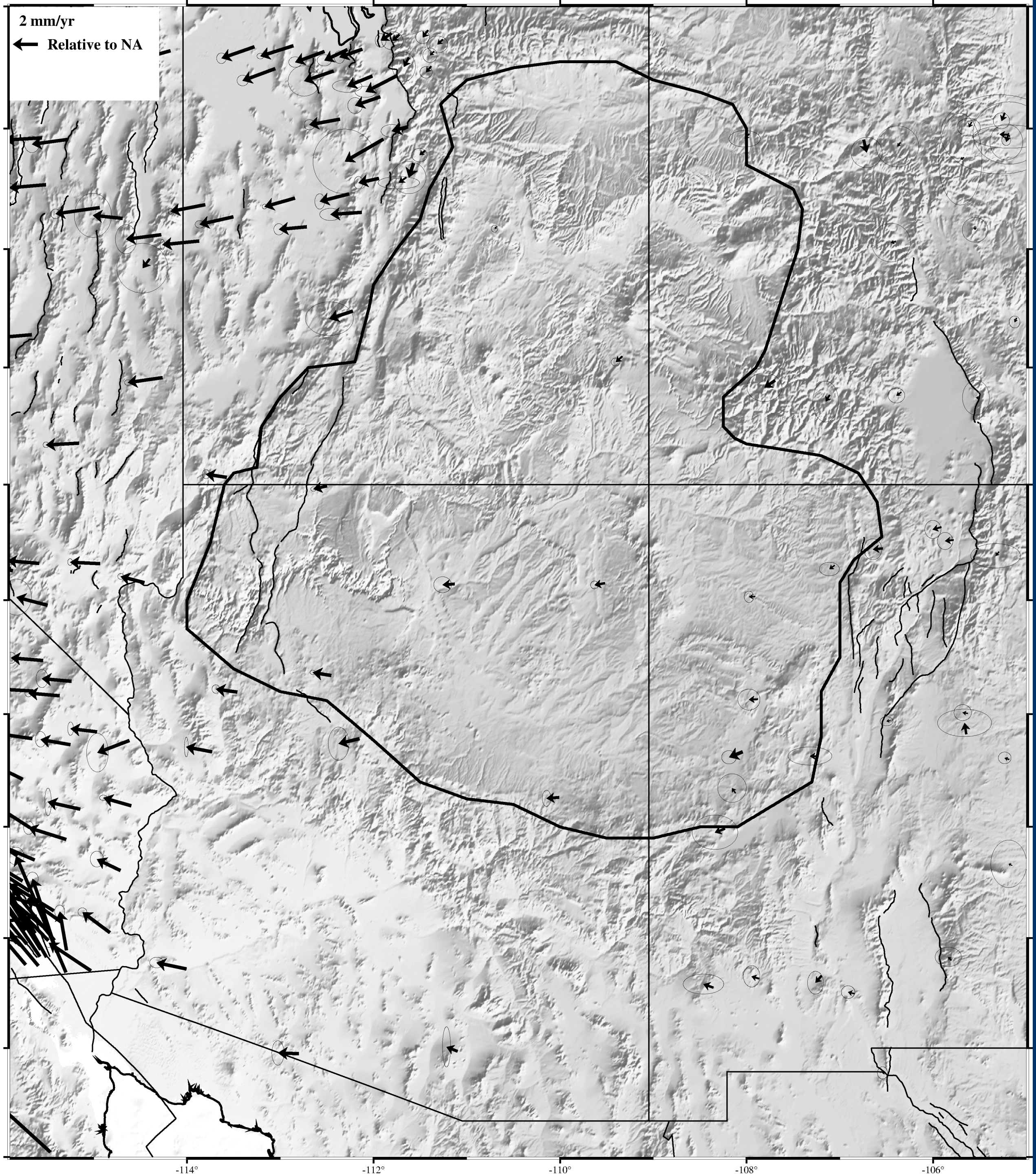

Regional Kinematics

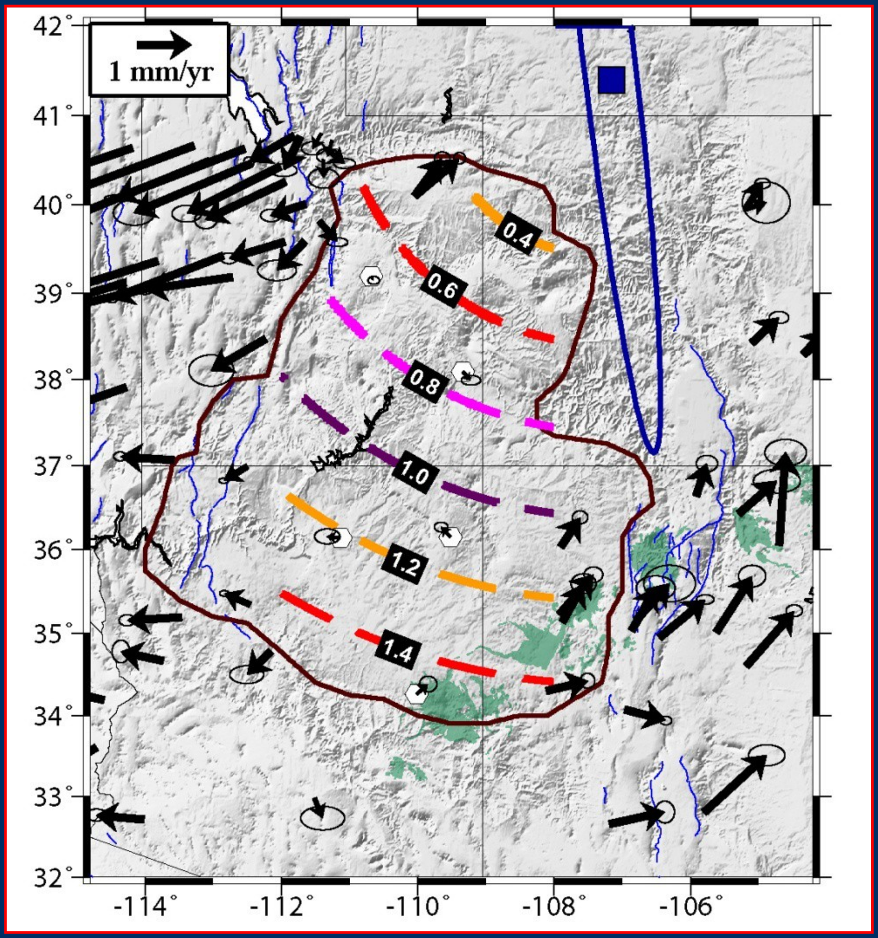

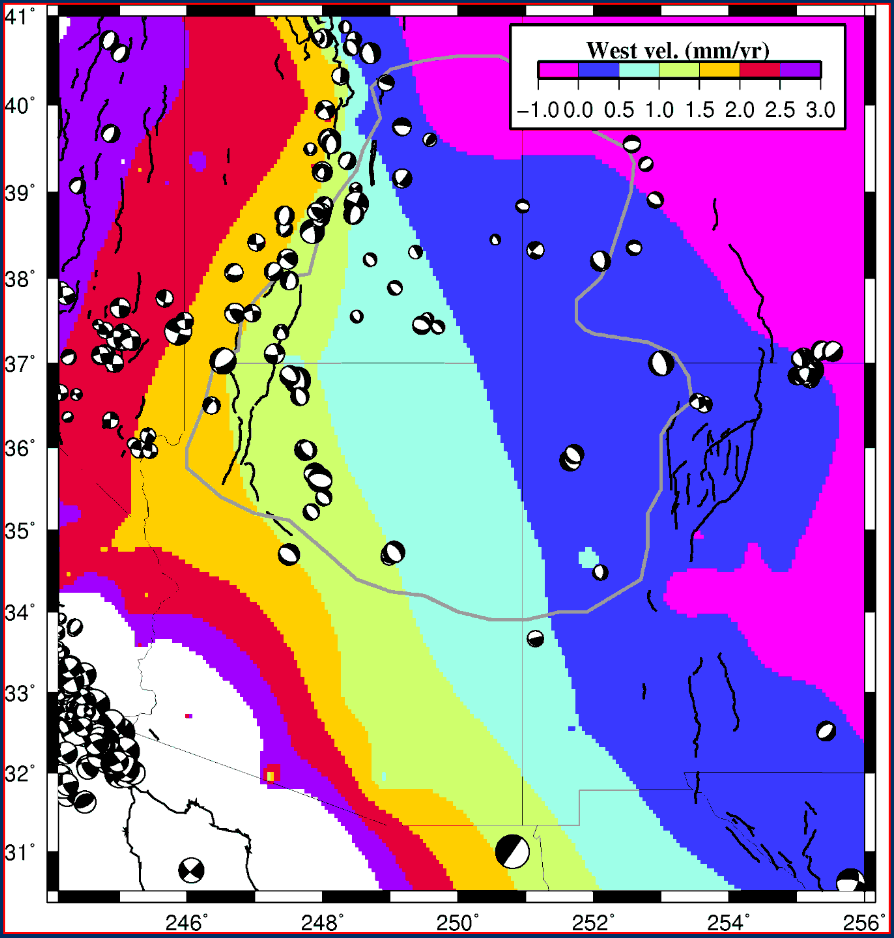

Kreemer et al., GRL, 2010

Pahranagat Shear Zone

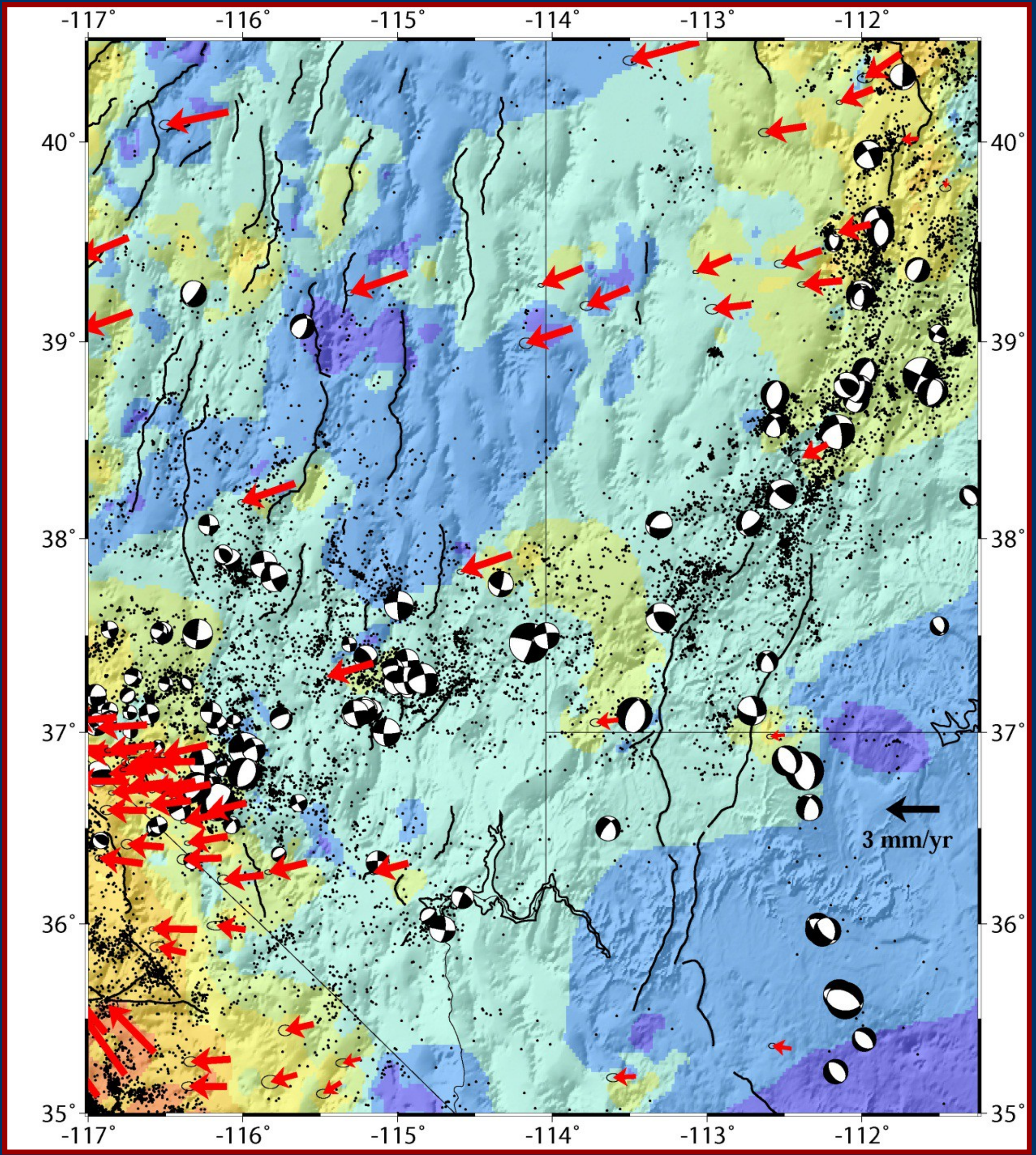

Pahranagat Shear Zone

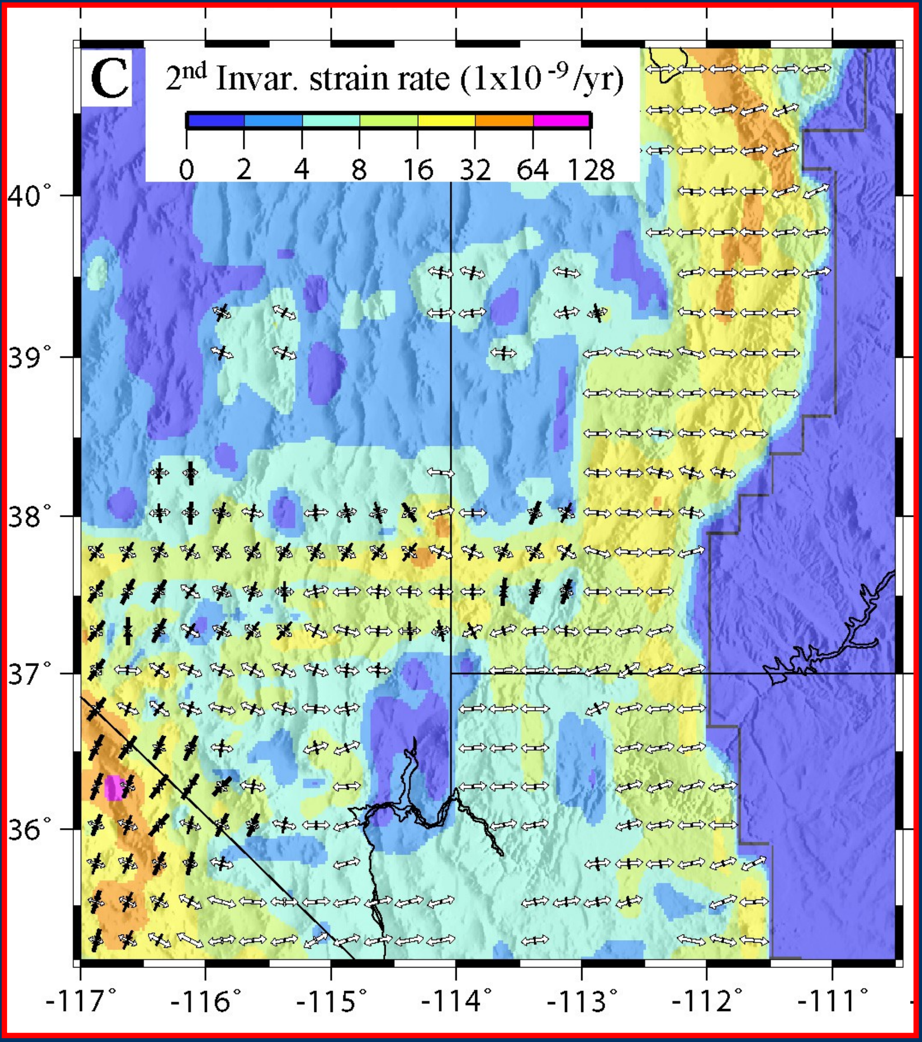

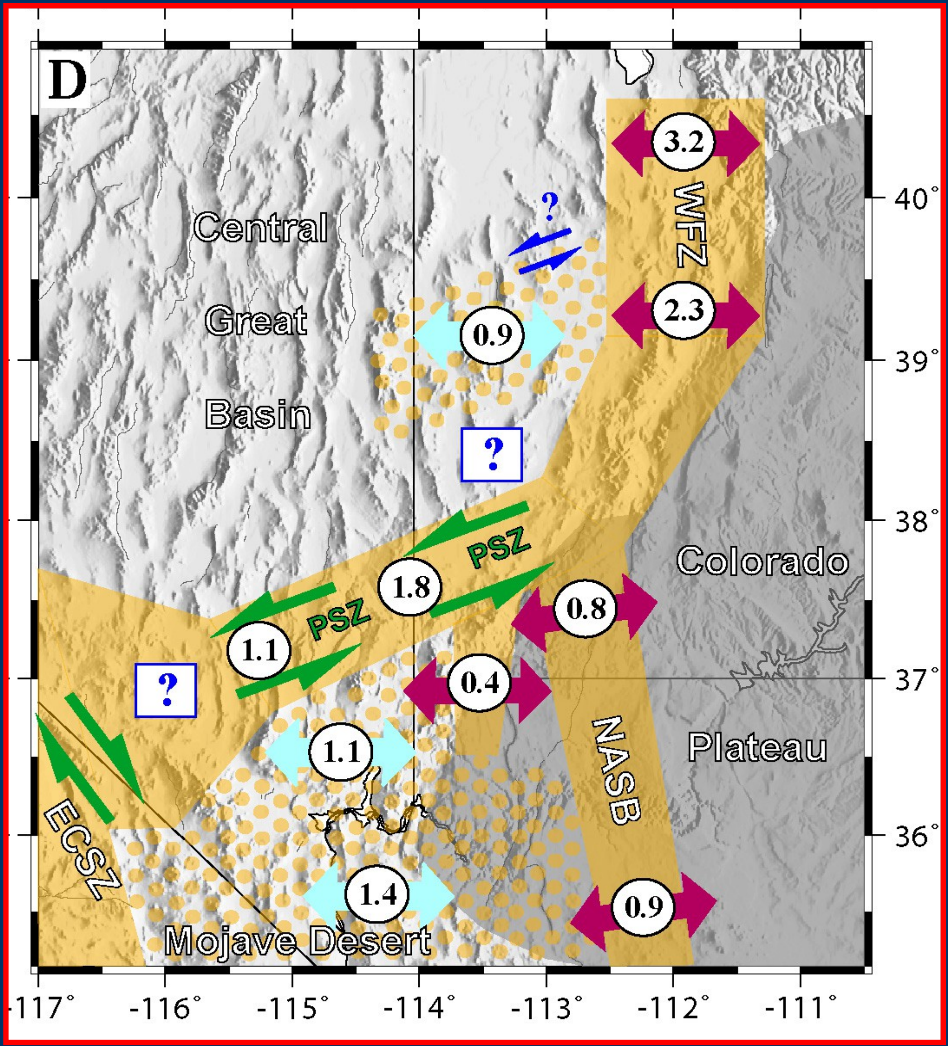

Kreemer et al., Geology, 2010

Pahranagat Shear Zone

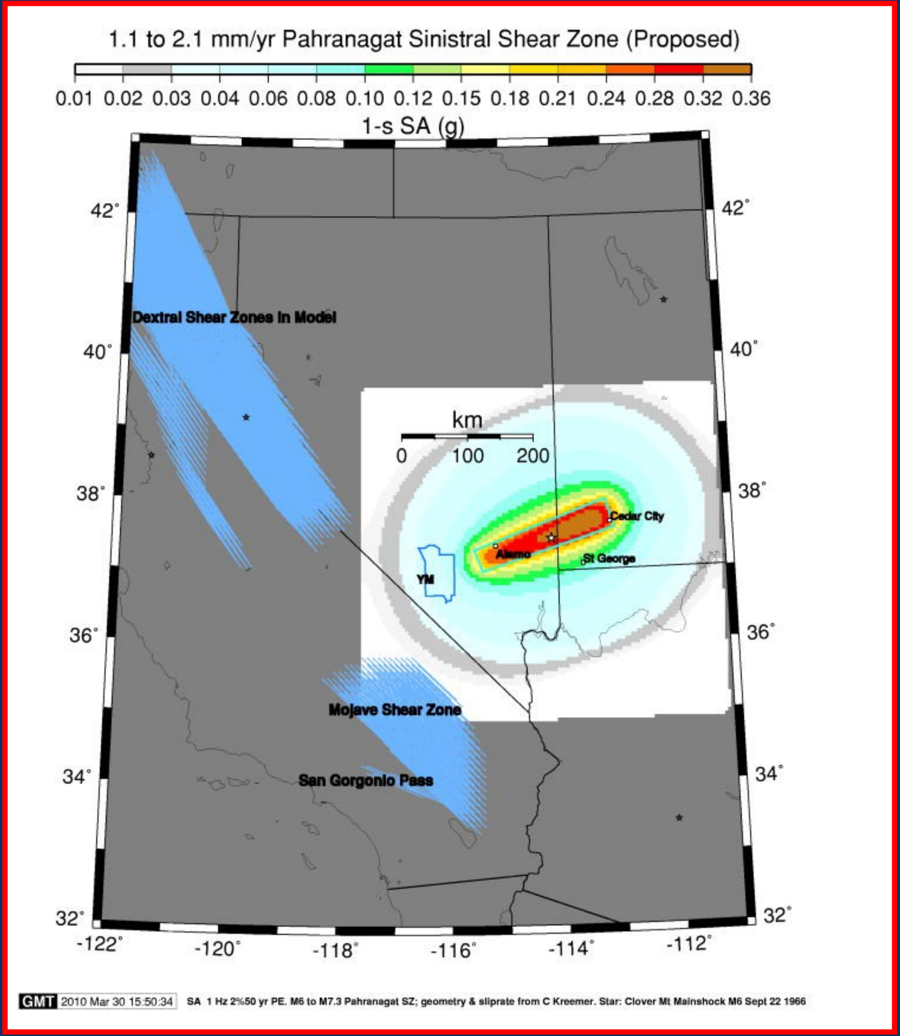

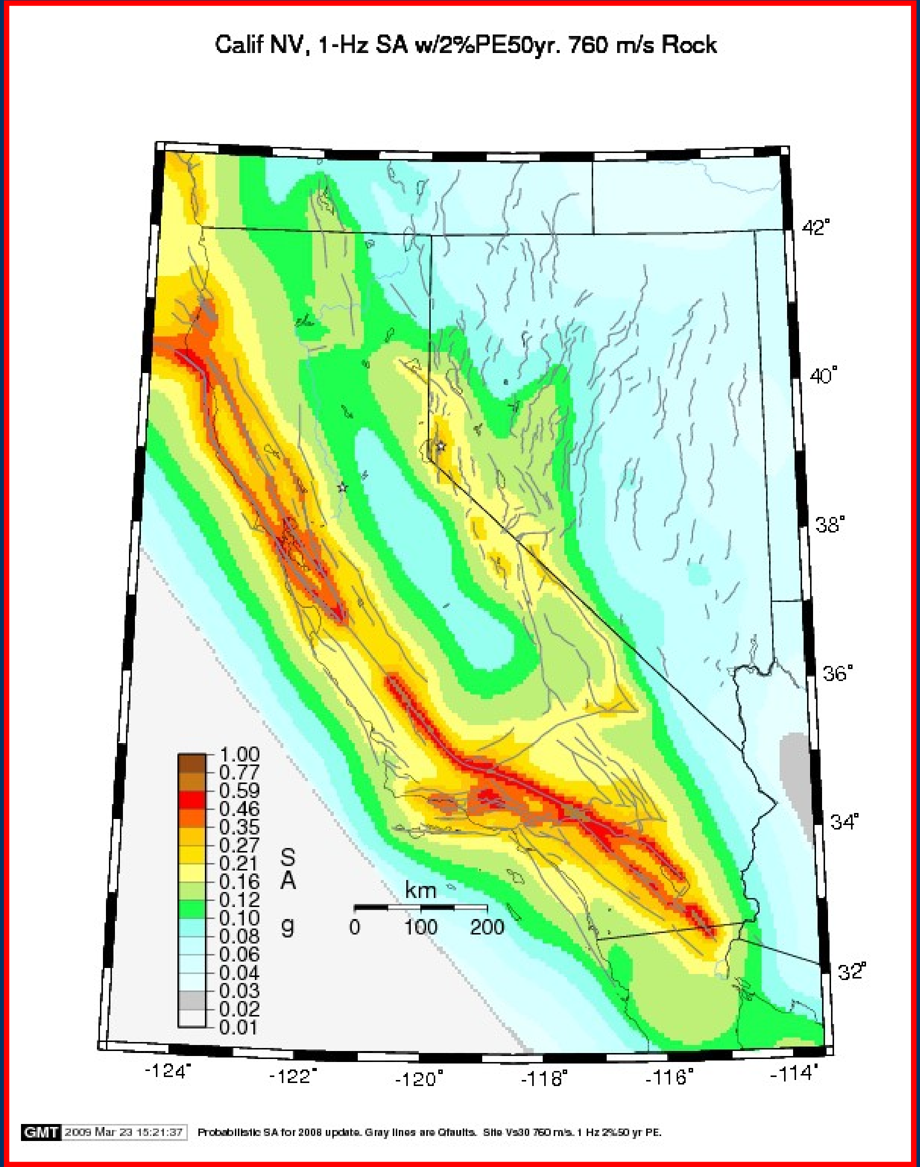

S. Harmsen, USGS, pers. comm., 2010

Kreemer et al., 2012

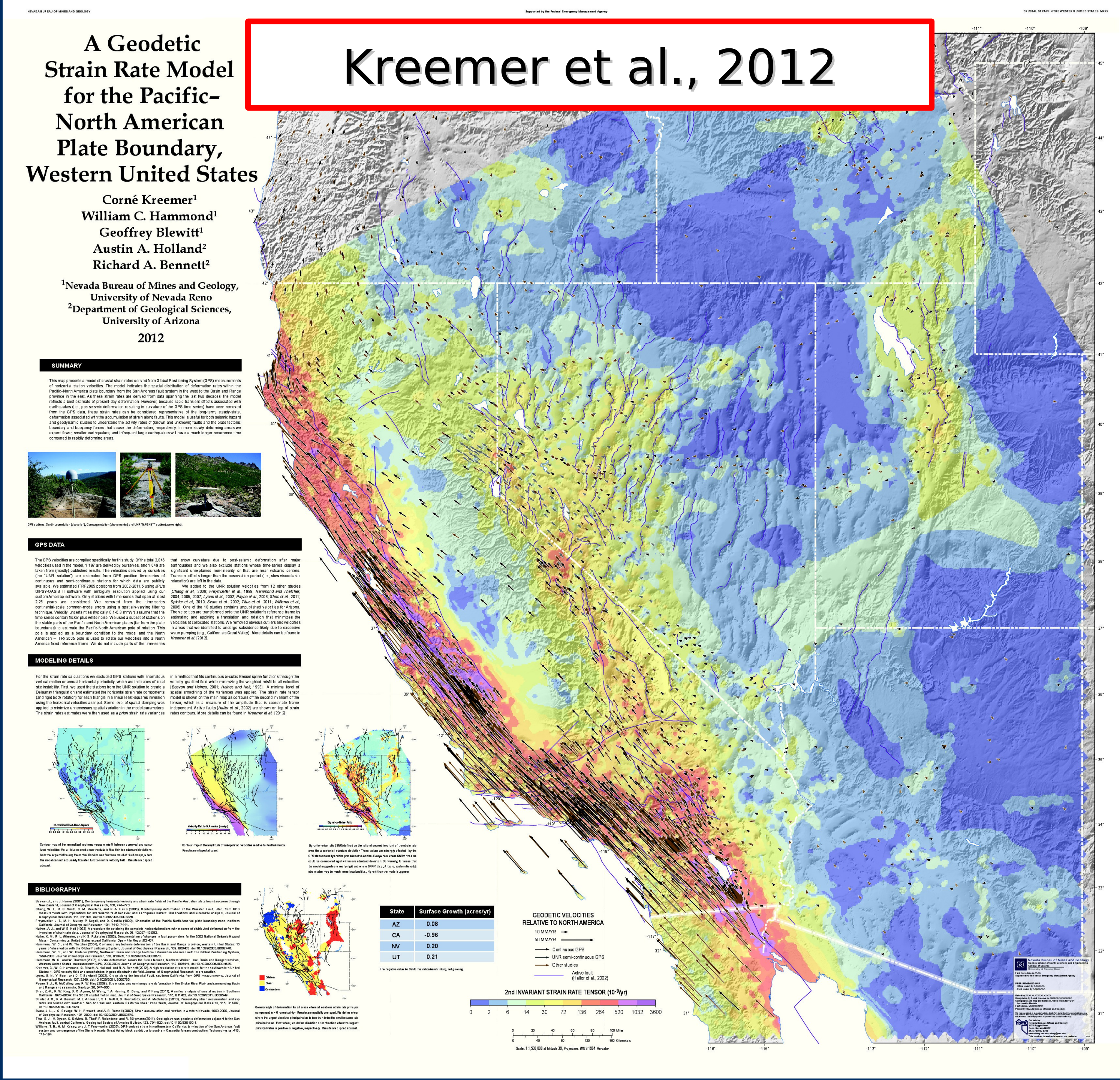

Signal-to-Noise Ratio

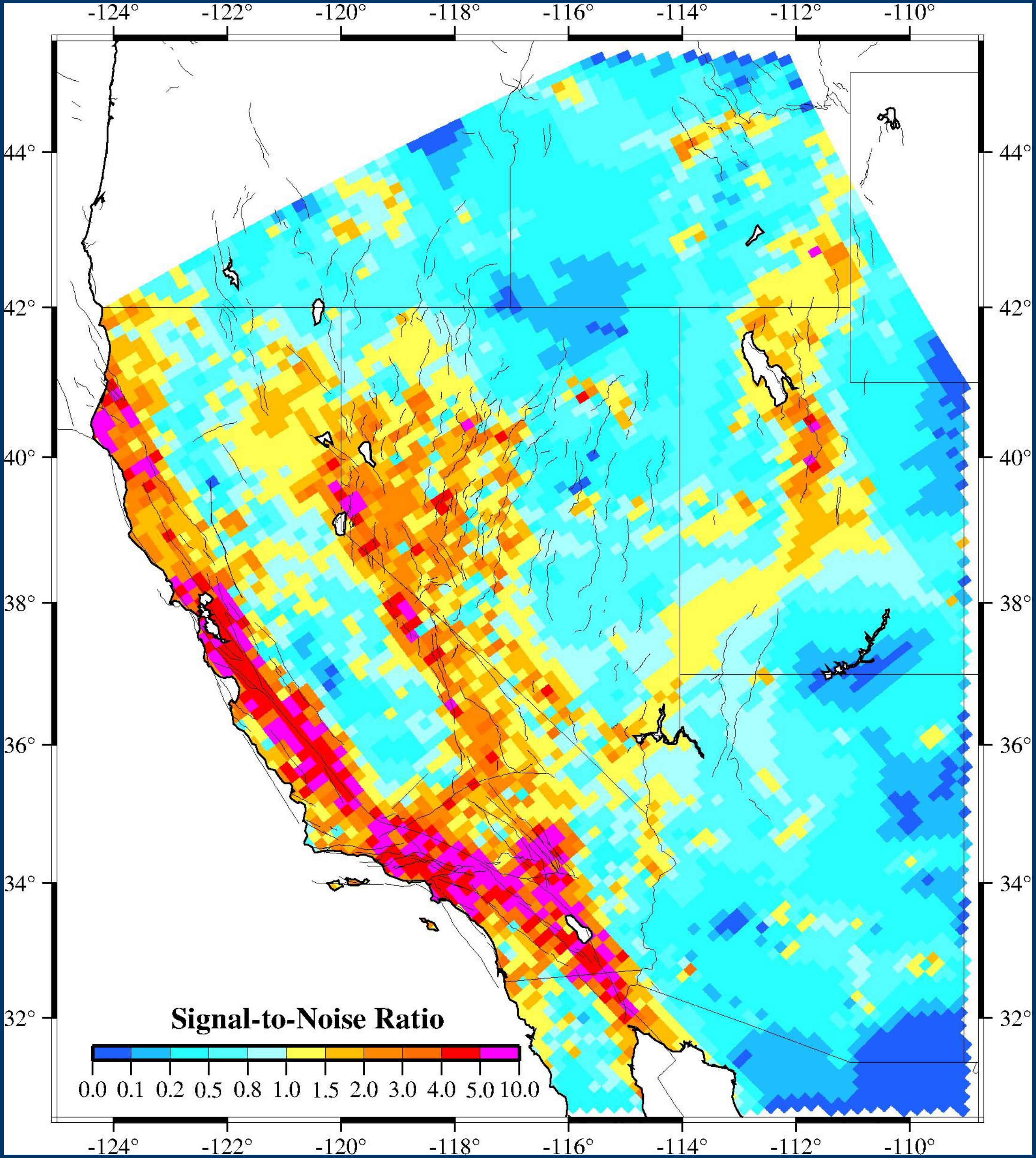

Continuous GPS Stations

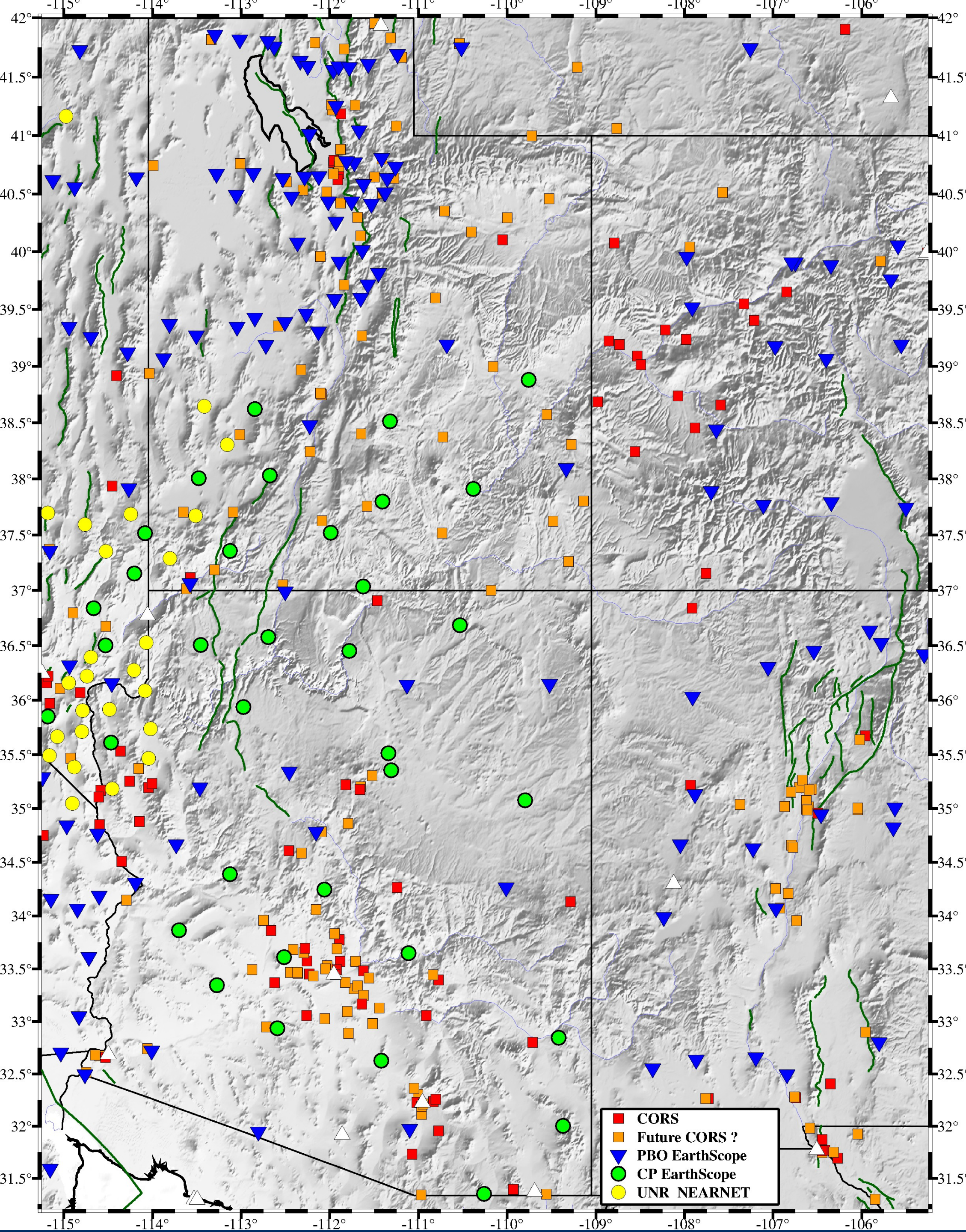

Many continuous GPS stations have been installed in the region (DOT, AZHMP, commercial), but we find that few are useful for tectonic studies

Monuments attached to bedrock are pertinent !!

We installed 34 continuous bedrock stations around western CP (Earthscope) and many more semi-continuous stations around LV (DOE, USGS)

Continuous GPS Stations

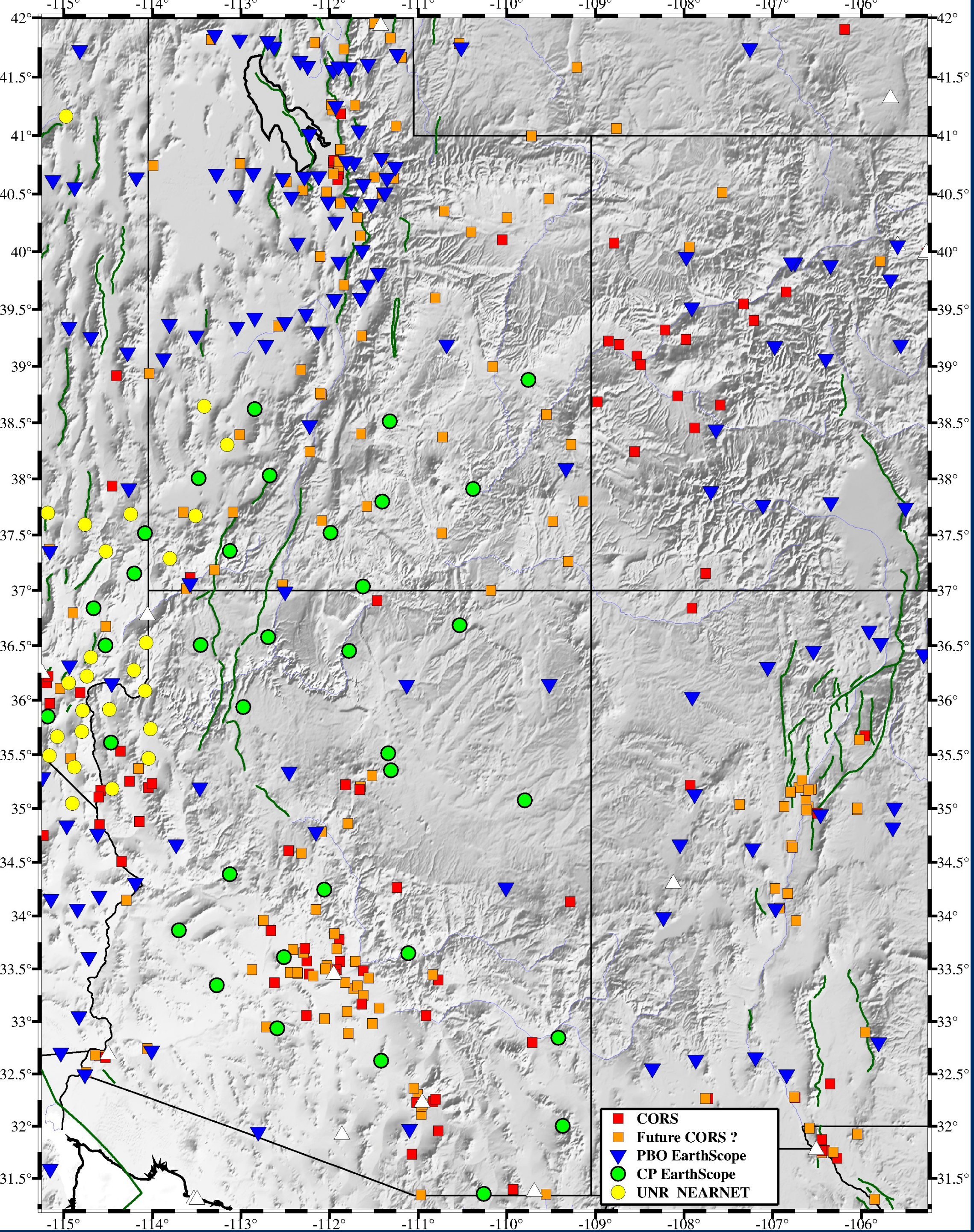

Coseismic Offsets El Mayor-Cucapah

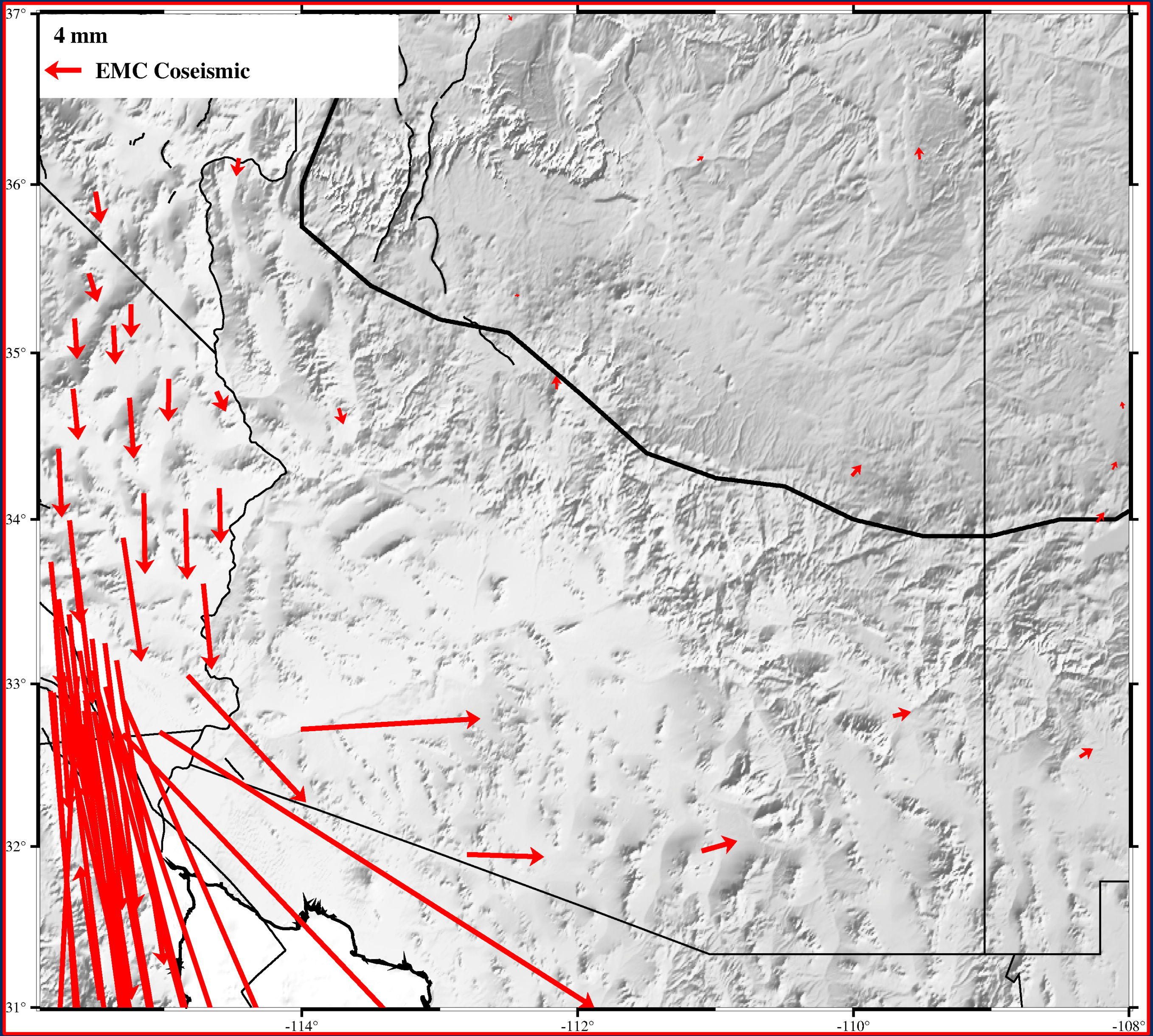

Effect of 2010 El Mayor-Cucapah

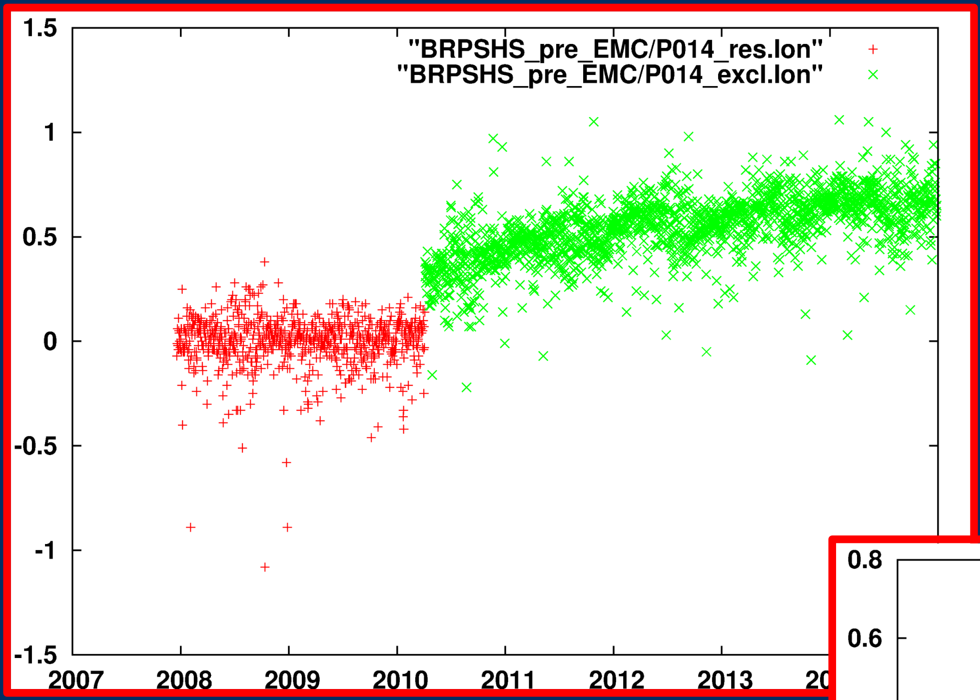

East component near Tucson

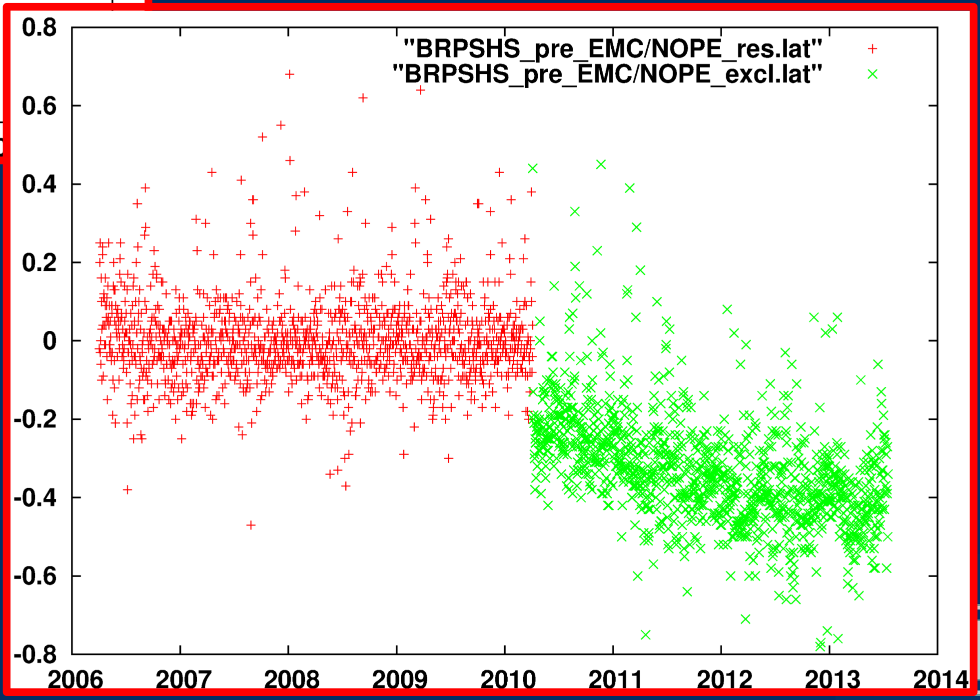

North component near Yucca Mountain

Velocity Change El Mayor-Cucapah

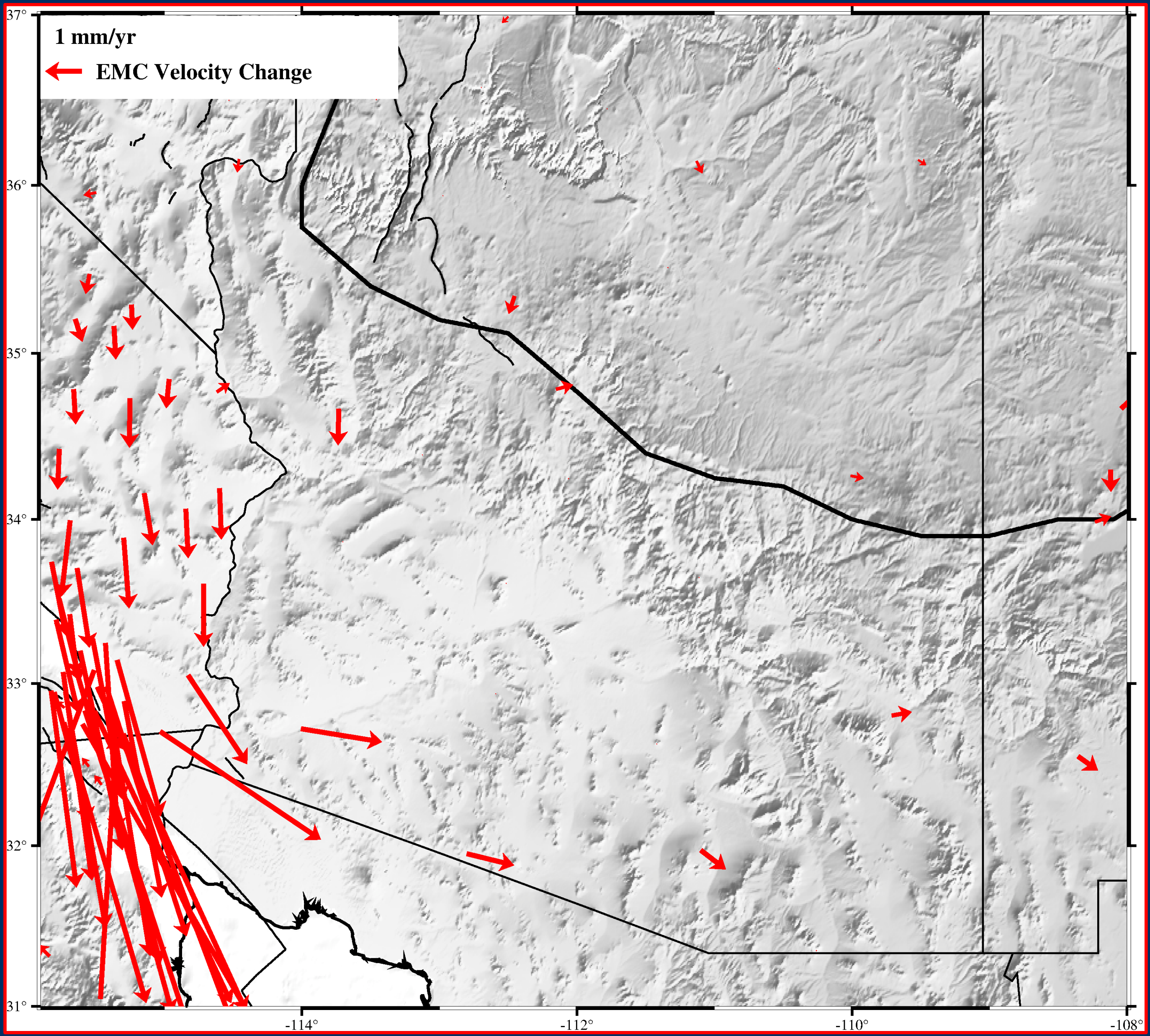

Velocities wrt NA

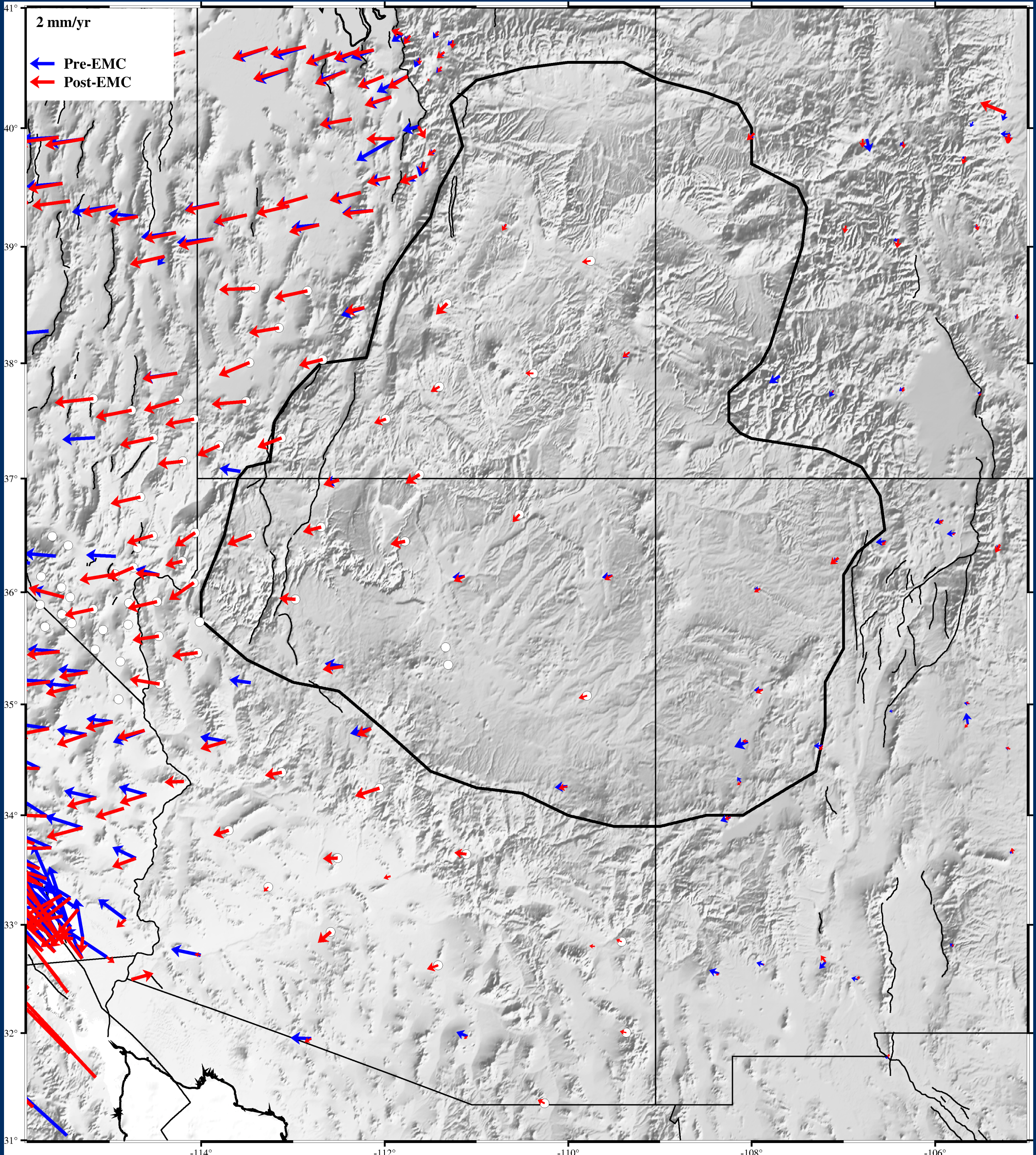

Before EMC
After EMC

Postseismic deformation following EMC shut off most of 2.5 mm/yr pre-EMC extension in southernmost AZ

Note our inability to infer velocity changes in southern NV due to termination of YM network

Strain Rate Before EMC

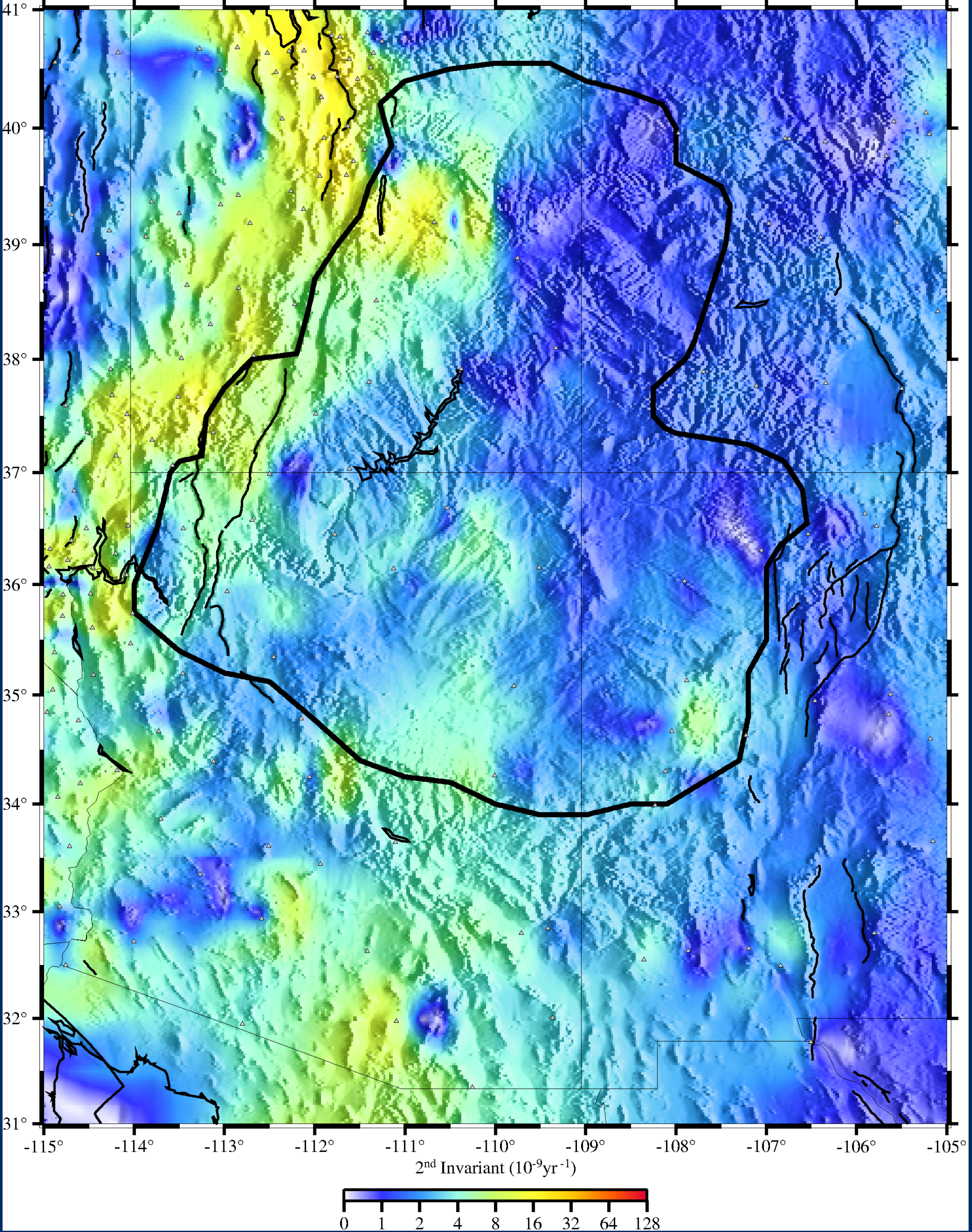

Strain Rate After EMC

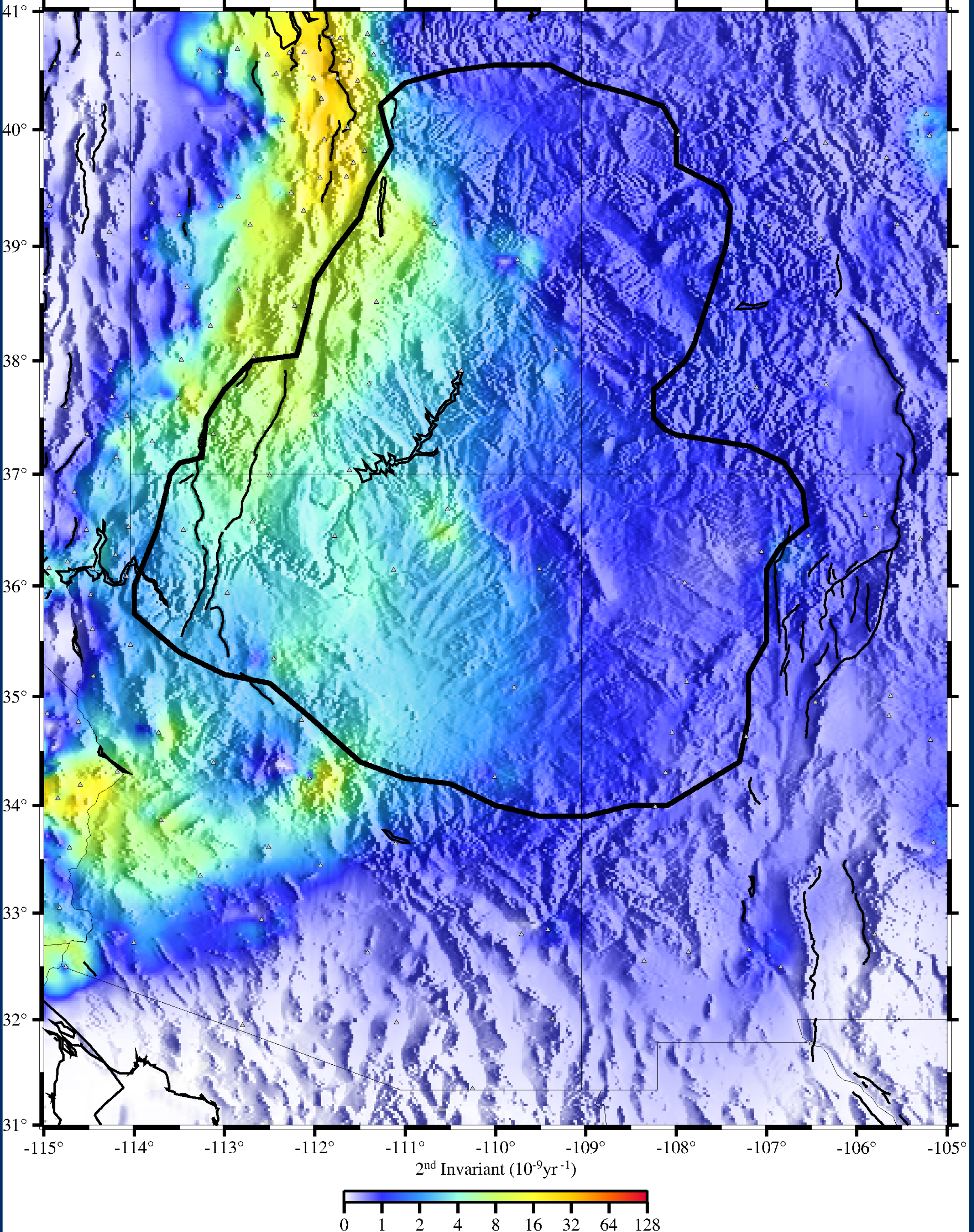

Visco-elastic Correction

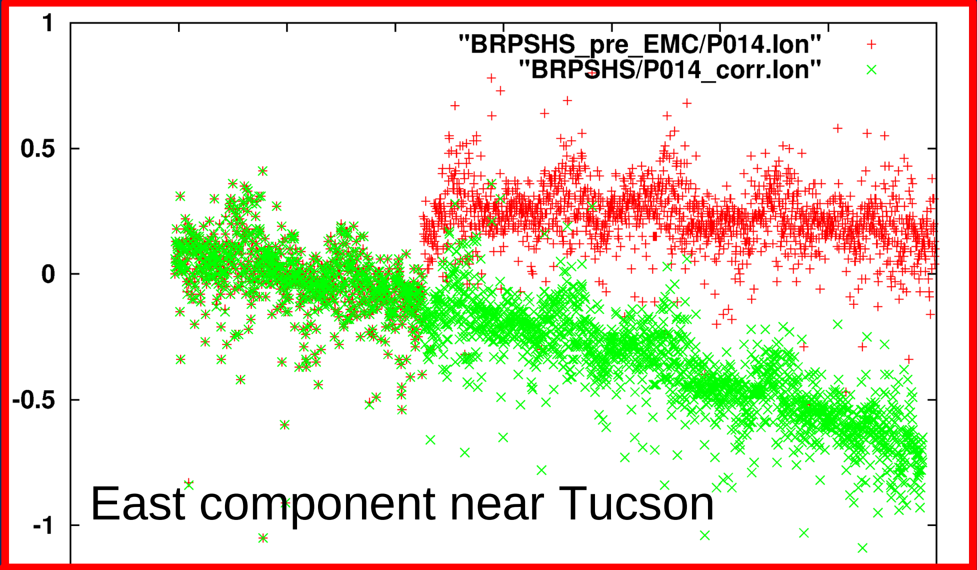

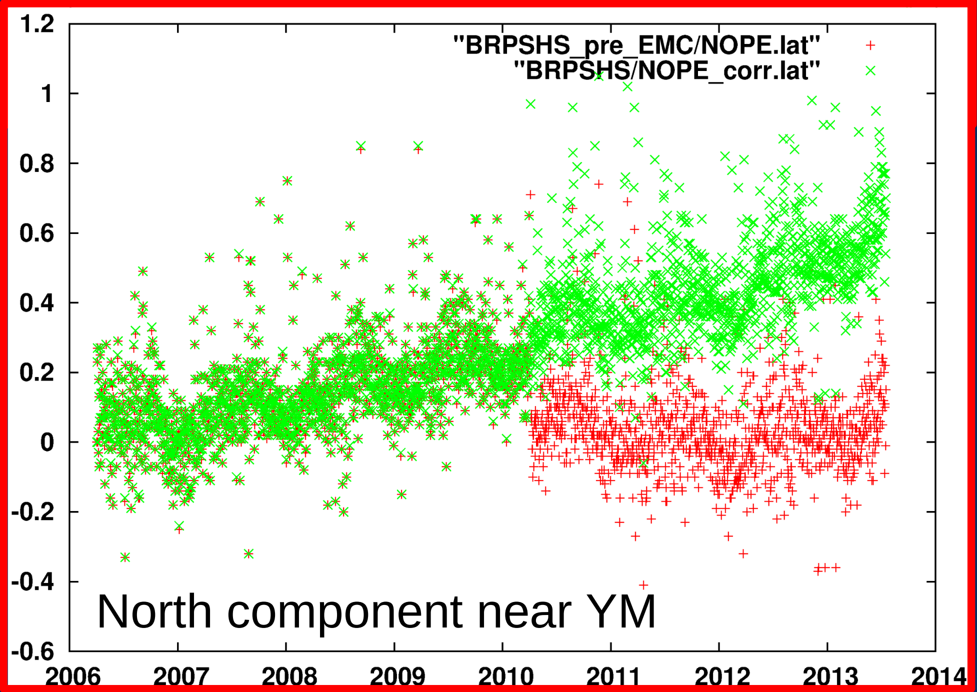

Effective correction for visco-elastic Relaxation using PSGRN/PSCMP by Wang (2006) using coseismic model of Wei et al. (2011)

Model uses simple viscoelastic structure with:

viscosity lower crust = 10^{20} Pa s
viscosity upper mantle = $10^{18.5}$ Pa s

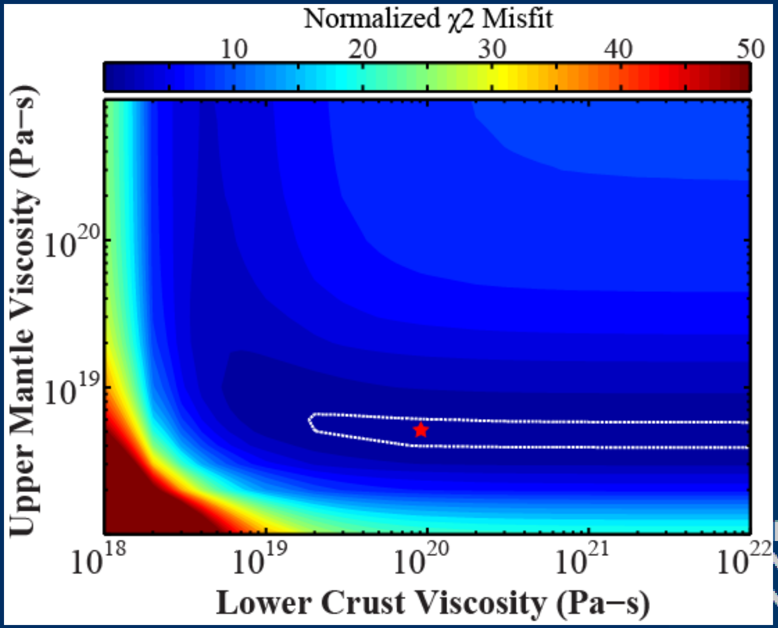

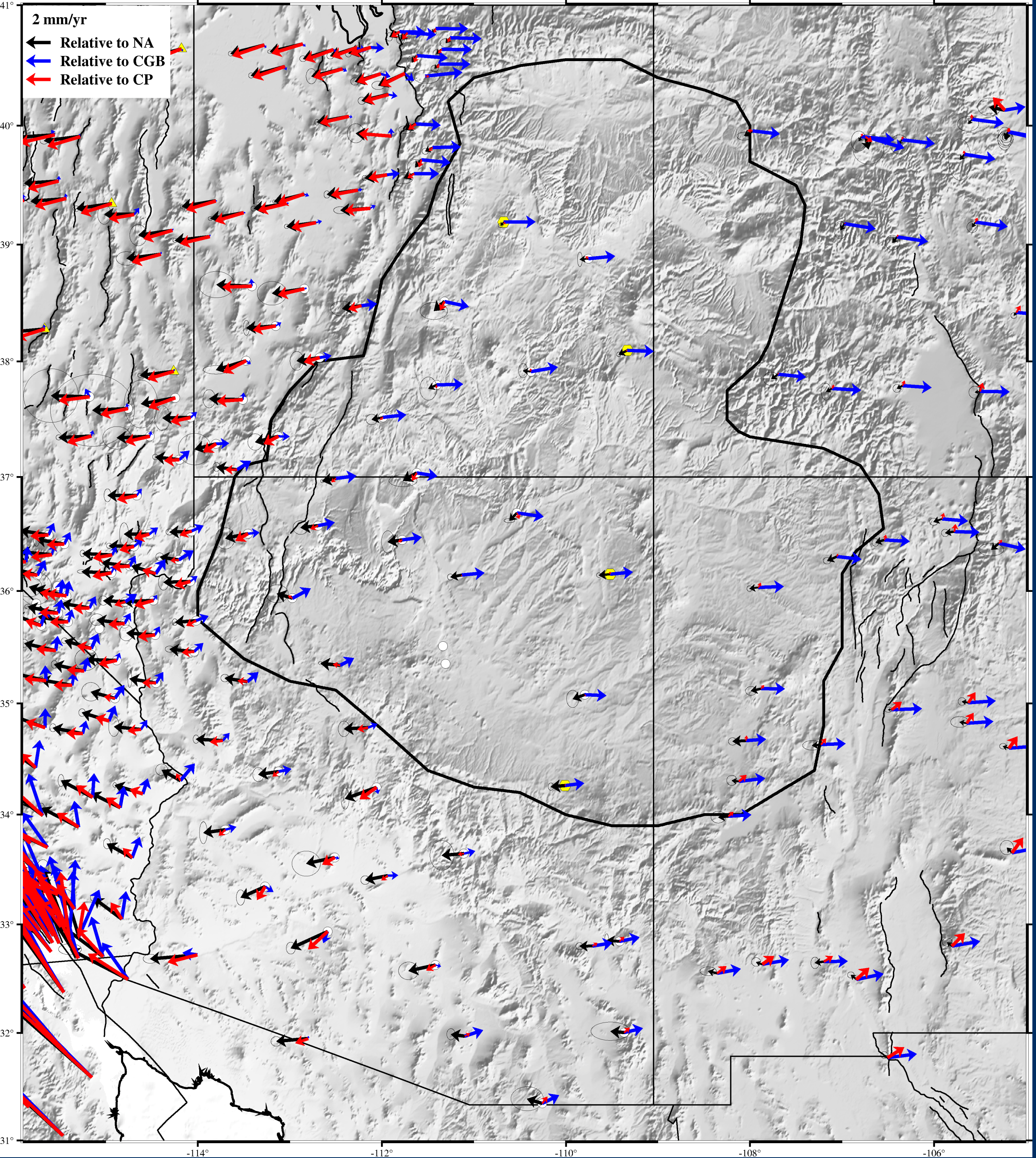

Corrected Velocities

wrt NA
wrt CGB
wrt CP

~2.5 mm/yr localized extension across Wasatch

0.4-0.5 mm/yr across Toroweap-Hurricane faults

No significant extension across Rio Grande Rift

Corrected Velocities

West Contours wrt NA

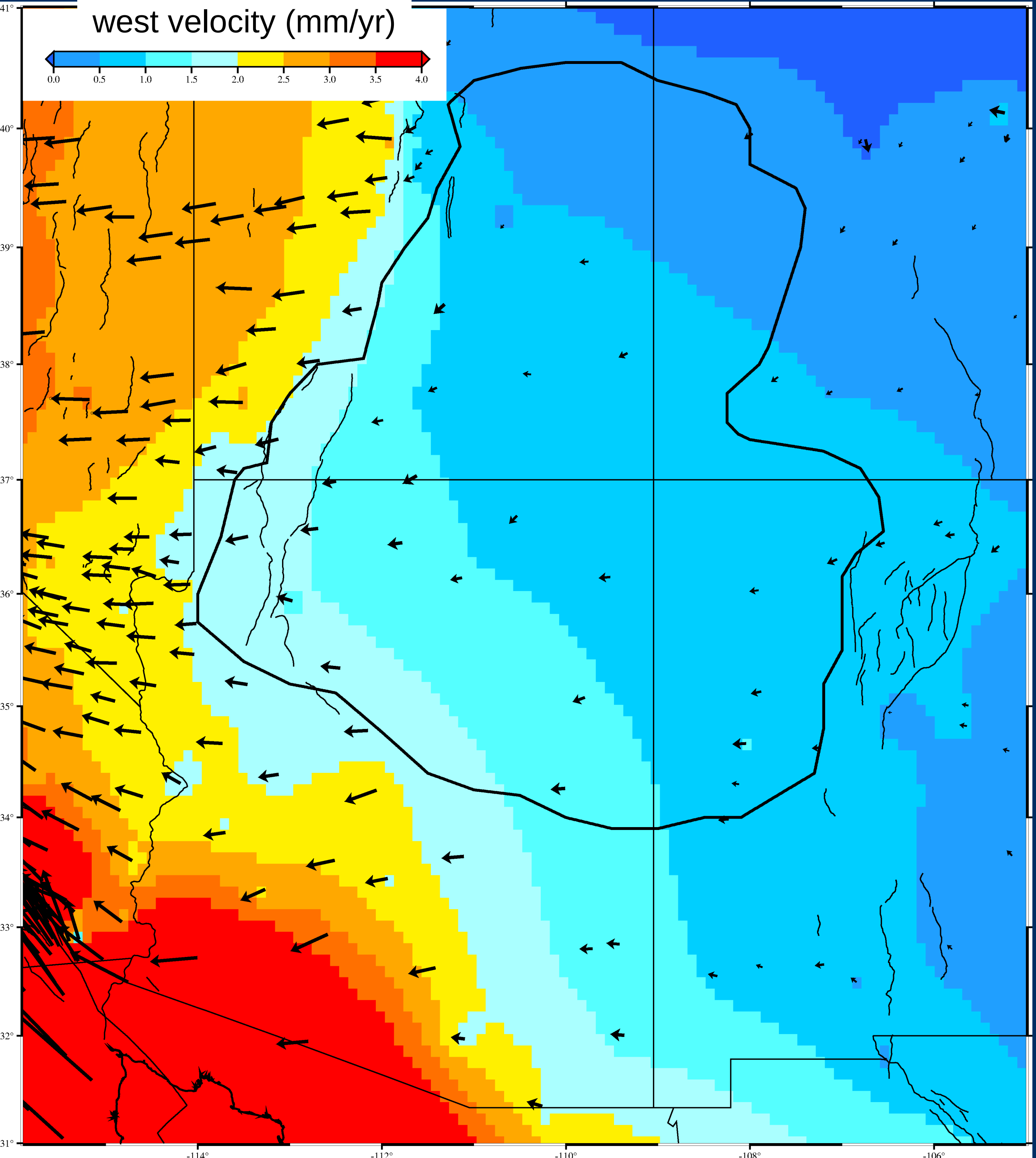

Visco-elastic Effects of Older Events

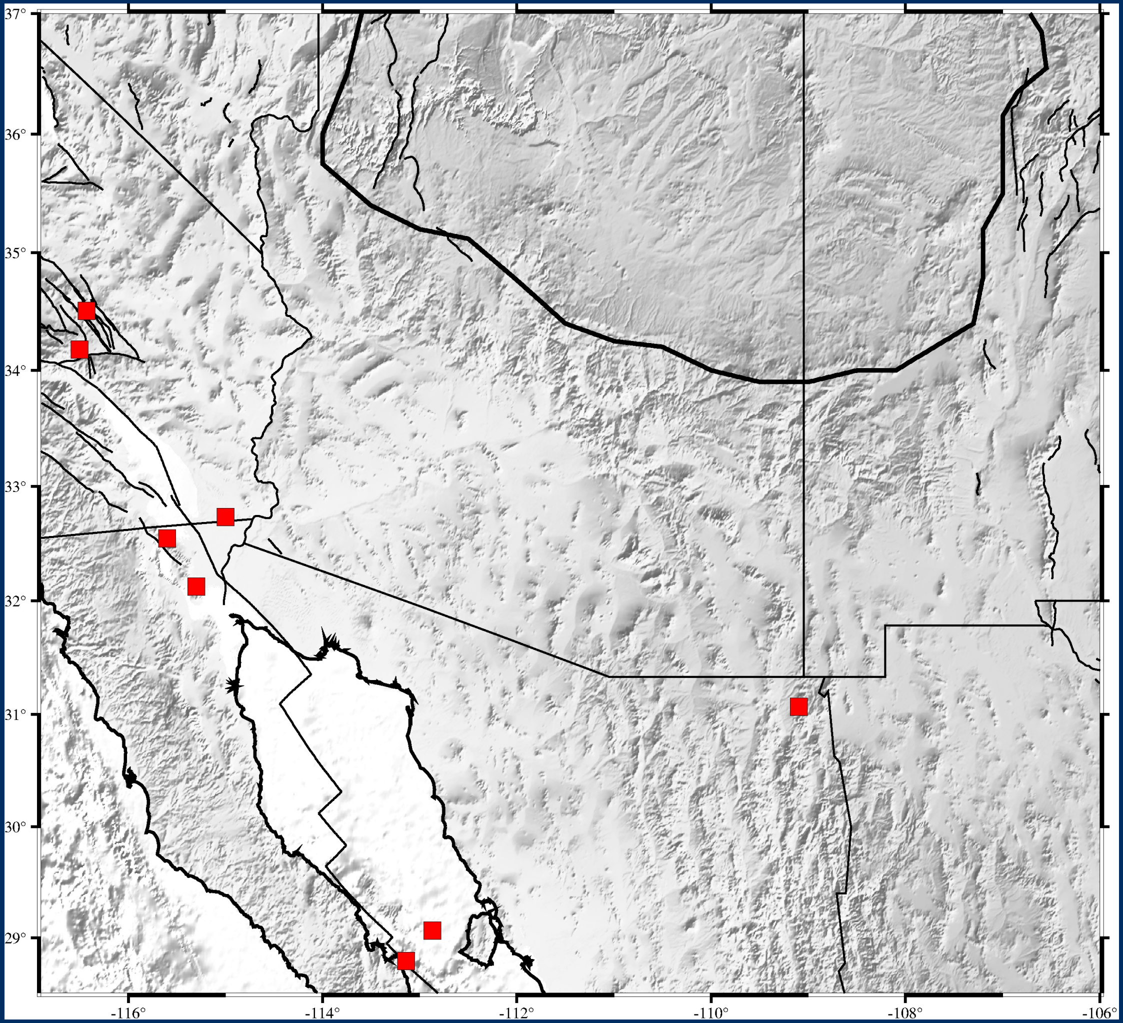

1887 M7.5 Sonora
1892 M7.2 Laguna Salada
1940 M6.9 Imperial Valley
1992 M7.3 Landers
1999 M7.1 Hector Mine
2009 M6.9 Baja California
2010 M7.2 El Mayor-Cucapah
2012 M6.9 Baja California

Visco-elastic Effects of Older Events

Effect of Landers in 2010

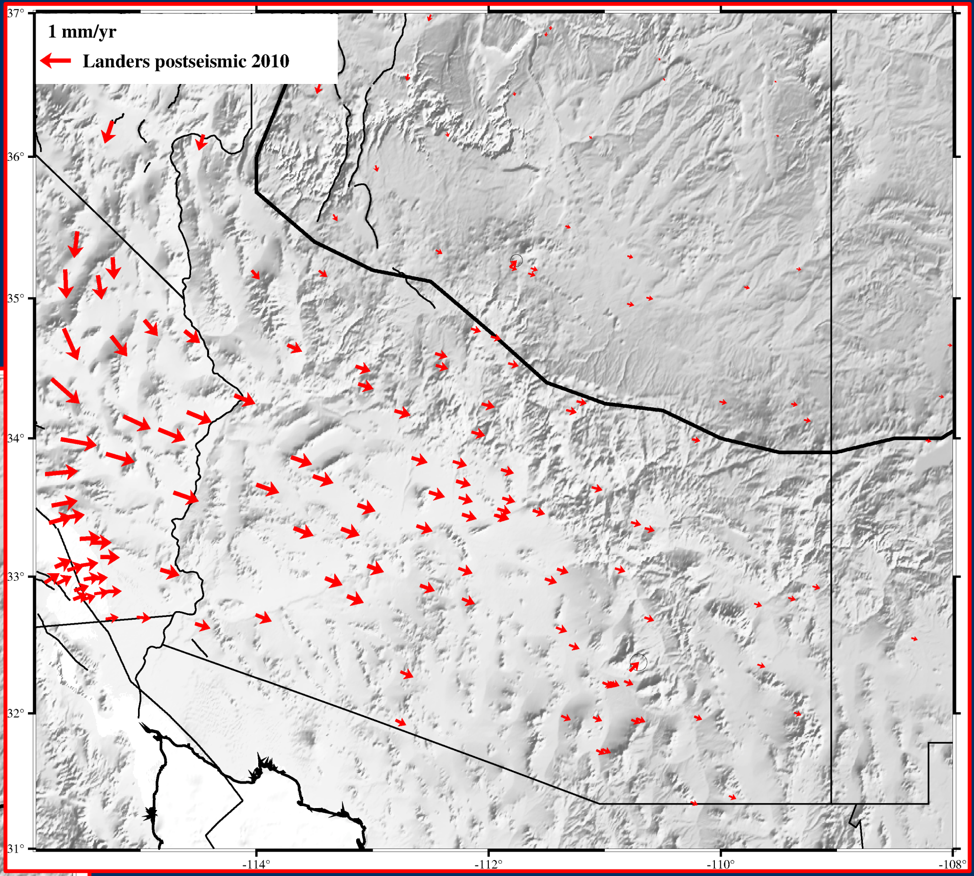

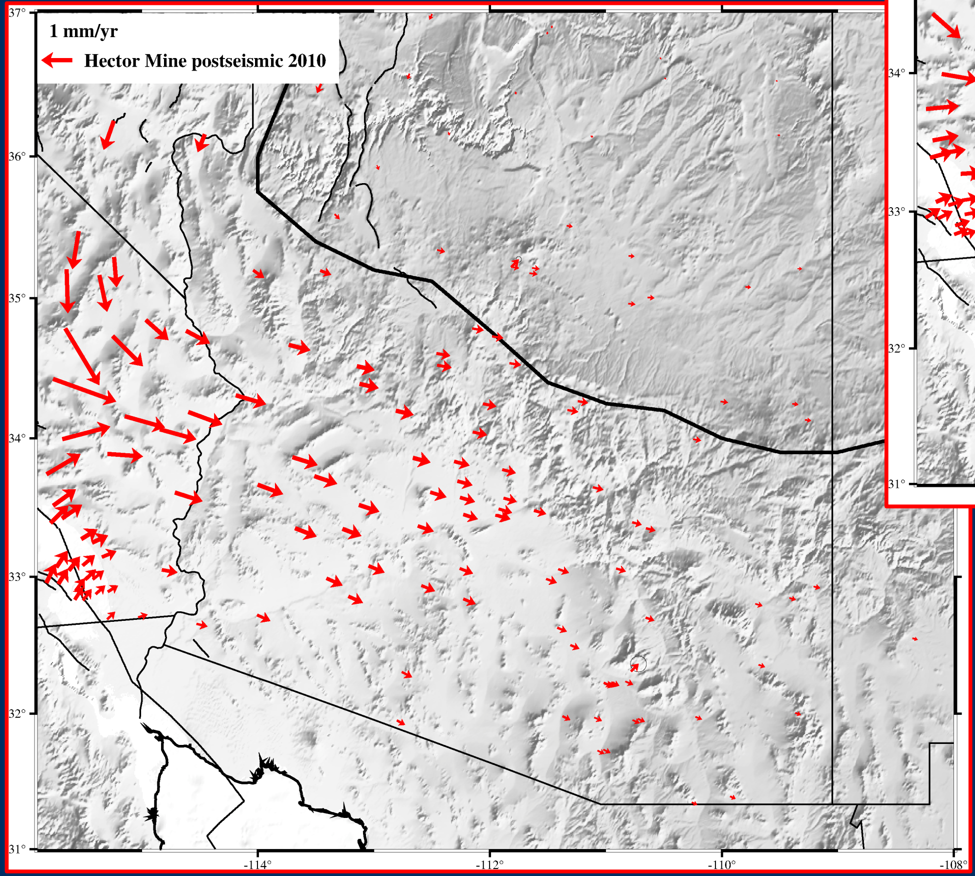

Effect of Hector Mine in 2010

Visco-elastic Effects of Older Events

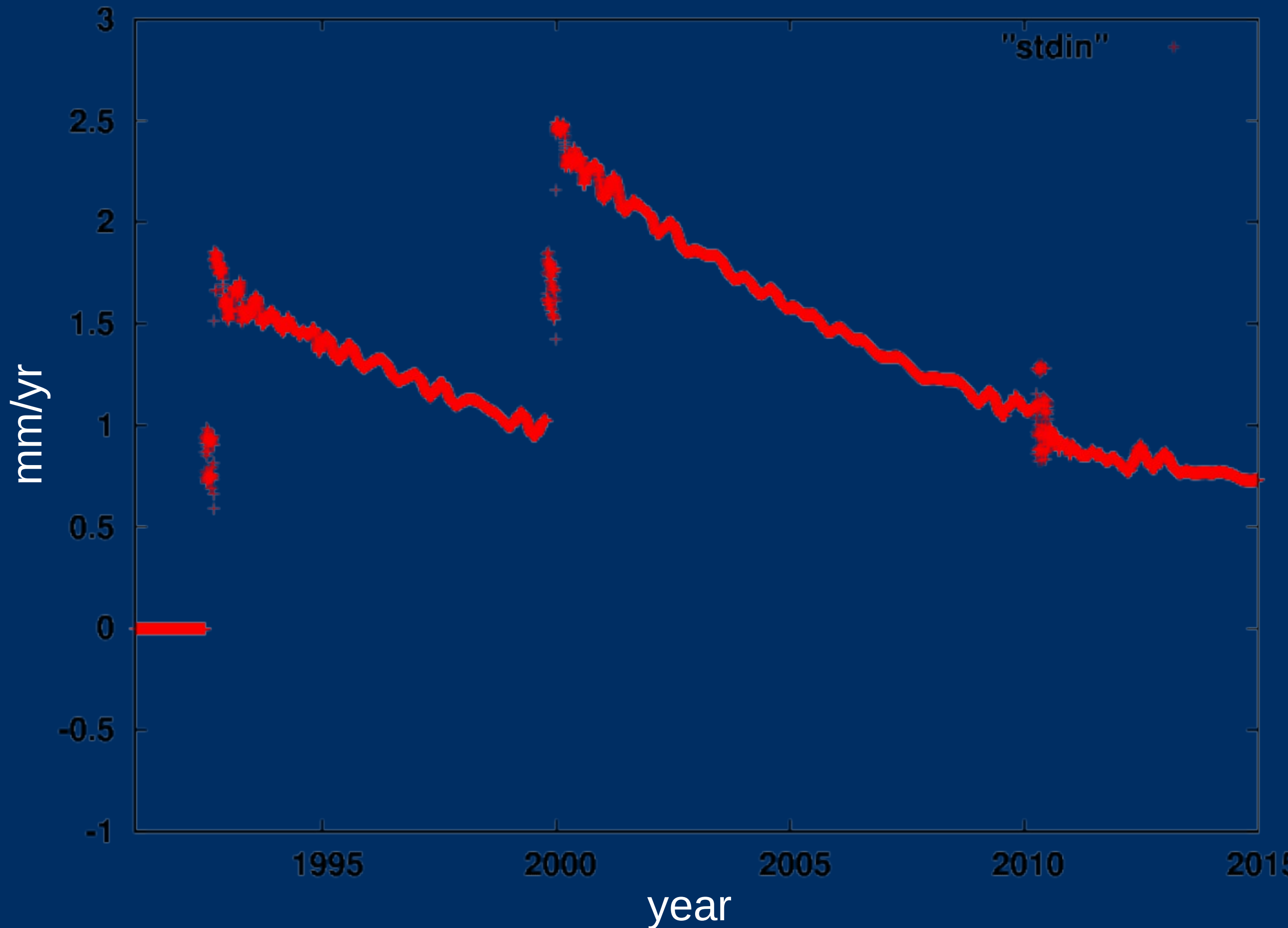

Change in baseline across southern AZ. Positive is contraction

Visco-elastic Effects of Older Events

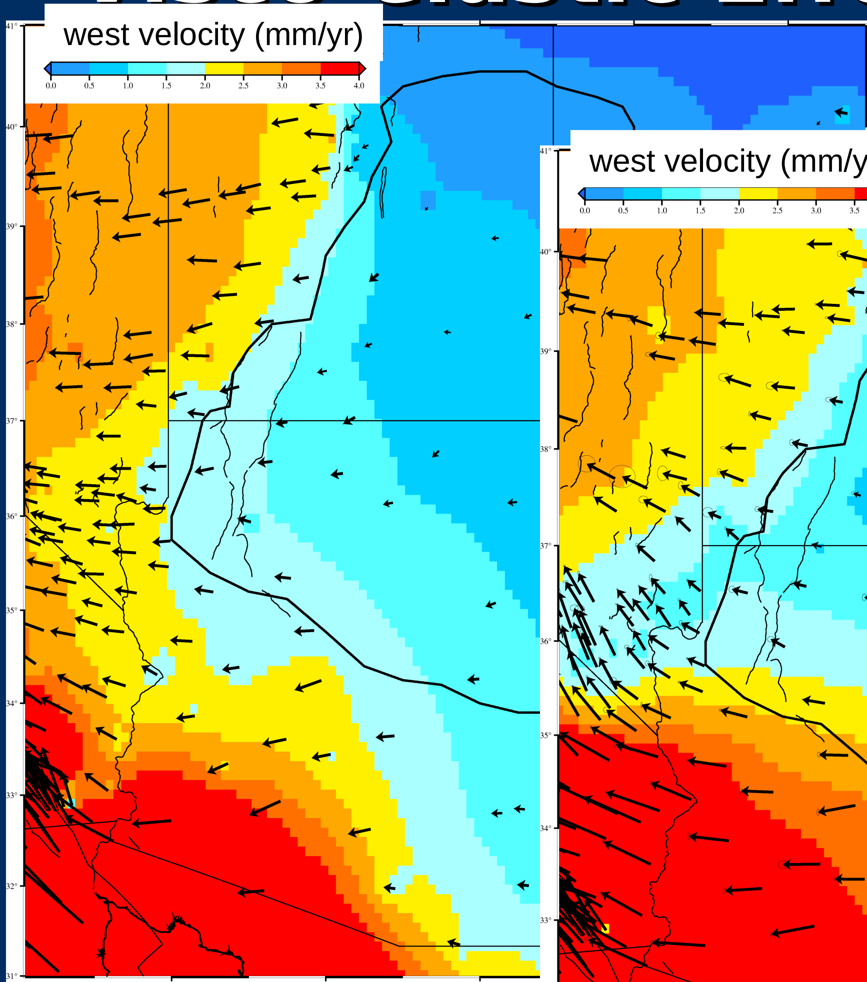

only used EMC in correction

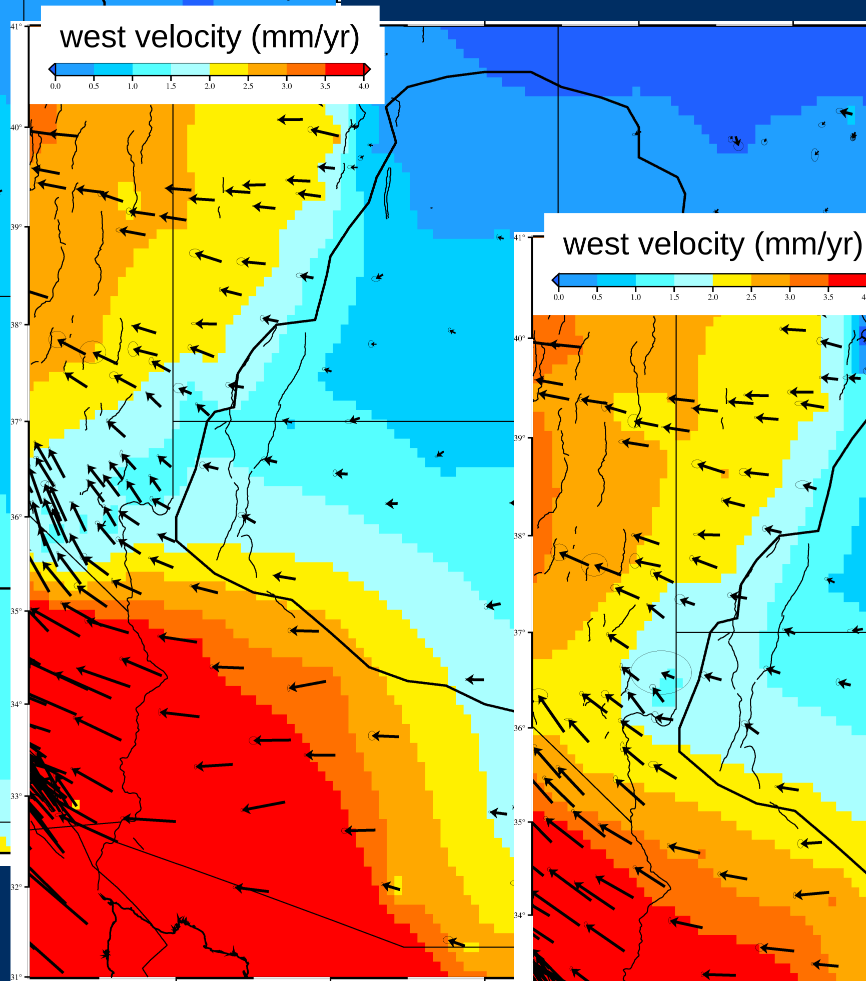

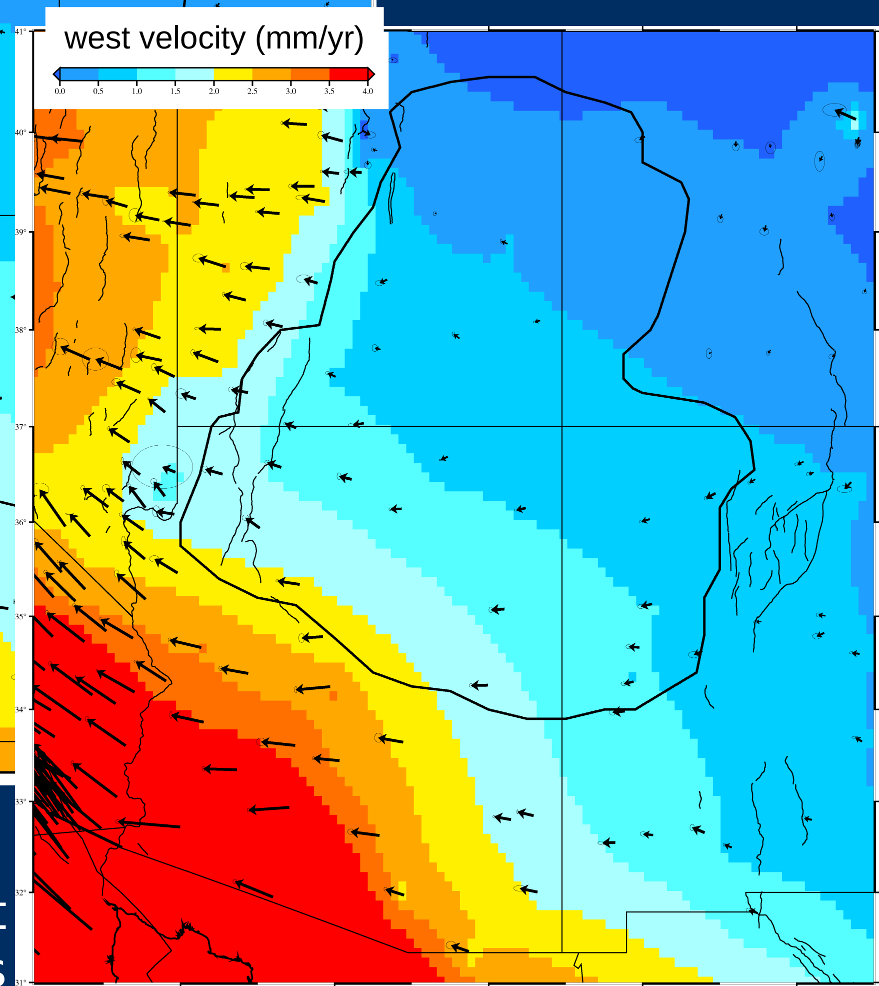

Used all in correction
But based on pre-EMC
velocities

Used all in correction, but
based on post-EMC velocities

Conclusions

Coverage of continuous GPS stations is growing, but only those in bedrock are useful

Earthquakes along southern SAF strongly modulate deformation in southern AZ. A long-term extension rate of >4 mm/yr is constantly superimposed with post-seismic contraction: <u>Difficult to assess long-term hazard</u>

Further north and east, results are less affected:

Extension rate of 2.4 mm/yr accommodated over

+ ~2.5 mm/yr localized extension across Wasatch

+ 0.4-0.5 mm/yr across Toroweap-Hurricane faults

+ No significant extension across Rio Grande Rift

UPDATE OF GPS DEFORMATION RATES IN THE SNAKE RIVER PLAIN

Suzette J. Payne[1], Robert W. King[2], Robert McCaffrey[3], and Simon A. Kattenhorn[4]
[1] Idaho National Laboratory, P.O. Box 1625, Idaho Falls, ID 83401-2203
[2] Department of Earth, Atmospheric and Planetary Sciences, Massachusetts Institute of Technology, Cambridge, MA 02139
[3] Department of Geology, Portland State University, Portland, OR, 97207
[4] ConocoPhillips Geological Technology, 600 N. Dairy Ashford, Houston, TX 77079
Senior author's email address: Suzette.Payne@inl.gov

Surface velocities at more than 400 Global Positioning System (GPS) sites during 1993–2014 are used to reveal rates of deformation in the Northern Basin and Range Province. Crustal deformation in the northern Basin and Range Province is extension while the Snake River Plain is overprinted by volcanism associated with the Yellowstone hotspot. The Snake River Plain by contrast is a seismically quiet, slowly deforming, low-relief volcanic province that extends from eastern Oregon through southern Idaho and into northwestern Wyoming. Adjacent Basin and Range Province regions are distinguished by higher elevations, higher rates of seismicity, and active normal faulting in the Centennial tectonic belt to the north and Intermountain seismic belt and Great Basin to the south of the Snake River Plain.

Interpretations of the GPS results extend the work of and are based on the work presented in Payne and others (2012; 2013) and McCaffrey and others (2013). We provide an update of the GPS velocity field from 1993 to 2014, which includes increased occupation times of continuous (cGPS) sites and additional survey-mode (sGPS) observations collected in 2012, 2013, and 2014. The GPS sites encompass the northwestern U.S. states of Idaho, Montana, Oregon, Washington, northern Utah, northern Nevada, and western Wyoming (figure 1). We analyze the GPS phase data using the GAMIT/GLOBK software (Herring and others, 2010) following the approach described in Section 2.2 of McCaffrey and others (2007). The velocities are determined relative to the Stable North American Reference Frame (PBO NAM08) by estimating a six-parameter transformation (three translation rates and three rotation rates), while minimizing the adjustments from the Plate Boundary Observatory velocity field of 150 continuous stations in North America. The error model incorporates both random and temporally correlated noise calibrated by examining the low-deforming region of eastern Oregon (described in McCaffrey and others, 2013). In the analyses and interpretations, we use only horizontal velocity estimates for which both components have one-sigma uncertainties less than 0.8 mm/yr, and set any uncertainties less than 0.2 mm/yr to 0.2 mm/yr. We discuss interpretations of Payne and others (2012, 2013), where we inverted GPS velocities and other kinematic data (e.g., earthquake slip vectors and dike-opening rates) using the block-model approach in TDEFNODE (McCaffrey, 2009). In these block models, the angular velocities and internal strain rates, ignoring locking on block-bounding faults, are estimated simultaneously by a least-squares linear inversion of all available data. From previous work, the block model boundaries (figure 2) were established through tests of statistical significance that one model with added boundaries has a better fit to the data over a second model without those boundaries (Payne and others, 2012; 2013; McCaffrey and others, 2013; Peterson and others, 2013). Previous work also shows that locking on the faults either does not occur or does not contribute noticeably to the velocities (Payne and others, 2012).

The velocities, together with geologic, volcanic, and earthquake data, reveal a large slowly deforming region within the Snake River Plain in Idaho and Owyhee-Oregon Plateau in Oregon separated by shear zones from the actively extending adjacent Basin and Range Province regions. Our latest 1993–2014 GPS results have reduced uncertainties and are otherwise very similar to those for 1994-2010 GPS results presented in Payne and others (2012). The latest results show a NE-oriented extensional strain rate of $5.4 \pm 0.4 \times 10^{-9}$ yr^{-1} (nanostrain/yr) in the Centennial tectonic belt and a ~E-W strain rate of $3.2 \pm 0.4 \times 10^{-9}$ yr^{-1} in the Great Basin (noted as the CTBt and EBnR blocks, respectively, in figure 2). These extensional rates contrast with the very low strain rate within the 125 km x 650 km region of the Snake River Plain and Owyhee-Oregon Plateau, which is indistinguishable from zero ($0.2 \pm 0.2 \times 10^{-9}$ yr^{-1}) (SRPn block in figure 2). A low rate of contraction ($-1.3 \pm 0.5 \times 10^{-9}$ yr^{-1}) is also shown for eastern Oregon (EOre block in figure 2), largely due to Cascadia subduction zone locking.

Using the 1994–2010 GPS data, Payne and others (2012) explicitly tested the likelihood that dike-opening of Snake River Plain volcanic rift zones are at rates comparable to GPS-derived extension rates across faults within the Centennial tectonic belt. Inversions of the velocities with dike-opening models indicate that rapid extension by dike intrusion in volcanic rift zones is not presently occurring in the Snake River Plain. If we assume the low rate of deformation is reflected in the length of time between eruptions on the order of 10^4 to $>10^6$ yrs, the interlude of a low-strain rate field in the Snake River Plain and Owyhee-Oregon Plateau would extend at least through the Quaternary.

The slow deformation within the Snake River Plain, in contrast to the rapidly extending adjacent Basin and Range Province regions, results in shear between them. We estimate right-lateral shear with slip rates of 0.3–1.4 mm yr^{-1} along the northern boundary of the Snake River Plain within the Centennial shear zone, and left-lateral oblique extension with slip rates of

0.5–1.5 mm yr^1 along the southeastern boundary adjacent to the Intermountain seismic belt (Payne and others, 2012). Further detailed evaluations of GPS velocities suggest that differential motion between the Centennial tectonic belt and eastern Snake River Plain is likely distributed across the Centennial shear zone rather than concentrated along any individual known fault. Surface velocity gradients observed in GPS data across the 40–45 km-wide Centennial shear zone reveal distributed deformation due to strike-slip faulting, distributed simple shear, regional-scale rotation, or some combination thereof (figure 3). In the Centennial shear zone, the fastest lateral shearing is closest to the Yellowstone Plateau, where fault plane solutions with components of right-lateral strike-slip are documented within a NE-trending zone of seismicity. Near the eastern end of the Centennial shear zone along the east-striking Centennial normal fault, right-lateral offsets are observed in Pleistocene age glacial moraines (Pierce and others, 2014).

The velocity field shows large-scale clockwise rotations, relative to North America, observed over the northern Basin and Range (figure 1). Estimates of rotation rates at every 1° of latitude and longitude derived from the observed velocities show that rotation extends from the Pacific coast to the Snake River Plain. The Pacific Coast has the highest rotation rate (1–2°/Ma) and rates decrease to about one-half that rate in Eastern Oregon and about one third in the Snake River Plain. The eastward decrease in rotation rates appear to agree with rates from the long term as seen in paleomagnetic declination anomalies (Mc-Caffrey and others, 2007; Wells and McCaffrey, 2013). The observed geodetic rigidity evidenced by little internal deformation in the Snake River Plain as well as eastern Oregon may result from mafic modifications that strengthen their crusts and allow them to rotate as large coherent regions. Additionally, regional velocity gradients are best fit by poles of rotation near the Idaho batholith. We attribute regional-scale rotation to gravitationally driven extension in the Basin and Range Province and Pacific-North America shear transferred through the Walker Lane belt aided by potentially strong pinning below the Idaho batholith (McCaffrey and others, 2013).

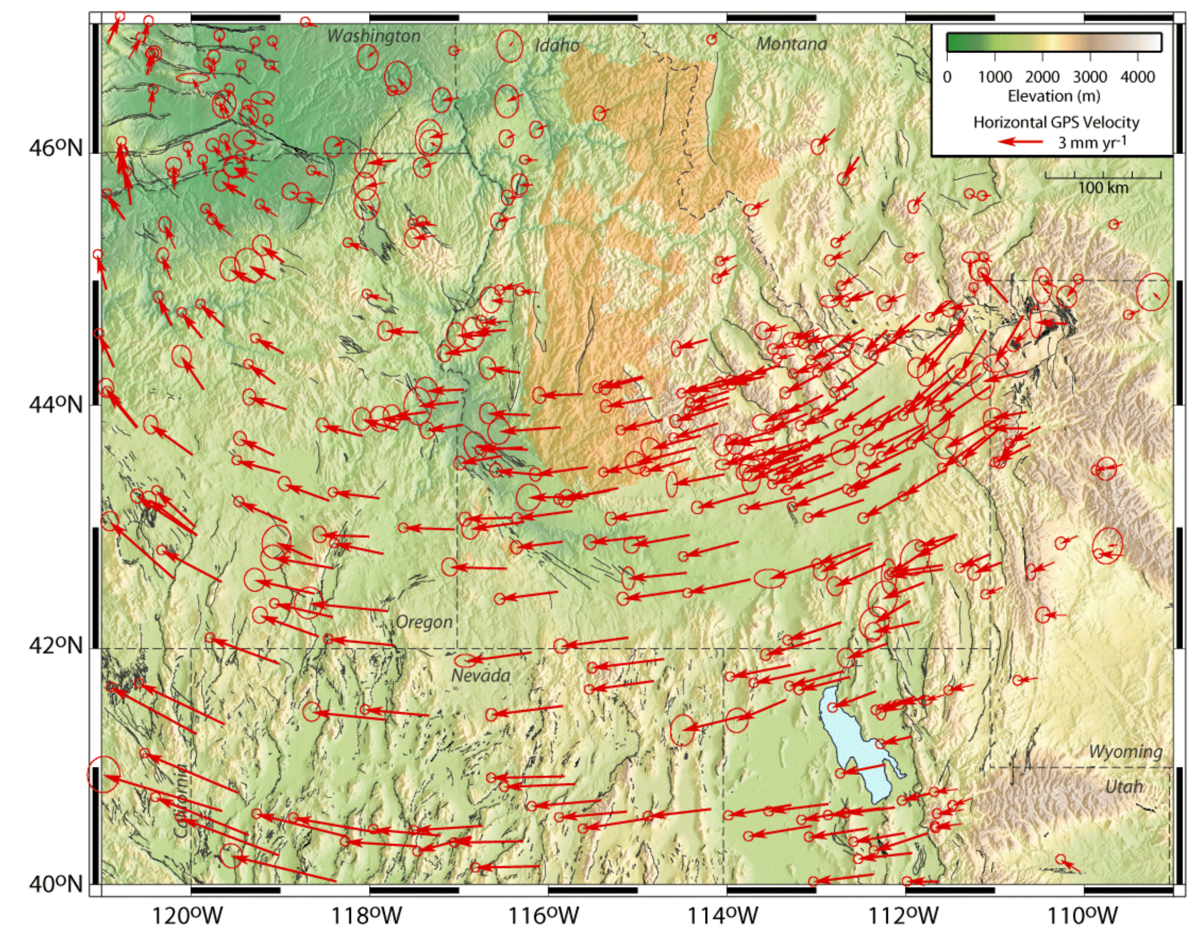

Figure 1. The 1994–2014 GPS velocity field (November 2014 solution). Error ellipses are 70% confidence. The field was generated using sGPS data acquired by Portland State University and Idaho National Laboratory in 2014 and in McCaffrey and others, 2013; Payne and others, 2008; 2012; the U.S. Geological Survey (USGS; http://earthquake.usgs.gov/monitoring/gps/; see also, Svarc and others, 2002), University of Utah, Central Washington University, the National Geodetic Survey, and Pacific Geoscience Centre. We also included our processing of cGPS data from the Pacific Northwest Geodetic Array (PANGA; Khazaradze and others, 1999; Miller and others, 2001; http://www.geodesy.cwu.edu/pub/data) and the Idaho National Laboratory network, and position estimates and covariances from the Plate Boundary Observatory (PBO) processing at New Mexico Tech (NMT) (ftp://data-out.unavco.org/pub/products/sinex).

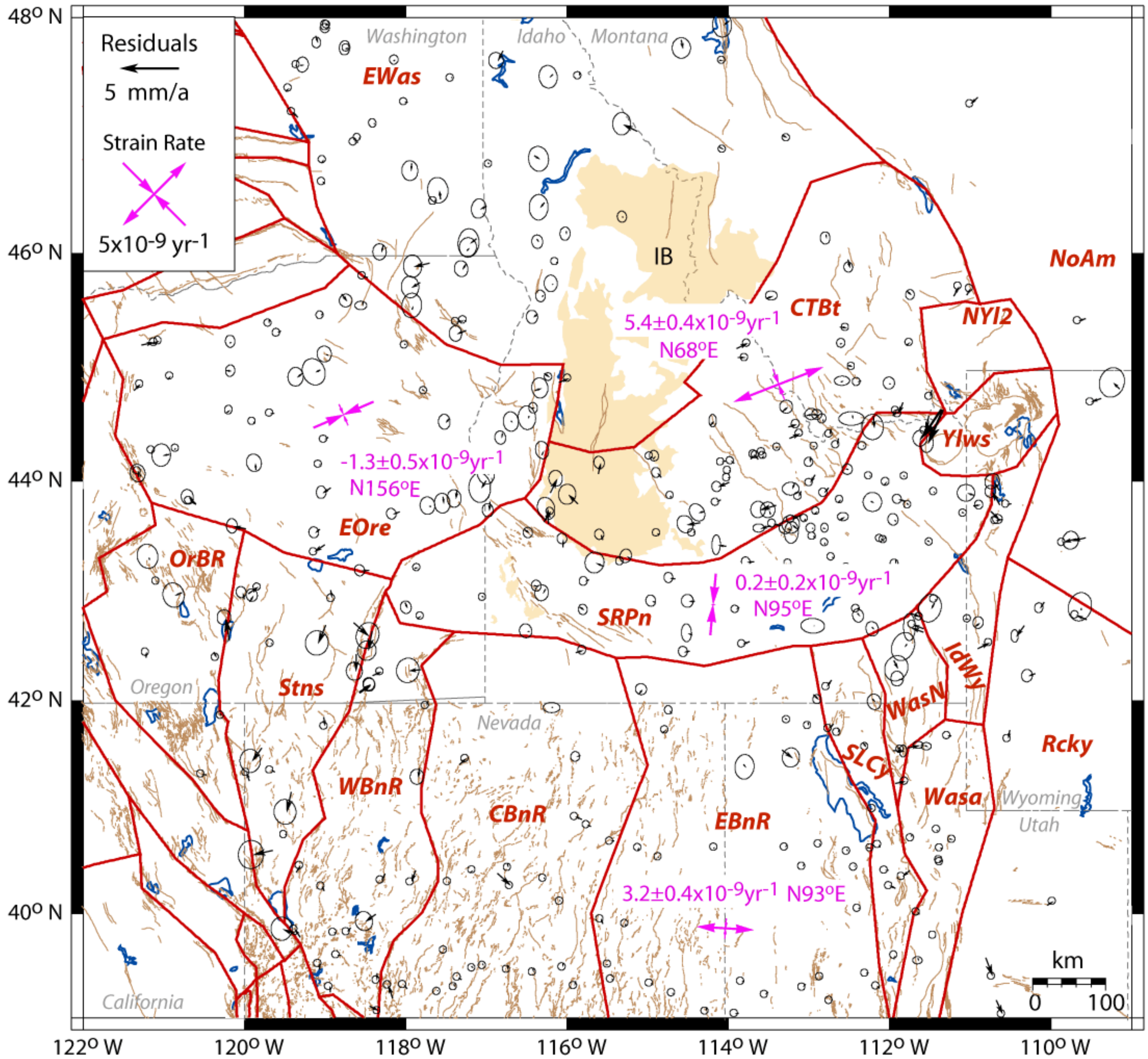

Figure 2. *Block model (red lines and letters) used to model 1993–2014 GPS velocities (model is from Peterson and others, 2013). Black vectors show residual velocities from the block model with 70% confidence ellipses. Principal horizontal strain rates (pink arrows) are labeled with magnitude, uncertainty, and orientation for the blocks discussed in the text. Brown lines show Quaternary faults and orange shading is the Idaho batholith (IB).*

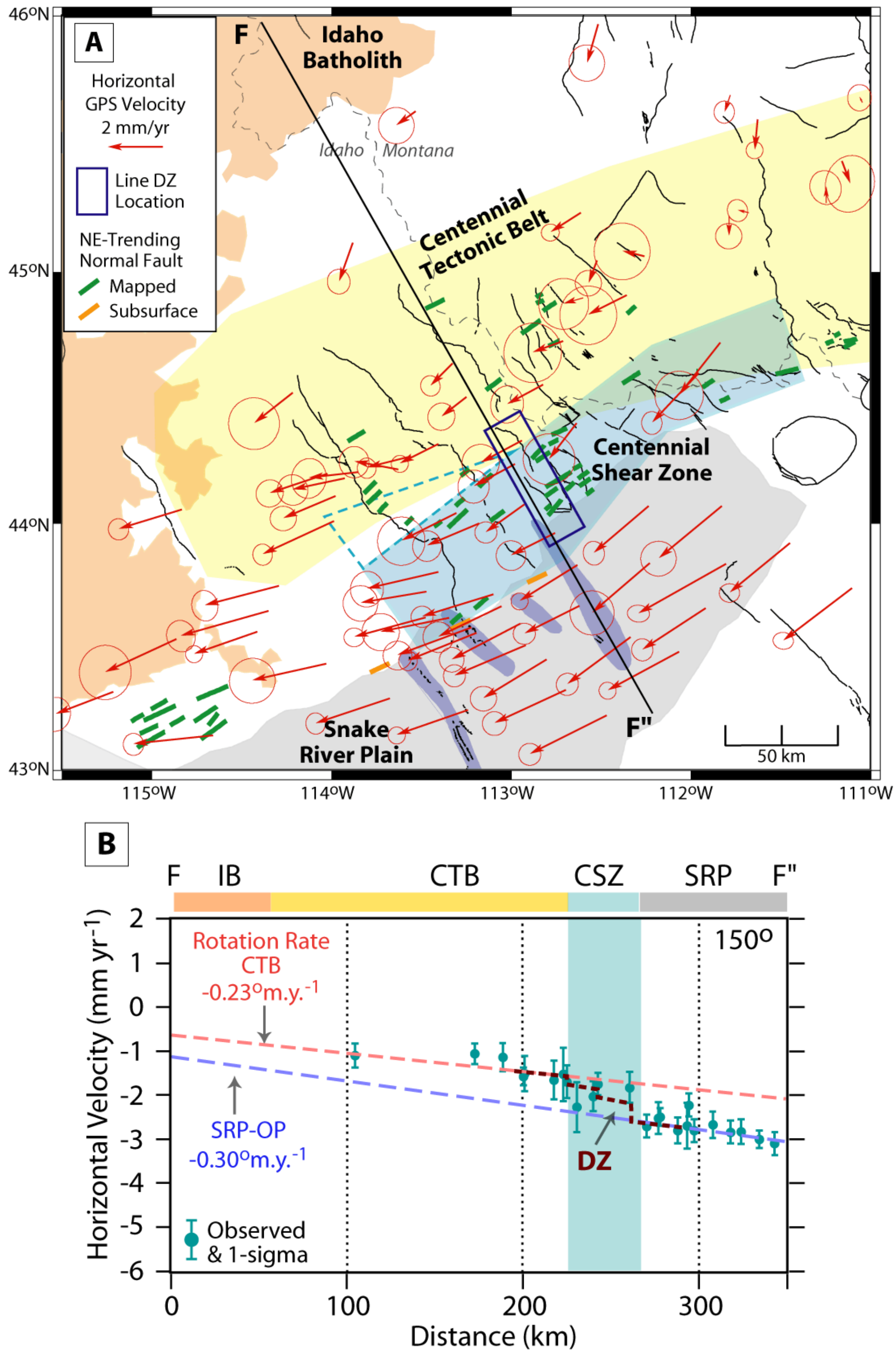

Figure 3. *(A) 1994–2010 observed horizontal GPS velocities with 70% confidence ellipses and locations of profile C-D and blue box for Deformation Zone (DZ). (B) Profile shows components of observed horizontal velocities and one-sigma uncertainties perpendicular to the direction of the profile indicating clockwise rotation or right-lateral shear or both for negative slopes. As an example, the dashed brown line "DZ" exhibits vertical steps where right-lateral shear is accommodated by strike-slip motion on discrete NE-trending faults (blue box in A). Line DZ decreases in slope from the NW to SE to match up with two regional-scale rotation rates for the Centennial tectonic belt - CTB (dashed light red line) and for Snake River Plain - Owyhee-Oregon Plateau (SRP-OP) (dashed light blue line). Blue shading for Centennial shear zone - CSZ (dashed where inferred), yellow for the CTB, and gray for the eastern Snake River Plain (ESRP). YP is Yellowstone Plateau and IB is the Idaho batholith. Figures modified from Payne and others (2013).*

REFERENCES

Herring, T.A., King, R.W. and McCluskey, S.C., 2010, Introduction to GAMIT/GLOBK: Release 10.4: Massachusetts Institute of Technology, 48 p. online, http://www-gpsg.mit.edu/~simon/gtgk/docs.htm.

Khazaradze, G., Qamar, A.I., and Dragert, H., 1999, Tectonic deformation in western Washington from continuous GPS measurements: Geophysical Research Letters, v. 26, p. 3153–3158.

McCaffrey, R., 2009, Time-dependent inversion of three-component continuous GPS for steady and transient sources in northern Cascadia: Geophysical Research Letters, v. 36, L07304, 5 p., doi:10.1029/2008GL036784.

McCaffrey, R., King, R.W., Payne, S.J., and Lancaster, M., 2013, Active tectonics of northwestern U.S. inferred from GPS-derived surface velocities: Journal of Geophysical Research, v. 118, p. 1–15, doi:10.1029/2012JB009473.

McCaffrey, R., Qamar, A.I., King, R.W., Wells, R., Khazaradze, G., Williams, C.A., Stevens, C.W., Vollick, J.J., and Zwick, P.C., 2007, Fault locking, block rotation and crustal deformation in the Pacific Northwest: Geophysical Journal International, v. 169, p. 1315-1340, doi:10.1111/j.1365-246X.2007.03371.x.

Miller, M., Dragert, H., Endo, E., Freymueller, J.T., Goldfinger, C., Kelsey, H.M., Humphpreys, E.D., Johnson, D.J., McCaffrey, R., Oldow, J.S., Qamar, A., and Rubin, C.M., 1998, Precise measurements help gauge Pacific Northwest's earthquake potential: EOS Transactions American Geophysical Union, v. 79, p. 269–275.

Payne, S.J., McCaffrey, R., and Kattenhorn, S.A., 2013, Extension driven right-lateral shear in the Centennial shear zone adjacent to the eastern Snake River Plain, Idaho: Lithosphere, v. 5, no.4, p. 407–419.

Payne, S.J., McCaffrey, R., and King, R.W., 2008, Strain rates and contemporary deformation in the Snake River Plain and surrounding Basin and Range from GPS and seismicity: Geology, v. 36, p. 647–650.

Payne, S.J., McCaffrey, R., King, R.W., and Kattenhorn, S.A., 2012, A new interpretation of deformation rates in the Snake River Plain and adjacent Basin and Range regions based on GPS measurements: Geophysical Journal International, v. 189, p. 101–122.

Petersen, M.D., Zeng, Y., Haller, K.M., McCaffrey, R., Hammond, W.C., Bird, P., Moschetti, M., Shen, Z., Bormann, J., and Thatcher, W., 2014, Geodesy- and geology-based slip-rate models for the western United States (excluding California) National Seismic Hazard Maps: U.S. Geological Survey Open-File Report 2013–1293, 80 p., http://dx.doi.org/10.3133/ofr20131293.

Pierce, K.L., Chesley-Preston, T.L., and Sojda, R.L., 2014, Surficial geologic map of the Red Rock Lakes area, southwest Montana: U.S. Geological Survey Open-File Report 2014-1157, 26 p.

Svarc, J.L., Savage, J.C., Prescott, W.H., and Murray, M.H., 2002, Strain accumulation and rotation in western Oregon, and southwestern Washington: Journal of Geophysical Research, v. 107, 11 p., 10.1029/2001JB000625.

Wells, R.E. and McCaffrey, R., 2013, Steady rotation of the Cascade arc: Geology, v. 41, no. 9, p. 1027–1030.

The following is a PDF version of the authors' PowerPoint presentation.

Update of GPS Deformation Rates in the Snake River Plain

Suzette Payne, Idaho National Laboratory
Robert King, Massachusetts Institute of Technology
Robert McCaffrey, Portland State University
Simon Kattenhorn, ConoPhillips

Basin and Range Province Seismic Hazards Summit III
January 16, 2014

Idaho National Laboratory

Overview

- Tectonics and seismicity
- 1994-2010 GPS data
- Interpretations of 1994-2010 geodetic results
  - Low deformation rate in the Snake River Plain
  - Right-lateral shear in the Centennial Shear Zone
- Quick look at the 1993-2014 GPS observations

Silicic and mafic volcanism are associated with initiation and migration of the Yellowstone Hotspot from ~17 Ma to present

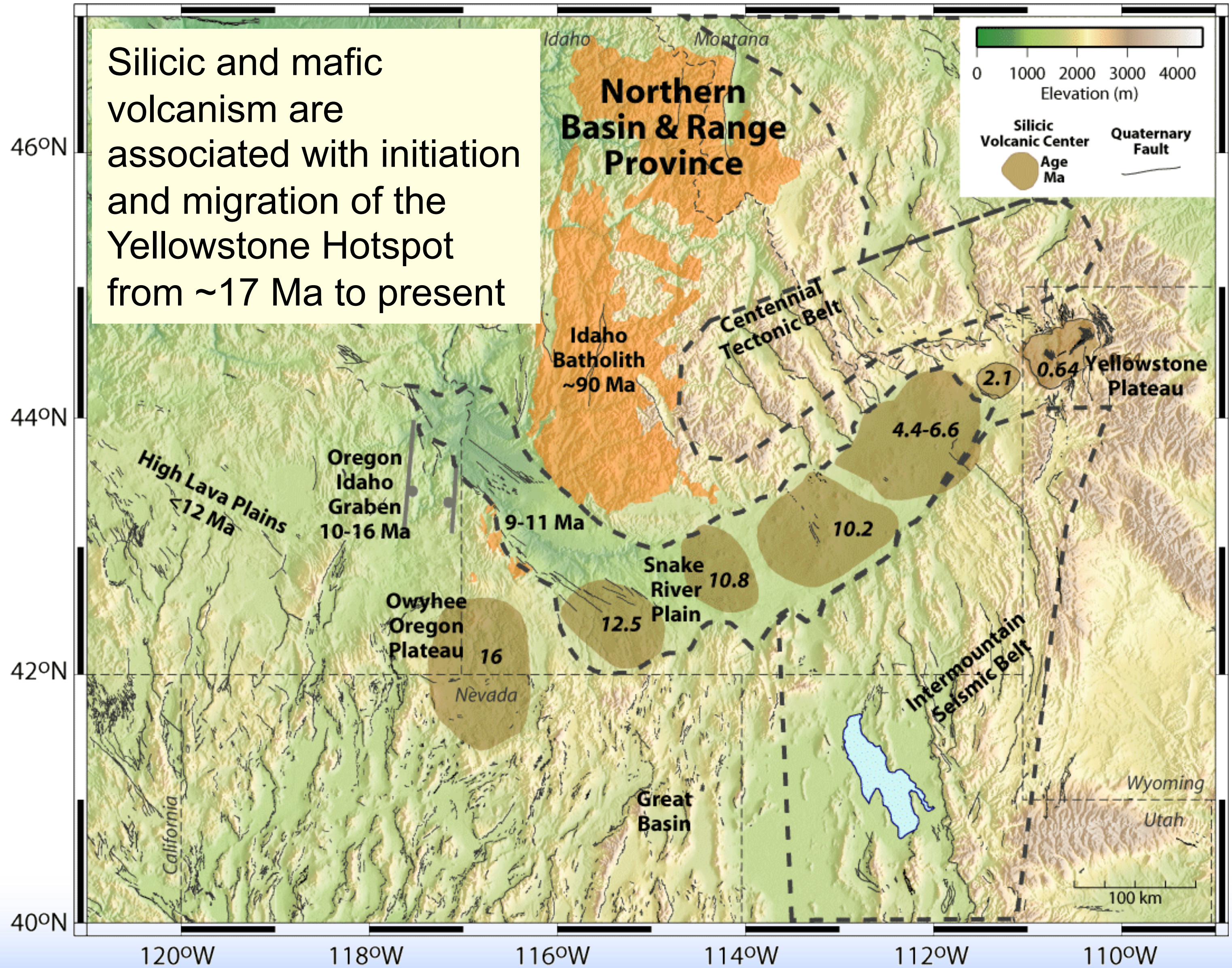

Idaho National Laboratory

Faults: http://earthquake.usgs.gov/regional/qfaults/
Calderas: Pierce & Morgan (1992); Morgan & McIntosh 2005; ISB: Smith & Arabasz (1991)
CTB: Stickney & Bartholomew (1987); OIG: Cummings et al. (2002)

Mafic volcanism continued into the Holocene & Pleistocene in regions deformed by the Yellowstone Hotspot

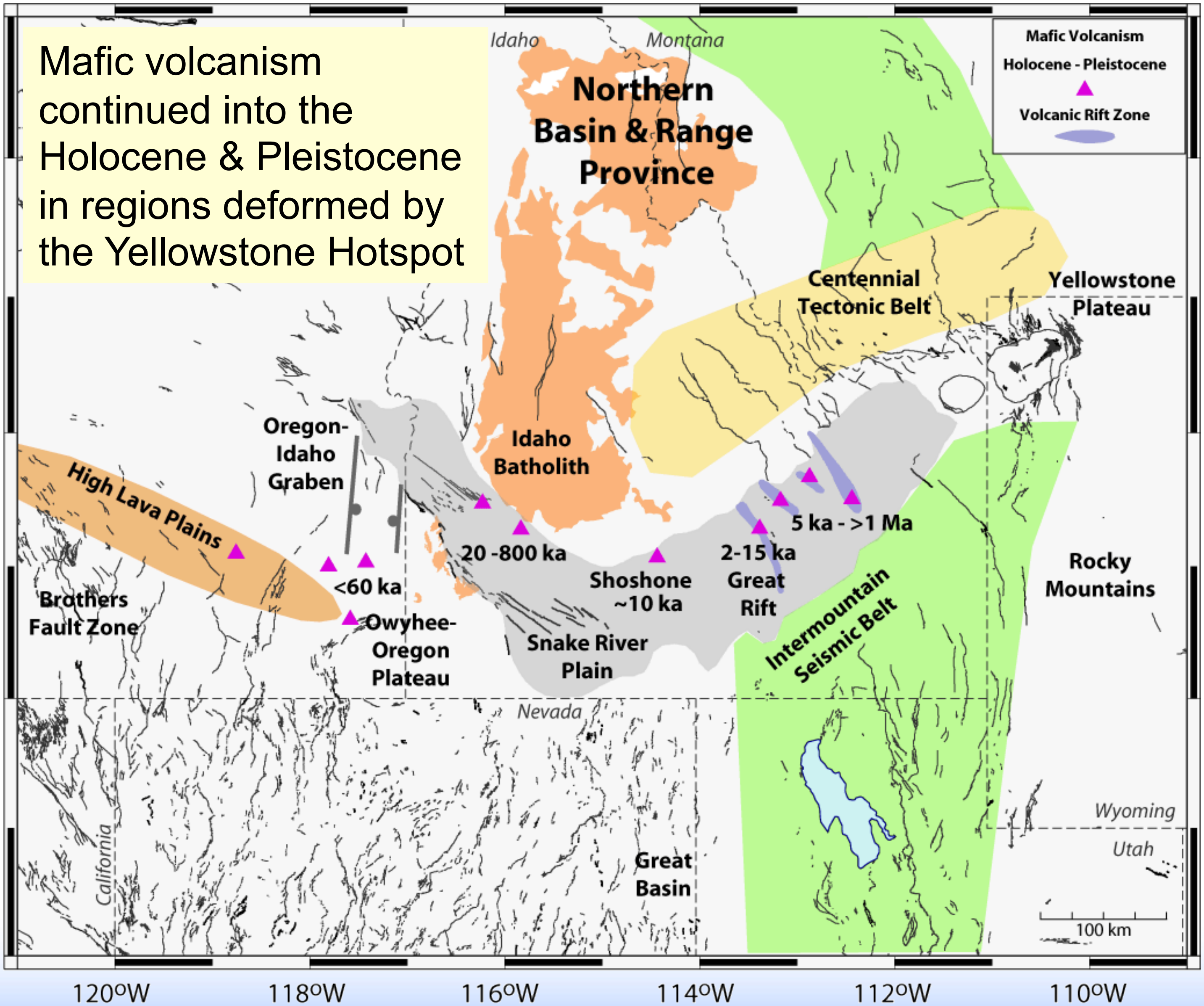

Idaho National Laboratory

Volcanic Rift Zones: Kuntz et al. (1986; 1994; 2004)
Vents: Siebert and Simkin (2002); Woods and Clemmens (2002)

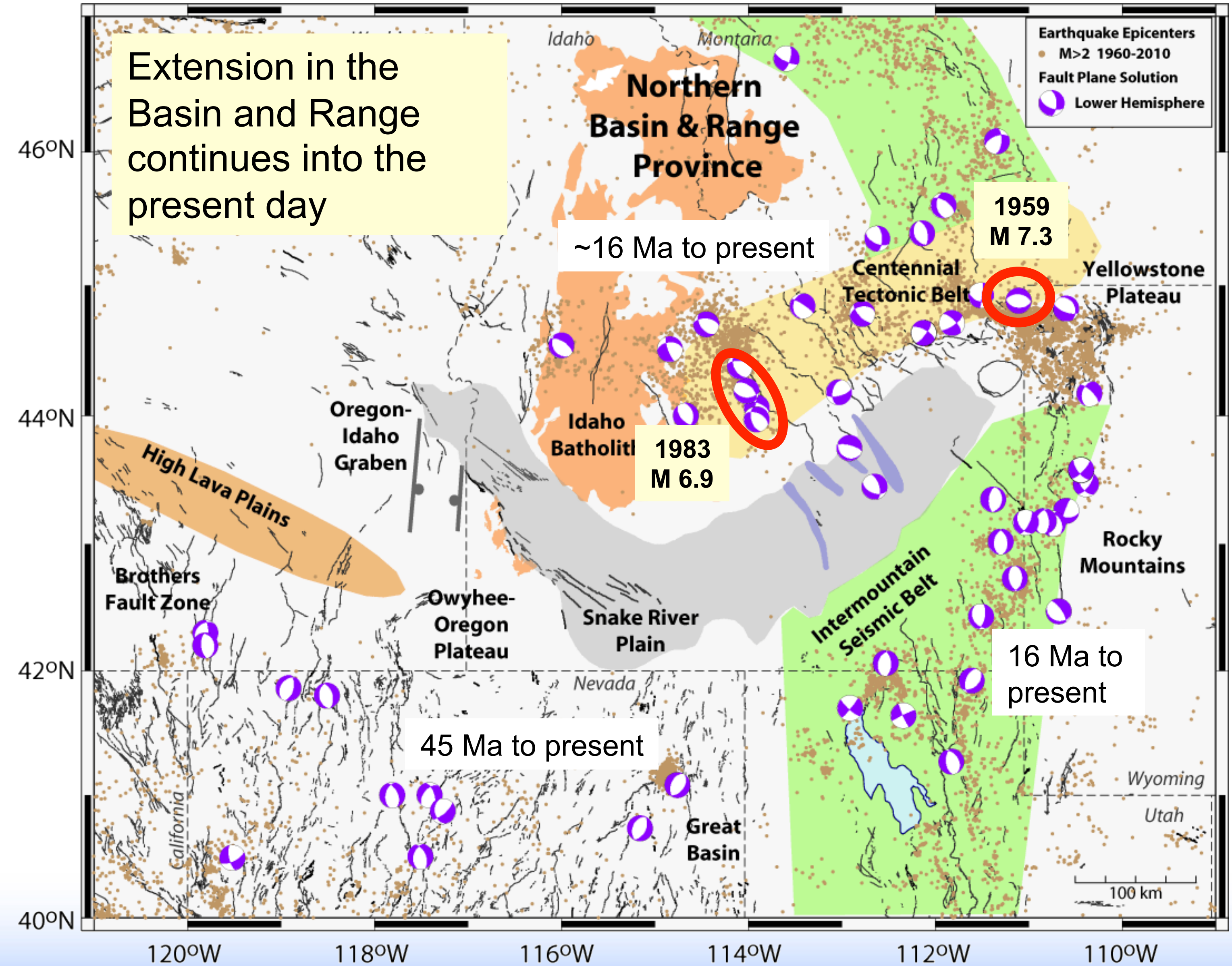

Idaho National Laboratory

Earthquakes: http://www.ncedc.org/anss/catalog-search.html
Focal Mechanisms: http://www.eas.slu.edu/Earthquake_Center/MECH.NA/index.html; http://www.seismology.harvard.edu/; Zollweg and Richins (1985); Doser and Smith (1985); Doser and Smith (1985); Doser (1989); Payne et al. (2007); Stickney (1997; 2007)

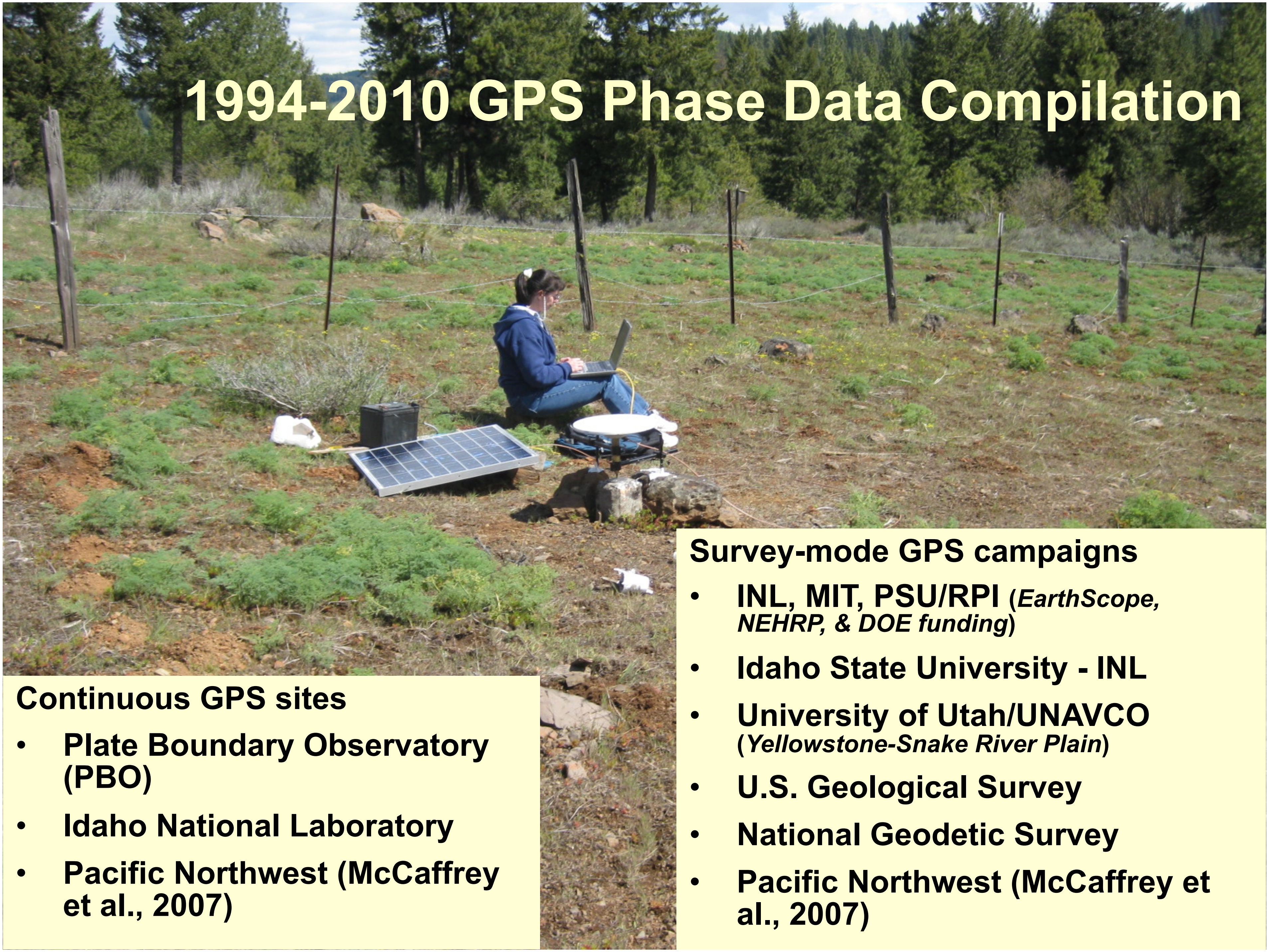

1994-2010 GPS Phase Data Compilation

Continuous GPS sites

- **Plate Boundary Observatory (PBO)**
- **Idaho National Laboratory**
- **Pacific Northwest (McCaffrey et al., 2007)**

Survey-mode GPS campaigns

- **INL, MIT, PSU/RPI (*EarthScope, NEHRP, & DOE funding*)**
- **Idaho State University - INL**
- **University of Utah/UNAVCO (*Yellowstone-Snake River Plain*)**
- **U.S. Geological Survey**
- **National Geodetic Survey**
- **Pacific Northwest (McCaffrey et al., 2007)**

GPS Velocities

- **Phase data processed by Dr. Robert King (MIT) using GAMIT/GLOBK software (*Herring et al., 2010*)**
- **Error model incorporates both random and correlated noise (*McCaffrey et al., 2007; 2013*)**
  - **Calibrated to obtain horizontal velocity uncertainties**
  - **Consistent with confidence level of the error ellipses**
- **Velocities determined relative to Stable North American Reference Frame**
- **Analysis uses velocities from >400 sites with uncertainties <0.8 mm yr^{-1} in either the N or E component**

1994-2010 Horizontal GPS Velocities

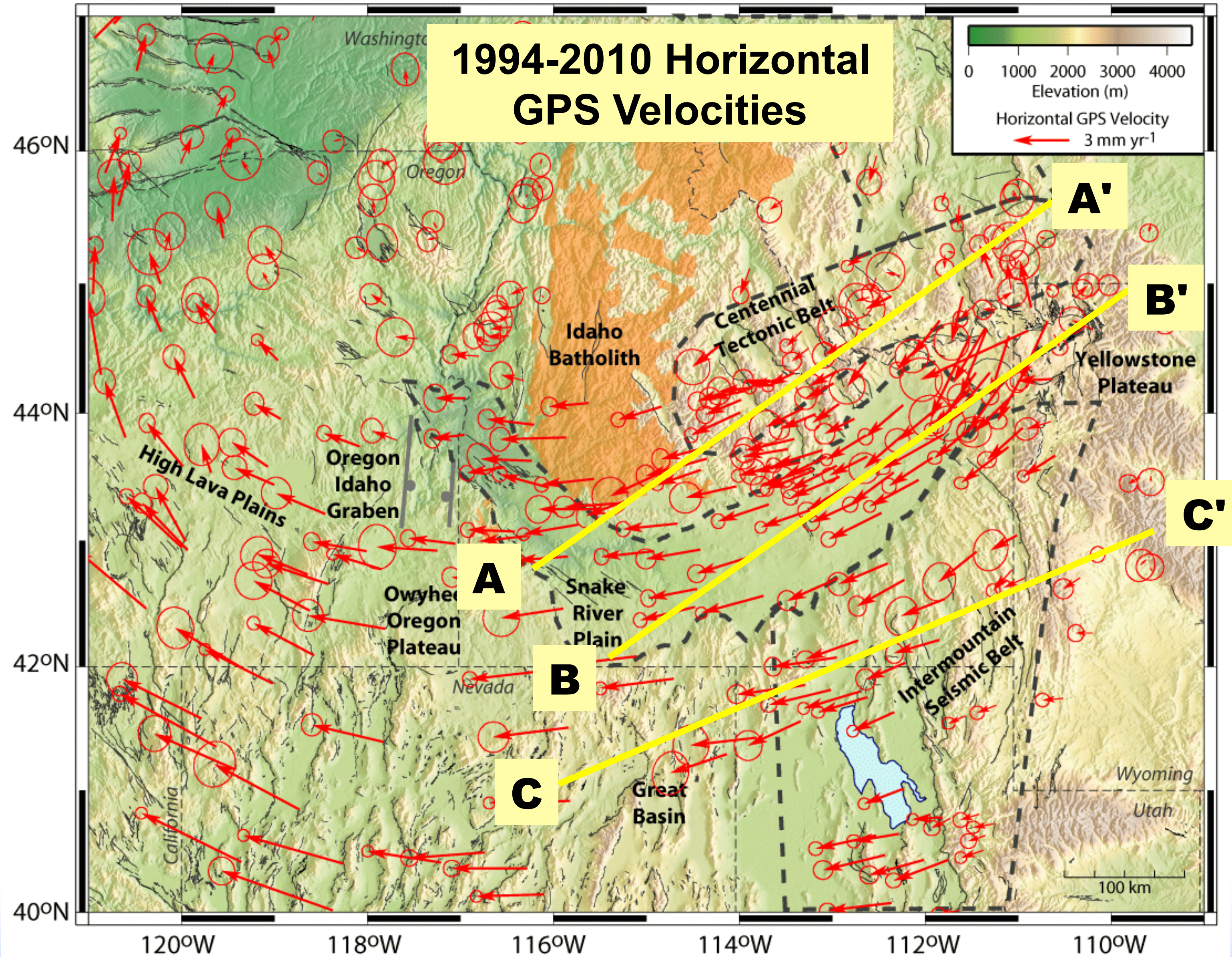

Idaho National Laboratory

Velocities in Stable North American Reference Frame

1994-2010 Observed GPS Velocities

• Components of velocities that are parallel to the direction of the profiles

• Positive velocity gradient indicates extension

•Basin and Range regions show positive slopes

•Snake River Plain shows nearly level slope

•Yellowstone Plateau shows steep positive slope and velocities are not corrected for transient motions

Slopes calculated using weighted-least squares linear regression

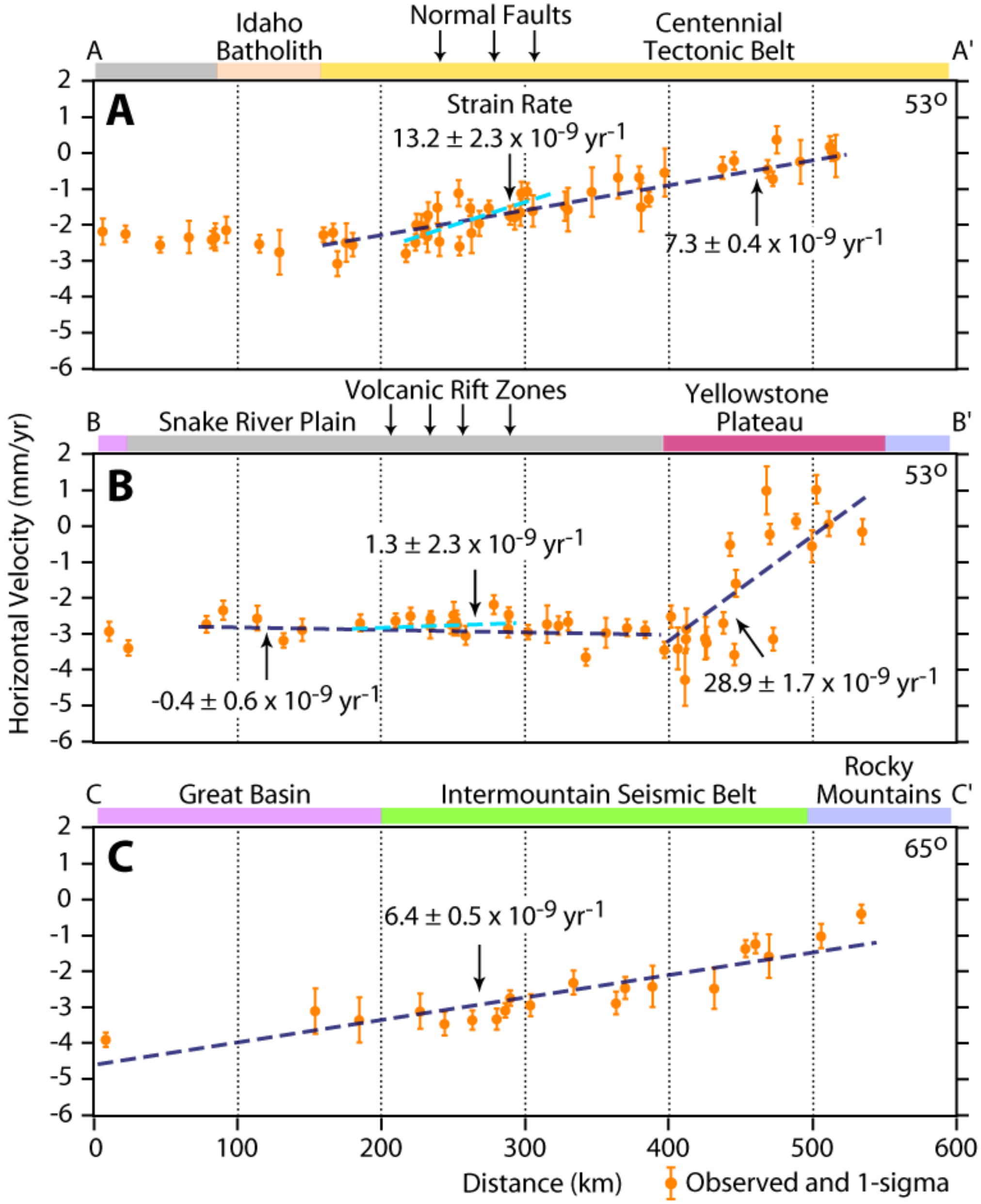

Payne et al. (2012)

Idaho National Laboratory

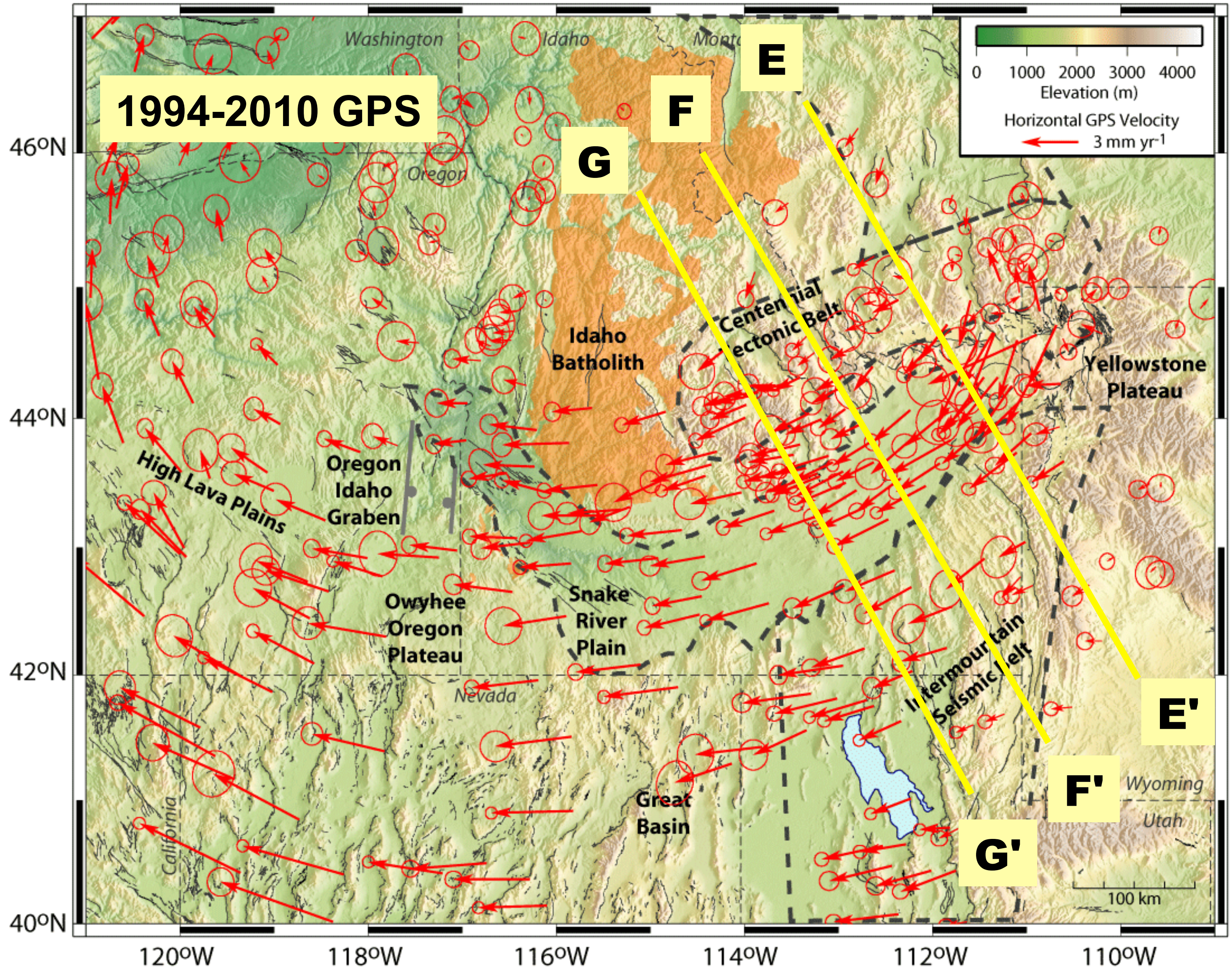

Idaho National Laboratory

Velocities in Stable North American Reference Frame

1994-2010 Observed GPS Velocities

- Components of velocities that are perpendicular to the direction of the profiles
- Negative velocity gradient indicates clockwise rotation or right-lateral shear or both
- Profiles all show negative trends or steps interpreted as zones of right-lateral shear
- Largest slip rate of right-lateral shear occurs across the Centennial fault

Slip rates calculated by taking the difference between weighted-averaged velocities on each side of the right-lateral shear zone

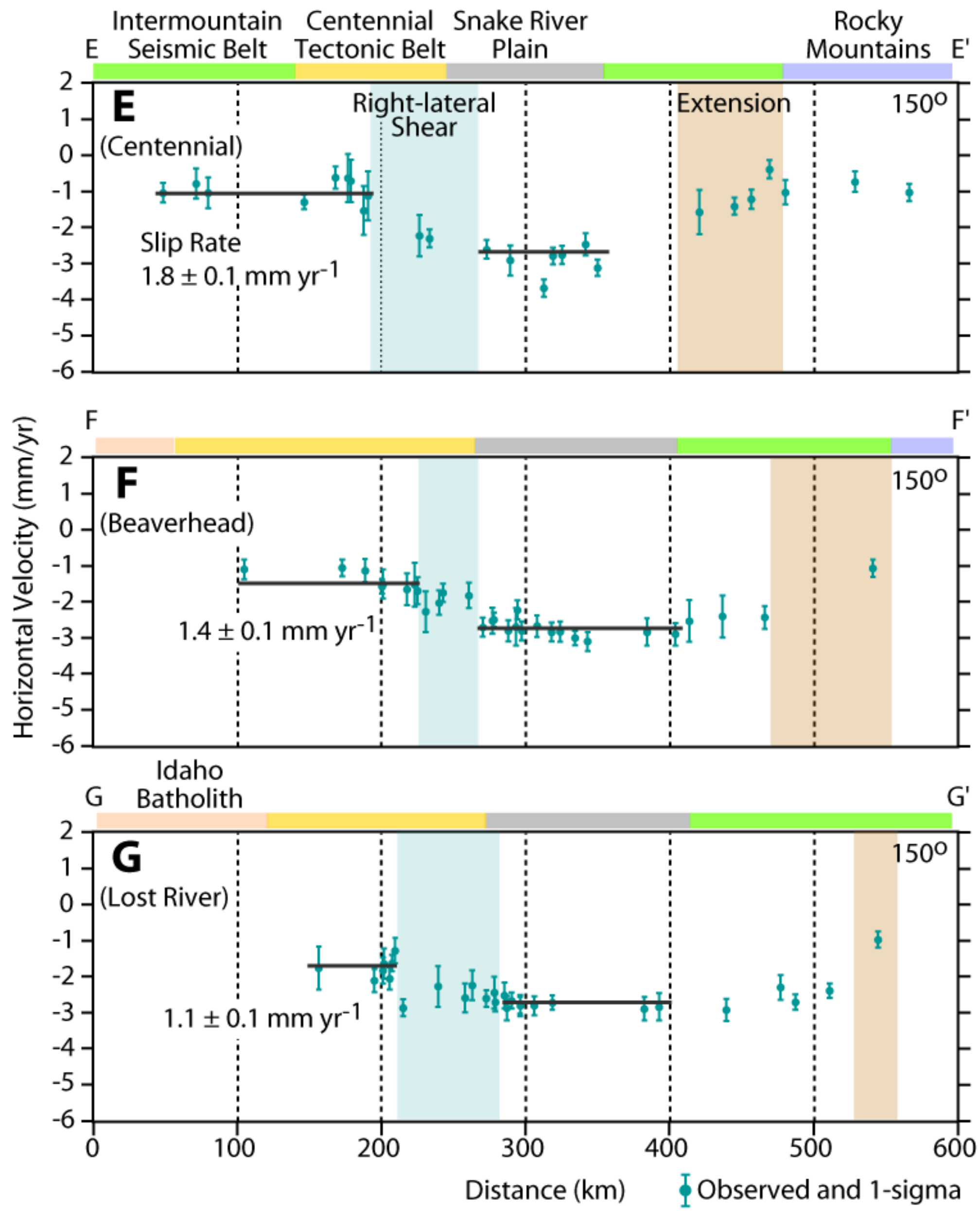

Payne et al. (2012)

Idaho National Laboratory

Kinematic Interpretations

- **Using the block-model inverse approach in TDEFNODE (McCaffrey, 2009)**
- **Invert horizontal GPS velocities and earthquake slip azimuths for:**
  - **Angular velocities of blocks**
  - **Horizontal strain rates within selected blocks**
- **Best-fit set of parameters**
  - **Simulated annealing (Press et al., 1989)**
  - **Minimizes reduced chi-square of the misfit to weighted data**
- **Compare models using F-Distribution Tests**
  - **Uses reduced chi-square and degrees of freedom**
  - **Apply 99% probability that one model with added boundaries has a better fit to the data than the other (Stein and Gordon, 1984)**

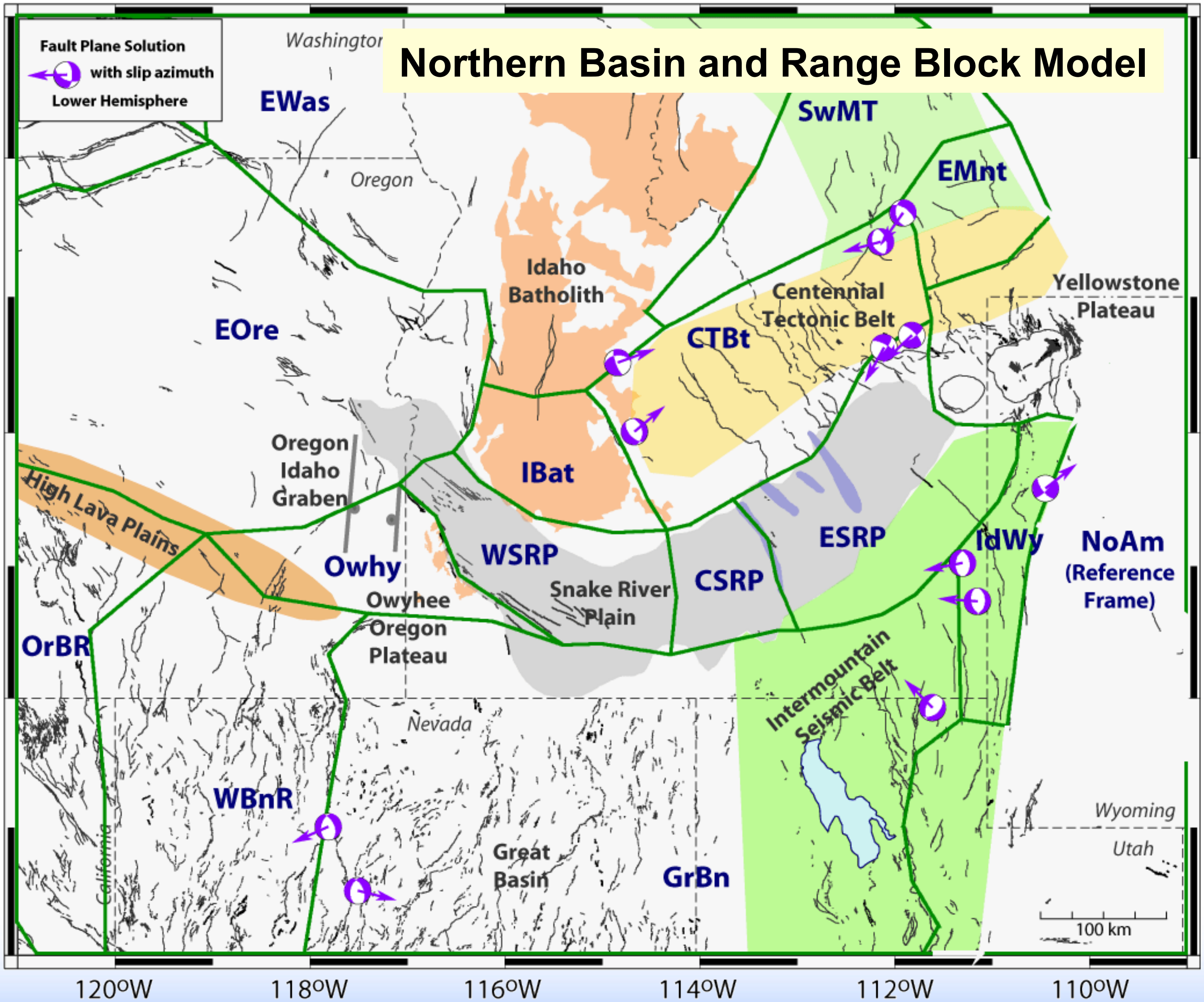

Payne et al. (2012)

Idaho National Laboratory

Test of Poles and Boundaries for Tectonic Provinces

One pole of rotation

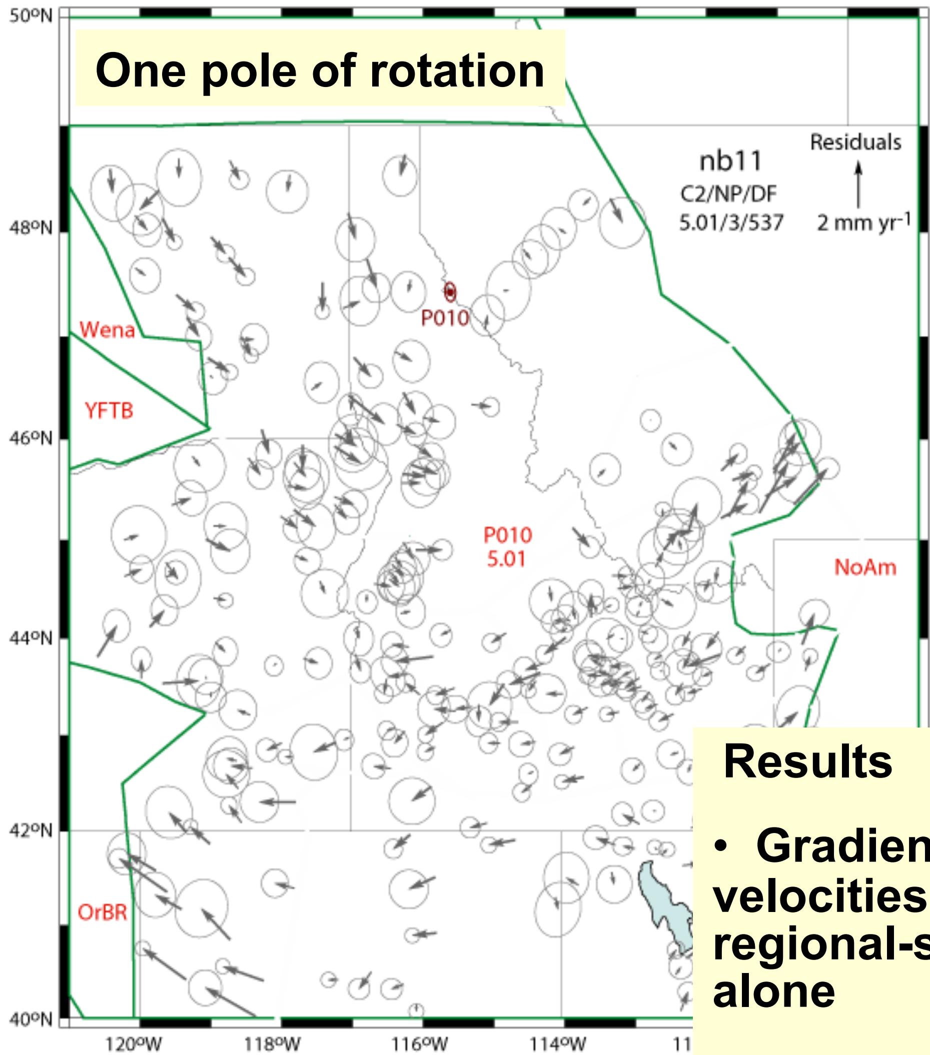

Seven poles of rotation

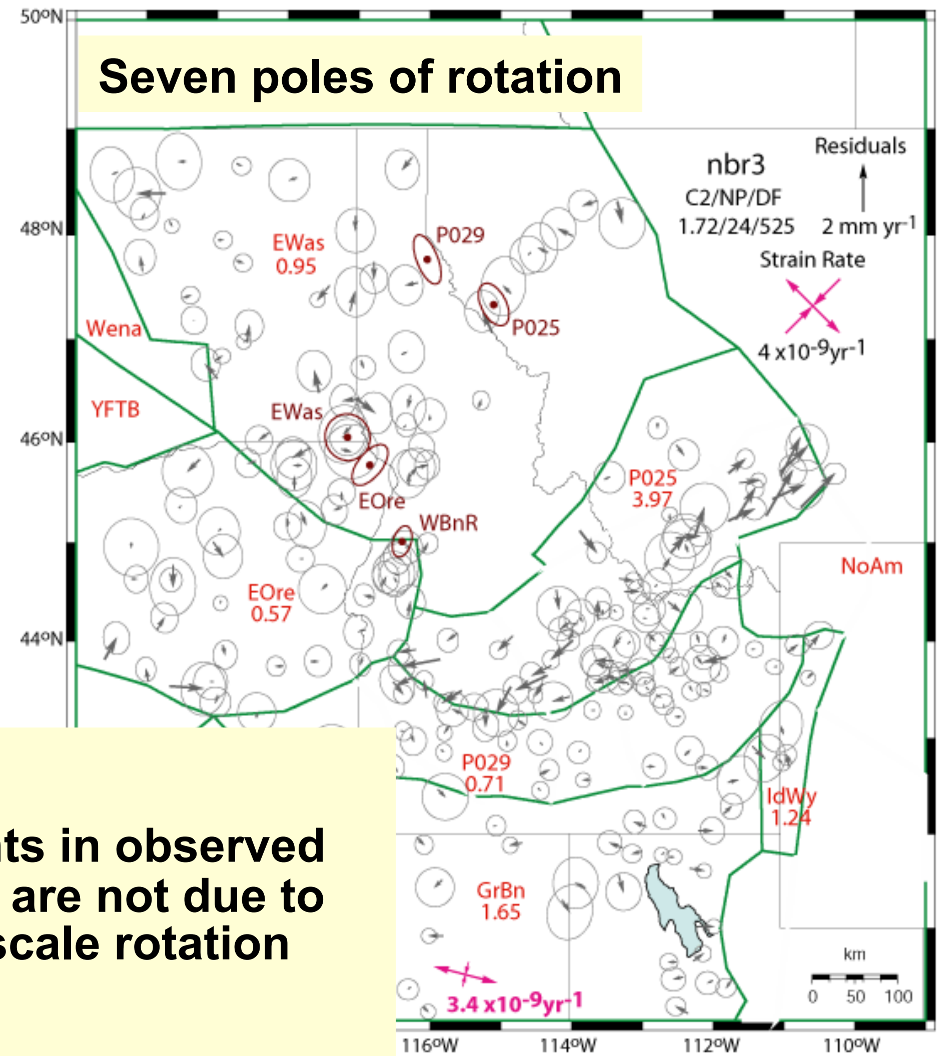

Results

- Gradients in observed velocities are not due to regional-scale rotation alone
- Separate block regions have nearby pole locations

Idaho National Laboratory

Payne et al. (2012)

Test of Boundaries for Centennial Tectonic Belt (CTB)

Separate Idaho Batholith Block

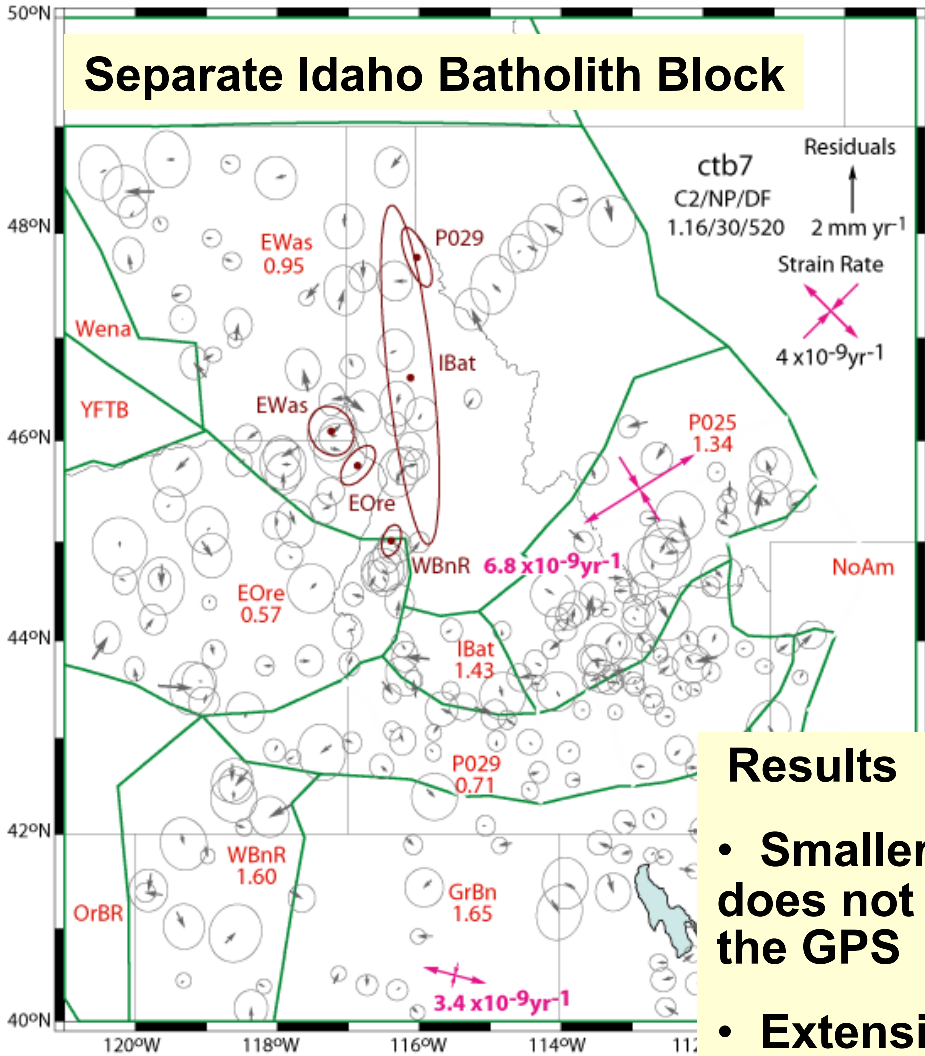

Combined with CTB

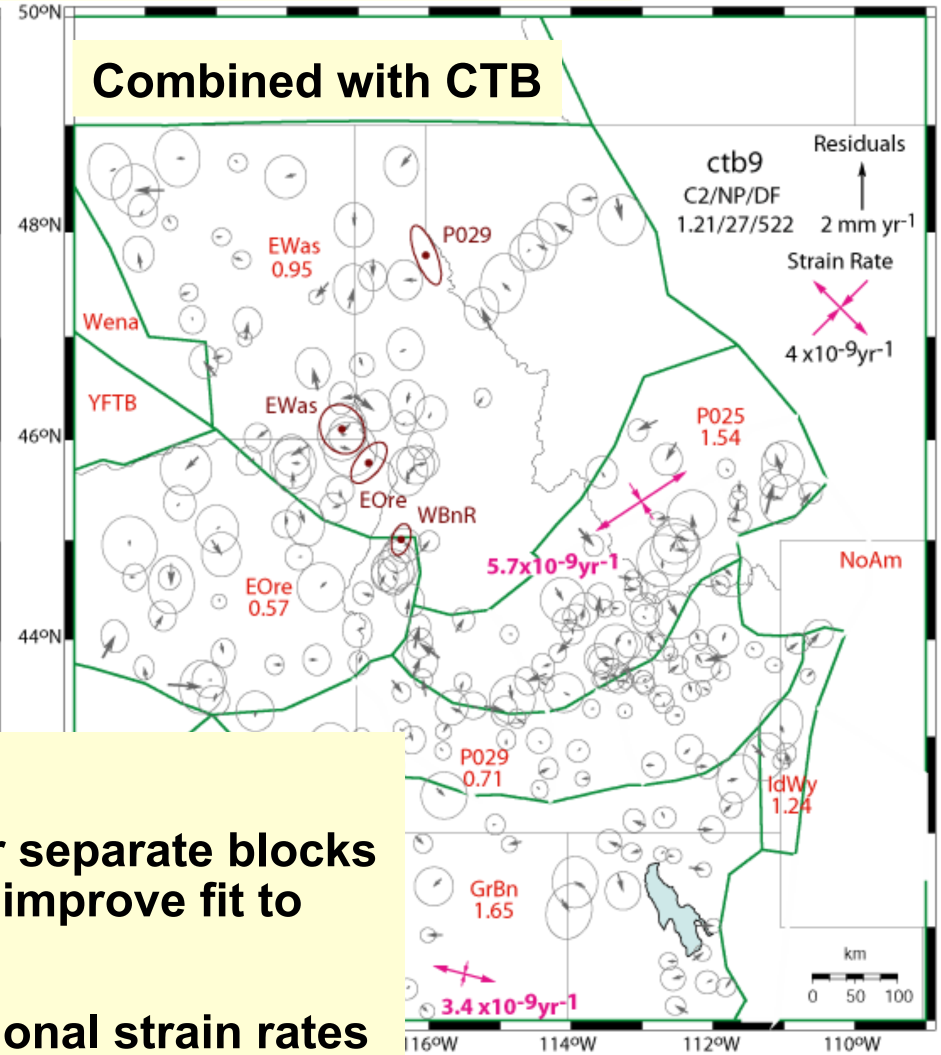

Results

- Smaller separate blocks does not improve fit to the GPS
- Extensional strain rates in the Centennial Tectonic Belt and Great Basin blocks

Payne et al. (2012)

Tests of Dike-Opening Rates Equal to GPS-Derived Normal Faulting Rates

Without Dike-opening Rates (<0.1 mm yr^{-1})

With Dike-opening Rates (0.96-1.02 mm yr^{-1})

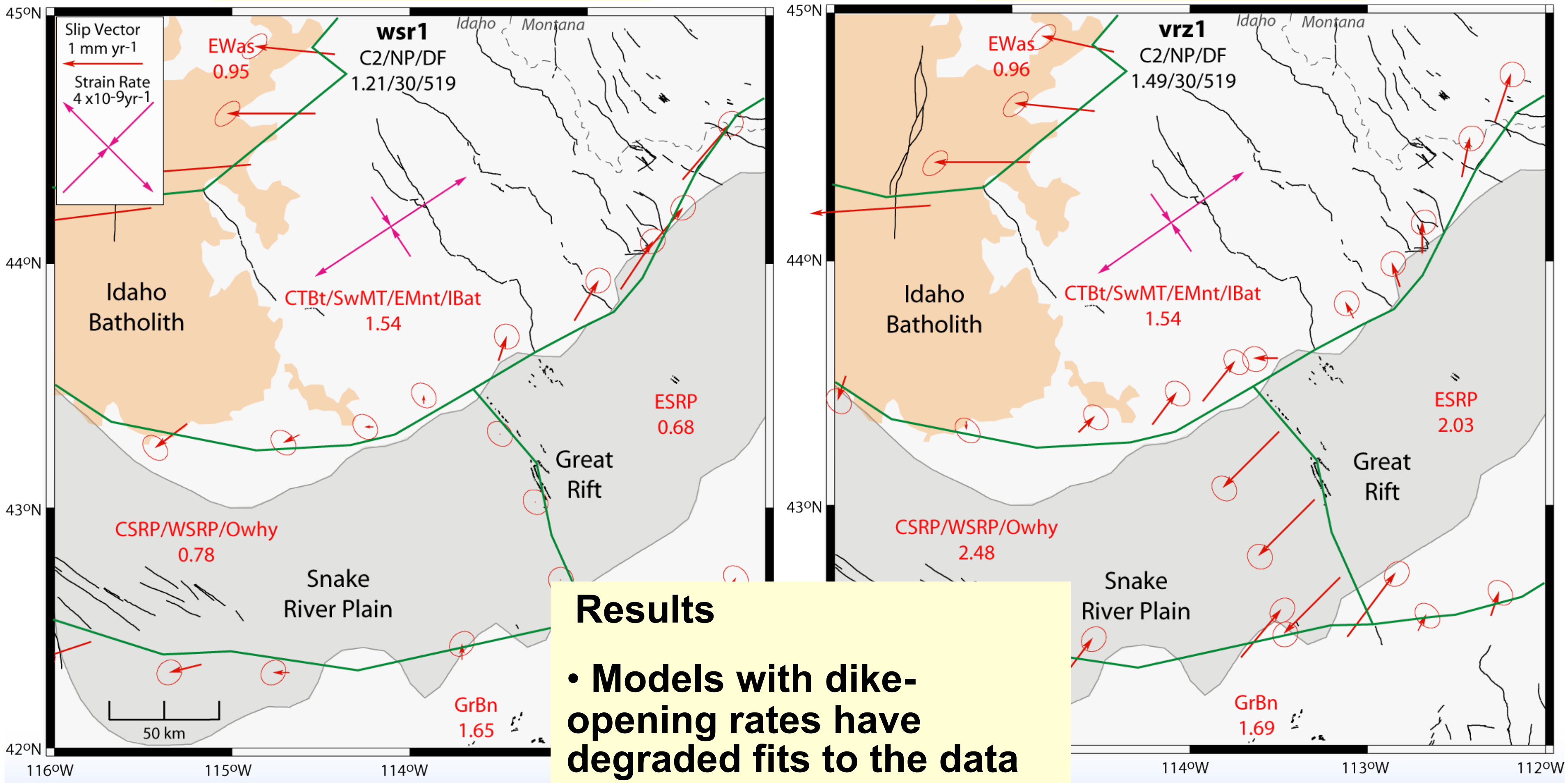

Results

- **Models with dike-opening rates have degraded fits to the data**
- **At present, volcanic rift zones are not significant**

Payne et al. (2012)

Idaho National Laboratory

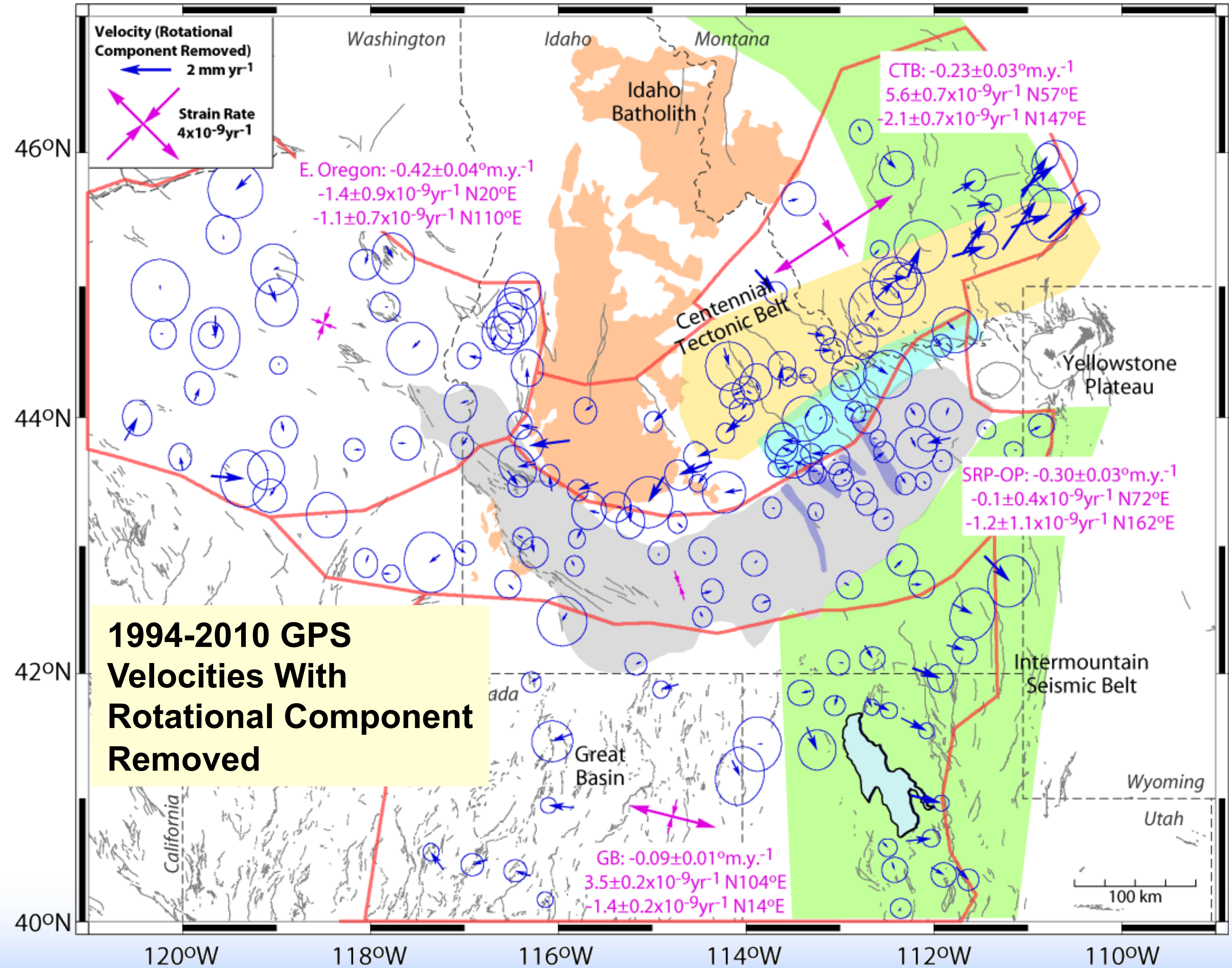

1994-2010 GPS Velocities With Rotational Component Removed

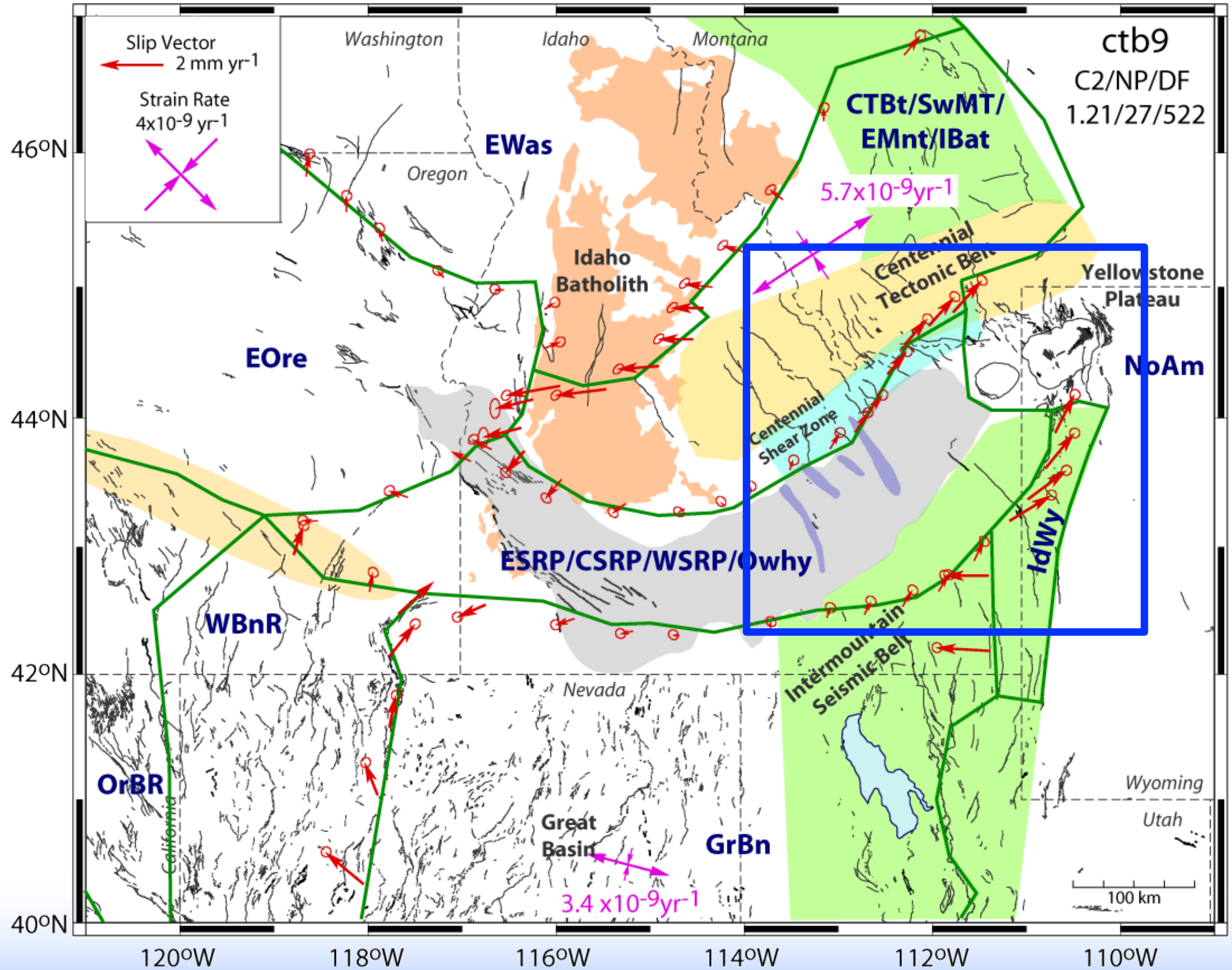

Idaho National Laboratory

Payne et al. (2012)

Interpretations

- At present, volcanic rift zones are not significant
- Combined Snake River Plain and Owyhee-Oregon Plateau (~125 km x 650 km region)
- Low deforming region consistent with
  - Infrequent small magnitude microearthquakes
  - Long time periods (10^4- >10^6 yrs) between mafic eruptions
- Rapid extension in Centennial Tectonic Belt and Great Basin
- Shear along the boundaries of the eastern Snake River Plain

Evaluate the Role of Shear

- **Shear drives extension**
  - Test hypothesis of McKenzie and Jackson (1986)
  - Bookshelf faulting across three NW-trending Basin and Range normal faults
  - Normal faulting is driven by edge shear stress
- **Extension drives shear**
  - Shear results from different strain rates between the Centennial Tectonic Belt and Snake River Plain
  - Distributed shear is localized within the Centennial Shear Zone

Two-dimensional Deformation Model

- System of small blocks bounded by parallel, equally spaced normal faults
- The component of strike-slip motion between the two plates is accommodated by
  - Clockwise rotation of the blocks between normal faults
  - Component of opposite (or left-lateral) slip on the block-bounding normal faults
- Only movement on the normal faults can produce a change in area; Line A-B remains parallel and a constant length

"Bookshelf Style Faulting"

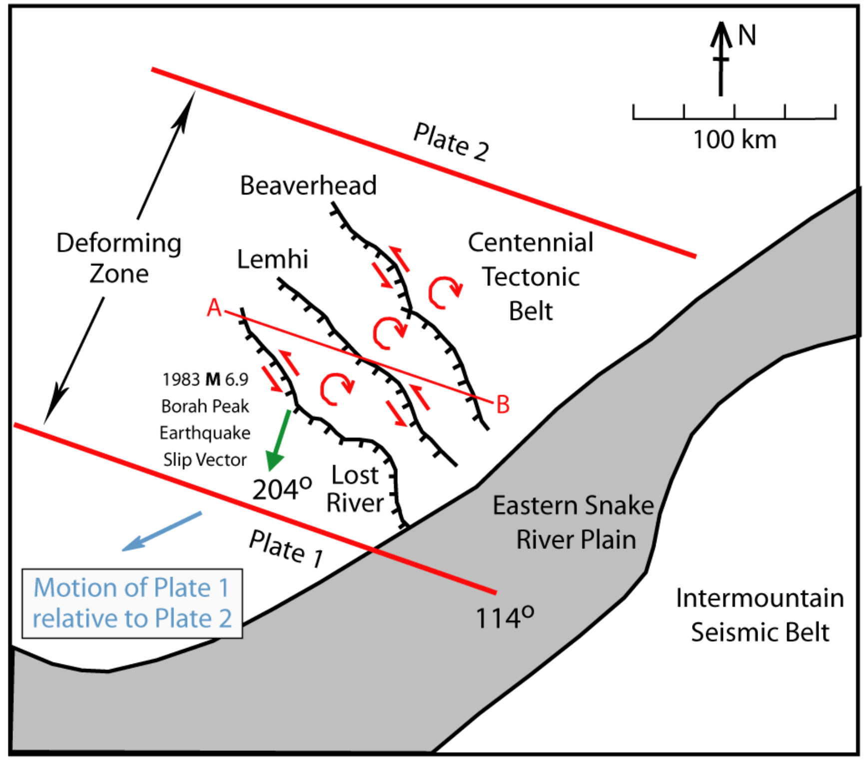

McKenzie and Jackson (1983; 1986)

Test Whether Ranges Rotate at Paleomagnetic Rate over ~48 m.y.

No Rotating Blocks

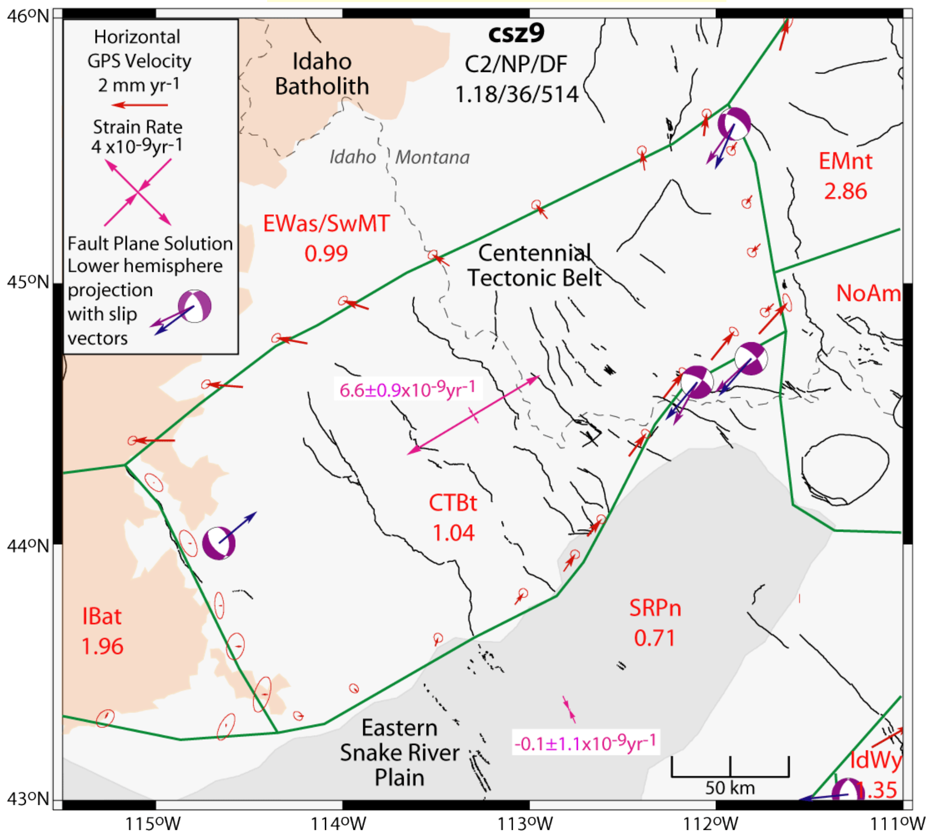

Rotation rates of -0.21 to -0.25 °m.y.$^{-1}$

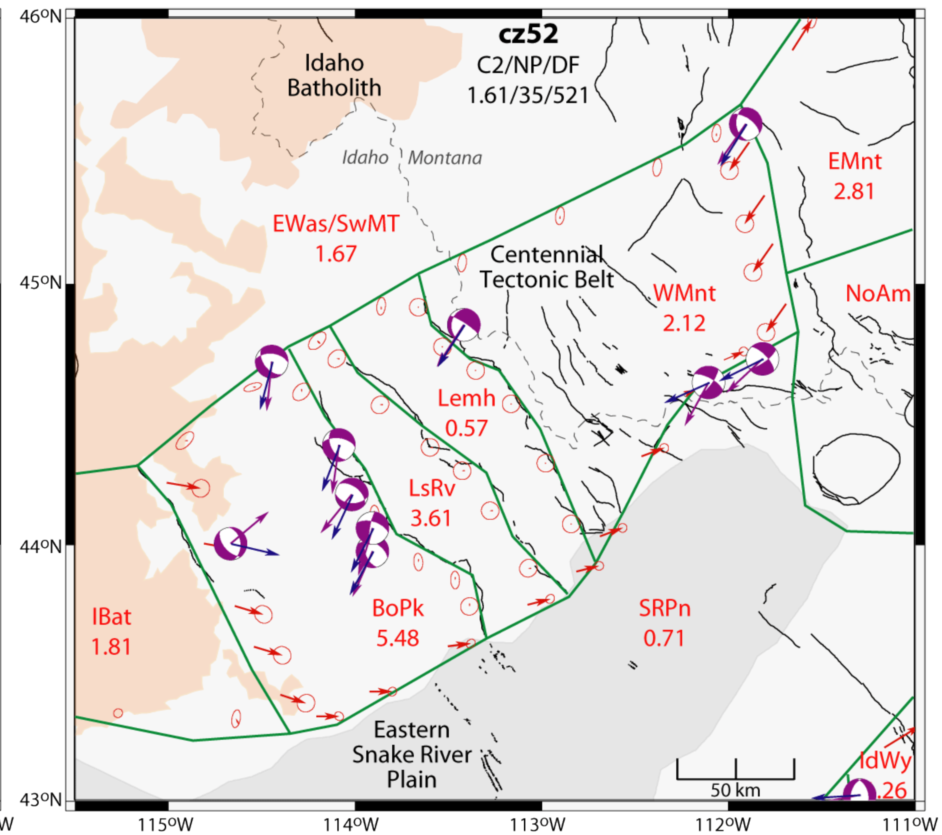

$\chi_\eta^2 = 1.18$ vs. $\chi_\eta^2 = 1.61$
F-Distribution Test = >99%

Idaho National Laboratory

Payne et al. (2013)

Extension along Line A-B

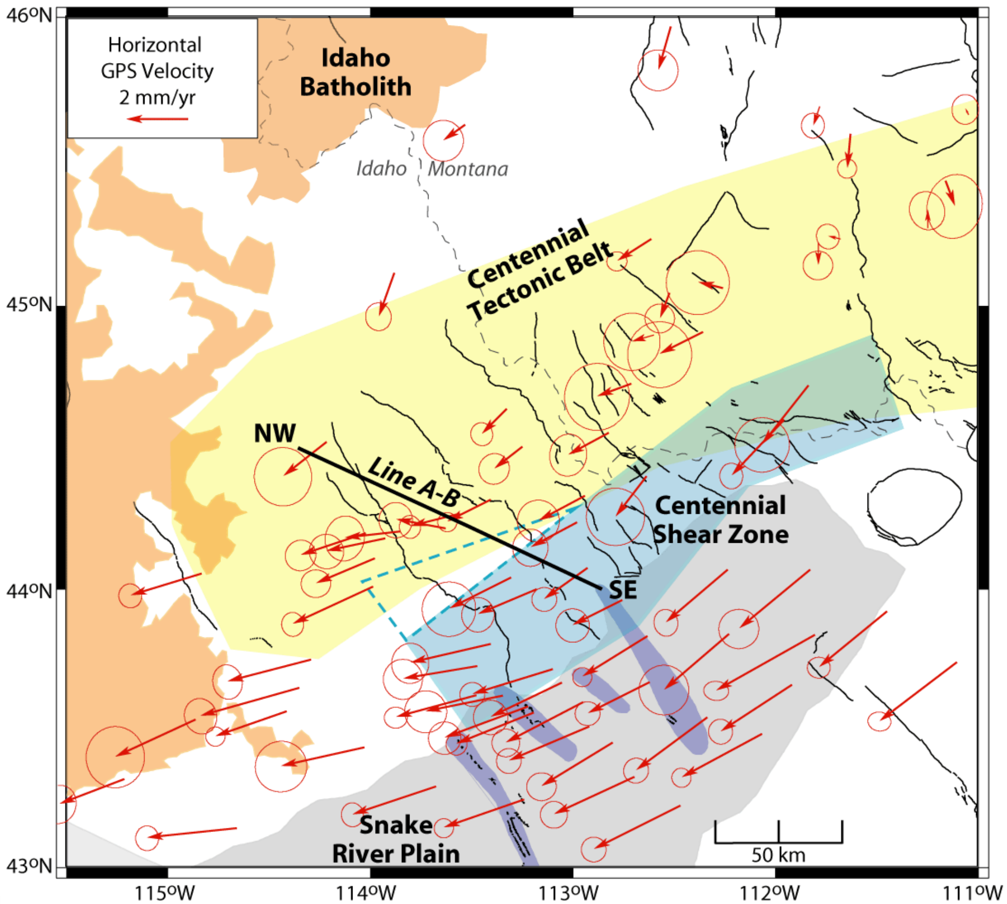

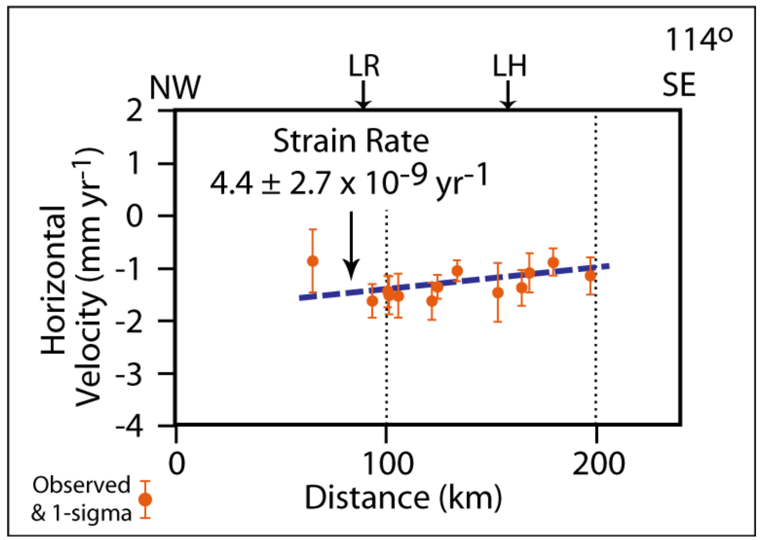

Components of velocities that are parallel to the direction of the profiles

Positive slope indicates extension

Idaho National Laboratory

Payne et al. (2013)

GPS Velocities in the Snake River Plain Reference Frame

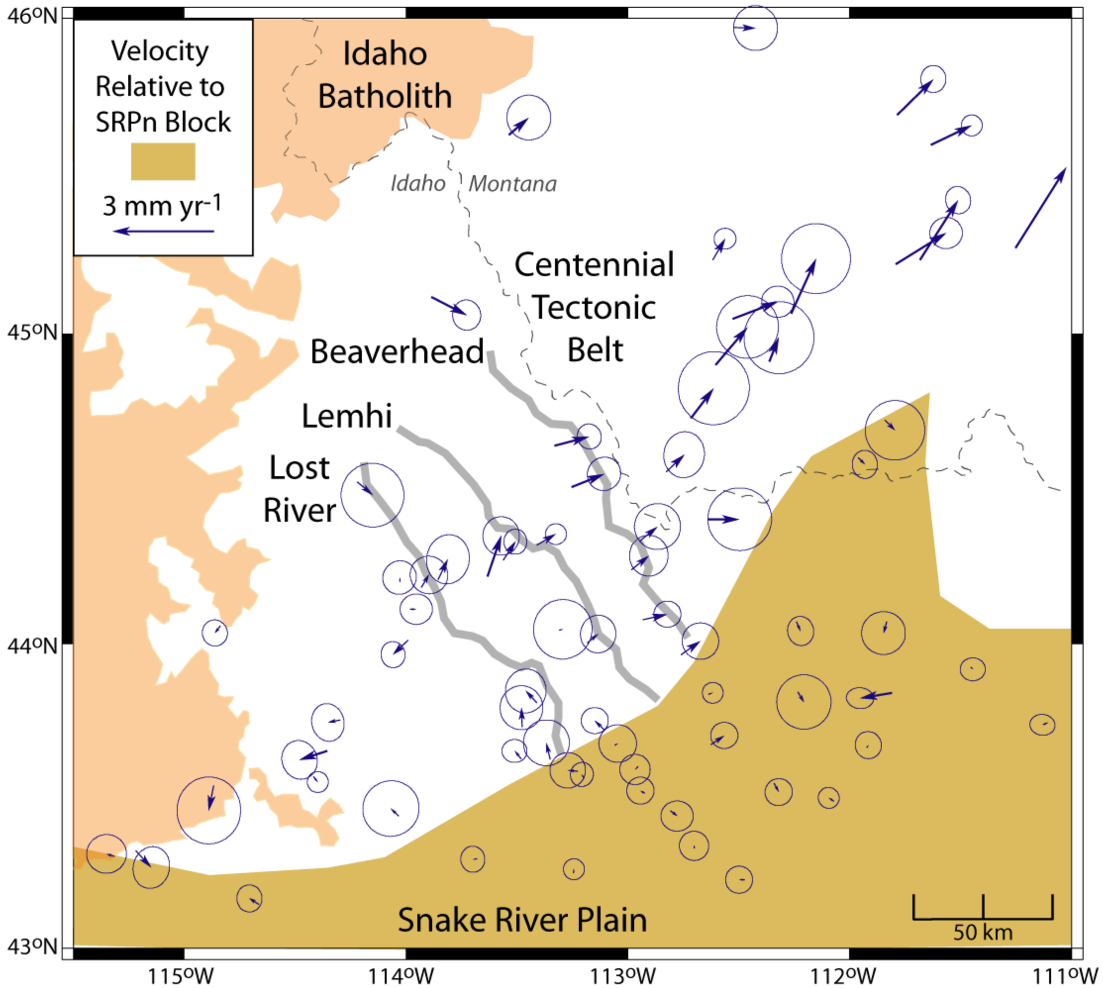

Rapid extension in the Centennial Tectonic Belt adjacent to the slowly deforming Snake River Plain produces shear between them

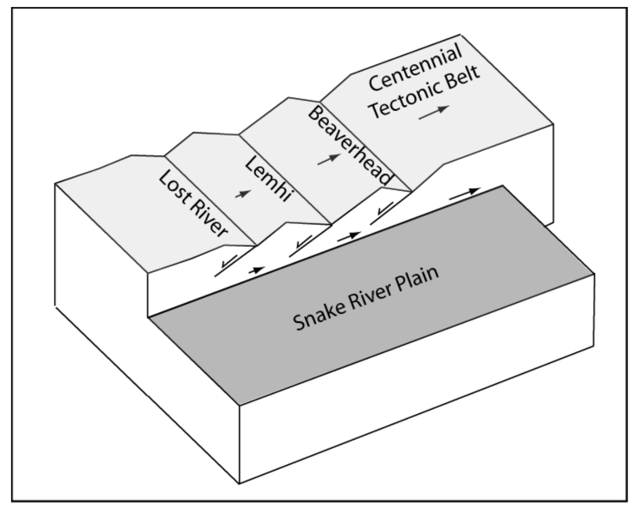

Payne et al. (2013)

Proposed Locations for Right-lateral Strike-slip Motion

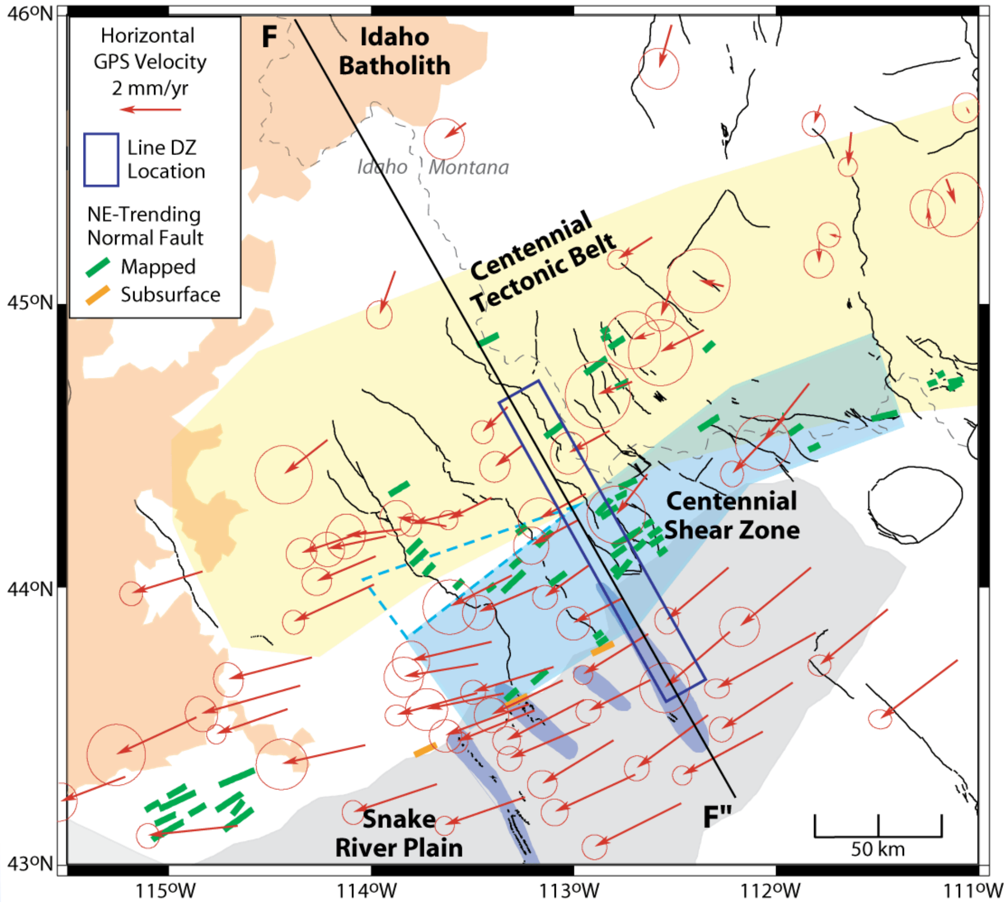

Deformation Zone (DZ) Example

- Strike-slip motions on existing NE-trending normal faults
- Regional-scale rotation

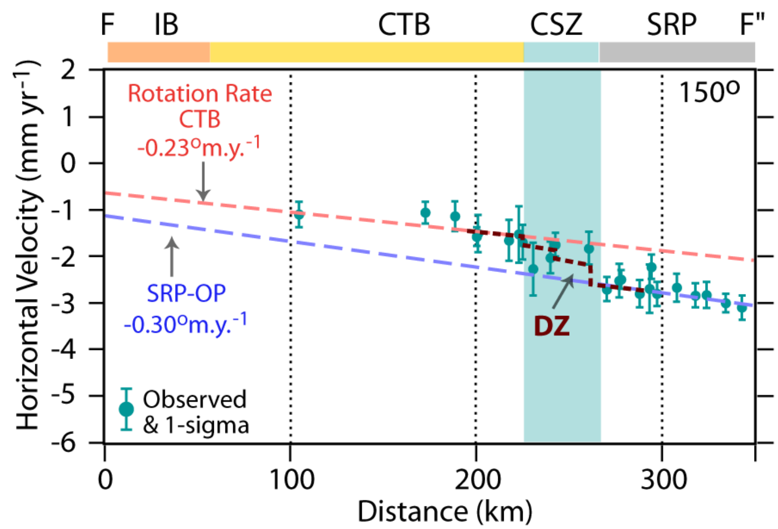

Velocities perpendicular to direction of profiles
Negative Slope = Clockwise rotation or right-lateral shear or both

Idaho National Laboratory

NE-trending faults: Zentner (1989); McQuarry & Rodgers (1998)
GPS results: Payne et al. (2013)

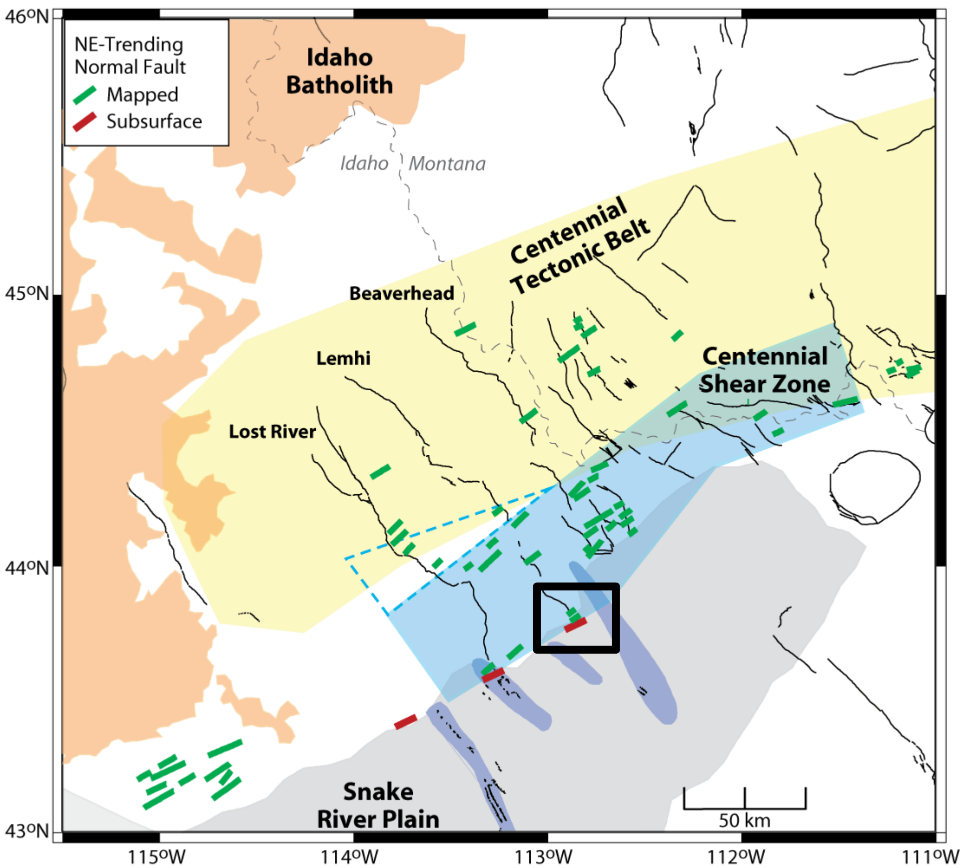

Bruhn et al. (1992)

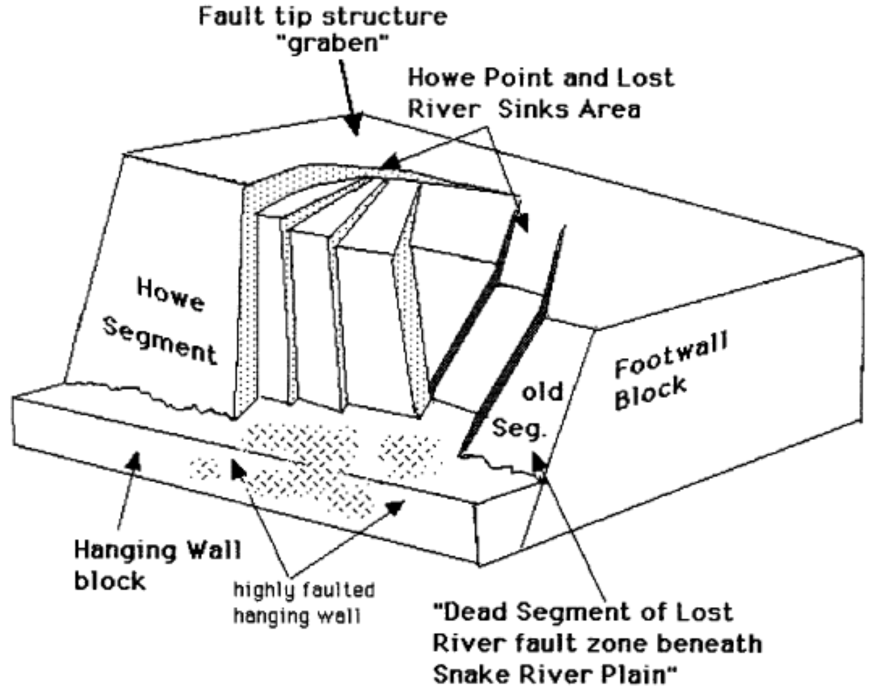

Note: Graben structure has been superimposed on Lemhi fault zone in last 4 m.y. as Howe segment continued to deform while Lemhi fault beneath Snake River Plain ceased to deform. This is indicated by asymmetry of graben structure in which deformation is concentrated at tip of Howe segment.

Figure 10: Tenative structural model for deformation at the southern tip of the Howe fault segment, Lemhi fault zone.

Idaho National Laboratory

Proposed Accommodation of Right-lateral Strike-slip Motion

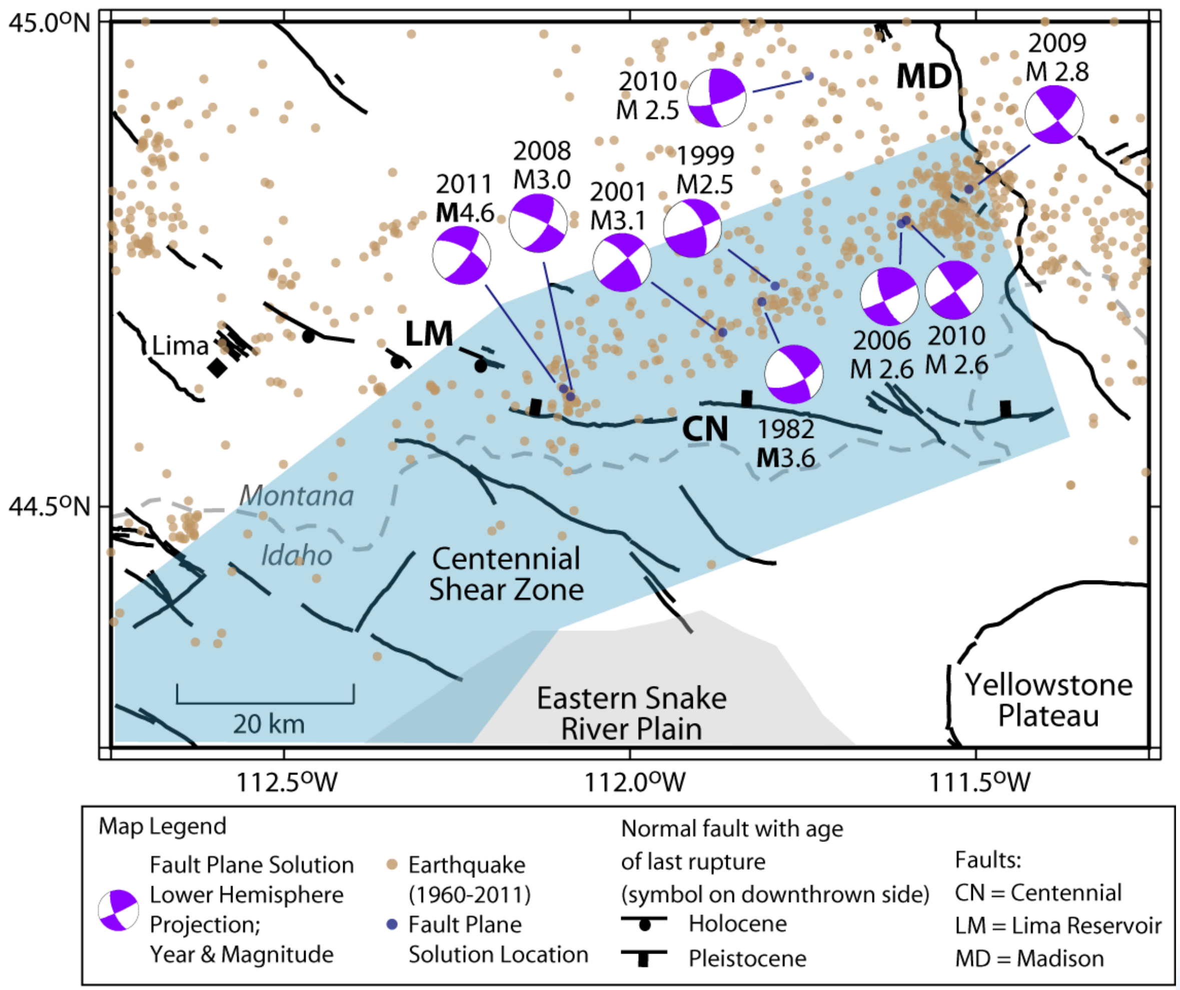

Idaho National Laboratory

Earthquakes: ANSS (2011); Fault Plane Solutions: Stickney (1997; 2007); Hermann et al. (2011)
Ages of last ruptures: Bartholomew et al. 2002; Petrik (2008); Anastasio et al. (2011)

1994-2010 GPS Results

- Rapidly extending Basin & Range
- Slowly deforming Snake River Plain
- Shear along the Snake River Plain boundaries
- In Centennial Shear Zone right-lateral shear may be accommodated by:
  - Strike-slip faulting on existing NE-trending faults
  - Localized bookshelf faulting within the zone
  - Regional-scale rotation
  - Some combination

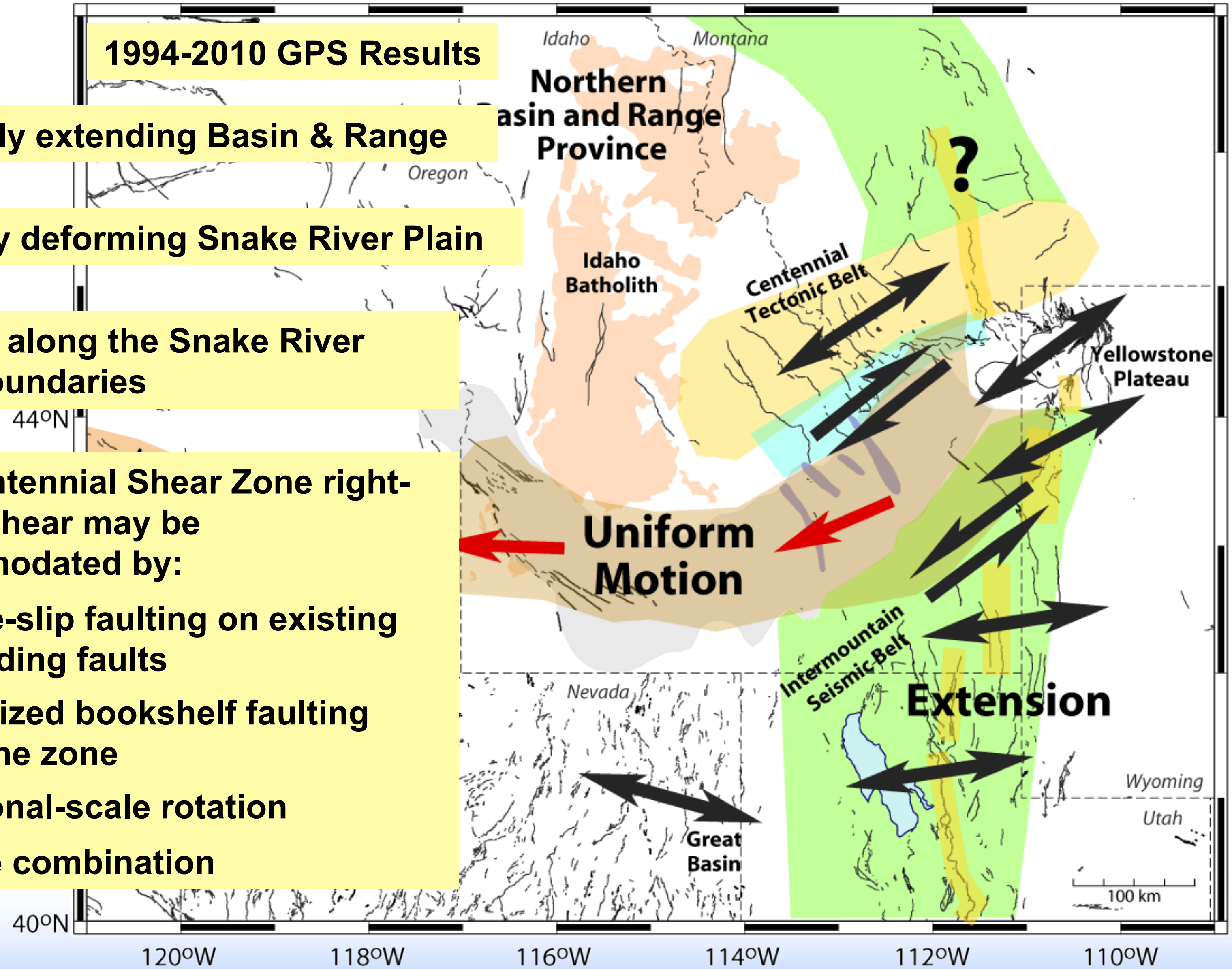

Payne et al. (2012)

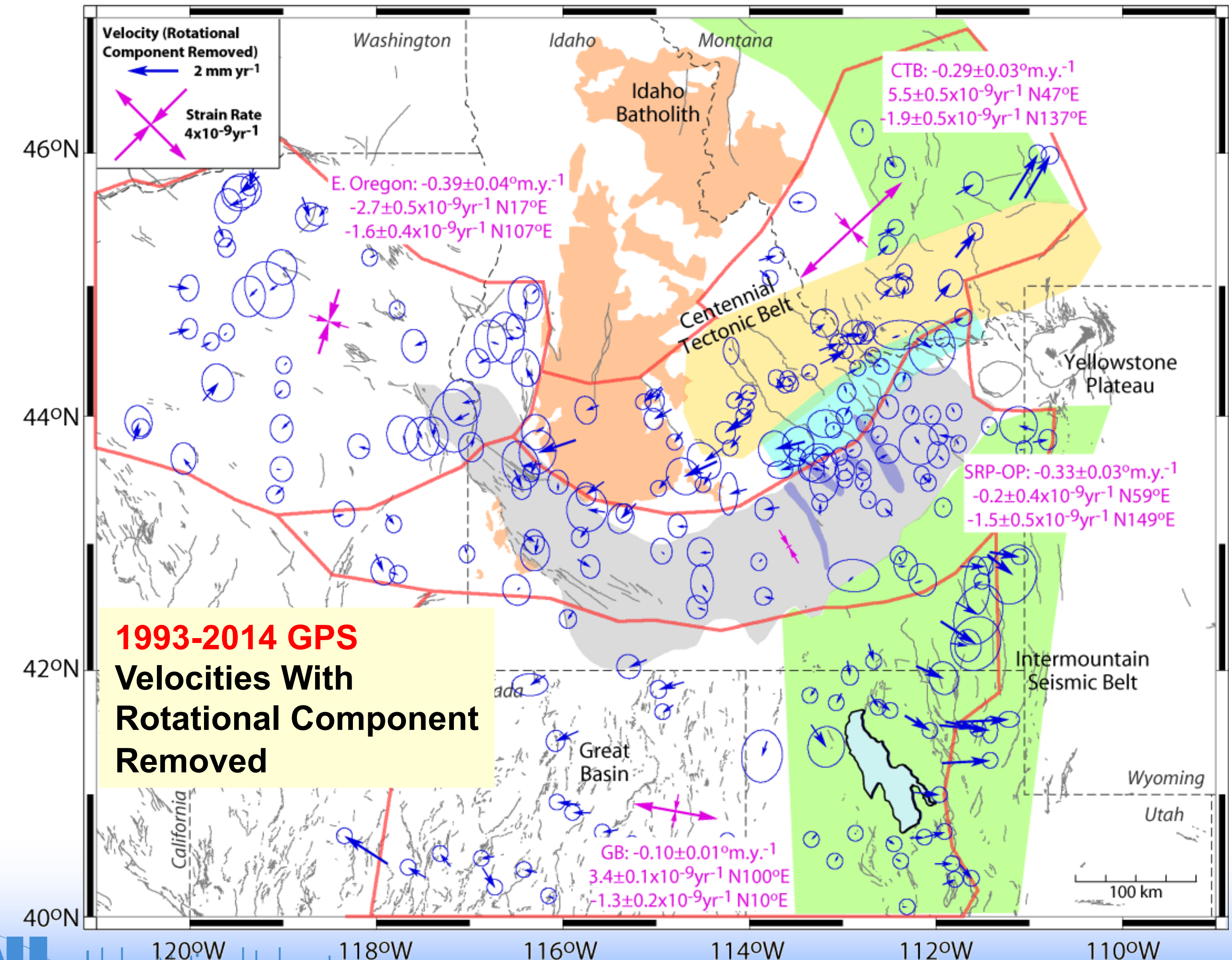

Idaho National Laboratory

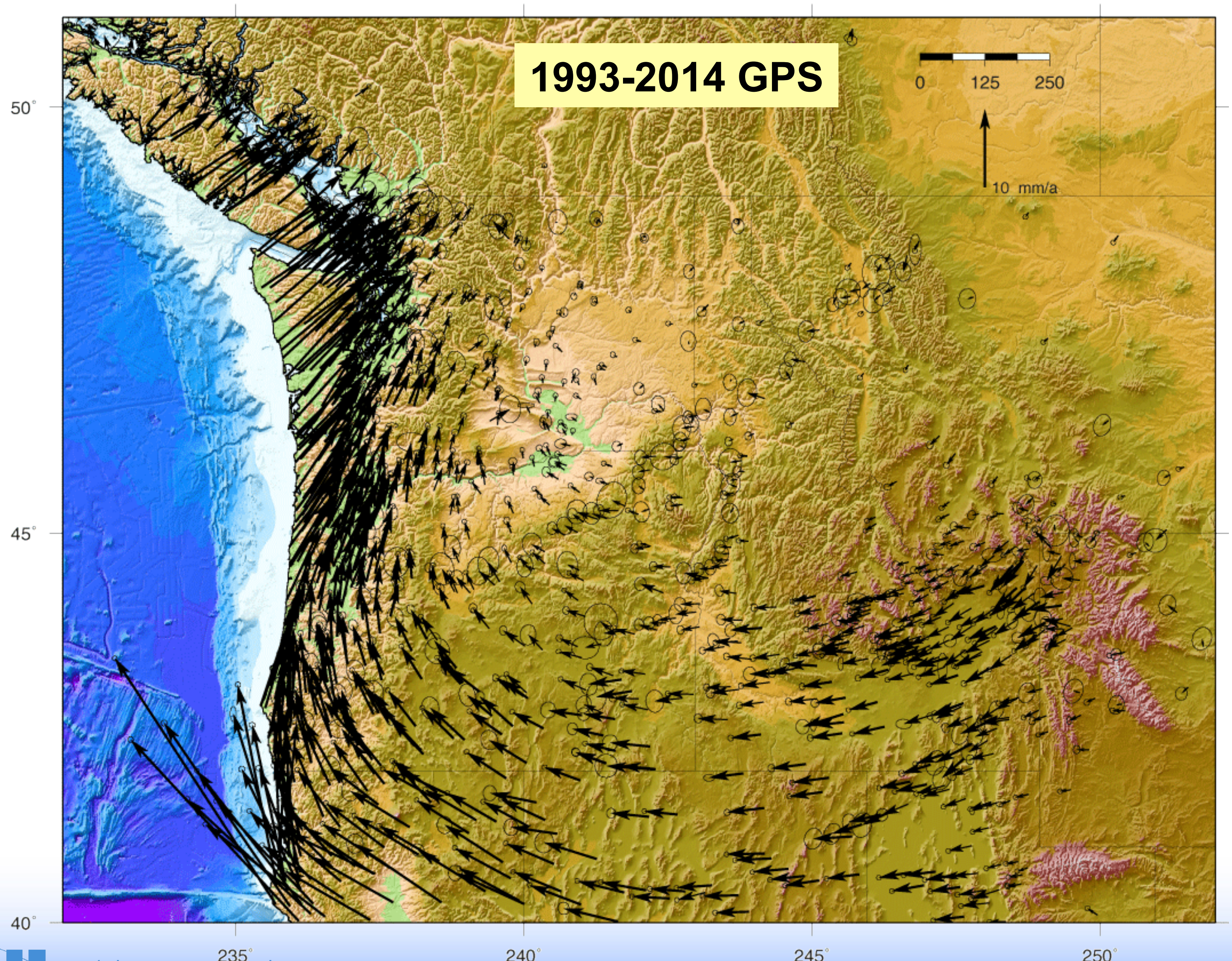

Idaho National Laboratory

Velocities in Stable North American Reference Frame

GEODETIC CONSTRAINTS ON KINEMATICS AND STRAIN RATES IN THE NORTHERN BASIN AND RANGE

Rebecca Bendick, Dylan Schmeelk, Yelebe Birhanu, and Cody Bomberger
University of Montana, Geosciences,
32 Campus Drive #1296, Missoula, Montana 59812-1296
Senior author email address: bendick@mso.umt.edu

The region of active extension north of the Snake River Plain (SRP) is of scientific interest for three reasons: (1) For continental dynamics, this region offers the best test of the hypothesis that a change in boundary conditions on the western North American margin from convergent to transform is the primary mechanism of Basin and Range extension. Specifically, if the total extension in Montana and Idaho (where the western margin is still Cascadian convergence) is comparable in magnitude and spatial distribution to that south of the latitude of the Mendocino triple junction, then boundary conditions cannot be the sole critical parameter for steady-state extension. (2) For regional kinematics, the rate and spatial distribution of extension north of the SRP places bounding constraints on either the shear required on the margins of the SRP or the amount of stretching that must be accommodated aseismically therein. Finally, (3) for regional seismic hazard, the slip rate, location, and structural geometry of major faults as measured by GPS provides measures of fault hazard independent of the sparse and poorly located seismic catalog. Geodetic assessments are especially important for the type of faults in the area: those with very limited paleoseismic data and low slip rates, but large lengths and offsets. Such faults are known from other locations to support rare, but large moment release, contributing substantial risk that is difficult to quantify with standard seismic statistical methods.

Two dense arrays of both continuous and campaign GPS installations inset into the Plate Boundary Observatory (PBO) network north of the SRP (figure 1) provide direct constraints on relative velocities across a broad zone of the northern Basin and Range Province, including several large normal faults, hence data relevant to all three applications above. We report the regional velocity and strain field, plus estimated slip rates for the Red Rock, Lemhi, Bitterroot, Mission, and Nine Mile faults of western Montana and northeastern Idaho. Additional scarp observations from LiDAR and Structure from Motion further constrain active fault trace location and scaling, and will contribute to future assessments of regional hazard. Finally, stacked synthetic aperture radar interferograms (InSAR) offer independent measures of tectonic deformation in the Lemhi fault-Borah Peak area.

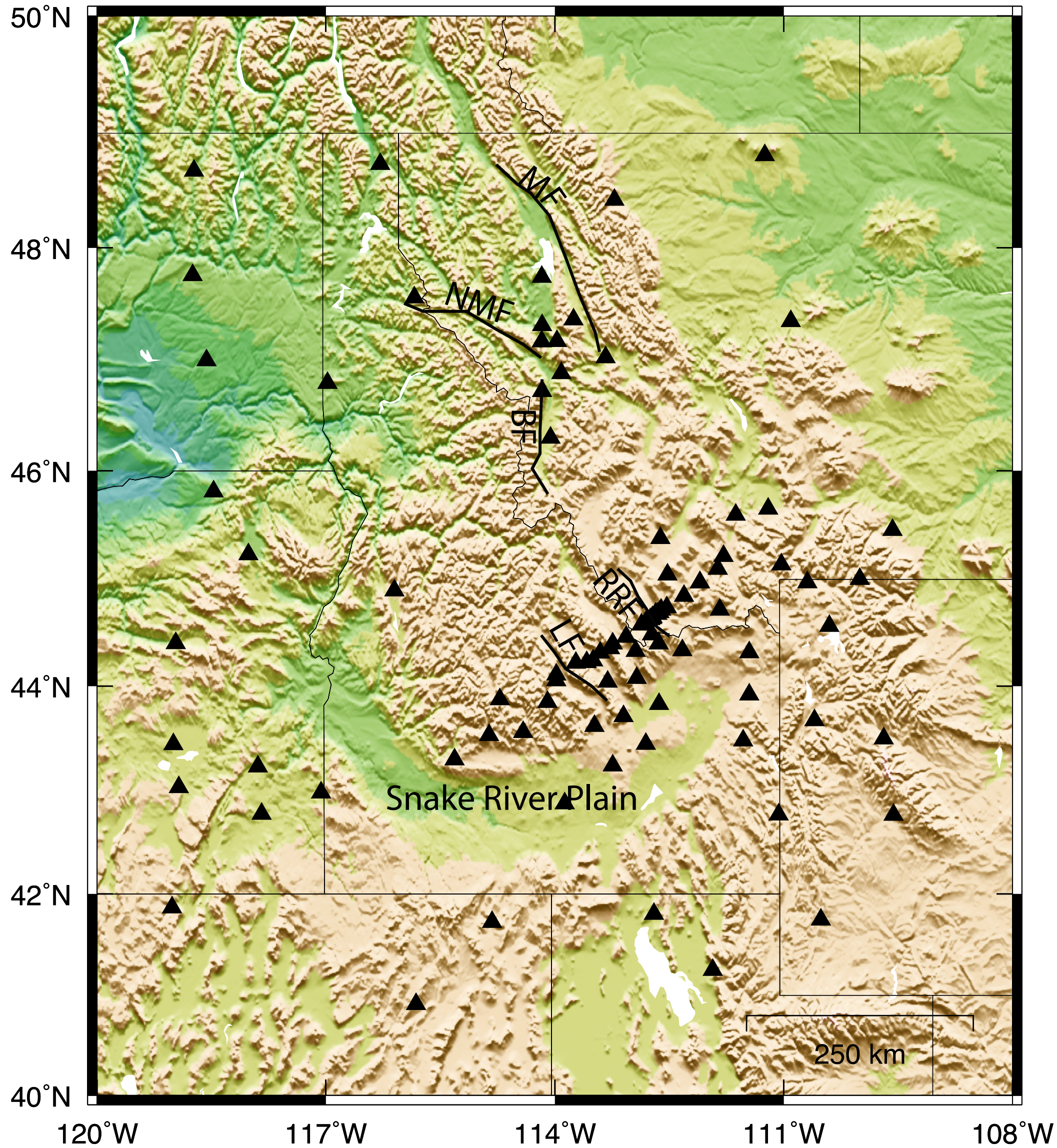

Figure 3. *Location of GPS sites used in this study. Seventy percent of the sites are continuously recording, installed either as part of the PBO network or a University of Montana, NSF-supported experiment. All continuous sites have at least four years of observations; some have more than ten years of observations. The remaining 30% are campaign sites measured sporadically over a period from 1998 to the present. LF - Lemhi fault, RRF - Red Rock fault, BF - Bitterroot fault, NMF - Nine Mile fault, and MF - Mission fault.*

The following is a PDF version of the authors' PowerPoint presentation.

Geodetic Constraints on Kinematics and Strain Rates in the Northern Basin and Range

Dylan Schmeelk, Rebecca Bendick, Yelebe Birhanu, and Cody Bomberger

Funding:

5yr NSF grant

Tectonic setting

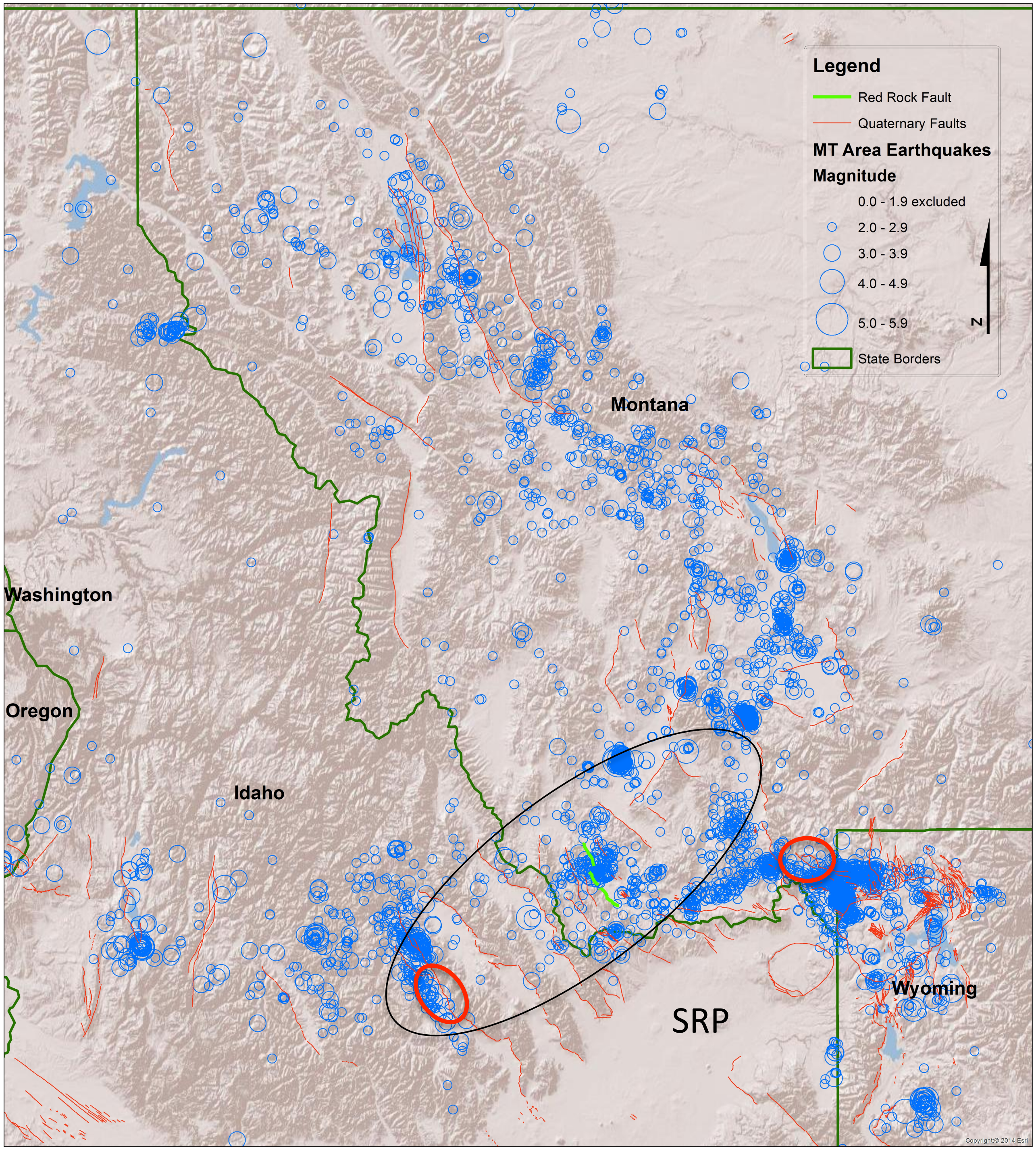

Seismic hazard implications

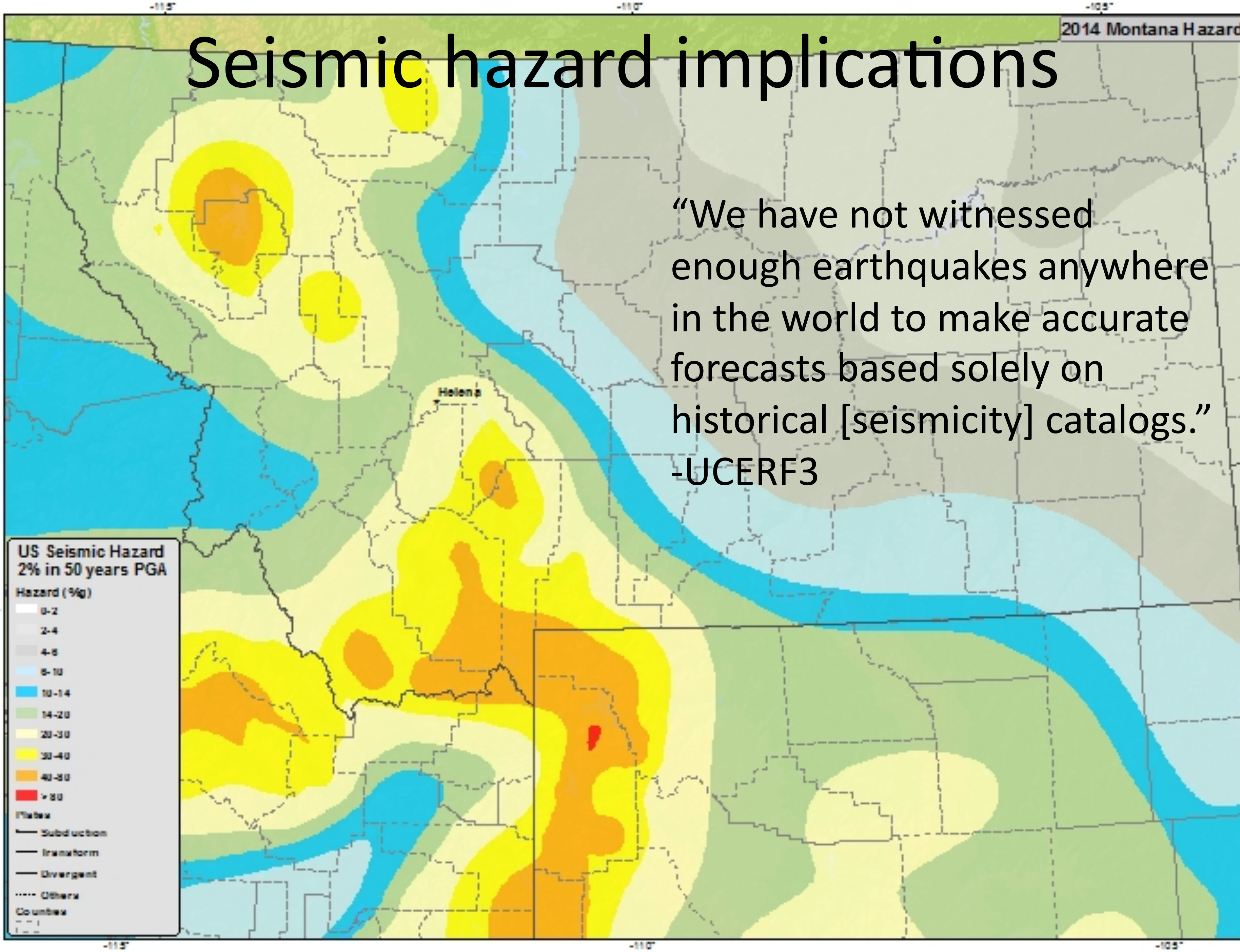

"We have not witnessed enough earthquakes anywhere in the world to make accurate forecasts based solely on historical [seismicity] catalogs."
-UCERF3

Geodetic deployment

Regional velocities

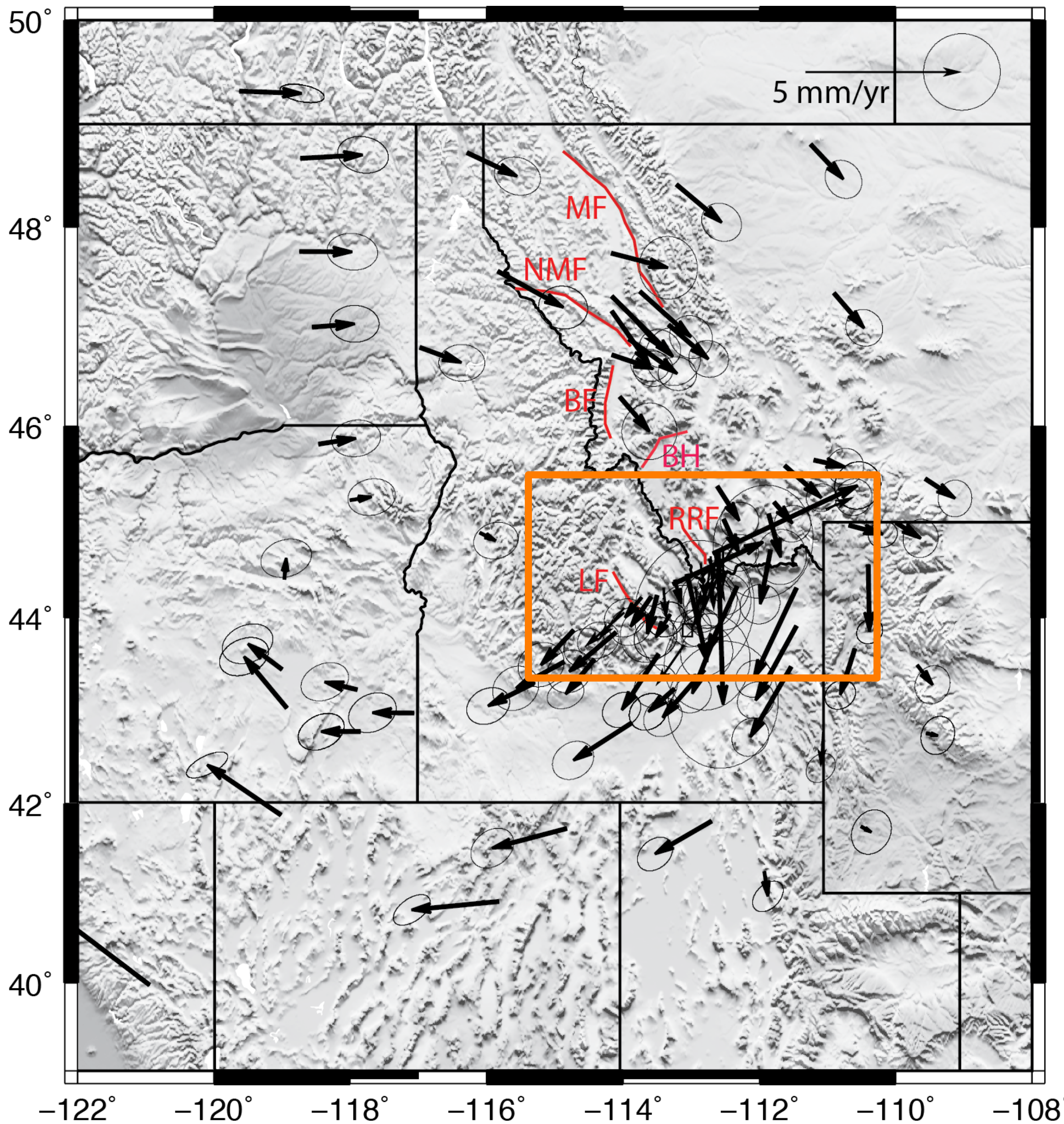

Local velocities

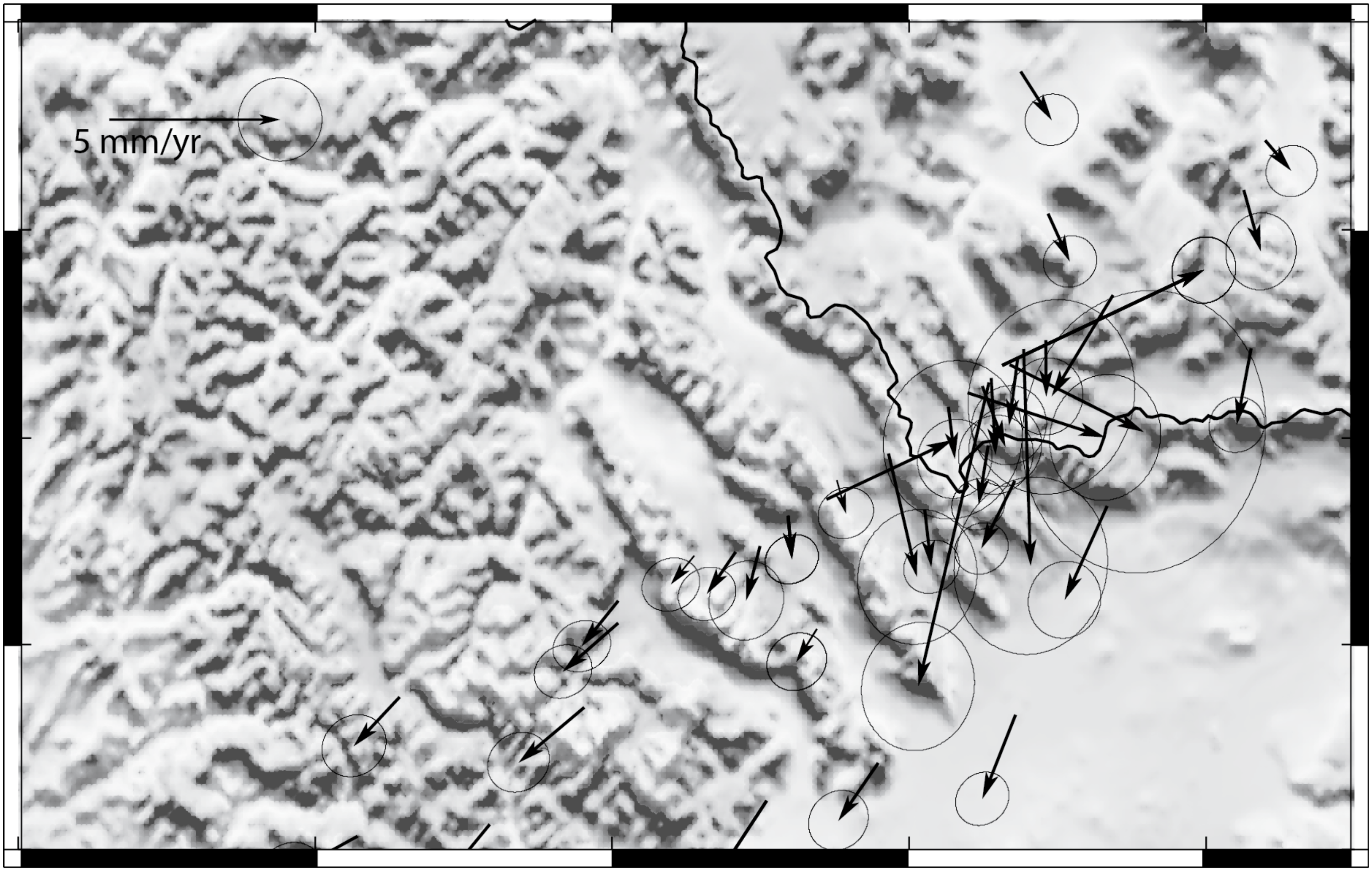

MT-ID border faults

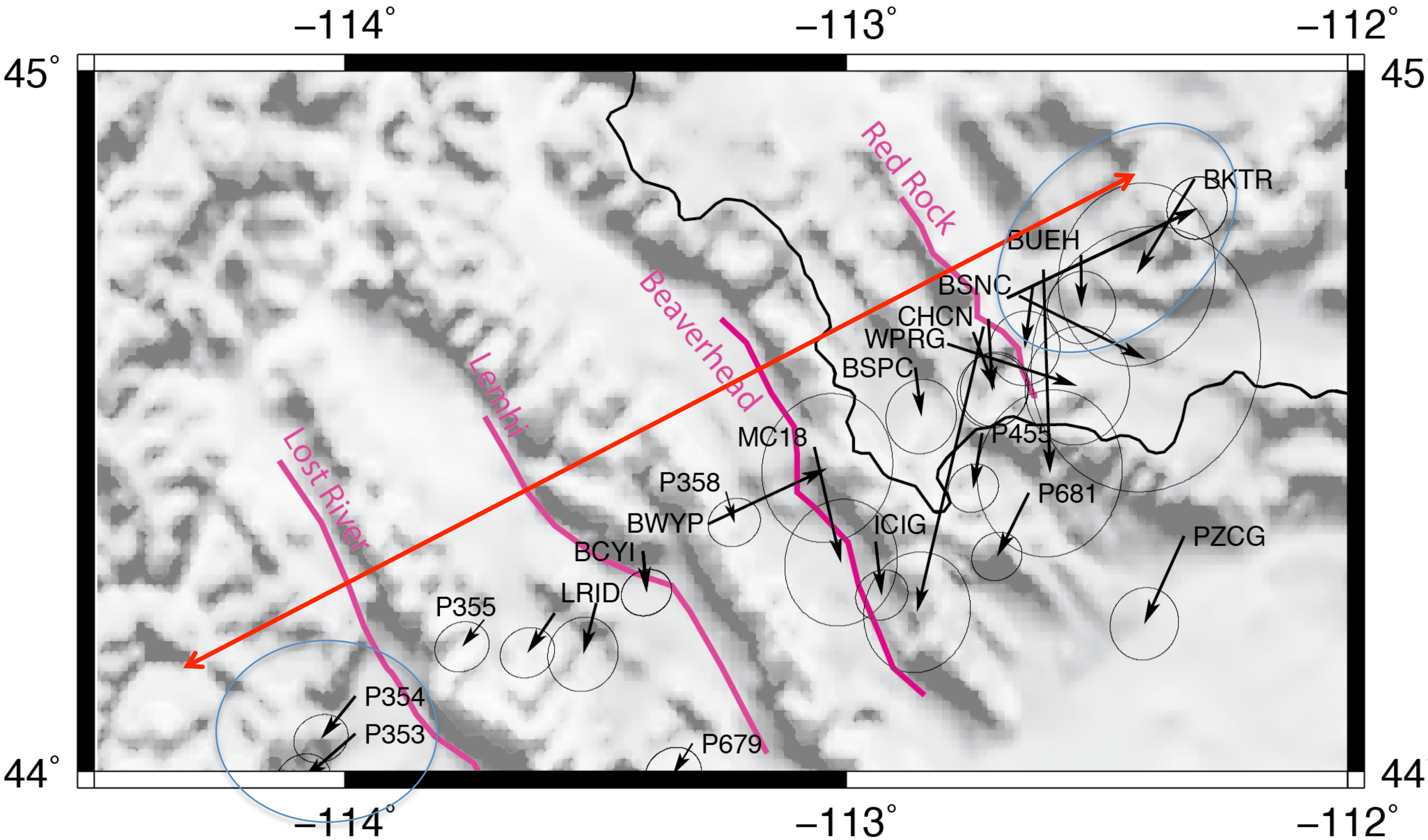

maximum extension = 4.4 ± 1 mm/yr

minimum extension = 1.4 ± 1 mm/yr

MT-ID border faults

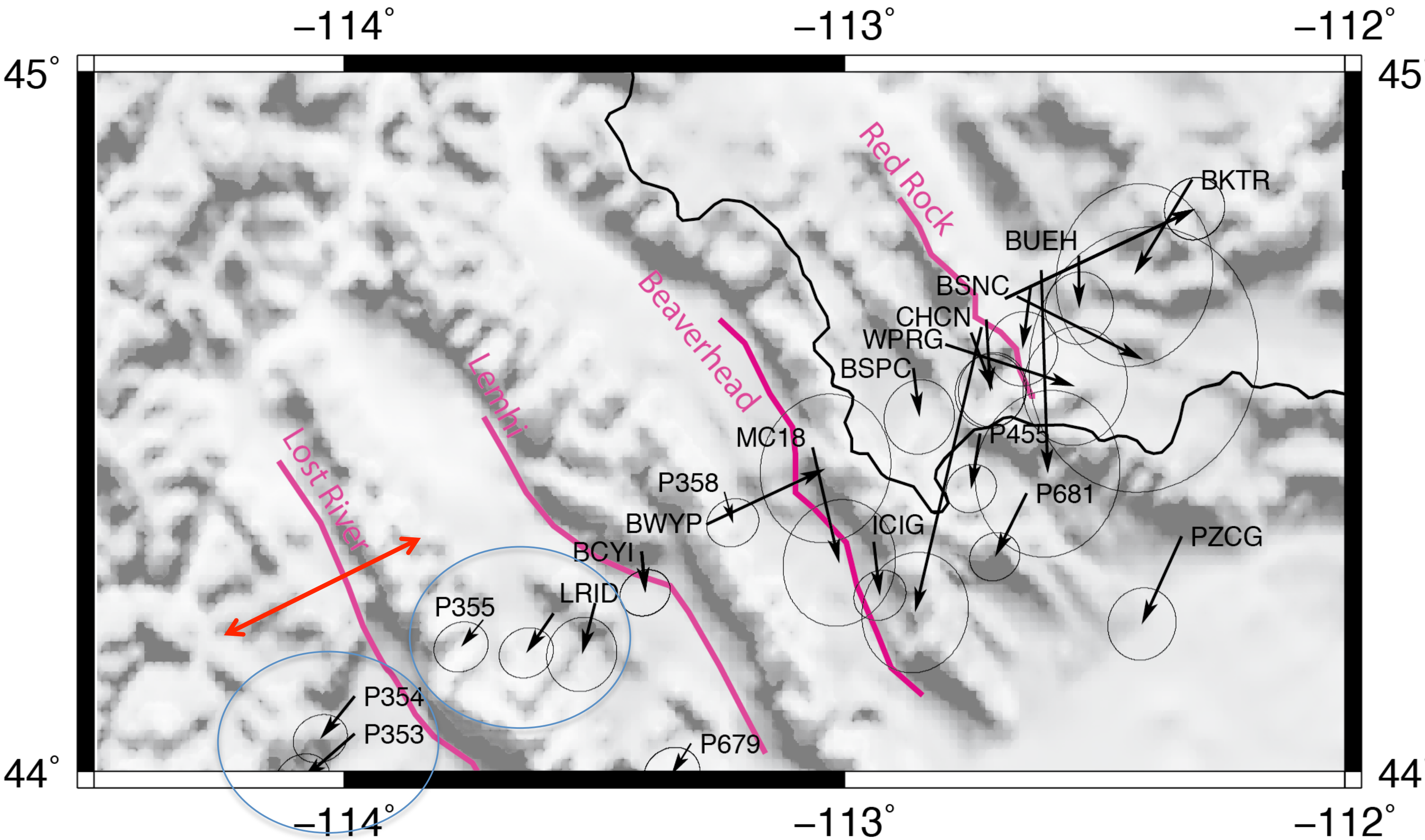

1 ± 0.5 mm/yr

Scarp from 1983 Bora Peak earthquake

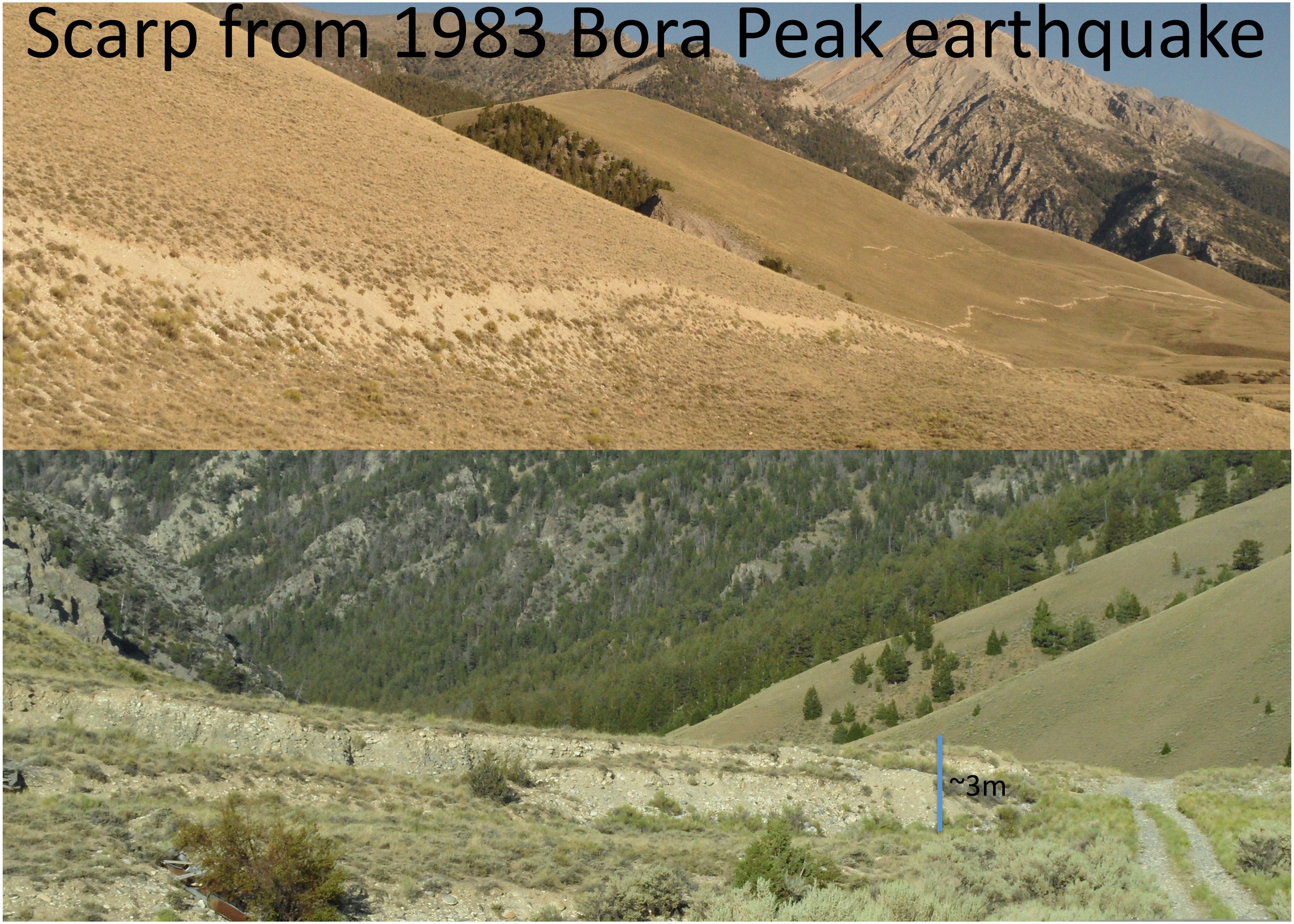

MT-ID border faults

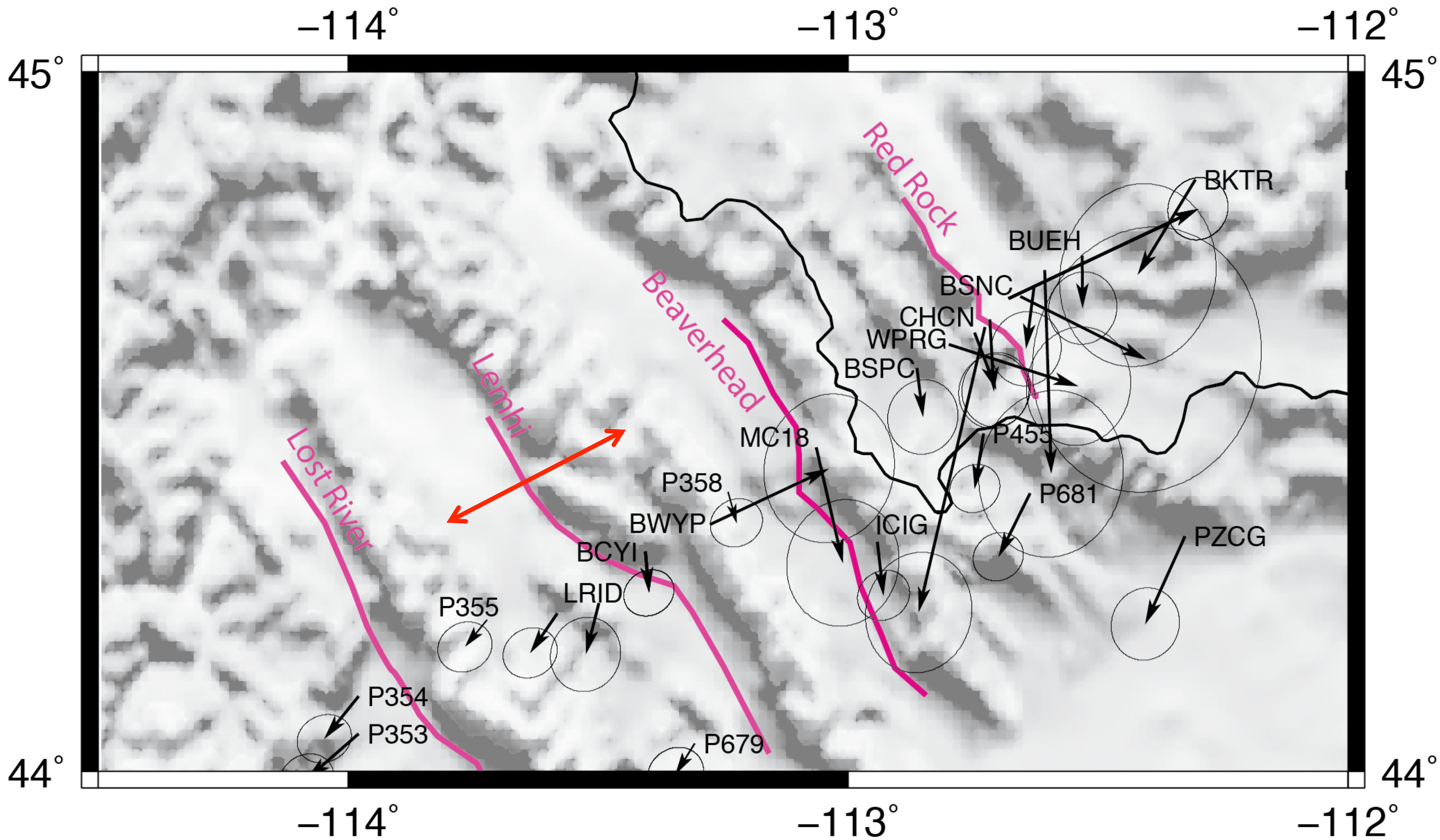

0.7 ± 0.5 mm/yr

MT-ID border faults

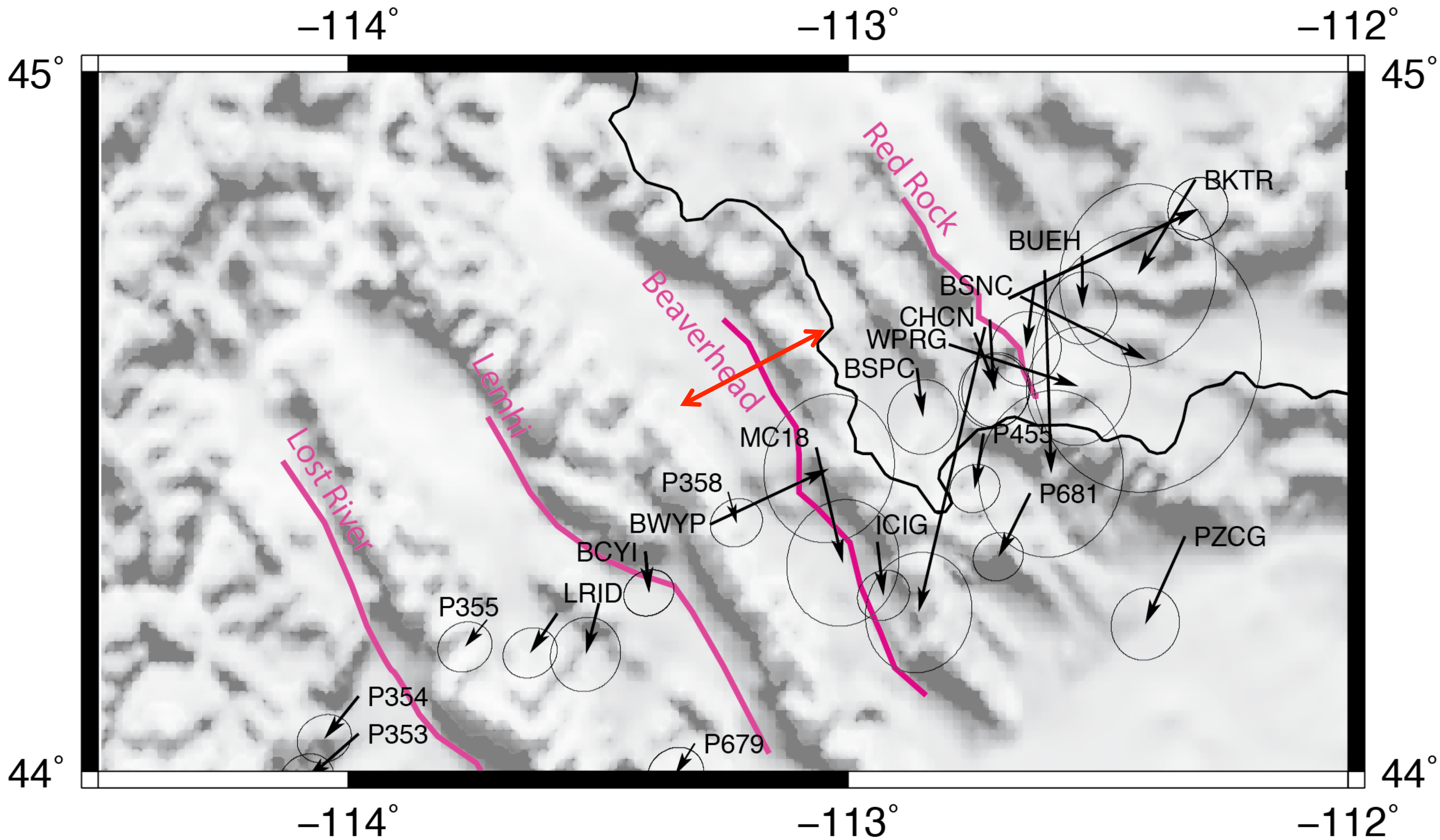

0.4 ± 0.5 mm/yr

MT-ID border faults

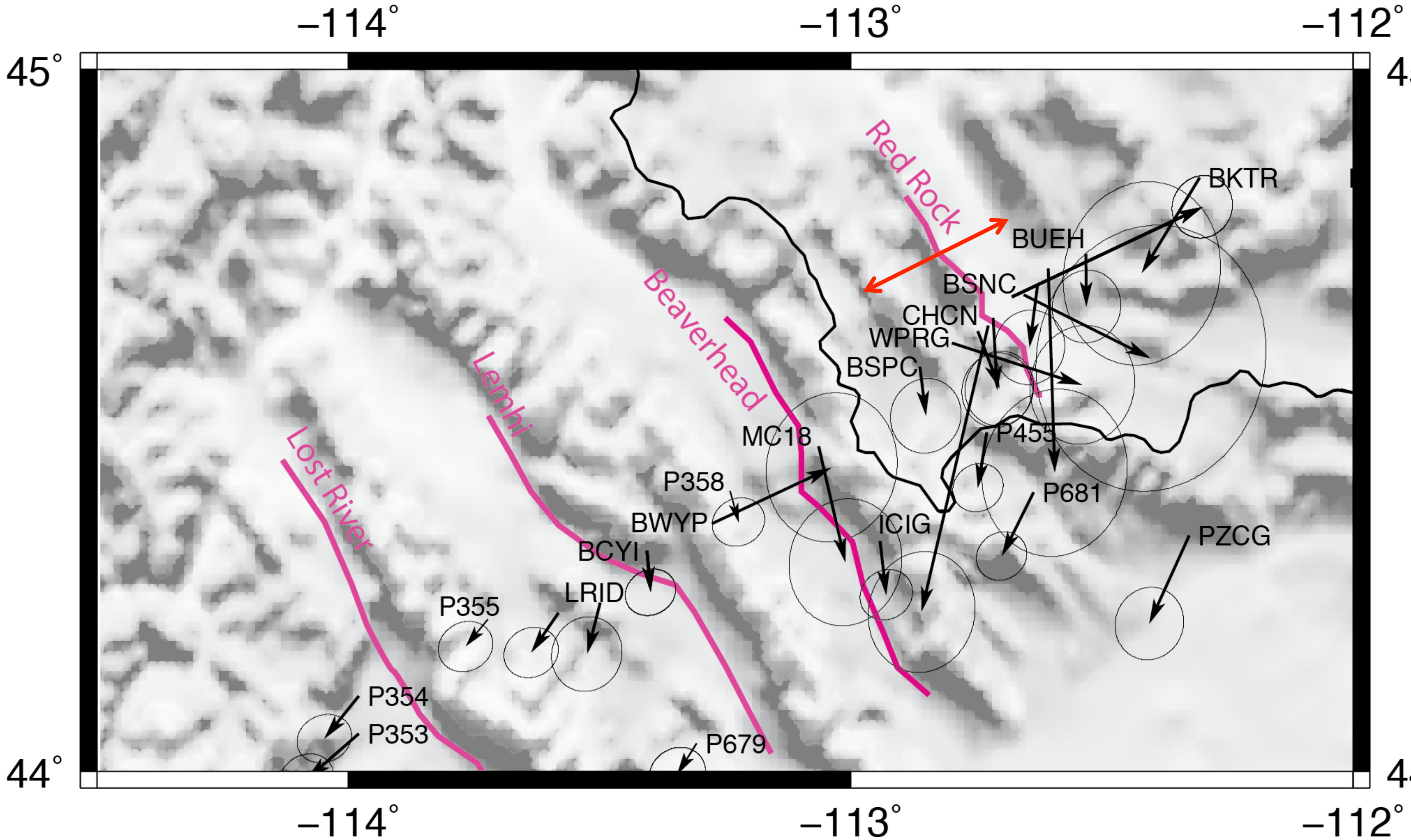

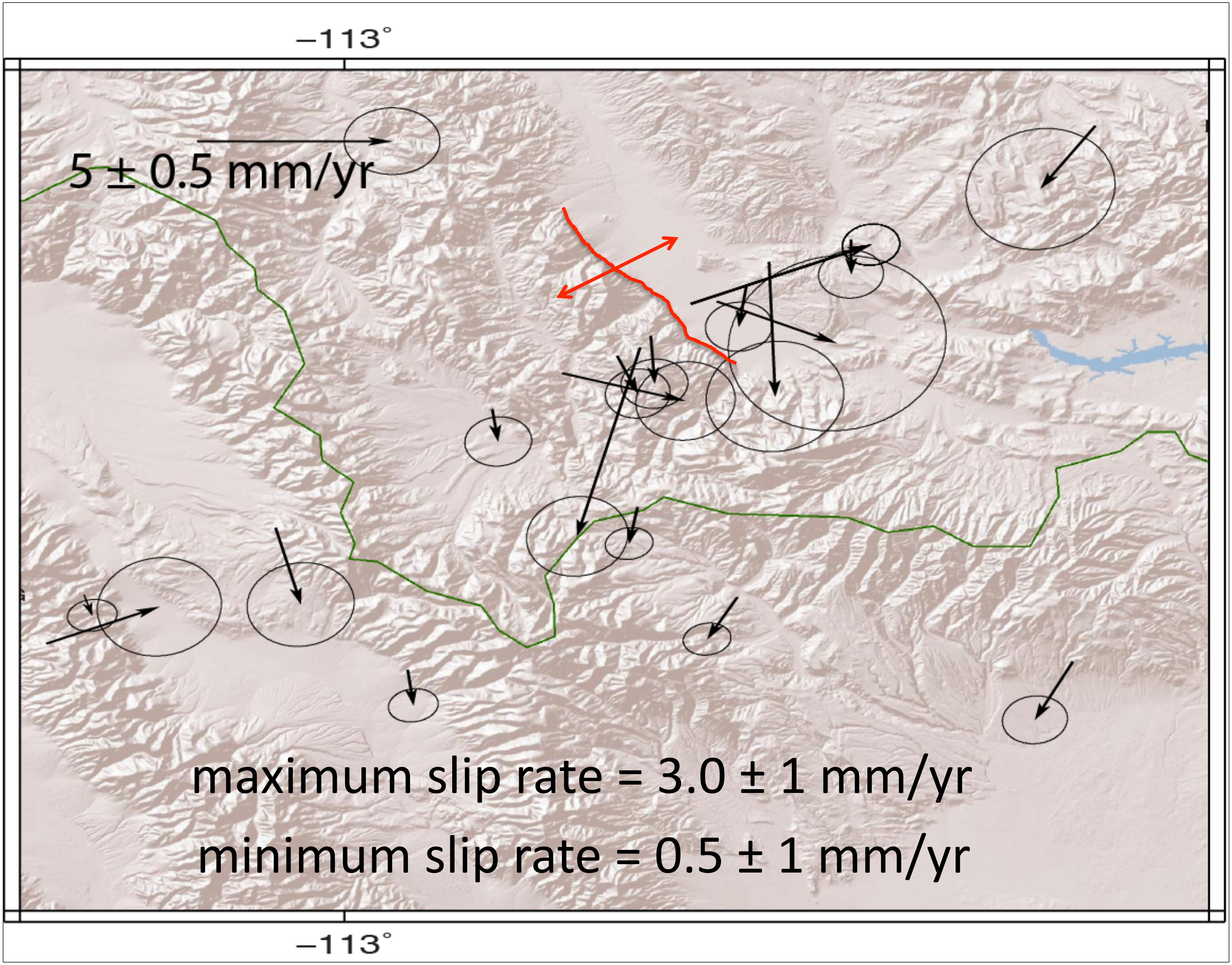
−113°
5 ± 0.5 mm/yr
maximum slip rate = 3.0 ± 1 mm/yr
minimum slip rate = 0.5 ± 1 mm/yr
−113°

MT-ID border faults

The Tendoy Mountains and Red Rock Fault, from Lima, MT

NW Montana

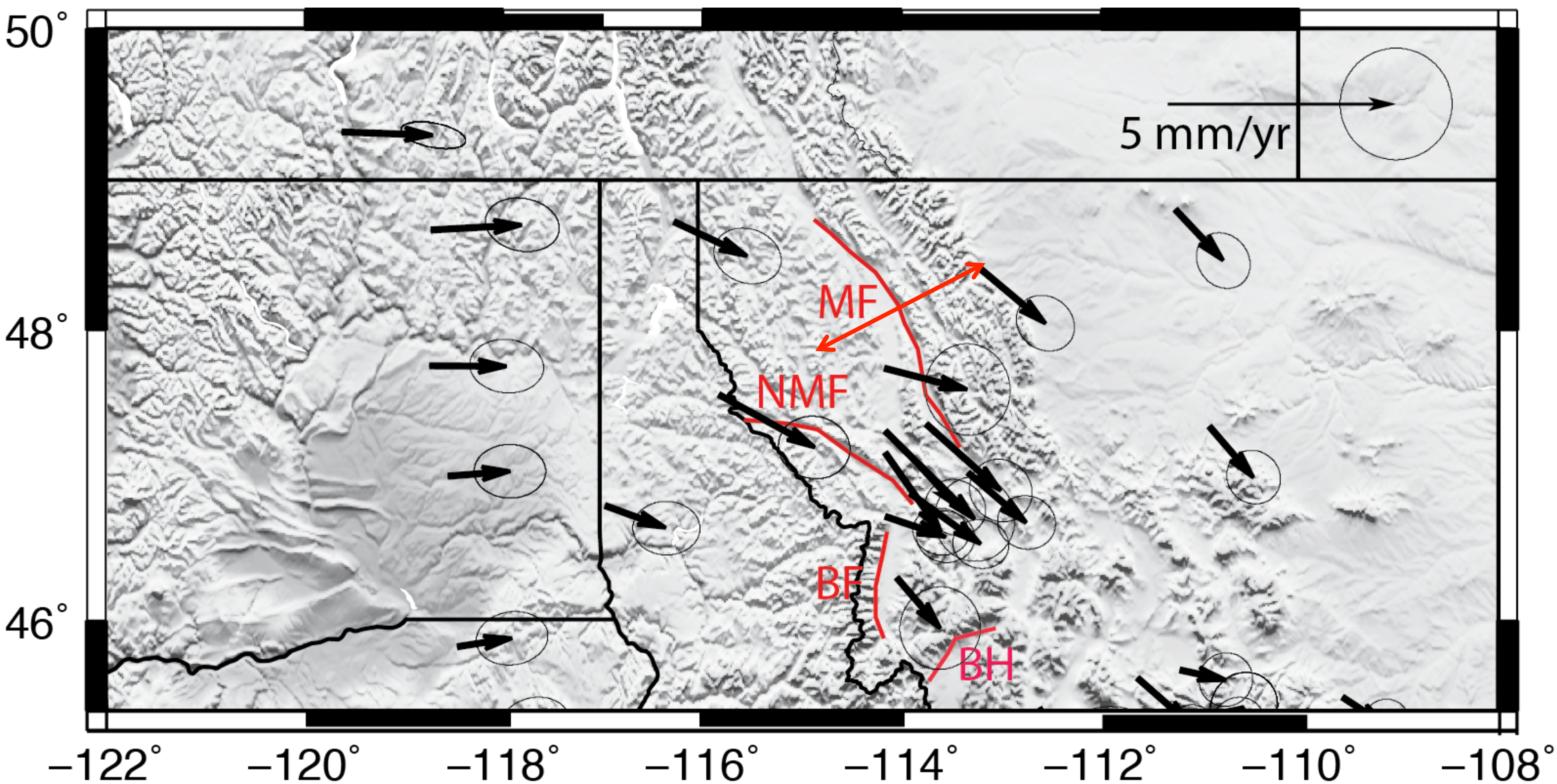

1.1 ± 0.5 mm/yr

NW Montana

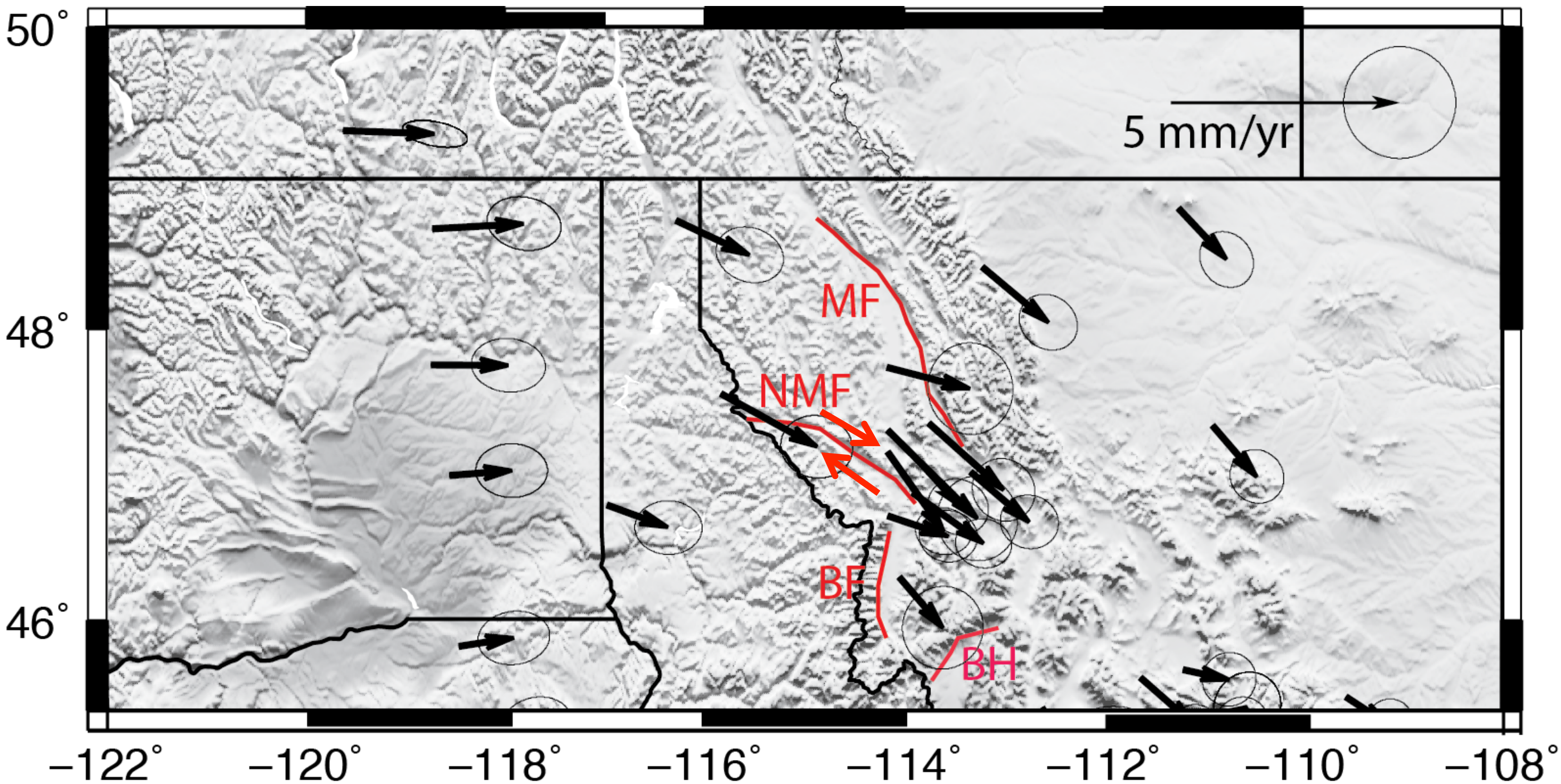

0.7 ± 0.5 mm/yr

NW Montana

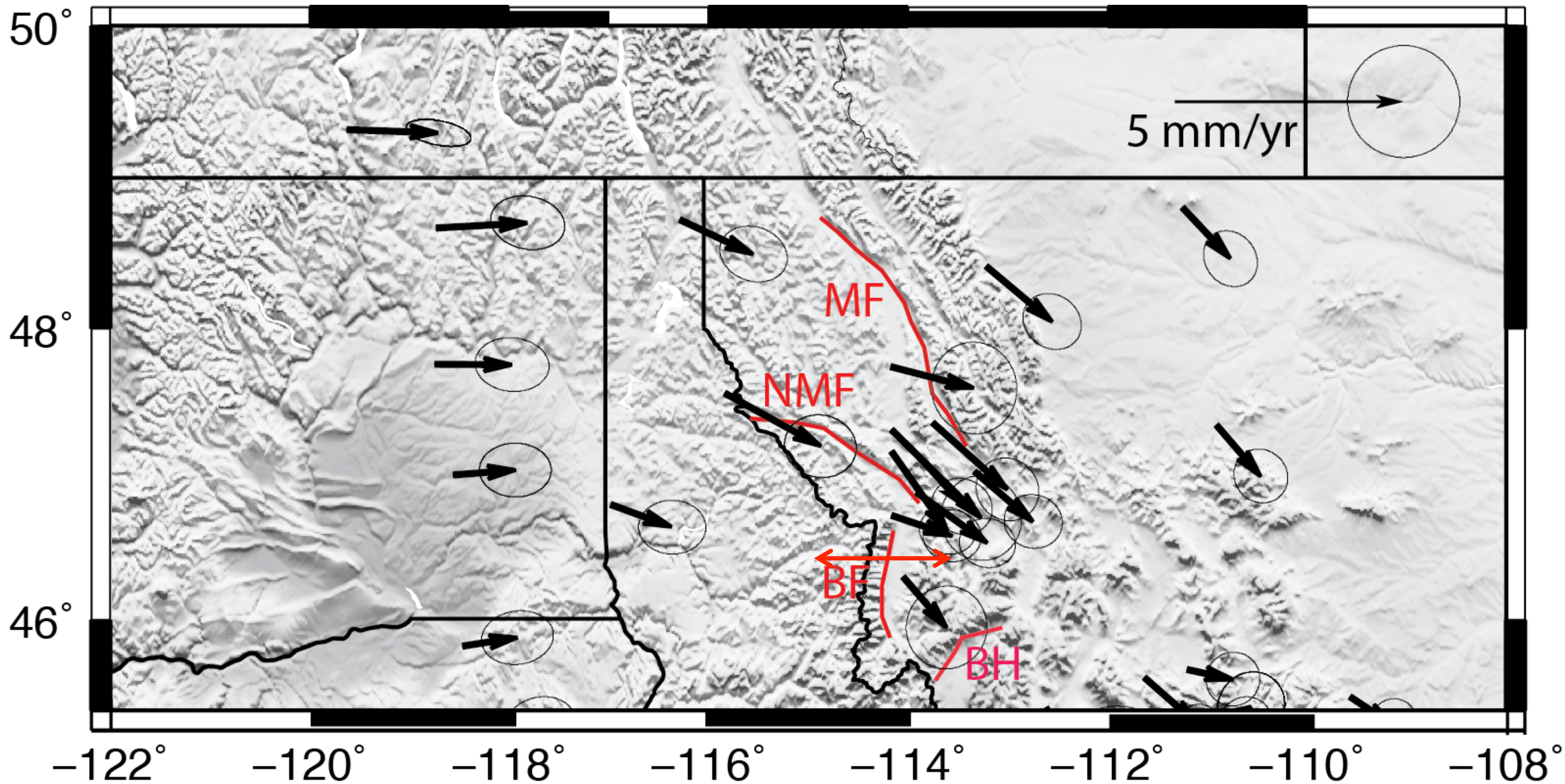

0.7 ± 0.5 mm/yr

SfM: Chute Canyon, Red Rock Fault

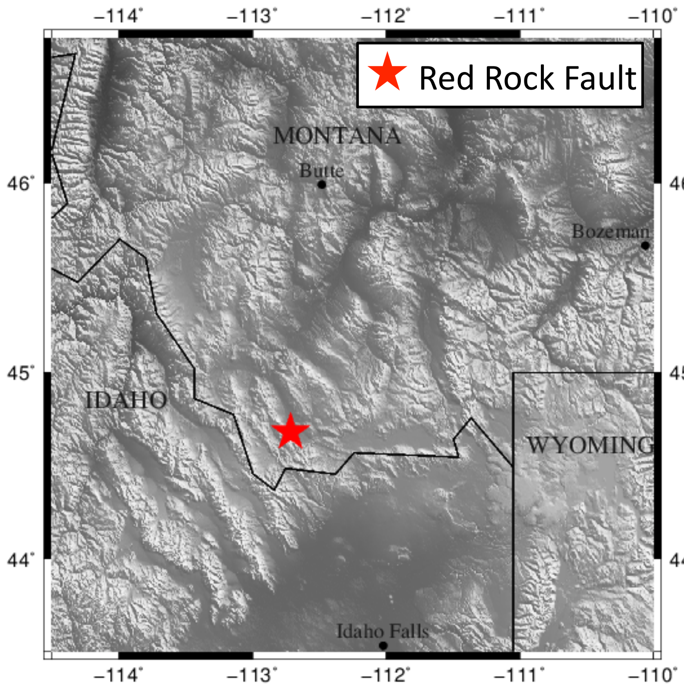

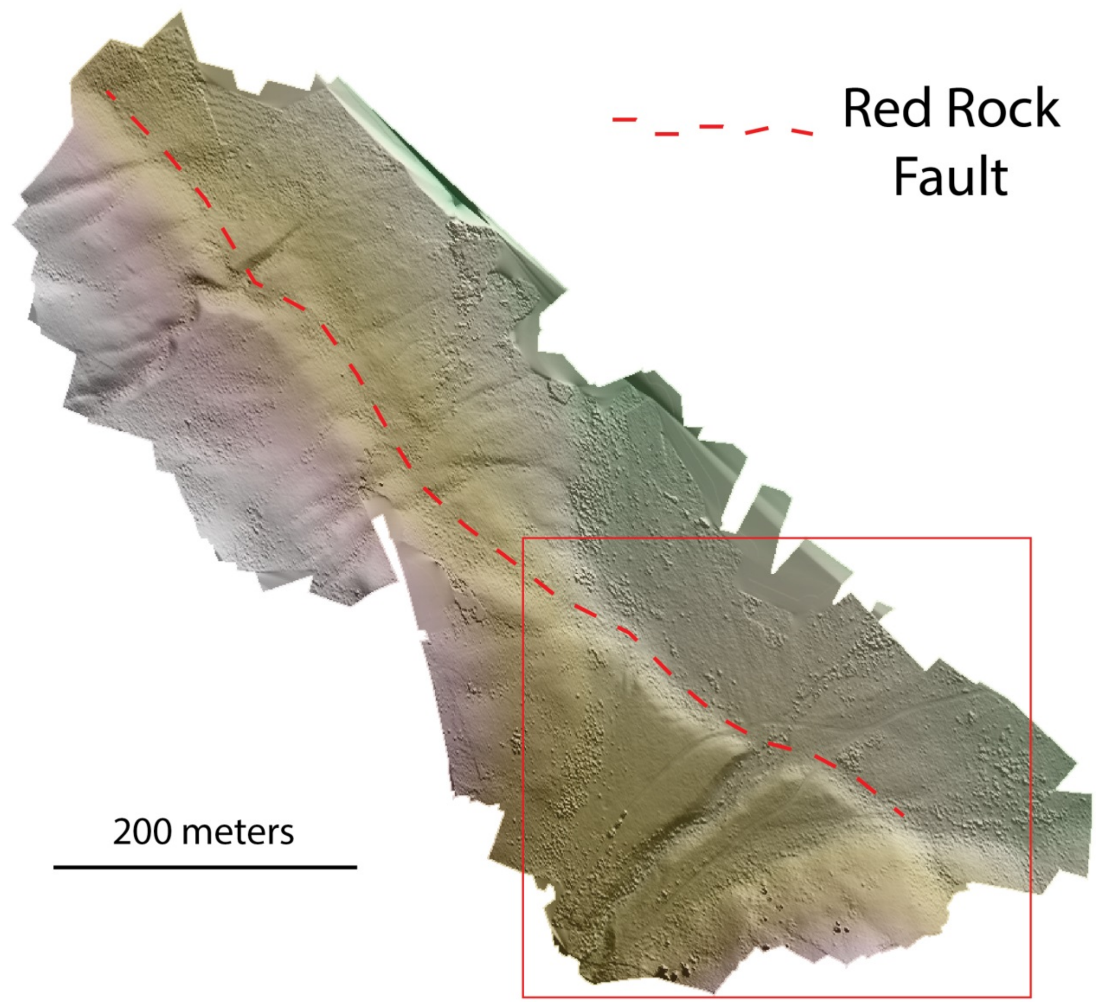

Courtesy K. Johnson, CSM

SfM: Chute Canyon, Red Rock Fault

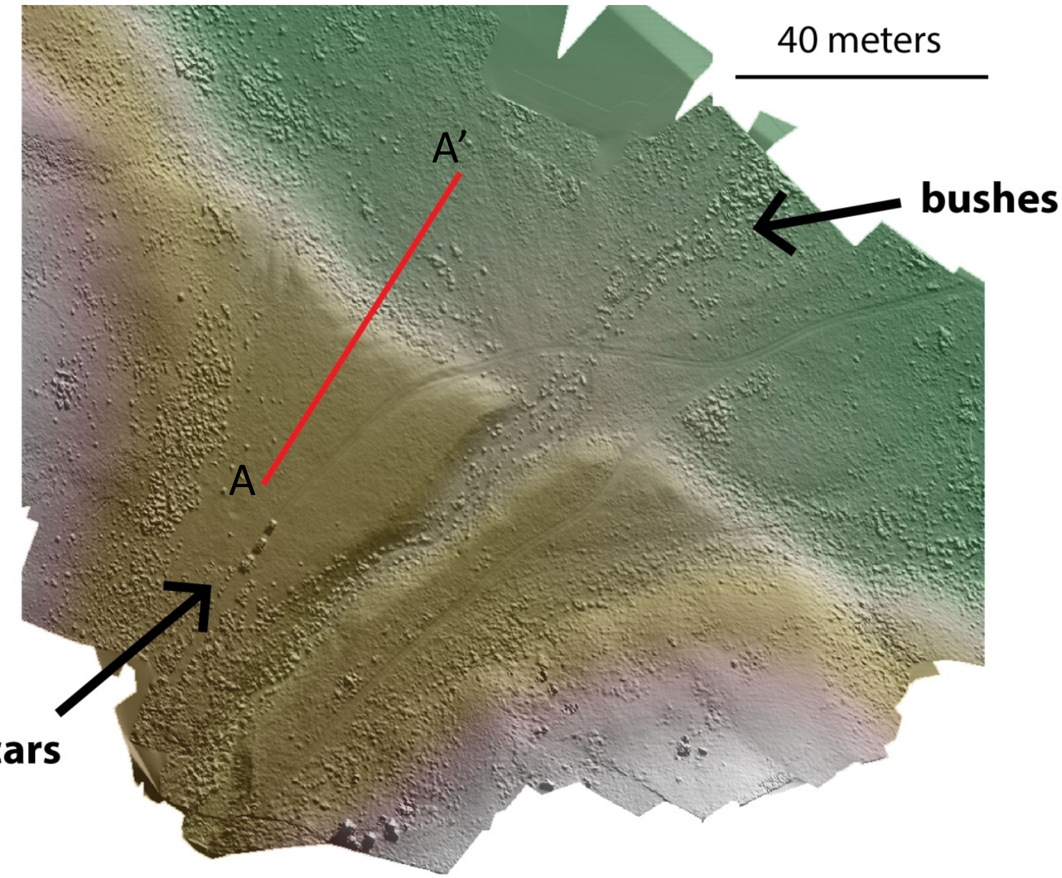

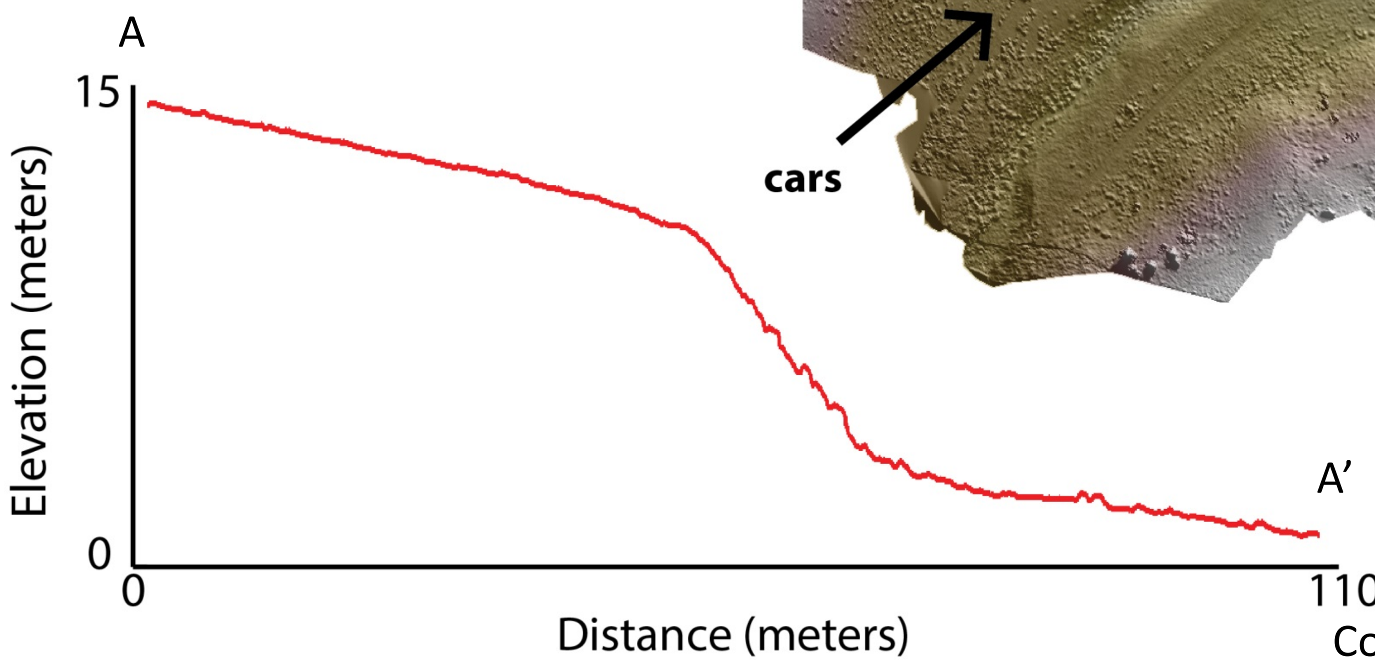

Courtesy K. Johnson, CSM

LiDAR: Bitterroot Fault

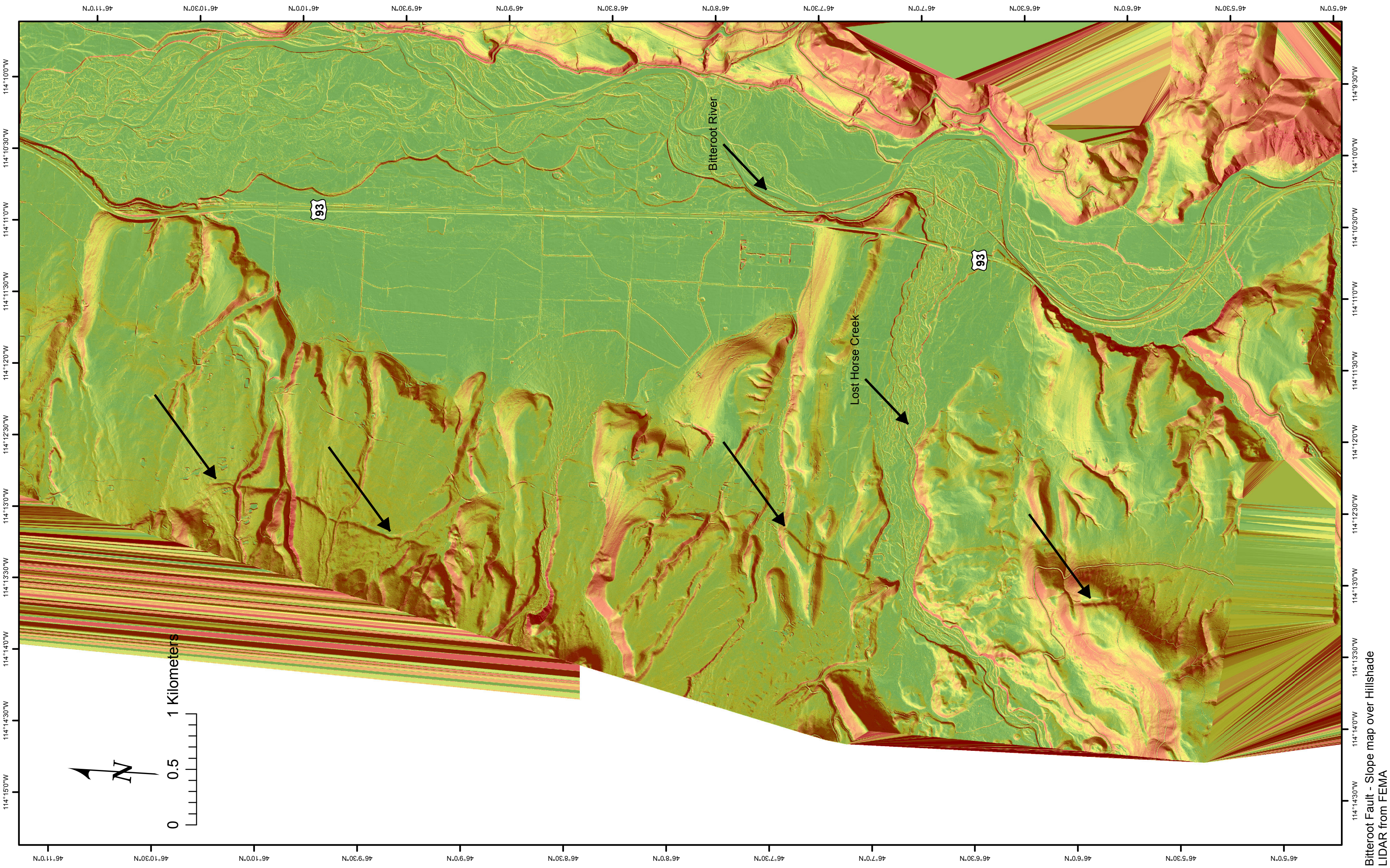

Seismic and paleoseismic

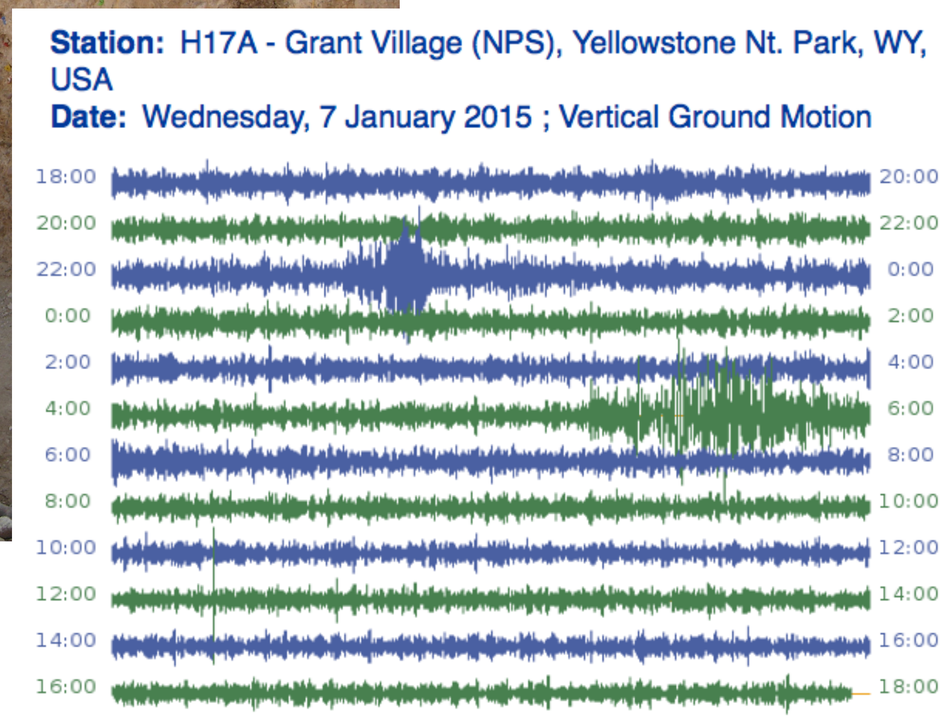

Current hazard assessment

Table 1. Missoula County Quaternary-age faults (Stickney et al., 2000)

Fault Name	Slip Rate (mm/yr)
Ninemile Fault	0.2(?)
Bitteroot Fault	0.2(?)
Jocko Fault	0.2(?)
Swan Fault	0.2(?)

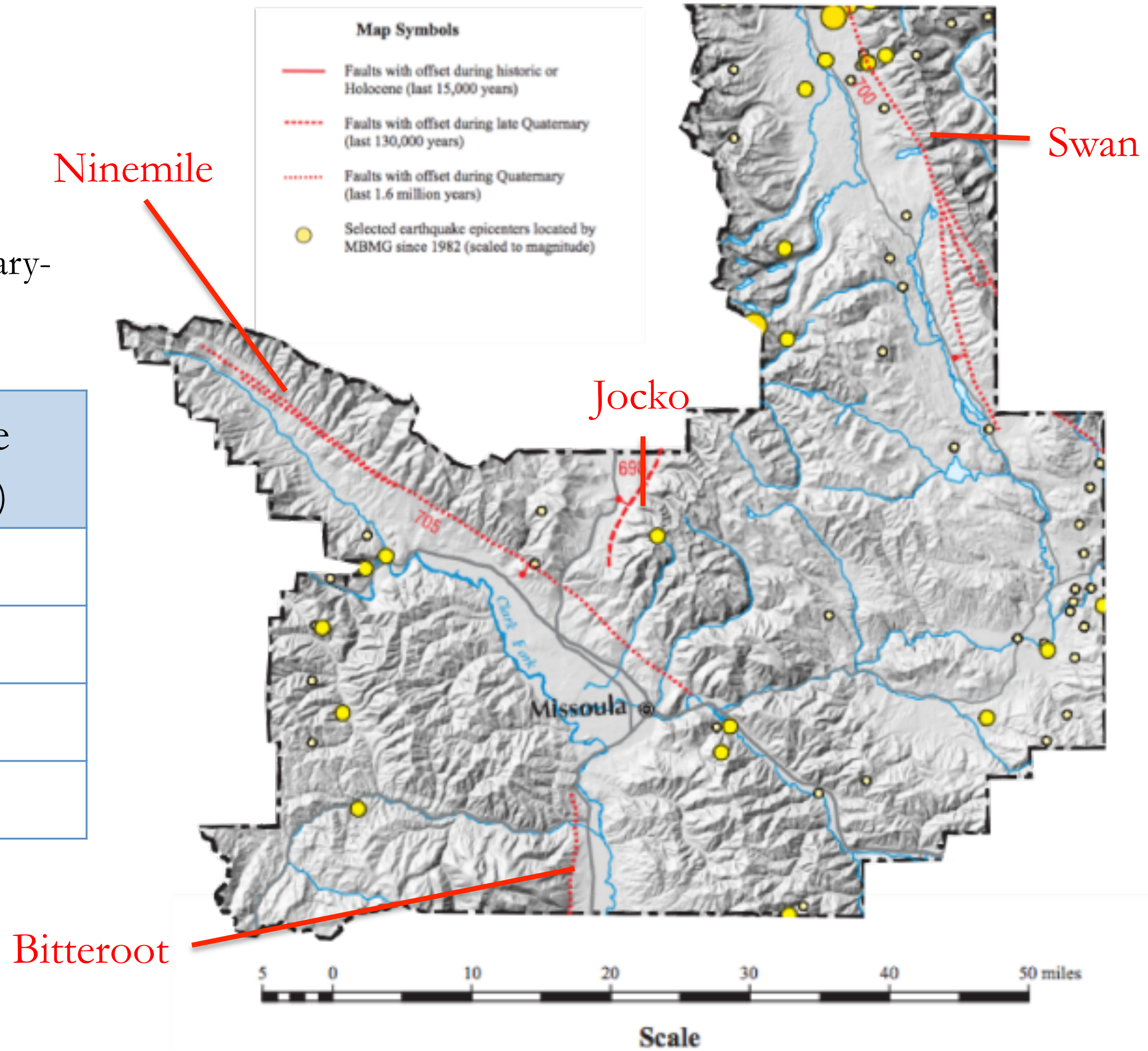

Figure 3. Mapped faults Missoula, County

http://www.mbmg.mtech.edu/pdf/SP114-earthquakemap.pdf

Current hazard assessment

Table 1. Miss... ...aternary-age fault... , 2000)

underestimates

Fault ...me	Slip Rate (m.../yr)
Ninemile ...ult	0.2(?)
Bitteroot Fau...	0.2(?)
Jocko Fa...	0.2(?)
Swan ...ault	...(?)

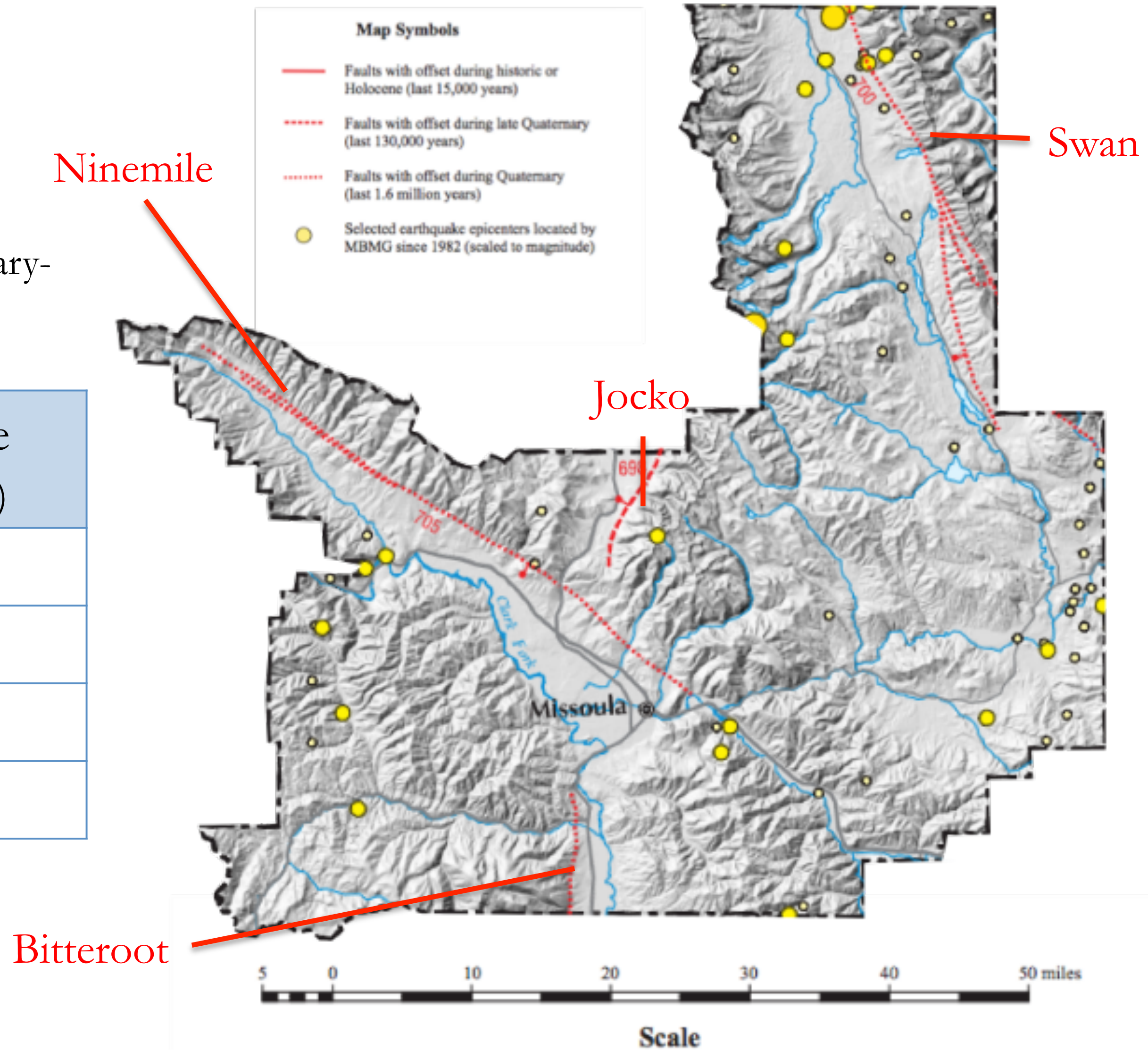

Figure 3. Mapped faults Missoula, County

http://www.mbmg.mtech.edu/pdf/SP114-earthquakemap.pdf

Goals

- Reduce slip-rate uncertainties
- Densify key transects for fault geometry
- Combine rates with recurrence data (when last events happened)
- Update regional hazard assessments to reflect higher slip rates
- Build regional kinematic model